Molecular function of the cytotoxic necrotizing factor CNF_Y and its impact on the virulence of *Yersinia pseudotuberculosis*

Von der Fakultät für Lebenswissenschaften

der Technischen Universität Carolo-Wilhelmina

zu Braunschweig

zur Erlangung des Grades einer

Doktorin der Naturwissenschaften

(Dr. rer. nat.)

genehmigte

D i s s e r t a t i o n

von Janina Nikola Georgia Schweer
aus Covington / USA

1. Referentin: Professorin Dr. Petra Dersch
2. Referent: Professor Dr. Michael Steinert
eingereicht am: 30.04.2014
mündliche Prüfung (Disputation) am: 26.06.2014

Druckjahr 2014

Vorveröffentlichungen der Dissertation

Teilergebnisse aus dieser Arbeit wurden mit Genehmigung der Fakultät für Lebenswissenschaften, vertreten durch die Mentorin der Arbeit, in folgenden Beiträgen vorab veröffentlicht:

Publikationen

Schweer J., Kulkarni D., Kochut A., Pezoldt J., Pisano F., Pils M. C., Genth H., Huehn J. & Dersch P.: The cytotoxic necrotizing factor of *Yersinia pseudotuberculosis* (CNF_Y) enhances inflammation and Yop delivery during infection by activation of Rho GTPases. *PLoS Pathog.* 9(11), e1003746. (2013)

Pisano F.[*], Heine W.[*], Rosenheinrich M., Schweer J., Nuss A. M., Dersch P.: Influence of PhoP and intra-species variations on virulence of *Yersinia pseudotuberculosis* during the natural oral infection route. (2014) Accepted at *PLoS ONE* ([*] shared first authorship)

Tagungsbeiträge

Schweer, J., Kochut, A. & Dersch, P. (2012) The cytotoxic necrotizing factor of *Yersinia pseudotuberculosis* YPIII -Characterization of a new virulence factor- (Vortrag). Symposium der Fachgruppe Mikrobielle Pathogenität der DGHM und VAAM, Bad Urach.

Schweer, J., Kochut, A. & Dersch, P. (2012) The cytotoxic necrotizing factor of *Yersinia pseudotuberculosis* YPIII -Characterization of a new virulence factor- (Vortrag). 3. nationales *Yersinia* Meeting, Tübingen.

Schweer, J., Kulkarni, D., Kochut, A., Pezoldt, J., Pisano, F., Pils, M. C., Genth, H., Hühn, J. & Dersch, P. (2013) The cytotoxic necrotizing factor of *Yersinia pseudotuberculosis* YPIII -Characterization of a virulence factor- (Poster). 5th Congress of European Microbiologists (FEMS 2013), Leipzig.

Table of Contents

List of figures

List of figures

List of figures

List of tables

Abbreviations

A	adenine
Ail	attachment and invasion locus
Amp	ampicillin
APC	antigen presenting cell
APS	ammonium persulfate
ATP	adenosine triphosphate
bp	base pairs
BHI	brain heart infusion
bla	ampicillin resistance gene (β-lactamase)
BSA	bovine serum albumin
C	cytosine
°C	degree Celsius
Cb	carbenicillin
CFU	colony forming units
CNF	cytotoxic necrotizing factor
Crp	cAMP receptor protein
Csr	carbon storage regulator
Da	Dalton
DAPI	49,6- diamidino-2-phenylindole
DC	dendritic cell
DNA	desoxyribonucleic acid
DNT	dermonecrotic toxin
dNTP	desoxy-ribonucleid-triphosphate
DYT	double yeast tryptone
et al.	et alii
ECM	extracellular matrix
EDTA	ethylenediaminetetraacetic acid
e.g.	for example
ETEM	YopE-β-lactamase
FAE	follicle associated epithel
F-actin	filamentous actin
FCS	fetal calf serum
FELASA	European Health Recommendations of the Federation of Laboratory Animal Science Associations
Fur	ferric uptake regulator
g	gram
G	guanine
G-actin	globular actin
GALT	gut-associated lymphoid tissue
GAP	GTPase-activating proteins
GDI	guanine-nucleotide-dissociation inhibitors
GEF	guanine-nucleotide-exchange factors
GFP	green fluorescent protein
GTP	guanosine triphosphate
GV-SOLAS	German Recommendations of the Society for Laboratory Animal Science
h	hour(s)
HBMEC	human brain microvascular endothelial cells

H & E	hematoxylin-eosin
HEp-2	human epithelial cells
HRP	horseradish peroxidase
IFN	interferon
IL	interleukin
IPTG	isopropyl-β-d-thiogalactopyranosid
IVIS	*in vivo* imaging system
kan	kanamycin
kb	kilobase
κB kinase β	IKKβ
kDa	kilo-Dalton
l	liter
lacZ	gene of β-galactosidase
LcrF	low calcium response F
LP	lamina propria
LPS	lipopolysaccharides
luxCDABE	luciferase operon (luciferase and its substrate)
M	molar
mA	milli-Ampère
MAPK	mitogen-activated protein kinase
M-cells	microfold cells
Mcs	multiple cloning site
MEK	mitogen-activated protein kinase kinases
min	minute
MMA	minimal medium A
μ	micro
ml	milliliter
MLNs	mesenteric lymph nodes
mm	millimeter
NCBI	National Center for Biotechnology Information
NCS	newborn calf serum
NEB	New England Biolabs
NF-κB	nuclear factor κB
ng	nanogram
NK	natural killer
nm	nanometer
nM	nanomolar
OD_{nm}	optical $density_{nm}$
OMV	outer membrane vesicle
ori	origin of replication
PAA	polyacrylamide
PAGE	polyacrylamide-gelelectrophoresis
PAK	p21-activated protein kinase
PBD	p21-binding domain
PBS	phosphate buffered saline
PCR	polymerase chain reaction
PFA	paraformaldehyde
PI	propidium iodide
PMN	polymorphonuclear neutrophil

PP	Peyer's patches
PRK2	protein kinase C-like 2
PVDF	polyvinylidene fluoride
pYV	*Yersinia* virulence plasmid
RBD	Rho-binding domain
ROS	reactive oxygen species
rpm	rotation per minute
RSK1	ribosomal protein S6 kinase
RT	room temperature
SDS	sodiumdodecylsulfate
SOC	super optimal broth
T	thymin
TBE	tris-borat EDTA-buffer
TCA	trichloracetic acid
TcdBF	toxin B of variant *Clostridium difficile* strain 1470 serotype F
TEER	trans epithelial electrical resistance
TLR	toll-like receptor
TNF	tumor necrosis factor
T3SS	type three secretion system
UPEC	uropathogenic *E. coli*
V	Volt
wt	wild-type
YadA	*Yersinia* adhesin A
YmoA	*Yersinia*-modulator A
Yop	*Yersinia* outer proteins

1 Introduction

Pathogenic bacteria possess different virulence factors, e.g. to evade the immune system or to efficiently colonize a host. Bacterial toxins are mostly essential virulence factors of the respective bacterium.

One of the first toxins, which were identified was the diphtheria toxin of *Corynebacterium diphtheriae* (Roux & Yersin, 1888). The identification of many other important toxins followed. Of particular interest are toxins functioning as biological weapons, like anthrax of *Bacillus anthracis*, but also toxins used in the pharmaceutical industry like botulinum toxin of *Clostridium botulinum*. Furthermore, inactivated bacterial toxins are commonly used as vaccines, stimulating the host's immune system to develop immunity against the respective bacterium.

This thesis has a focus on an A-B toxin, the cytotoxic necrotizing factor CNF_Y, which is expressed by the enteropathogen *Yersinia pseudotuberculosis*, a model organism widely applied in fundamental research.

1.1 The genus *Yersinia*

Yersiniae are gram-negative rod shaped bacteria, which facultatively grow in aerobic conditions and are psychrotolerant. They are able to grow at 4°C as well as 43°C with an optimum between 20 - 30°C. At moderate temperatures outside the host they are mostly motile and lose this feature inside the host at 37°C (Kapatral & Minnich, 1995).

The genus *Yersinia* belongs to the group of *Enterobacteriaceae* and was first described by the Swiss tropical physician Alexandre Yersin in 1894. He was able to isolate the most known species *Y. pestis* out of plague-spots of human dead bodies (Treille & Yersin, 1894). In total, 18 species belong to the genus *Yersinia* (Savin *et al.*, 2014), but only three of them are human pathogens, the above mentioned *Y. pestis* and two enteropathogenic species, namely *Y. enterocolitica* and *Y. pseudotuberculosis* (Carniel *et al.*, 2006; Chen *et al.*, 2010). Transmission of all human pathogenic *Yersinia* strains occurs by animals. These infections are referred to as zoonoses. Furthermore, isolates of these pathogens have in common a tropism for lymphatic tissue. Within these tissues the bacteria are able to replicate efficiently and escape or inhibit the innate immune response of the host (Grosdent *et al.*, 2002; Heesemann, 1994; Naktin & Beavis, 1999).

Up to now plague is one of the most dangerous infectious diseases and still not eradicated. New infections with *Y. pestis* are reported regularly, e.g. epidemics in Madagascar or even in the United States of America due to persistance of the bacteria in rodents. *Y. pestis* is transmitted to the host by infected fleas, which serve as vectors. The bite induces the regurgitation of the contaminated stomach content of the flea into the bloodstream of the host (Hinnebusch, 1997). Rodents often show no symptoms of disease, whereas a *Y. pestis* infection in humans leads to bubonic or pneumonic plague. These diseases cause rapid death of the patient without antibiotic treatment (McCrumb *et al.*, 1953; Quenee & Schneewind, 2009).

In comparison, infections by the enteropathogenic strains, *Y. enterocolitica* or *Y. pseudotuberculosis*, are less dangerous. These bacteria are transmitted via contaminated food or water, e.g. raw meet or milk (Lynch *et al.*, 2006). An infection with these species induce Yersiniosis, a variety of gut-associated diseases like enteritis and diarrhea or it can rarely cause autoimmune diseases like erythema nodosum or reactive arthritis (Lamps, 2003; Lamps *et al.*, 2003). Yersiniosis is the third most abundant bacterial zoonotic infectious disease in Germany and the European Union (Rosner *et al.*, 2010). With an intact immune system of the host, these infections are self limiting and do not require antibiotic treatment (Abdel-Haq *et al.*, 2000).

Although these three human pathogenic species belong to the same genus, they vary significantly in the type of transmission (see above). The genetically higher degree of relationship is between *Y. pseudotuberculosis* and *Y. pestis*. It could be shown that *Y. pestis* evolved out of *Y. pseudotuberculosis* about 1,500 – 20,000 years ago (Achtman *et al.*, 1999). Nevertheless, these two species show important differences in the progress and severity of disease. Responsible therefore are differences in the genome, mostly the extra chromosomal DNA.

All human pathogenic strains harbour a very similar virulence plasmid with a size of around 70 kb, which is needed for infection. However, there are 13% of genes inactive in *Y. pestis*, of which most of them are important for a successful *Y. pseudotuberculosis* infection (Chain *et al.*, 2004). For example the gene *yadA* (*Yersinia* adhesin A), encoded on the virulence plasmid, is needed for adhesion to and invasion into the eukaryotic cells by the enteropathogenic strains, whereas it is inactive in the *Y. pestis* strains (Neyt *et al.*, 1997). In addition to the virulence plasmid pYV, which is harboured by all pathogenic strains, *Y. pestis* carries two other plasmids, pFRA (100 kb) and pPLA (9.5 kb). These

two extrachromosomal elements are of high importance for the infection, because they are needed for the survival in the flea and the transmission via the blood of the host (Sebbane *et al.*, 2009).

The enteropathogenic species consist of many different serotypes. The two species show a weak sequence-identity of around 50% in the genome, and differ in their gene expression pattern (Brenner *et al.*, 1976). The *Y. enterocolitica* strains are classified in biogroups based on biochemical features and in serogroups, depending on their O-antigen immune reactivity (Brenner *et al.*, 1976). Many of these serogroups are known to induce diseases in humans, but the most common serogroup in Germany with about 90% of all *Y. enterocolitica* infections is the serogroup O:3/biotype 4 (Rosner *et al.*, 2010). The *Y. pseudotuberculosis* strains are categorized in 21 serogroups, whereas the majority of diseases are caused by the serogroups O:1 and O:3 (Dube, 2009). Several differences among the *Y. pseudotuberculosis* strains were described. A few isolates e.g. carry the intact gene for the cytotoxic necrotizing factor *cnfY*, whereas this gene is mutated in other sequenced *Y. pseudotuberculosis* strains (Lockman *et al.*, 2002).

Due to their ability to colonize and invade different hosts, enteropathogenic *Yersinia* species are used for fundamental research on the infection mechanism (e.g. in mice). The detailed path of infection of the enteric species is described below.

1.2 Pathogenesis of enteropathogenic *Yersinia* strains

The uptake of enteropathogenic *Yersinia* species takes place by ingestion of contaminated food or water. Raw or undercooked pork is the main source of infection, because many pigs are colonized by *Y. enterocolitica* without showing any symptoms of disease (Fosse *et al.*, 2009; Fredriksson-Ahomaa *et al.*, 2006). Additionally, the bacteria are able to grow at 4°C in the fridge.

Infection with both enteric *Yersinia* species is considered as biphasic, divided into early and late infection phase. The early phase starts with the uptake of the bacteria in the human body, where an immediate shift in temperature and pH occurs, to which the bacteria need to adjust rapidly. These changes in the environment of the bacteria lead to the expression of stress adaption and virulence factors. The coding genes are located both on the chromosome and on the virulence plasmid pYV (Pepe *et al.*, 1994). This expression is important for the bacteria to pass through the stomach with its acidic pH (Young *et al.*, 1996). Subsequently, the bacteria reach the small intestine and the terminal ileum, where the *Yersinia* are able to adhere to specialized enterocytes, the

microfold cells (M-cells) and invade therein (see Figure 1.2.1). Up to this step the bacteria are motile, but lose this characteristic during the progress of infection.

The M-cells belong to the follicle-associated epithelial layer (FAE) of the gut, which covers the Peyer's patches (PP). These cells have a flat form and fewer, wider and less pronounced microvilli compared to the absorptive enterocytes of the gut (Grutzkau *et al.*, 1990). M-cells possess β_1-integrins, which are important receptors for the adhesion, invasion and ultimately the induced transcytosis of *Yersinia* through the gut epithelial layer. They initiate the process of transcytosis, by recognizing antigens on their apical side, take them up in vesicles and transport them to their basolateral side into the PP (Neutra *et al.*, 1999). With the transcytosis of the enteric *Yersinia*, the late infection phase starts.

The bacteria are able to colonize the PP, which leads to a proinflammatory response characterized by the infiltration of phagocytes (Grutzkau *et al.*, 1990) and the release of proinflammatory cytokines (see 1.3). To evade or protect themselves against the ongoing immune response, *Yersinia* possess different virulence factors, e.g. the *Yersinia* outer proteins (Yops) (see 1.4.2), which expression is associated with the late infection phase (Cornelis & Wolf-Watz, 1997; Revell & Miller, 2001).

In the next step, the bacteria leave the PP and spread via the lymphatic system to the mesenteric lymph nodes (MLNs). From there they are able to spread to the systemic organs liver, spleen and kidneys. It is also believed, that the enteropathogenic *Yersinia* species can, in some cases, travel directly from the small intestine through the blood stream to the systemic organs like liver and spleen and bypass the MLNs (Autenrieth & Firsching, 1996). In the organs, *Yersinia* replicates mostly extracellularly, which leads to the formation of microcolonies and abscesses (Autenrieth & Firsching, 1996; Isberg & Van Nhieu, 1994). Additionally, there is evidence that some strains of the enteropathogenic species are able to survive and even replicate within the macrophages (Brzostek *et al.*, 2003; Cavanough & Randall, 1959; Pujol & Bliska, 2005; Tsukano *et al.*, 1999). This would be another factor helping the bacteria to hide and thereby evade their elimination by the host's immune system.

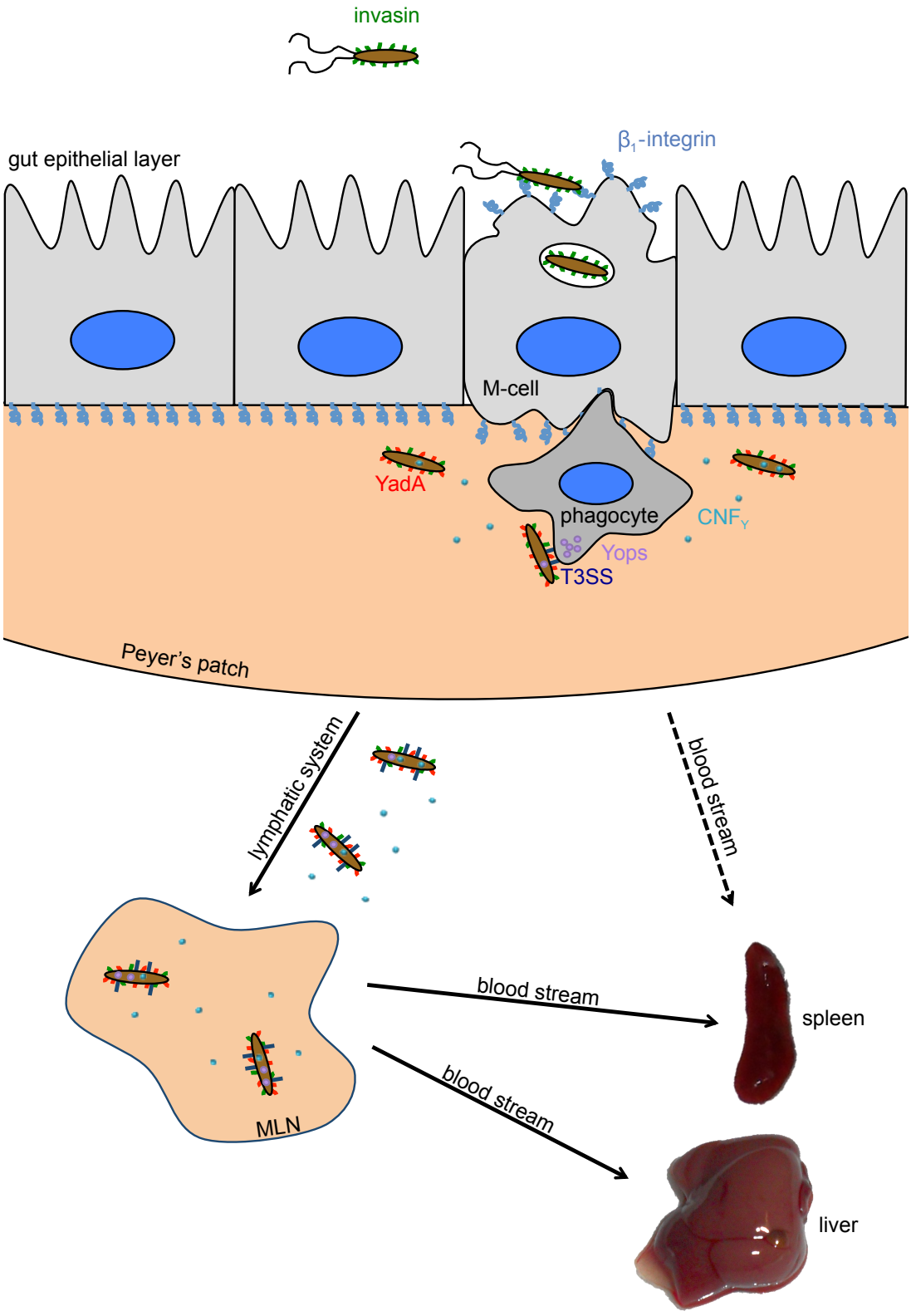

Figure 1.2.1: Infection route of enteropathogenic *Yersinia* species through the gut.
The yersiniae are ingested by contaminated food or water, reach the small intestine and transcytose via M-cells, localized in the terminal ileum. After the transcytosis mediated by β_1-integrin receptors, the bacteria reach the Peyer's patches, travel through the lymphatic system and reach the MLN. From there they spread to the systemic organs liver and spleen. It is assumed that some of the bacteria can bypass the MLNs and reach the systemic organs directly from the PP via the blood stream (Autenrieth & Firsching, 1996).

1.3 Enteropathogenic *Yersinia* and the host's immune response

All enteropathogenic bacteria come into contact with the largest and most complex part of the host immune system, the intestinal immune system. It has evolved a local and systemic tolerance for the commensals, the oral tolerance, in which the M-cells play a key role (Strobel & Mowat, 1998). This differentiation between harmful pathogenic and harmless commensal bacteria is highly important. If the immune system overshoots constantly with commensal bacteria, inflammatory disorders like coeliac disease or Crohn's disease may occur. If the immune system does not react properly in case of invading pathogens, an infection with severe disease symptoms can result.

A characteristic for an enteropathogenic bacterium is its ability to invade into or transpass the gut epithelial barrier. By invading in the small intestine, the pathogenic bacteria come into contact with the largest proportion of immune cells in the gut. These cells belong to the gut-associated lymphoid tissue (GALT), which is divided into two parts, the lymphocytes in the epithelial layer and lamina propria (LP) and the lymphocytes in the PP. Enteropathogenic yersiniae are known to enter through the M-cells in the terminal ileum and reach the PP as described. The PP are formed of large B cell follicles (60% B cells), intervening T cell areas (25% T cells), dendritic cells (DCs) (10%), and macrophages and polymorphonuclear leukocytes (PMNs) (together < 5%) (Jung *et al.*, 2010). The entry of the yersiniae into the PP leads to the induction phase of the innate immune response of the host, as described in detail below (see Figure 1.3.1).

At the early stage of an infection with enteropathogenic *Yersinia* species, the bacterial numbers decrease significantly, probably due to the fast influx of macrophages and neutrophils in answer to the penetration. This was especially shown after an i.v. injection, mimicking a systemic infection of the bacteria (Conlan, 1997). These cell types and also the DCs are very important during this step of the host's immune response, because of their phagocytic behaviour and their release of proinflammatory cytokines. The release is triggered by the activation of the Toll-like receptors on these cell types upon contact with the pathogen. It was shown for enteropathogenic yersiniae, that the binding of the invasin to the β_1-integrins of enterocytes can additionally trigger the release of proinflammatory cytokines (Kampik *et al.*, 2000; Schulte *et al.*, 1996). Whether other factors like LPS or YadA also contribute to the recruitment of the immune cells is still unclear.

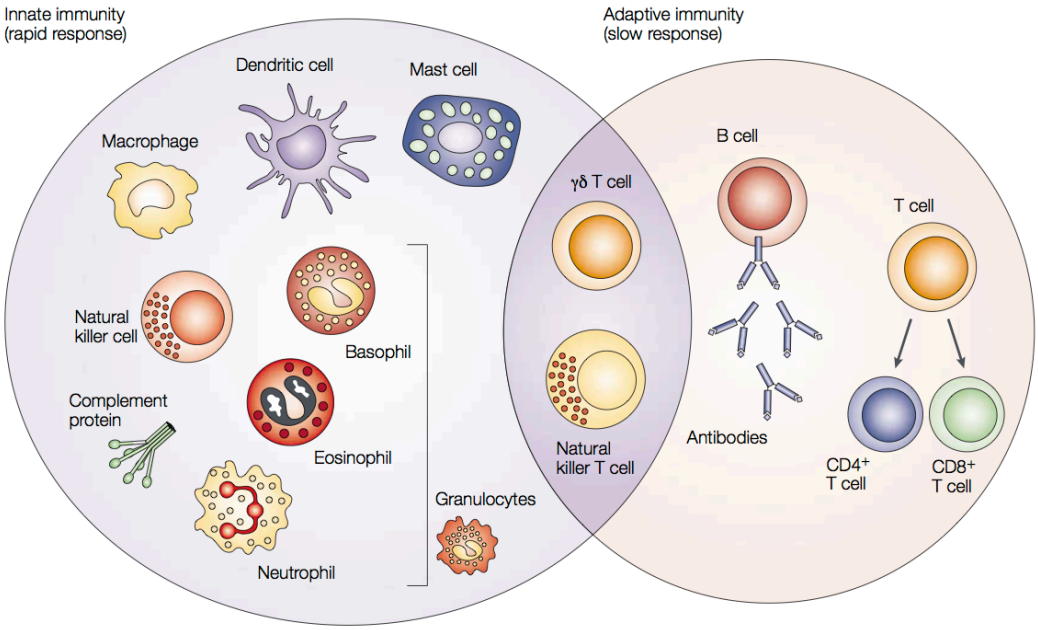

Figure 1.3.1: Overview of the cells of the innate and adaptive immunity (Dranoff, 2004)**.**
The innate immunity forms the first line of defence against an invading bacterium. In contrast, the adaptive immunity is slower, but more specific.

In the PP, DCs are mainly responsible for the antigen sampling. They take up the bacteria and act as antigen presenting cells (APCs) for T cells. However, also macrophages and especially PMNs are recruited to the PP and defend the host against the pathogen by phagocytizing the bacteria. Upon a *Yersinia* infection, the infiltrating immune cells as well as the enterocytes (Eckmann *et al.*, 1995) have been shown to produce proinflammatory cytokines, especially IL-1 (Autenrieth & Firsching, 1996; Beuscher *et al.*, 1992), leading to the recruitment and maturation of additional phagocytes. One day after an oral infection of mice, microabscesses and residing bacteria can be detected in the PP (Autenrieth *et al.*, 1996; Hanski *et al.*, 1989).

In the next step, the bacteria exit the PP through the lymphatics or the blood and reach the MLNs, the largest lymph nodes of the human body, or the systemic organs (see 1.2), respectively. It has been suggested that some phagocytes may also be involved in the dissemination of yersiniae from the PP (Autenrieth *et al.*, 1996). These cells are proposed to function as vehicles transporting the intracellular bacteria through the blood like trojan horses.

Different cytokines, mainly produced by macrophages, e.g. IL-12 or IL-18 lead to the stimulation of NK cells and T cells and the antigen presentation of the APCs, which constitutes the cross point between the innate and adaptive immune response. It is

known that the concerted activities of the adaptive immune cells, T helper cells ($CD4^+$), and cytotoxic T cells ($CD8^+$), and the innate immune cells, the activated macrophages are required to control a *Yersinia* infection efficiently. T cells control the infection (1) with their ability to kill infected cells, (2) by helping macrophages to eliminate the internalized bacteria, and (3) by activation of B cells for antibody production (Autenrieth *et al.*, 1992, 1993a; Bohn & Autenrieth, 1996). But, particularly the T cell activated macrophages have been shown to kill enteric *Yersinia* species efficiently (Autenrieth & Heesemann, 1992; Zhang & Bliska, 2005).

Even though the enterophathogenic *Yersinia* species harbour defence mechanisms to evade the host immune system, infections in humans are mostly self-limiting after triggering the immune response, and end with a complete clearance of the bacteria. However, in small children, elderly persons, immunosuppressed patients or in conditions involving iron overload (Adamkiewicz *et al.*, 1998; Chiu *et al.*, 1986; Autenrieth *et al.*, 1993a, b), bacteria are able to evade the immune system by injecting different effector proteins into the immune cells and impairing the complement system with virulence factors (see 1.4).

1.4 Virulence factors of enteropathogenic *Yersinia*

The virulence factors of the enteropathogenic *Yersinia* species are encoded both on the chromosome as well as on the virulence plasmid pYV (Portnoy & Falkow, 1981). In recent years, it was possible to sequence and annotate whole genomes of different *Yersinia* strains. Thereby, new virulence genes and partially their mode of action in the host-pathogen interaction have been identified (Thomson *et al.*, 2006).

The virulence gene expression is tightly regulated and influenced by temperature, the pH or nutrients (Pepe *et al.*, 1994). The regulation occurs on the transcriptional as well as on the post-transcriptional level and involves different regulators (Darwin & Miller, 1999; Gort & Miller, 2000; Young & Miller, 1997).

The main pathogenicity factors for infection and resistance against the innate immune system of the host are encoded on the virulence plasmid (Revell & Miller, 2001). The gene products are categorized in four groups:

1. Secreted antiphagocytic effector proteins (Yops)
2. Ysc proteins of the type-III-secretion system (T3SS) involved in the production and secretion of the Yops

3. The Y*ersinia* adhesin A (YadA), necessary for the bacteria's adhesion and invasion to/into the eukaryotic cell
4. The regulatory protein LcrF of *Y. pseudotuberculosis* and *Y. pestis* or VirF (98% sequence-identity) of *Y. enterocolitica* (Hoe *et al.*, 1992)

Without the virulence plasmid, the pathogenicity of the *Yersinia* species is massively diminished and the bacteria are no longer able to reach the systemic organs (Cornelis *et al.*, 1998; Straley *et al.*, 1993).

In addition to the plasmid-encoded virulence factors, three other important factors are encoded on the chromosome:

1. The attachment and invasion locus (*ail*), coding for a 17 kDa integral outer membrane protein
2. The pH6 antigen, which forms a 16 kDa pilus like structure
3. The *invA* gene, coding for the invasin

The Ail protein has been shown to play four different roles in the *Yersinia* infection process. It is important for the serum resistance of the bacteria, the adhesion to and internalization into eukaryotic cells, the Yop translocation into the host cells and it is able to inhibit the inflammatory response of the host (Bartra *et al.*, 2008; Felek & Krukonis, 2009; Hinnebusch *et al.*, 2011; Kolodziejek *et al.*, 2007, 2010; Tsang *et al.*, 2010). Ail is expressed anaerobically at 37°C in both enteropathogenic species. However, no difference in the virulence was observed in an isogenic *ail* mutant strain for the enteropathogenic species (Isberg, 1996; Wachtel & Miller, 1995). In contrast, an isogenic *Y. pestis ail* mutant strain was attenuated in virulence (Hinnebusch *et al.*, 2011).

The pH6 antigen was shown to promote adhesion to the host cell, the induction of hemagglutination, and possesses anti-phagocytic properties towards macrophages. Nevertheless, because of its expression profile at 37°C and low pH, it is believed that it supports survival of the bacteria in the phagolysosome during the late infection phase (Huang & Lindler, 2004; Yang & Isberg, 1997; Yang *et al.*, 1996).

1.4.1 Invasins and adhesins

The virulence factors inducing adhesion (adhesins) to and internalization (invasins) into the host cells are of high importance for the infection of enteropathogenic *Yersinia* strains.

Yersiniae exploit the zipper mechanism to initiate their invasion into the host cell (see Figure 1.4.1) (Finlay & Cossart, 1997; Galan, 1994). The initial contact to the eukaryotic cell is ensured by adhesins. Two of them are mainly needed, YadA and especially InvA (see below). The adhesion activates signaling pathways in the host cell. Subsequently, cytoskeletal actin rearrangements are induced and thereby the internalization of the bacterium into membrane-bound vacuoles is initiated, forming the bacterial phagosome.

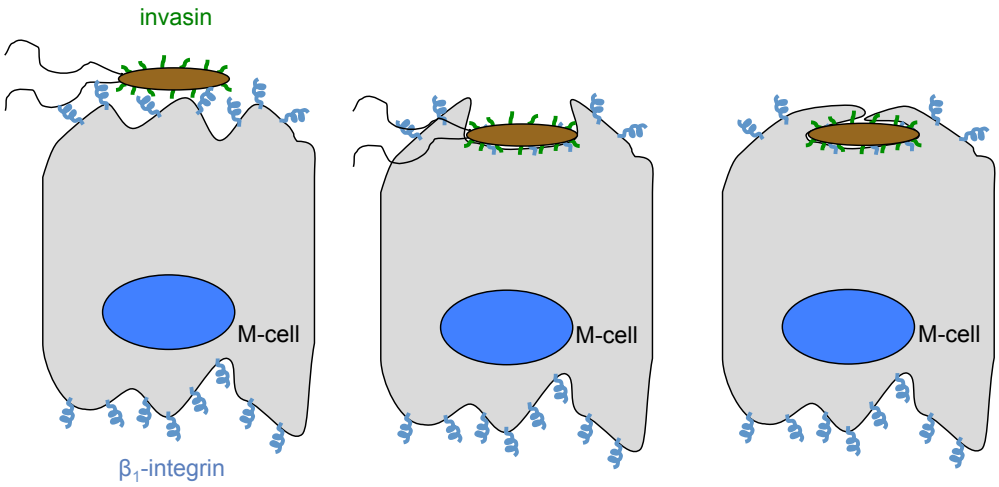

Figure 1.4.1: Invasion of enteropathogenic *Yersinia* by InvA induced zipper mechanism.
Schematic description of the zipper mechanism. *Yersinia* binds to the M-cell receptors (β_1-integrins) in the intestine with invasin by high affinity binding. This leads to actin cytoskeleton rearrangements and the formation of membrane protrusions. The bacterium is taken up by the cell into a bacterial phagosome (Isberg, 1989).

1.4.1.1 Invasin

Invasin (InvA) is the most important invasion protein of the enteropathogenic *Yersinia* species. This protein is involved in both the adhesion to and the invasion into the M-cells of the gut epithelial layer (Dersch & Isberg, 2000). Its expression in non-invasive *Escherichia coli* enables these bacteria to invade into human epithelial cells (HEp-2) (Isberg & Falkow, 1985; Miller & Falkow, 1988). The *invA* gene expression *in vitro* is temperature-, pH-, and growth phase-dependent. Maximal expression is obtained at 25°C during late stationary phase in nutrient rich medium with low osmolarity (Isberg *et al.*, 1988; Pepe *et al.*, 1994).

This 108 kDa outer membrane protein consists of an N-terminal outer membrane anchoring domain and five β-barrel domains in *Y. pseudotuberculosis* (see Figure 1.4.2). The invasin binds to β_1-integrins anchored in the host cell membrane and thereby leads to a clustering of these receptors. Responsible for the binding are the head domains D4 and D5 (Clark *et al.*, 1998; Tran Van Nhieu & Isberg, 1993). After binding, clustering of the integrins is induced through multimerization of invasin via domain D2 (Dersch & Isberg, 1999). This leads to the initiation of signaling cascades in the host cell, which trigger internalization (zipper mechanism) of the bacteria (see Figure 1.4.1) (Dersch & Isberg, 1999, 2000).

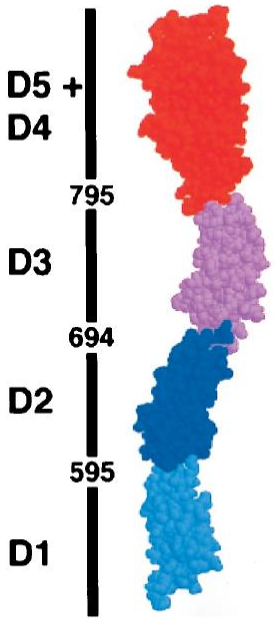

Figure 1.4.2: The invasin (InvA) structure of *Y. pseudotuberculosis*.
InvA consists of 5 domains, with domains D4 and 5 responsible for the β_1-integrin binding. Domain 2 of *Y. pseudotuberculosis* leads to a multimerization of InvA, which in turn induces a clustering of the β_1-integrin receptors (Dersch & Isberg, 1999).

1.4.1.2 YadA

The virulence factor YadA is another important adhesin of enteropathogenic yersiniae. It binds to proteins of the extracellular matrix (ECM), e.g. laminin or collagen and thereby enables the bacterium to adhere to the host cell (Flügel *et al.*, 1994; Heise & Dersch, 2006; Tertti *et al.*, 1992).

The *yadA* gene encodes for an outer membrane protein, which is exclusively expressed at 37°C (Barocchi *et al.*, 2005; Linke *et al.*, 2006). Depending on the *Yersinia* species, it possesses an atomic mass of around 200 - 240 kDa. The trimeric protein has a „lollipop“

like structure and covers the surface of the bacterium like a capsule (Hoiczyk *et al.*, 2000).

Structure analyses revealed that YadA from *Y. pseudotuberculosis* carries an additional domain at its N-terminus, which is absent in *Y. enterocolitica*. This domain of YadA induces, besides adhesion, also the invasion of *Y. pseudotuberculosis* into the eukaryotic cell, by binding to the natural ligand of the $\alpha_5\beta_1$-integrin receptors, fibronectin. Furthermore, YadA of *Y. enterocolitica* preferentially binds to collagen and laminin of the ECM (Heise & Dersch, 2006).

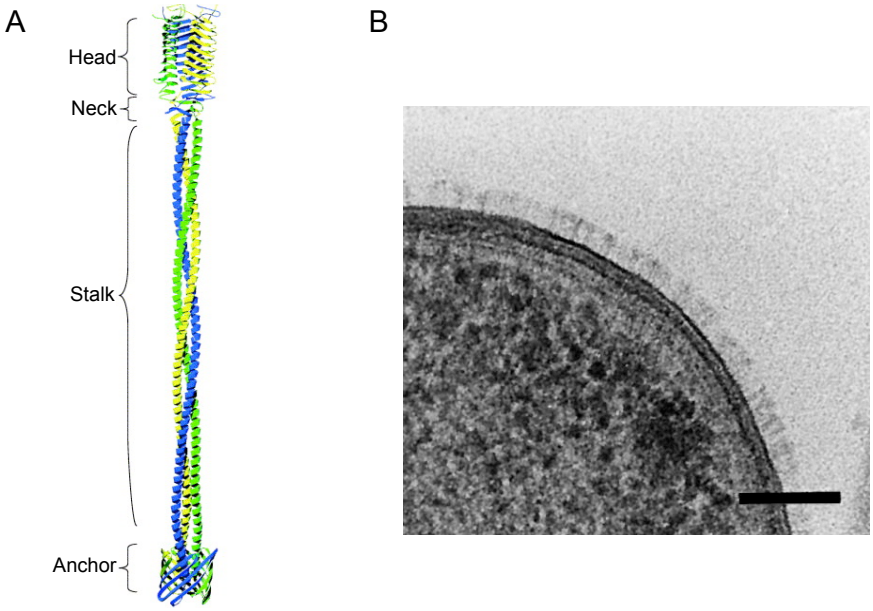

Figure 1.4.3: The virulence factor YadA.
A: Schematic illustration of the trimeric protein YadA, consisting of an anchor-, stalk-, neck-, and head-domain (Linke *et al.*, 2006).
B: Electron microscopic picture of a bacterium with the capsule like arranged YadA proteins. Bar indicates 100 nm (Hoiczyk *et al.*, 2000).

YadA of both species also induces an inflammatory response by triggering the expression of the proinflammatory cytokine interleukin 8 (IL-8) (Eitel *et al.*, 2005; Schmid *et al.*, 2004). An additional function of the protein is the protection of the bacterium against the immune system of the host. It binds components of the complement system, like the factor H, and inhibits thereby the opsonation of the bacterium preventing its elimination (Balligand *et al.*, 1985; Biedzka-Sarek *et al.*, 2008; Kirjavainen *et al.*, 2008; Pilz *et al.*, 1992).

1.4.2 The Yop virulon

The T3SS forms a syringe like structure with a needle surface to inject effector proteins into host cells (Kudryashev *et al.*, 2013). The genes encoding the T3SS are organized in different operons on the pYV by their function, whereas the translocated Yops are distributed all over the plasmid (Cornelis, 1998, 2002a; Pujol & Bliska, 2005). The expression of this system and therefore the injection of the effector proteins is dependent on temperature and Ca^{2+} ionic concentration, conditions present in the surroundings during infection. Moreover, it is activated by the transcriptional activator low calcium response F (LcrF), which in turn is repressed by the global virulence regulator *Yersinia* modulator A (YmoA) at conditions found outside the host (25°C). The seven translocated Yop proteins so far known are exotoxins, named YopE, YopH, YopJ/P, YopK/Q, YopM, YopO/YpkA and YopT. They help the bacterium to manipulate the host cell functions, e.g. the cytokine production or the actin dynamics, to prevent their elimination by the host immune system, mostly by preventing phagocytosis (see Figure 1.4.5) (Cornelis, 2002a; Viboud & Bliska, 2005).

The T3SS of *Yersinia* consists of three parts, (1) the pore forming complex, (2) the needle structure and (3) the basal body (see Figure 1.4.4). For the assembly of the basal body, multi-ring structures consisting of different Ysc proteins are integrated in the outer- and inner-membrane of the bacterium. At first, YscC oligomerises and forms the outer-membrane ring, which stretches into the periplasm (Diepold *et al.*, 2010; Koster *et al.*, 1997). In the next step, the inner-membrane ring is formed by YscD, which connects the inner- and outer-membrane rings (Diepold *et al.*, 2010; Ross & Plano, 2011; Spreter *et al.*, 2009). Subsequently, YscJ oligomerises and completes the inner-membrane ring (Yip *et al.*, 2005). Furthermore, a cytosolic energy producing ATPase, YscN is recruited and surrounded by the proteins YscK and YscL (Blaylock *et al.*, 2006). In the next step, YscQ assembles at the cytoplasmic site of the T3SS (Diepold *et al.*, 2010). Finally, the export machinery is formed, containing the proteins YscRSTUV which are positioned in the inner-membrane ring.

The secretion needle formed by the protein YscF is secreted through the basal body. YscI is positioned first and seems to allow the crossing of substrates through the inner membrane (Allaoui *et al.*, 1995; Marlovits *et al.*, 2006). YscF is translocated through the YscI channel and polymerizes to form the needle structure (Diepold *et al.*, 2012). The length of the needle varies from ~41 nm in *Y. pestis* to ~58 nm in *Y. enterocolitica* and

possesses an inner diameter of ~2 - 3 nm (Hoiczyk & Blobel, 2001; Journet *et al.*, 2003; Kubori *et al.*, 2000). YscP appears to regulate the length of the secretion needle (Journet *et al.*, 2003; Payne & Straley, 1999; Stainier *et al.*, 2000). The substrate specificity of the needle seems to be determined by YscU, which possesses an inner-membrane anchoring- and a cytosolic-domain (Allaoui *et al.*, 1994; Edqvist *et al.*, 2003). YscP was shown to induce the autocleavage of YscU after completion of the needle assembly (Agrain *et al.*, 2005; Lavander *et al.*, 2003; Sorg *et al.*, 2007). This step is needed to continue the secretion of the proteins for the formation of the pore complex and the proper secretion of the Yop proteins (Björnfot *et al.*, 2009; Riordan & Schneewind, 2008).

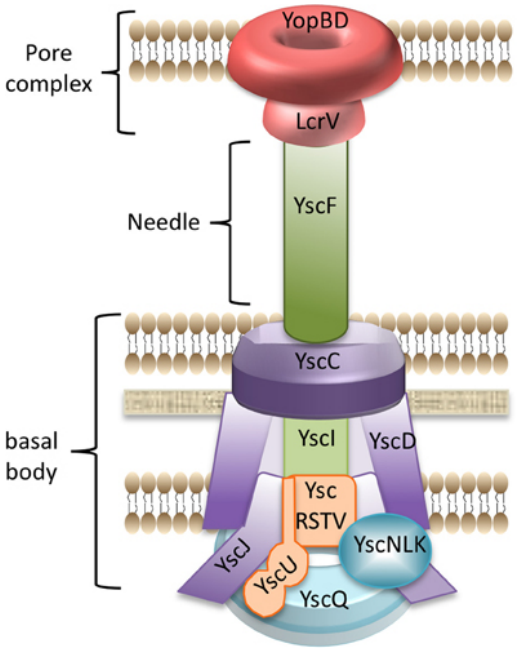

Figure 1.4.4: The type III secretion system of *Yersinia* (Dewoody *et al.*, 2013)**.**
Schematic model of the T3SS of *Yersinia*. Colours indicate the different structures and functions. Blue: components of the C- ring and ATPase in the bacterial cytoplasm; orange: proteins of the export apparatus; purple: scaffold proteins of membrane ring structures; green: rod and needle components; red: pore complex.

The Yop effector proteins should ideally be released upon host cell contact, which can also be mimicked *in vitro* by depletion of calcium in the medium (Lee *et al.*, 1998; Yother & Goguen, 1985). To prevent a premature release of the effectors, the needle is blocked for the effector Yop proteins by a complex consisting of YopN, TyeA, YscB and SycN, which is called the calcium plug (Forsberg *et al.*, 1991). In the next step, LcrV is secreted and forms a needle tip (Mueller *et al.*, 2005), at which the pore complex - consisting of YopD and YopB - is positioned. These two proteins (YopD/B) are able to insert

themselves into the host cell membrane to form a translocation pore (Hakansson *et al.*, 1993, 1996a; Neyt & Cornelis, 1999; Rosqvist *et al.*, 1995). With the assembly of YopD and YopB, the complex T3SS is completed and able to inject the effector Yops into the host cell upon cell contact. Most of these effector proteins require their own chaperone for correct folding and guidance to the secretion needle, but are injected into the cytosol of the host cell on their own.

Seven cytotoxic effector proteins are translocated into phagocytes, interfering with cell signaling pathways and preventing phagocytosis (Viboud & Bliska, 2005). YopE, YopO and YopT belong to the group of bacterial toxins interacting with Rho-GTPases (see 1.7) (Barbieri *et al.*, 2002). YopE is mimicking the Guanine-exchange proteins (GAPs) of the small Rho-GTPases RhoA, Rac1 and Cdc42, leading to a continuous hydrolysis of GTP (Von Pawel-Rammingen *et al.*, 2000). YpkA of *Y. pseudotuberculosis* and YopO, the homolog in *Y. enterocolitica* are serine/threonine kinases binding to RhoA and Rac1 (Viboud & Bliska, 2005; Wong & Isberg, 2005). This binding leads to the autophosphorylation of the Yop, which then controls the eukaryotic cell rounding and blocks the phagocytosis of the bacterium (Galyov *et al.*, 1993; Grosdent *et al.*, 2002; Hakansson *et al.*, 1996b). YopT forms a cysteine protease, which leads to the removal of the GTPases RhoA, Rac, and Cdc42 from the membrane of the cell (Shao *et al.*, 2003), causing the disruption of actin fibres, cell rounding, and inhibition of the bacterial internalization (Cornelis, 2002b; Viboud & Bliska, 2005).

YopH is a tyrosine phosphatase that blocks actin cytoskeletal dynamics, thus leading to the inhibition of phagocytosis by immune cells (Grosdent *et al.*, 2002). It was shown to dephosphorylate mostly proteins of the focal adhesion complex (Black & Bliska, 1997; Bliska *et al.*, 1991; Grosdent *et al.*, 2002; Guan & Dixon, 1990; Persson *et al.*, 1997). YopJ of *Y. pseudotuberculosis* and the *Y. enterocolitica* homolog YopP, seem to be particularly important in the defence against the adaptive immune system of the host (Viboud & Bliska, 2005). YopP/J are cysteine proteases inhibiting different signaling pathways in the host cell by binding to the mitogen-activated protein kinase (MAPK) kinases (MEKs), the inhibitor κB kinase β (IKKβ), and the counterregulators of the Toll-like receptor-4 triggered apoptotic pathway. These interactions lead to the inhibition of cytokine expression and the apoptotic cell death of macrophages and DCs (Erfurth *et al.*, 2004; Lemaitre *et al.*, 2006; Monack *et al.*, 1997; Mukherjee *et al.*, 2006; Zhang & Bliska, 2010; Zheng *et al.*, 2011).

YopM is a leucine-rich protein with no enzymatic activity (Viboud & Bliska, 2005). This protein appears to act like an adaptor protein, forming complexes with the ribosomal protein S6 kinase 1 (RSK1) and the protein kinase C-like 2 (PRK2) (McDonald *et al.*, 2003). YopM travels to the nucleus of the host cell and is essential for *Yersinia* to persist in the systemic organs liver and spleen by blocking the innate immune response. It was shown to downregulate proinflammatory cytokines, e.g. IL-1β, IL-12 or TNF-α and causes the depletion of NK cells (Kerschen *et al.*, 2004; Skrzypek *et al.*, 1998). YopK of *Y. pseudotuberculosis* and the *Y. enterocolitica* homolog YopQ seem to regulate the translocation pore size by affecting the pore-forming proteins YopB and YopD (Holmstrom *et al.*, 1997). Both proteins seem to influence the amount of delivered proteins, to prevent neutrophil death and further activation of inflammatory responses. The translocation of YopH, YopM and YopE appear to be most important for the protection of *Yersinia* against the immune response of the host (Kerschen *et al.*, 2004; Logsdon & Mecsas, 2003; Trülzsch *et al.*, 2004).

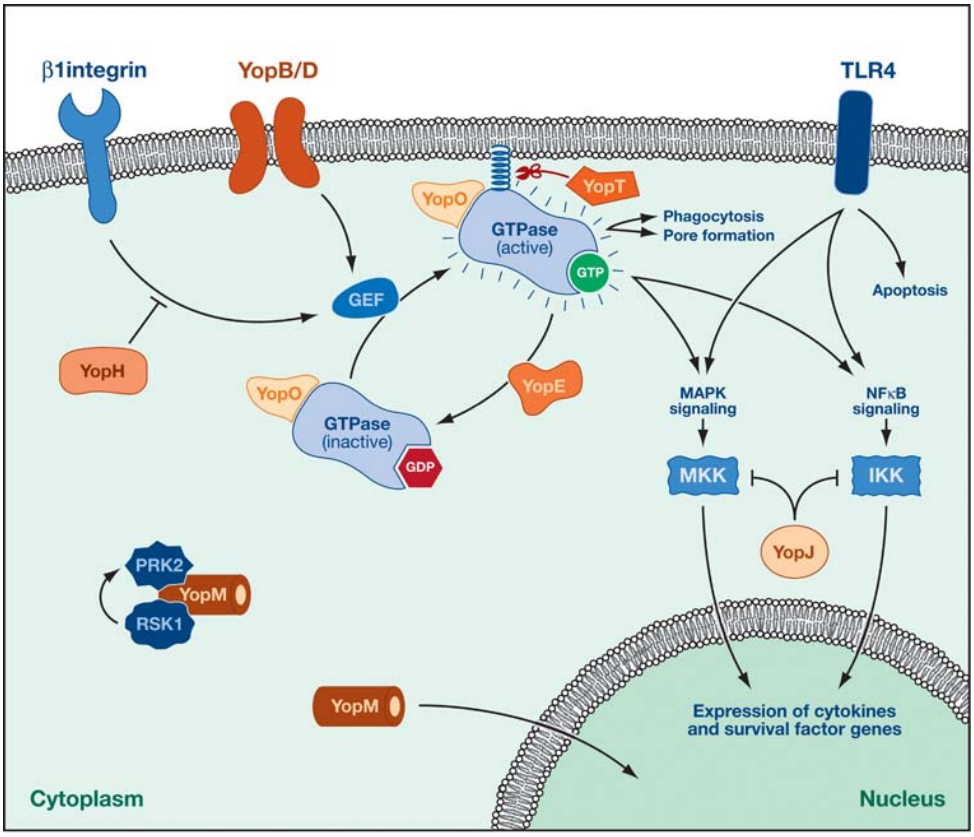

Figure 1.4.5: Overview of the different effector Yops and their influence in the host signaling pathways (Viboud & Bliska, 2005)**.**

Yop proteins are injected into the host cell by the T3SS. YopE, YopT, and YopA/O target and manipulate the small Rho-GTPases blocking mostly phagocytosis. YopJ/P inhibits the Toll-like receptor 4 (TLR4) signaling pathways and thereby inhibits inflammatory responses and induces apoptosis in macrophages. YopH blocks phagocytosis by immune cells. YopM is able to enter the nucleus, thus interfering in gene expression.

1.5 The actin cytoskeleton

The actin cytoskeleton is involved in many cellular functions like cell motility, cell adhesion or the cellular shape and polarity (Le Clainche & Carlier, 2008; Galletta & Cooper, 2009; Pollard & Borisy, 2003), but also in the defence against bacteria like in phagocytosis by macrophages or the migration of immune cells (Hoffmann & Schmidt, 2004).

The actin structure constantly rearranges, and this is achieved by fast polymerization and depolymerization of actin filaments. Thereby the actin alters between its monomeric form, the globular-actin (G-actin) and its multimeric form, the filamentous-actin (F-actin). G-actin is a 42 kDa protein forming tube-like structures (F-actin), consisting of two twisted strands (see Figure 1.5.1) (Winder & Ayscough, 2005).

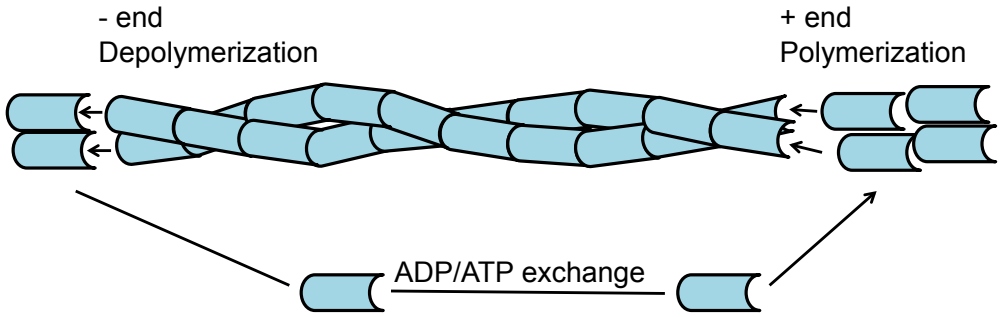

Figure 1.5.1: Actin polymerization and depolymerization dynamics.
G-actin (ATPase) polymerizes at the plus end of the F-actin. At the minus end, the ATPase is activated and cleaves the ATP in ADP+P, resulting in the dissociation of the G-actin from the filament. This dynamics lead to rearrangements of the actin cytoskeleton.

The G-actin is an ATPase and exists in two states, the ATP bound and the ADP bound state. If associated with ATP, it polymerizes at the plus end of the F-actin. At the minus end, the ATPase is activated and thereby the ATP is cleaved into ADP+P, which leads to the dissociation of the G-actin from the F-actin. This dynamic results in conformational changes of the actin cytoskeleton. Many signaling pathways and proteins are involved in the regulation of this process (Pollard & Borisy, 2003). Crucial are the small GTPases of the Rho-family (see 1.6). Many pathogenic bacteria are able to alter the actin cytoskeleton of the host cell by interacting with the dynamic to their advantage. This leads for example to the inhibition of their phagocytosis by macrophages, to the induction of their invasion by non-phagocytic cells or to the destruction of a barrier to reach the underlying tissue (Bhavsar *et al.*, 2007; Gouin *et al.*, 2005).

1.6 Small Rho-GTPases

The Rho-GTPases belong to the Ras super-family and are small monomeric G-proteins with a size of 21 - 25 kDa. The *rho* gene was discovered in 1985 and named after its homology to *ras*, Ras homolog (Madaule & Axel, 1985). The Rho-GTPases are very homologous among each other and show an amino acid sequence-identity of about 40 - 95% in their GTPase domain (Wennerberg & Der, 2004). Due to their differences in the sequence, the 23 so far known Rho-GTPases are categorized in six subfamilies, Rho, Rac, Cdc42, RhoBTB and RhoT/Miro (Bustelo *et al.*, 2007).

The Rho-GTPases are involved in many signaling pathways in the eukaryotic cell, like the regulation of the actin cytoskeleton, the gene expression, the cell cycle or the phagocytosis (Van Aelst & D'Souza-Schorey, 1997; Etienne-Manneville & Hall, 2002). The GTPases cycle from the active GTP-bound form to the inactive GDP-bound form is regulated and coordinated by three different protein classes (see Figure 1.6.1):

1. Guanine-nucleotide-exchange factors (GEFs): these factors are responsible for the exchange of the GDP against the GTP (Symons & Settleman, 2000).
2. GTPase-activation proteins (GAPs): these factors activate the GTPase, which leads to the hydrolysis of the bound GTP.
3. Guanine-nucleotice-dissociation inhibitors (GDIs): these factors lead to the stabilization of the GDP-bound inactive form in the cytosol (Van Aelst & D'Souza-Schorey, 1997; Nomanbhoy *et al.*, 1999).

The activation of the GTPases is triggered by extracellular signals like cytokines or by adhesion- or G-protein-associated receptors (Rossman *et al.*, 2005). They possess isoprenylated cysteins at their C-terminus, with which they are able to bind membrane-anchored lipids and subsequently interact with their effectors. In the inactive state, the Rho-GTPases are coupled with the GDIs at their isoprenylated cysteins (DerMardirossian *et al.*, 2004). Morphologically, the activation of the Rho-GTPases leads to the formation of different cell fibres: RhoA induces the formation of stress fibres, Rac1 of lamellipodia and Cdc42 of filopodia (see Figure 1.6.1) (Ahmadian *et al.*, 2002). Additionally, it was shown that Cdc42 leads to the activation of Rac, which in turn leads to the activation of Rho (Nobes & Hall, 1995). Thereby, the Rho-GTPases are affecting each others activity.

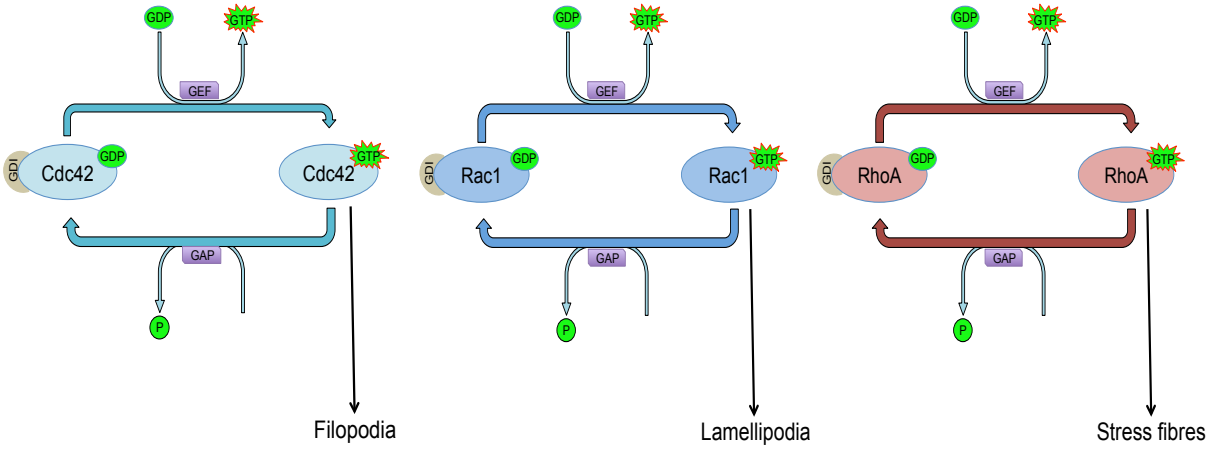

Figure 1.6.1: The GTPase cycle of Cdc42, Rac1 and RhoA and their influence on the actin cytoskeleton.
The activation of Cdc42, Rac1, and RhoA leads to the formation of filopodia, lamellipodia, and stress fibres, respectively. The GTPases cycle from the inactive form (GDP-associated) to the active form (GTP-associated). This transition is accomplished by the GEF proteins, which are exchanging the GDP against GTP. Upon activation of the GTPase by the GAP proteins, the GTP is cleaved in GDP+P, leading to an inactive state. This state is stabilized by the GDI proteins in the cytosol.

Many bacterial virulence factors are known to interact in the cycle of the most investigated GTPases, Rho, Rac and Cdc42 (Symons & Settleman, 2000). These factors help the bacterium for example to control the actin cytoskeletal rearrangements for their invasion process into the cell (Barbieri *et al.*, 2002). Enteric yersiniae are able to interfere in the Rho-GTPase cycles at different steps, e.g. *Y. pseudotuberculosis* is interfering in the cycle of Rac1 during the β_1-integrin induced phagocytosis (Alrutz *et al.*, 2001). Thereby the binding of InvA leads to a local activation of Rac1 (Del Pozo *et al.*, 2002; Wong & Isberg, 2005). In contrast, RhoA was observed to inhibit an InvA-induced bacterial invasion (Black & Bliska, 2000; Leeuwen *et al.*, 1997; Tosello-Trampont *et al.*, 2003). Thus, RhoA must be blocked to enable an efficient invasin-induced bacterial invasion by Rac1 activation (Wong *et al.*, 2006). However, InvA influences the GTPases indirectly by the activation of β_1-integrin signaling pathways, whereas most GTPase-interfering toxins act directly.

1.7 Bacterial toxins interacting with Rho-GTPases

Because of its diverse functions in bacterial defence, the actin cytoskeleton is a frequent target of bacterial toxins. Toxins modulating the actin cytoskeleton can be categorized into four groups, (1) toxins that covalently modify actin, (2) toxins that modulate the cytoskeleton as adenylate cyclases, (3) toxins that modulate the nucleotide state of the Rho-GTPases and (4) toxins that covalently modify GTPases (Barbieri *et al.*, 2002). The

third group is subdivided into two subgroups, the activators and inhibitors. The first two groups are directly influencing the actin cytoskeleton, whereas the toxins of group 3 and 4 are acting indirectly by interfering in the small Rho-GTPase cycle (Barbieri *et al.*, 2002; Boquet & Lemichez, 2003). Figure 1.7.1 shows a summary of different bacterial toxins and their mode of action with the Rho-GTPases.

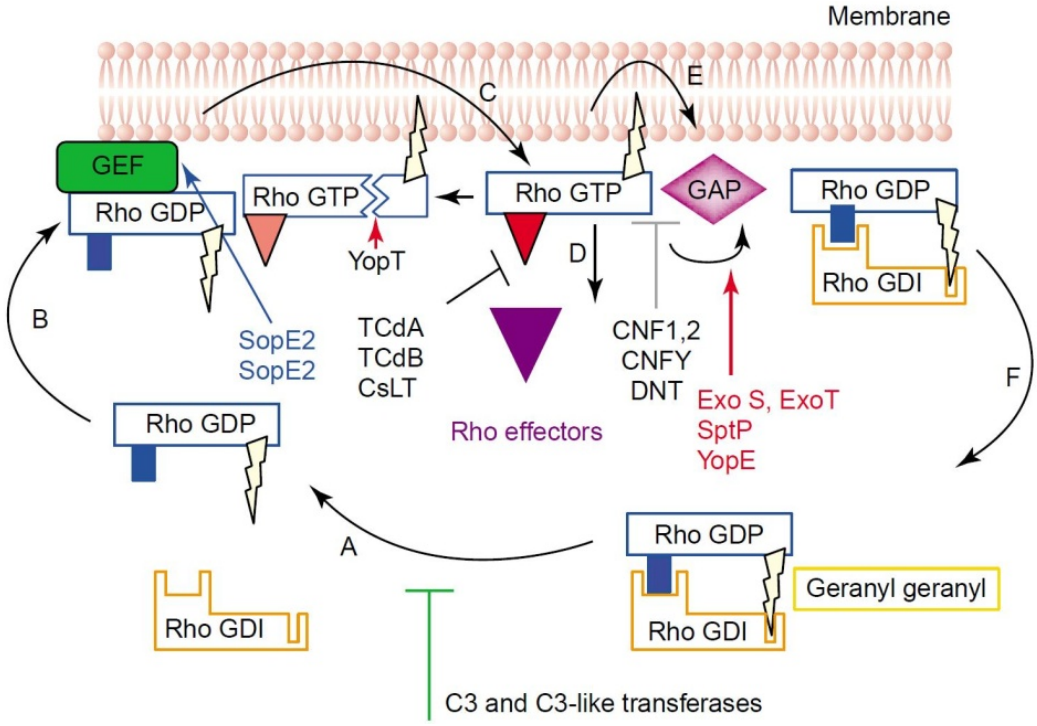

Figure 1.7.1: Different Rho-GTPase modifying toxins.
This scheme shows the regulating influence of the toxins in the different steps of the GTPase cycle. Included are the cytotoxic necrotizing factors of *E. coli* and *Y. pseudotuberculosis* (Boquet & Lemichez, 2003).

Bacterial toxins mostly lead to the inactivation of the Rho-GTPases by either covalently modifying the GTPase itself or by the imitation of GAP proteins, leading to a constitutive GTPase activity (Fiorentini *et al.*, 2003). Inactivating toxins are for example YopE of the enteric *Yersinia* species, which imitates Rho-GTPase inactivating Rho GAPs (Black & Bliska, 2000; Fu & Galan, 1999), YopT of *Y. pseudotuberculosis*, which lead to the dissociation of the GTPase from the membrane (Shao *et al.*, 2002) or the C3 toxin of *Clostridium botulinum*, which leads to an ADP-ribosylation of RhoA, B and C, thus inducing a strong interaction of the GTPase with the GDI. This in turn results in a blockage of the GTPase recruitment and subsequently to the inhibition of its activation (Aktories & Hall, 1989; Vogelsgesang *et al.*, 2007).

In comparison, only a small group of toxins lead to a constitutive or non-constitutive activation of the Rho-GTPases by inhibiting the GTPase activity or the GAPs. Activating toxins are for example the dermonecrotic toxin (DNT) of *Bordetella* (Masuda *et al.*, 2000) or the cytotoxic necrotizing factors (CNFs) of *Y. pseudotuberculosis* (Hoffmann *et al.*, 2004; Knust & Schmidt, 2010; Lockman *et al.*, 2002) or *E. coli* (Fiorentini *et al.*, 1997), which all lead to the constitutive activation of the Rho-GTPases (see 1.7.1).

1.7.1 Cytotoxic necrotizing factors

In 1984, the first CNF-producing *E. coli* strain was isolated from enteritis patients. The toxin caused dermonecrotic lesions and multinucleation plus enlargement of eukaryotic cells (Caprioli *et al.*, 1984). Three CNFs of *E. coli* (CNF_{1-3}) have been described so far, mostly produced by extraintestinal pathogenic strains. Additionally, a CNF beyond the species *E. coli* was identified in the *Y. pseudotuberculosis* wild-type strain YPIII (Lockman *et al.*, 2002).

These toxins were all shown to induce actin cytoskeletal rearrangements and multinucleation in different eukaryotic cells due to an inhibition of cytokinesis and ongoing cell cycle progression (Falzano *et al.*, 1993a; Huelsenbeck *et al.*, 2009). Furthermore, they possess the identical superior structure and consist of three functional domains: (1) the N-terminal host-cell binding domain, (2) the central translocation domain, and (3) the C-terminal catalysis domain (see Figure 1.7.3). Due to their structure, CNFs are categorized into the group of A-B toxins (Fabbri *et al.*, 1999; Fiorentini *et al.*, 1997).

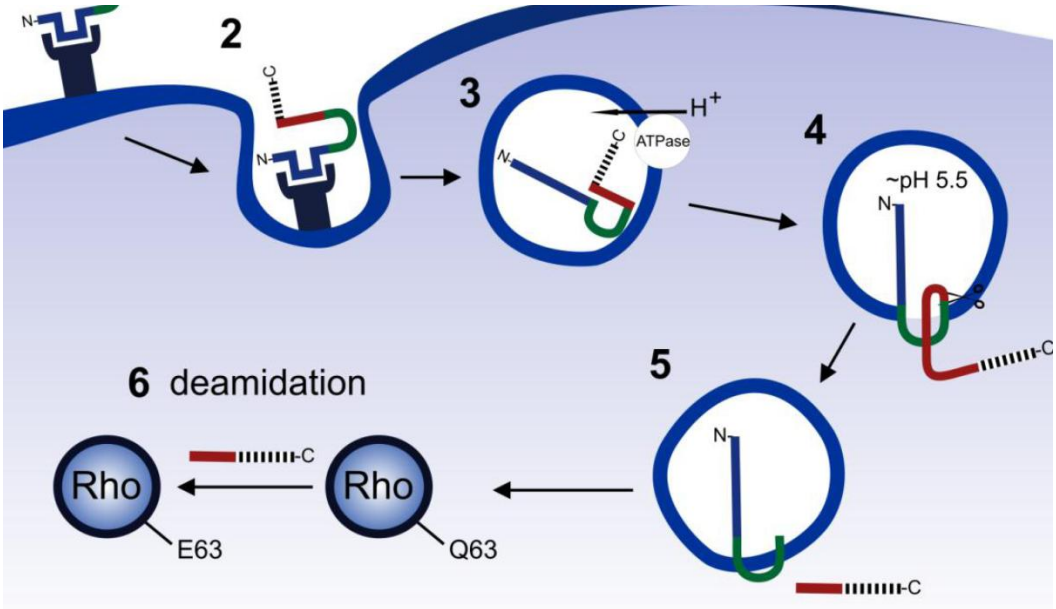

Figure 1.7.2: Receptor-mediated endocytosis of the CNFs into the eukaryotic cell.
The CNF binds to its receptor on the eukaryotic cell and is endocytosed into an endosome. The toxin containing endosome becomes acidic, leading to a conformational change of the CNF. Thereby, the translocation domain is integrated into the endosomal membrane, which leads to the cleavage and secretion of the catalytical domain into the cytosol. In there, this domain can deamidate the GTPases (Knust & Schmidt, 2010).

Bacterial A-B toxins follow the mechanism of the receptor-mediated endocytosis induced by the binding of the N-terminal domain. Two different processes and subsequent catalytic reactions of bacterial A-B toxins in eukaryotic cells can be distinguished: (1) The toxins evade the degradative pathway and reach the Golgi apparatus (Falnes & Sandvig, 2000) or (2) the toxin containing endosomes become acidic, induce a conformational change of the toxins, leading to the autocatalytical cleavage of the catalytic domain and its subsequent secretion into the cytosol (Fabbri *et al.*, 1999; Lemichez *et al.*, 1997). The CNFs use the second mechanism whereby the cleaved catalytic domain interacts with the Rho-GTPase (Contamin *et al.*, 2000; Knust & Schmidt, 2010) (see Figure 1.7.2).

The CNFs are toxins interfering with the Rho-GTPase cycle by a constitutive activation of Rho, Rac or Cdc42. This permanent activation is accomplished by the deamidation of a conserved glutamine (61/63) to glutamate in the catalytic center of the GTPase. Subsequently, the GAP catalyzed hydrolysis of the bound GTP is inhibited, leading to a permanent activated state of the GTPase (Rittinger *et al.*, 1997).

CNF_1 is the best characterized toxin of the CNF toxin family. It is a 108 kDa sized protein, mainly produced by uropathogenic *E. coli* strains (UPEC), which cause extraintestinal infections (Blanco *et al.*, 1992; Landraud *et al.*, 2000). Moreover, it could be detected in *E. coli* K1 strains, which cause neonatal meningitis (Bonacorsi *et al.*, 2000). CNF_1 leads to the constitutive activation of the Rho-GTPase subfamilies RhoA, Rac1, and Cdc42.

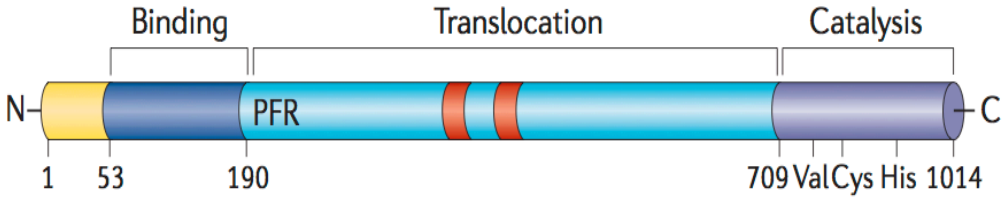

Figure 1.7.3: Structure of the cytotoxic necrotizing factor of *E. coli* CNF_1 (Aktories, 2011)**.**
The toxin belongs to the group of A-B toxins and consists of three domains, the binding, translocation and catalysis domain. With the binding domain, CNF_1 binds to its receptor on the eukaryotic cell and subsequently gets endocytosed. After a change of the pH, the translocation domain inserts into the endosomal membrane and leads to the secretion of the catalysis domain into the cytosol.

The *cnf1* gene is encoded on the chromosome on a pathogenicity island (Blum *et al.*, 1995) and is secreted and transfered to the host cell by outer membrane vesicles (OMVs) (Davis *et al.*, 2006; Kouokam *et al.*, 2006). The receptor-mediated endocytosis of CNF_1 seems to be independent of clathrin and lipid rafts (sphingolipid/cholestrol rich microdomains) (Blumenthal *et al.*, 2007; Contamin *et al.*, 2000), but it was shown that binding to the 67 kDa laminin receptor induces the internalization of CNF_1-expressing *E. coli* into human brain microvascular endothelial cells (HBMEC) (Kim *et al.*, 2005).

This toxin was demonstrated to induce the formation of actin stress fibres, filopodia and lamellipodia (Fiorentini *et al.*, 1997), caused by the 55 kDa catalytical domain, which is essential for the biological activity of CNF_1 (Schmidt *et al.*, 1998). The crystallized catalytical domain shows a unique fold with a β-sheet surrounded by α-helices and loops (Buetow *et al.*, 2001). Different functions for CNF_1 have been demonstrated, e.g. the induction of phagocytosis by non-phagocytic cells, the inhibition of phagocytosis by phagocytic cells (Falzano *et al.*, 1993b; Hofman *et al.*, 2000; Visvikis *et al.*, 2011) or the impairment of the barrier function of epithelial layers (Gerhard *et al.*, 1998; Hopkins *et al.*, 2003).

1.7.1.1 CNF_Y

Some *Y. pseudotuberculosis* strains of the serogroup O:3, e.g. the pathogenic isolate YPIII, have been shown to produce a CNF called CNF_Y (Lockman *et al.*, 2002). Due to mutations and deletions over the complete *cnfY* gene, the toxin is not expressed or inactive in many sequenced *Y. pseudotuberculosis* strains of the serogroup O:3 (Lockman *et al.*, 2002). This is also true for the *Y. pestis* strain CO92, which contains a sequence (Parkhill *et al.*, 2001) with 99% sequence-identity to *cnfY* of *Y. pseudotuberculsosis*. However, the gene in *Y. pestis* harbours a deletion at the C-terminus in the catalytical domain (see Figure 1.7.4) (Lockman *et al.*, 2002). So far no *Y. enterocolitica* strain was described to harbour the toxin gene in its genome.

The CNF_Y toxin is homolog to the CNF_1 toxin of *E. coli*, with a sequence-identitiy of around 65% over the whole gene (Lockman *et al.*, 2002). The *cnfY* gene is encoded on the chromosome of *Y. pseudotuberculosis* and flanked by a transposase and an oxidoreductase, indicating that the gene was acquired from another bacterium, like *E. coli*. The produced toxin has a size of about 115 kDa and leads to the formation of multinucleated giant HeLa cells, like its homolog CNF_1 (Lockman *et al.*, 2002).

However, CNF_Y seems to address a different receptor in comparison to CNF_1 as the preincubation of cells with inactive CNF_1 does not block CNF_Y activity completely (Blumenthal *et al.*, 2007). Moreover, antibodies against CNF_1, which prevented multinucleation by CNF_1 expressing *E. coli* lysates, could not prevent the CNF_Y activity in the eukaryotic cells (Lockman *et al.*, 2002). However, it was demonstrated that CNF_Y binds to heparan sulfate proteoglycan, a co-receptor of CNF_1 (Blumenthal *et al.*, 2007).

Subsequently, after binding to its receptor CNF_Y is taken up by receptor-mediated endocytosis into endosomes like CNF_1, as the internalization of the toxin is inhibited by blocking the acidification of the early endosome (Blumenthal *et al.*, 2007). In the cytosol of the eukaryotic cell, the catalytically active domain of CNF_Y functions similarly to the domain of CNF_1 as the three recombinantly purified GTPases RhoA, Rac1, and Cdc42 were also shown to serve as substrates for CNF_Y. Nevertheless, CNF_Y preferentially deamidates/activates RhoA over Rac or Cdc42 in human epithelial cells leading predominantly to the formation of actin stress fibres and of multinuclear giant cells (Hoffmann *et al.*, 2004).

So far, beyond elucidating the molecular mechanism of the toxin (primarily by intoxication of epithelial cells) in reference to its ability to activate the Rho-GTPase

RhoA, no further research has been performed on CNF_Y. However, different effects on the cells were attributed to the constitutively activation of RhoA by CNF_Y. For instance, it was demonstrated by incubating cells with CNF_Y that the RhoA activation is exclusively responsible for inhibition of cytokinesis (Huelsenbeck *et al.*, 2009), which was described before as a consequence of CNF intoxication (Falzano *et al.*, 1993a). Furthermore, CNF_Y was demonstrated to (1) decrease the endothelial barrier function (Baumer *et al.*, 2008), (2) to increase cell-matrix adhesion and subsequent cell spreading (May *et al.*, 2012), (3) to induce apoptosis in prostate cancer cells (Augspach *et al.*, 2013), and (4) to induce immunity of mice against a subsequent *Y. pseudotuberculosis* infection when applied subcutaneously (Mou *et al.*, 2012).

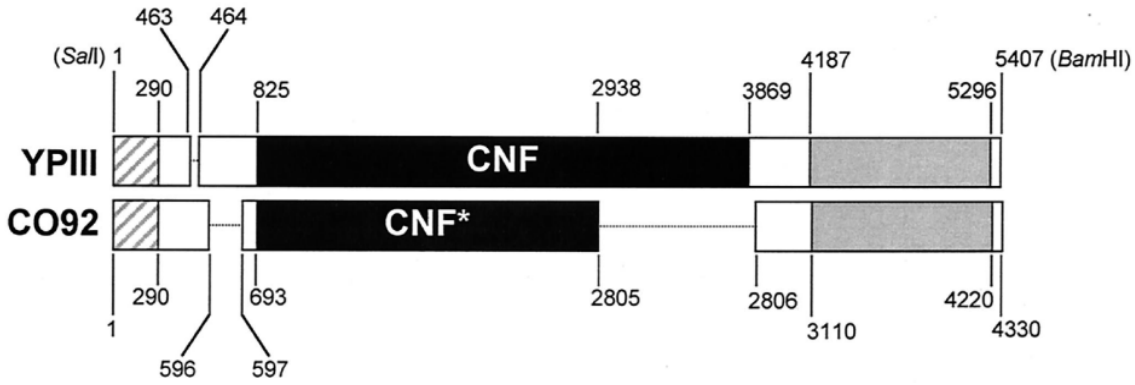

Figure 1.7.4: Comparison of the CNF_Y sequences of *Y. pseudotuberculosis* YPIII and *Y. pestis* CO92 (Lockman *et al.*, 2002)**.**

The dotted lines indicate deletions in the CNF_Y gene of *Y. pestis* CO92 and the boxes indicate sequences that show a sequence-identity of >99%. Left and right are indicated the putative transposase and the putative oxidoreductase, respectively.

1.8 Aim of this study

As mentioned above, the clinical isolate *Y. pseudotuberculosis* YPIII harbours the toxin gene *cnfY*, which has a sequence-identity to the *cnf1* of uropathogenic *E. coli* K1 strains of about 65% (Lockman *et al.*, 2002). Incubation of eukaryotic cells with CNFs results in a constitutive activation of the small Rho-GTPases Rho, Rac, and Cdc42, whereby CNF_Y predominantly activates RhoA (Flatau *et al.*, 1997; Hoffmann *et al.*, 2004). This activation leads to rearrangements of the actin cytoskeleton, and the formation of giant, multinucleated cells (Falzano *et al.*, 2006; Huelsenbeck *et al.*, 2009).

Previous studies focused on the molecular mechanism of the CNF_Y toxin were primarily focused on epithelial cells. However, little was known about the role of this toxin during pathogenesis of *Y. pseudotuberculosis* and the consequences of the constitutive activation of the Rho-GTPases in the infection process. Hence, the aim of this study was to investigate the molecular function of CNF_Y and its impact on the virulence of *Y. pseudotuberculosis*.

To address this aim, the expression conditions of *cnfY in vitro* as well as *in vivo* in the mouse model, the secretion conditions of CNF_Y, and the molecular function of CNF_Y regarding the activation of the Rho-GTPases and the influence on the morphology of intoxicated eukaryotic cells should be investigated. The main focus was on deciphering the role of CNF_Y during the infection process. For this purpose, the impact of CNF_Y on the bacterial colonization ability in the different tissues, the histology of the infected tissues, and the immune response should be assessed.

Additionally, the interplay and cooperation of CNF_Y with the T3SS and the Yop effector proteins *in vitro* and during the infection in mice should be examined. Moreover, it should be investigated whether CNF_Y plays an additional role in the host-pathogen interaction beside the amplification of crucial virulence factor functions. Furthermore, long-term effects on the immune system after infection with avirulent/low virulent *Y. pseudotuberculosis* mutant strains should be analyzed.

2 Material and methods

2.1 Material

2.1.1 Equipment and material

Equipment and material of the following companies were used: BD Biosciences, Biochrom, Biometra, Bio-Rad, Brand, Consort, Eppendorf, Gilson, Greiner, Heraeus, Heidolph, Hirschmann EM, Ibidi, Infors AG, Integra Biosciences, Janke & Kunkel IKA-Labortechnik, Laboport, Marienfeld, Millipore, Microflex Corporation, PeqLab, Roth, Sarstedt, Sartorius, Schott, Sigma Aldrich, Sorvall, TPP, Thermo Scientific, Oregon Scientific, VWR International, Whatman Schleicher & Schüll GmbH and Zeiss. Special equipment or materials used are mentioned in the text.

2.1.2 Chemicals and buffers

Chemicals and buffers of the following companies were used: Applichem, BD Biosciences, Biochrom, BioLegend, BioMoll, BioXCell, Difco, eBioscience, Fermentas, Fischer Scientific, Fluka, GIBCO, Invitrogen, Jackson ImmunoResearch, J.T. Baker, Life Technologies, Merck, Metabion, New England Biolabs Inc. (NEB), PAA, Pierce, Perkin Elmer, PeqLab, Promega, PromoCell, Qiagen, Roche, Roth, Sigma Aldrich, Serva, T. H. Geyer and Zeiss. Special chemicals used are mentioned in the text. If not noted otherwise all buffers and solutions were prepared with distilled water. Sterilization was accomplished by autoclaving for 20 min. at 121°C and 1 bar. Temperature sensitive substances were instead filtered using a pore size of 0.2 µm.

Table 2.1: Buffers and solutions

Buffer/solution	Chemicals and concentrations
3 x gel buffer	3 M Tris, 1 M HCl, 0.3% SDS
Acetate buffer	0.5 M NaCl, 0.1 M ammonium acetate; pH 4
Aceto-SDS solution	87.5% acetone, 0.25% SDS
Binding buffer J774A.1 & HEp-2	RPMI 1640 + GlutaMax-I + 0.4% BSA + 20 mM HEPES pH 7.0
Binding buffer RAW264.7	IMDM + 0.4% BSA + 20 mM HEPES pH 7.0
Coomassie staining solution	20% isopropanol, 10% acetic acid, 0.05% Coomassie^{TM} Brilliant Blue G250

Coupling buffer (antibody purification)	0.5 M NaCl, 0.1 M $NaHCO_3$; pH 8.3
Elution buffer 1	50 mM Tris-HCl, 100 mM NaCl, 150 mM imidazole
Elution buffer 2	50 mM Tris-HCl, 100 mM NaCl, 250 mM imidazole
Elution buffer (antibody purification)	0.2 M glycine, 0.15 M NaCl; pH 2.2
Erythrolysis buffer	7.8 mM NH_4Cl, 10 mM $KHCO_3$, 100 µM EDTA
FACS buffer	PBS + 0.2% BSA
Lysis buffer (protein purification)	50 m M Tris-HCl, 300 mM NaCl, 10 mM imidazole
Neutralizing buffer	0.5 M NaCl, 0.1 M Tris-HCl; pH 8
ONPG solution	4 mg/ml ONPG
PBS (10x)	80 g/l NaCl, 2 g/l KCl, 14.4 g/l Na_2HPO_4, 2.4 g/l KH_2PO_3; pH 7.4
SDS running buffer	33 mM Tris-HCl pH 8.3, 192 mM glycine, 0.1% SDS
SDS sample buffer	3 g/l Tris pH 8.3, 14.4 g/l glycine, 0.1% SDS
SDS running gel buffer	500 mM Tris-HCl, 4% SDS, pH 6.8
SDS stacking gel buffer	1.5 M Tris-HCl, 4% SDS, pH 8.8
TAE buffer (Tris-acetate-EDTA) (1x)	40 mM Tris-acetate, 2 mM EDTA, pH 8.0
TBST buffer	20 mM Tris-HCl pH 7.5, 150 mM NaCl, 0.05% Tween-20
TBSTB buffer	3% BSA in TBST
TBSTM buffer	5% skim milk powder in TBST
TFB1 buffer	30 mM potassium acetate, 10 mM $CaCl_2$, 50 mM $MnCl_2$, 100 mM RbCl, 15% glycerin, pH 5.8
TFB2 buffer	10 mM MOPS, 75 mM $CaCl_2$, 10 mM RbCl, 15% glycerin, pH 6.5
Transblot buffer	25 mM Tris, 192 mM glycine, 20% MetOH
Transformation buffer	272 mM sucrose, 15% glycerol, sterile filtrated
Washing buffer	50 mM Tris-HCl, 300 mM NaCl, 20 mM imidazole
Z-buffer	100 mM sodium phosphate buffer pH 7, 1 mM Mg_2SO_4

2.1.3 Media and supplements

Media used in this study are listed in Table 2.2. If not noted otherwise all media were prepared with distilled water. For selective media sterile antibiotics were added (see Table 2.3).

Table 2.2: Media

Media	Chemicals and concentrations
BHI broth (brain-heart infusion)	37 g/l BHI
CRMOX	40 g/l Tryptic Soy agar, 80 ml/l 0.25 M di-sodium oxalate, 80 ml/l 0.25 M magnesium chloride, 10 ml/l 20% galactose,5 ml/ congo red
Caco-2 medium	MEM + 10% FCS
DYT broth (Double Yeast Tryptone) complex medium (Miller, 1992)	10 g/l yeast extract, 5 g/l NaCl, 16 g/l tryptone
Freezing medium for eukaryotic cells	90% FCS + 10% DMSO
HEp-2 medium	RPMI 1640 + 1% GlutaMax-I + 7.5% NCS
J774A.1 medium	RPMI 1640 + 1% GlutaMax-I + 5% FCS
LB broth (Sambrook *et al.*, 1989)	5 g/l yeast extract, 5 g/l NaCl, 10 g/l tryptone
LB solid medium	LB-medium + 18 g/l agar
MMA (minimal medium A) (Sambrook *et al.*, 1989)	10.5 g/l K_2HPO_4, 4.5 g/l KH_2PO_4, 1 g/l $(NH_4)_2SO_4$, 0.5 g/l sodiumcitrate
Raw264.7 medium	Iscove Basal medium with stable glutamine (IMDM) + 10% FCS
SOC medium (super optimal broth) complex medium	5 g/l yeast extract, 0.5 g/l NaCl, 10 ml/l 1M $MgCl_2$, 20 g/l tryptone, 2.5 ml/l 1M KCl, 10 ml/l $MgSO_4$
Yersinia medium	*Yersinia* selective agar base and *Yersinia* selective supplement (Oxoid)

Table 2.3: Supplements and inhibitors

Supplement/inhibitor & function	End concentration	Concentration stock solution & manufacturer
Carbenicillin (antibiotic)	100 µg/ml	100 mg/ml in H_2O (Roth)
Chloramphenicol (antibiotic)	30 µg/ml	30 mg/ml in 70% EtOH (Roth)

CNF_Y (cytotoxic necrotizing factor of YPIII)	1 - 25 nM	1 - 5 mg/ml (this study)
CT04 (C3 Transferase; Rho Inhibitor I)	0.5 - 1 µg/ml	0.1 µg/µl (Cytoskeleton)
Cytochalasin-D (inhibitor)	5 µg/ml	5 mg/ml in DMSO (Sigma)
FCS (fetal calf serum; growth factor)	10%- 5%	100% (Biochrom)
Gentamycin (antibiotic)	50 µg/ml	50 mg/ml (Sigma)
HEPES (buffer)	10 mM	1 M (Biochrom)
Kanamycin (antibiotic)	50 µg/ml	50 mg/ml in H_2O (Merck)
NCS (newborn calf serum; growth factor)	7.5%	100%
Probenecid (inhibitor)	1.5 mM	150 mM (Sigma)
TcdBF (Toxin B serotype F; Rac1/2/3 inhibitor)	85 - 250 ng/ml	850 µg/ml (H. Genth, Institute for Toxicology, Medical School Hannover)

2.1.4 Enzymes and antibodies

Enzymes used in this study are listed in Table 2.4 and were applied with the provided buffers. Antibodies used for western blotting or flow cytometry are listed in Table 2.5.

Table 2.4: Enzymes

Manufacturer	Enzyme
Bioline	Mango*Taq*™ DNA polymerase
Finnzymes	Phusion® High-Fidelity DNA Polymerase
NEB	Antarctic phosphatase Benzonase LongAmp *Taq* DNA polymerase Restriction enzymes *Taq* DNA polymerase T_4-DNA ligase
Sigma Aldrich	Trypsin-EDTA Cytochalasin-D
Qiagen	RNaseA

Table 2.5: Antibodies

Manufacturer	Antibody (dilution and buffer)
Antibodies for western blotting	
Ake Forsberg	Anti-Yop all (TBSTB)
Cell Signaling	Anti-Cdc42 (1:1,000 in TBSTB)
	Anti-mouse-HRP (1:5,000 in TBSTB/TBSTM)
	Anti-Pan-Actin (1:1,000 in TBSTB)
	Anti-rabbiT HRP (1:5,000 in TBSTB/TBSTM)
	Anti-Rac1/2/3 (1:1,000 in TBSTB)
	Anti-RhoA (1:1,000 in TBSTB)
David's Biotechnology	Anti-CNF_Y (1:1,000 in TBSTB)
Sigma	Anti-polyHistidin (1:2,000 in TBSTM)
Antibodies for Flow Cytometry*	
BD Biosciences	Anti-CD3-Biotin
	Anti-CD3-PE
	Anti-Ly6G-PE-Cy7
	Streptavidin-FITC
BioLegend	Anti-CD11c-PE-Cy7
	Anti-CD19-FITC
	Anti-CD25-APC
	Anti-CD49b-Biotin
	Anti-Ly6C-APC
BioXCell	Anti-mouse CD16/CD32
eBioscience	Anti-CD3-APC
	Anti-CD3-PE-Cy7
	Anti-CD4-PerCP-Cy5.5
	Anti-CD4-APC-eF780
	Anti-CD8-eFluor450
	Anti-CD335-PerCP-Cy5.5 (NKp46)
	Anti-CD11b-Pacific Blue
	Anti-CD11c-APC

	Anti-CD19-Biotin Anti-CD45R-PerCP-Cy5.5 (B220) Anti-CD11c-APCeFluor780 Anti-F4/80-PE Anti-Gr1-A700 Anti-NKp46-PE Streptavidin-PerCP-Cy5.5

*all antibodies were titrated for optimal staining conditions

2.1.5 Commercial kits

In Table 2.6 are listed all kits used in this study. Kits were employed according to the manufacturer's protocol, unless differently stated.

Table 2.6: Commercial kits

Manufacturer	Kit	Application
Cell Biolabs	Cdc42 and Rac Activation Assay	Pull down of active Rac and Cdc42 GTPases
Invitrogen	Live/dead Fixable Blue Dead Cell Stain Kit	Live/dead staining of cells for flow cytometry analysis, UV excitation
Life Technologies	LiveBLAzer-FRET B/G Loading Kit	Yop delivery assay
Millipore	Rho Activation Assay Kit MILLIPLEX MAP Mouse Cytokine/Chemokine Magnetic Bead Panel - Premixed 32 Plex - Immunology Multiplex Assay Kit	Pull down of active Rho GTPases Measurement of cytokine level
Perkin Elmer	Western Lightning ECL II Kit	Detection of HRP conjugated secondary antibodies (western blot)
Pierce	Coomassie (Bradford) Protein Assay Kit	Detection and quantification of total protein amount

Qiagen	QIAquickTM Gel Extraction Kit	Gel extraction of PCR products and plasmids
	QIAquick^{TM} PCR Purification Kit	Purification of PCR products
	QIAprep^{TM} Spin Miniprep Kit	Isolation and purification of plasmids

2.1.6 Oligonucleotides and plasmids

2.1.7 Oligonucleotides

Metabion performed the synthesis of all used oligonucleotides (see Table 2.7). Each primer stock solution was 100 µM and was diluted for PCR reactions to 10 µM. Underlined nucleotides mark integrated restriction sites or overlapping regions as indicated. Plasmids used in this study are listed in Table 2.8.

Table 2.7: Oligonucleotides

Name	Sequence 5' - 3'	Description
I661	GTGTAGGCTGGAGCTGCTTC	sense for synthesis of *kan*-cassette of pKD3/4
I662	CATATGAATATCCTCCTTAGTTCC	anti-sense for synthesis of *kan*-cassette of pKD3/4
I984	TAAGAAACCATTATTATCATGAC	sequencing primer for pFU vector system, binds in P1-site
I987	TCTAGGGCGGCGGATTTG	sequencing primer for pFU vector system, binds in P2-site
II306	GCACTGGATCCTAGTATCTGGAATAGACAACGAAAG	sense for 5'UTR of *yopE*
II371	CGGACTAGTGATGGGCAAATTGAAGCAC	sense for upstream region of *lcrQ*
II372	CGGGCATGCGCCCACTGGTAATGCAGG	anti-sense for downstream region of *lcrQ*
II794	GGGGCTAGCATGAAAAATCAATGGCAA	sense for CNF_Y overexpression (*NheI*)
II795	GGGCTCGAGTTAAAAGTCTTTTTGTAA	anti-sense for CNF_Y overexpression (*XhoI*)
II894	ACATAATGTATTCTAATAAAAACATTC	sense for *cnf*$_Y$ sequencing

II895	TAAATGATAATTTTGGTTTTACTGGTG	anti-sense for cnf_Y sequencing
II896	GGGGGGGATCCTATTGACAAACAAAATGAAGCAAGATAG	sense for promoterregion of *cnfY* (*BamHI*)
II898	GGGGGGTCGACTTAGCCATTGATTTTTCATAAACACTCC	anti-sense for promoterregion of *cnfY* (*SalI*)
III710	CCGGGGAGCTCGACAAACAAAATGAAGCAAGATAGTTTTACATG	sense for *cnfY* mutagenesis, upstream region (*SacI*)
III711	CCGGGGAGCTCTTTTTGGCGATGCCACCTACCC	sense 900 bp upstream of *cnfY* (*SacI*)
III712	CCGGGGAGCTCATTTTCTGGCGGGGTGTGACCA	anti-sense for *cnfY* mutagenesis, downstream region (*SacI*)
III713	CCGGGGAGCTCCTACGCCATGTTTCCGAAACCCAG	anti-sense 1000 bp downstream of *cnfY* (*SacI*)
III714	GGAACTAAGGAGGATATTCATATGTAATGTTTTACAAAAAGACTTTTAAATCTTAAGTCTC	sense for *cnfY* mutagenesis (downstream region) with homologous *kan* region
III715	GAAGCAGCTCCAGCCTACACAAACACTCCTTTTATTGACGATGCACAATG	anti-sense for *cnfY* mutagenesis (upstream region) with homologous *kan* region
III727	CCGGGGGATCCATGAAAAATCAATGGCAACATCAATATTT	test for *cnfY* loss
III680	TCTCCACCCAAGCGGCCG	anti-sense *kan* region, testing for genomic integration
III681	CGATTCGCAGCGCATCGC	sense *kan* region, testing for genomic integration
IV16	GGGGGGCGGCCGCTTAAAAGTCTTTTTGTAAAAC	anti-sense for *cnfY* complementation (*NotI*)
IV48	GTAAAGATGAATATGAATTCTCTATTGATGC	sense sequencing *cnfY*
IV49	CCTCAAGCGCAATTTTTATACC	anti-sense sequencing *cnfY*
IV474	CCCCCGCGGCCGCTTAGTGGTGATGGTGATGATGAAAGTCTTTTTTGTAAAA CATTAAACAC	anti-sense for C-terminal His tag of *cnfY* (*NotI*)

V439	AGACAGCGGCCGCTCAGCTAC TTAGCATGCTGAGTAAACTTGG TCTGACAGT	anti-sense test for TEM integration
V553	CCGGGGAGCTCAGATGGGTTT TAATATATCTTGACTGAAT	sense for *yopE* mutagenesis, upstream region (*SacI*)
V554	GAAGCAGCTCCAGCCTACACTT CTCCTACGCTGCTAGATCC	anti-sense for *yopE* mutagenesis (upstream region) with homologous *kan* region
V555	GGAACTAAGGAGGATATTCATA TGTATTGATAAAAACAAGGGGA TAGTGTT	sense for *yopE* mutagenesis (downstream region) with homologous *kan* region
V556	CCGGGGAGCTCAATGTACCTG TGAGCCATCG	Anti-sense for *yopE* mutagenesis, downstream region (*SacI*)
V557	CACCGGTCGCAGGATCAA	sense 1000 bp upstream of *yopE*
V558	TCTGTTGAGCATTCCACACT	anti-sense 1000 bp downstream of *yopE*

Table 2.8: Plasmids

Plasmid	Characteristics	Source/reference
pAKH3	pGO704, *sacB*$^{+}$, Amp^{R}	(Nagel *et al.*, 2001)
pCP20	pSC101$_{ts}$, *flp*, Amp^{R}, Cm^{R}	(Datsenko & Wanner, 2000)
pET28a	T7 promoter based expression vector, Kan^{R}	Novagen
pFU54	promoterless *luxCDABE*, pSC101* ori, Amp^{R}	(Uliczka *et al.*, 2011)
pFU58	promoterless *gfpmut3.1*, pSC101* ori, Amp^{R}	(Uliczka *et al.*, 2011)
pFU68	promoterless *lacZ*, pSC101* ori, Amp^{R}	(Uliczka *et al.*, 2011)
pFU166	*gapA-luxCDABE*, colE1 ori, Amp^{R}	(Uliczka *et al.*, 2011)
pFU228	*gapA-dsRed2*, colE1 ori, Cm^{R}	(Uliczka *et al.*, 2011)
pFU234	*ifp*$^{+}$, pSC101* ori, Kan^{R}	(Uliczka *et al.*, 2011)
pKD3/4	Kanamycin cassette template, Kan^{R}	(Datsenko & Wanner, 2000)

pSR47s-E-TEM2	YopE-TEM1; Kan^R	(Harmon *et al.*, 2010)
pJNS01	pET28a, *cnfY*, Kan^R	(Schweer *et al.*, 2013), this study
pJNS02	P_{cnfY}-*luxCDABE*, pSC101* ori, Amp^R	(Schweer *et al.*, 2013)
pJNS03	P_{cnfY}-*gfpmut3.1*, pSC101* ori, Amp^R	(Schweer *et al.*, 2013), this study
pJNS04	P_{cnfY}-*lacZ*, pSC101* ori, Amp^R	(Schweer *et al.*, 2013)
pJNS05	pAKH3, *cnfY*::kan^R, $sacB^+$, Amp^R	(Schweer *et al.*, 2013), this study
pJNS09	pFU234, Amp^R	(Schweer *et al.*, 2013), this study
pJNS10	pJNS09, $cnfY^+$, pSC101* ori, Amp^R	(Schweer *et al.*, 2013), this study
pJNS11	pJNS09, pSC101* ori, Amp^R	(Schweer *et al.*, 2013), this study
pJNS12	pJNS09, $cnfY^+$, C-terminal 6xHis, pSC101* ori, Amp^R	(Schweer *et al.*, 2013), this study
pJNS13	pAKH3, *yopE*::kan^R, $sacB^+$, Amp^R	(Schweer *et al.*, 2013), this study

2.1.8 Bacterial strains and cell lines

All bacterial strains and eukaryotic cell lines used in this study are listed in Table 2.9 and Table 2.10, respectively.

Table 2.9: Bacterial strains

Bacterial strain	Description	Reference
Escherichia coli K-12		
DH10β	F^- *endA1 recA1 galE15 galK16 nupG rpsL* Δ*lacX74* Φ80*lacZ*ΔM15 *araD139*Δ*(ara,leu)7697 mcrA* Δ*(mrr-hsdRMS-mcrBC)*λ^-	(Casadaban & Cohen, 1980)
BL21 λDE3	F^- *ompT gal dcm lon hsdSB(rB2 mB2) gal* λDE3	(Studier & Moffatt, 1986)
CC118 λ*pir*	F^- Δ(*ara-leu*)7697 Δ(*lacZ*)74 Δ(*phoA*)20 *araD139 galE galK thi rpsE rpoB* $arfE^{am}$ *recA1*	(Manoil & Beckwith, 1986)

S17-1 λ*pir*	*recA thi pro hsdR*$^{-}$*M*$^{+}$*(*RP4-2 Tc::Mu-Km::Tn*7), λpir*	(Simon *et al.*, 1983)
Yersinia pseudotuberculosis		
YPIII	pIB1, wild-type	(Bolin *et al.*, 1982)
YP12	pIB1^{-}	(Bolin *et al.*, 1982)
YP101	YPIII Δ*yscS*	(Schweer *et al.*, 2013), Steinmann
YP147	pIB1, Δ*cnfY*, Kan^{R}	(Schweer *et al.*, 2013), this study
YP149	YPIII *phoPQ*^{IP32953}	(Schweer *et al.*, 2013)
YP150	YP147, pIB1^{-}	This study
YP173	YPIII ETEM, amino acids 1 to 100 of YopE+TEM1	(Schweer *et al.*, 2013)
YP174	YPIII Δ*yscS* ETEM, amino acids 1 to 100 of YopE+TEM1	(Schweer *et al.*, 2013)
YP188	YP149 Δ*cnfY*, Kan^{R}	(Schweer *et al.*, 2013), this study
YP216	YP147, Kan^{S}	This study
YP217	YP147 ETEM, amino acids 1 to 100 of YopE+TEM1	(Schweer *et al.*, 2013), this study
YP275	pIB1, Δ*yopE*, Kan^{R}	(Schweer *et al.*, 2013), this study
YP298	YP101, Δ*cnfY*, Kan^{R}	This study

Table 2.10: Cell lines

Cell line	Description	Reference
Caco-2	Human colonic Adenocarcinoma cell line	(Fogh & Trempe, 1975)
HEp-2	Human Larynx carcinoma cell line	(Toolan, 1954)
J774A.1	Murine monocytes/macrophages cell line	(Ralph & Nakoinz, 1975)
RAW 264.7	Murine macrophages leukemia cell line	(Ralph & Nakoinz, 1977)

2.1.9 Software and databases

Software applied in this study was Graph Pad PRISM 5.0 (Graphpad Software, Inc.), FlowJo (Tree Star Inc.), and FACSDiva™ (BD Bioscience). Databases used in this study were the National Center for Biotechnology Information (NCBI; www.ncbi.nlm.gov), and uniprot (www.uniprot.de).

2.2 Methods

All microbiological, molecular, biochemical and cell biological methods used in this study are listed in the following passages. Used materials are summarized in chapter 2.1 or either mentioned in the text.

2.2.1 Microbiological methods

2.2.1.1 Sterilization

Sterilization of solutions and media was accomplished by autoclaving for 20 min at 121°C and 1 bar. Temperature sensitive substances were filtered, using a filter pore size of 0.2 µm (Filtropure S 0.2, Sarstedt). Glassware was dry heat sterilized at 180°C. Heat labile equipment and workbenches were disinfected with 70% ethanol or 7% Pursept®.

2.2.1.2 Growth conditions

Y. pseudotuberculosis was cultured under aerobic conditions at 25°C, whereas cultures of *E. coli* were incubated at 37°C if not noted otherwise. Cultivation took place either on agar plates (Heraeus incubator) or in liquid culture (Infors incubation shaker) at 200 rpm in test tubes or Erlenmeyer flasks. Supplements, if required for the experiment, are listed in Table 2.3. If not noted otherwise, bacteria were grown in LB broth or on LB agar plates. Specially used media were: *Yersinia*-agar plates, BHI, SOC, DYT, MMA and RPMI.

2.2.1.3 Determination of cell density

The cell density of bacterial cultures was measured via the optical density (OD_{600}) at 600 nm wavelength with a spectrophotometer (Ultraspec 3100 pro, Ambersham Biosciences). A bacterial culture with an OD_{600} of 1 correlates with a cell density of approx. 1 x 10^9 bacteria/ml (Sambrook *et al.*, 1989). Reference for the measurement was the corresponding growth medium.

2.2.1.4 Storage of bacteria

For short- or middle-term storage periods the bacteria were grown on agar plates and stored at 4°C. Long-term storage was accomplished in the corresponding culture medium with 30% glycerol at -80°C. Therefore, overnight grown bacteria (1.25 ml) were mixed with 0.75 ml of 80% sterile glycerol.

2.2.1.5 Curing of the virulence plasmid of *Y. pseudotuberculosis*

To remove the virulence plasmid pIB1 from *Y. pseudotuberculosis* strains, the curing method of Riley & Toma (1989) was used. The method is based on the detection of the virulence associated calcium-dependency and Congo-red absorption of the pIB1 carrying *Yersinia*. Therefore, the bacteria were grown on CRMOX plates for 24 h at 37°C to built up selection pressure on the plasmid-cured bacteria (pIB1$^-$). Bacteria colonies without the plasmid appeared bright and big, whereas bacteria still carrying the plasmid formed small red colonies. To verify the loss, bacteria were tested by colony-PCR against a plasmid-encoded gene.

2.2.1.6 Yop secretion assay

The Yop secretion assay was performed as described previously (Cornelis *et al.*, 1987). Bacteria were grown overnight at 25°C in LB medium, diluted 1:50 in fresh LB medium and grown at 25°C to an OD_{600} of about 0.4 - 0.5. The cultures were shifted to 37°C for 3 - 4 h in the absence or presence of 20 mM Mg^{2+} and 20 mM sodiumoxalate, a Ca^{2+} chelator. The OD_{600} of the different strains was adjusted to the strain with the lowest OD_{600} (18 ml). After harvesting the bacteria by a centrifugation step (10 min, 4°C, 27,000 x g), the supernatant was sterilized with a 0.2 µm filter. To precipitate the proteins of the supernatant, 2 ml of 100% trichloroacetic acid (TCA) were added and incubated for 30 min on ice. The denatured proteins were harvested by centrifugation (10 min, 4°C, 27,000 x g). After discarding the supernatant, the pellet was resuspended in 2 ml Aceto-SDS and incubated for 20 min on ice. Subsequently, the mixture was centrifuged (10 min, 4°C, 27,000 x g) and the pellet washed with 500 µl aceton. After another centrifugation step (10 min, 4°C, 27,000 x g) the pellet was dried and resuspended in 50 µl 3 x SDS sample buffer. The samples were boiled for 5 min at 95°C, separated on 12% SDS polyacrylamide gels and visualized by Coomassie brilliant blue staining (see 2.2.4.4).

2.2.2 Cell biological methods

2.2.2.1 Cultivation and passage of eukaryotic cells

The cultivation conditions of eukaryotic cells were 37°C with 5% CO_2 in a cell incubator. The cells, if not noted otherwise, were cultured in 75 cm^2 cell culture flasks with 20 ml medium and passaged every 2 - 3 days.

2.2.2.1.1 Cultivation and passage of HEp-2 and Caco-2 cells

Cultivation of the human epithelial cell line HEp-2 was performed in RPMI medium supplemented with 7.5% NCS. Caco-2 cells were cultured in DMEM medium supplemented with 10% FCS and 10 mM HEPES. To detach the adherent cells off the culture flask bottom, the cells were washed once with 5 - 10 ml PBS and subsequently treated with 2 ml trypsin-EDTA for 5 min at 37°C. The trypsin reaction was stopped by addition of 5 x the volume of culture medium. After resuspension, the cells were diluted 1:10 with fresh medium and transferred into a new flask.

2.2.2.1.2 Cultivation and passage of J774A.1 and RAW264.7

The adherent murine macrophage cell lines J774A.1 and Raw264.7 were cultured in RPMI or IMDM (respectively) and both supplemented with 10% FCS. For the passage, cells were washed once with PBS and scraped off the bottom of the culture flask. After resuspending the cells in 10 ml fresh culture medium, cells were diluted 1:20 with medium and transferred into fresh flasks.

2.2.2.2 Determination of cell count

For the determination of the cell amount per ml cell suspension, cells were diluted 1:10 in trypan-blue to exclude the dead cells from the count. Trypan-blue is not able to penetrate the cytoplasmic membrane, hence the dye invades selectively dead cells, which appear blue under the light microscope. The average cell number of 4 squares of a Neubauer counting chamber was determined and multiplied by 10^4. Calculation took account of used dilutions prior to cell counting.

2.2.2.3 Freezing and thawing of eukaryotic cells

For freezing/storage, eukaryotic cells were cultured in 75 cm^2 cell culture flasks to a subconfluent level. Cells were detached from the surface as described in 2.2.2.1.1 and 2.2.2.1.2. After centrifugation (5 min, 25°C, 172 x g), the pellet was resuspended in 1 ml freezing medium and transferred into cryotubes. Subsequently, the cells were cooled down slowly to -80°C and long-term stored in liquid nitrogen at -170°C.

For thawing, the cryotubes were incubated shortly at 37°C and afterwords the cells were taken up in 9 ml fresh medium followed by centrifugation (5 min, 25°C, 172 x g). After resuspending the pellet in 20 ml fresh culture medium, the cells were transferred into a 75 cm^2 cell culture flask and cultivated at 37°C with 5% CO_2.

2.2.2.4 Incubation of eukaryotic cells with CNF_Y

The incubation of eukaryotic cells with CNF_Y took place in the respective culture medium (concentration 1, 10 or 25 nM). For this purpose, cells were seeded one day prior to toxin treatment and washed once with PBS before addition of CNF_Y. Incubation took place for 30 min - 24 h in a cell incubator.

2.2.2.5 Multinucleation assay

The multinucleation assay is based on the ability of CNF_Y to interfere in the cell cycle of the eukaryotic cell, leading to the formation of multinucleated giant cells. Hence, multinucleation assays were performed to determine the activity or in case of a Δ*cnfY* mutant strain, the loss of CNF_Y. In order to test this, eukaryotic cells were incubated over 48 h with lysates of whole bacterial cell extracts and visualized afterwards.

To prepare bacteria lysates, different *Yersinia* strains were grown at 37°C overnight in BHI medium to get a high CNF_Y expression. After measuring the OD_{600} of the cultures the OD_{600} were adjusted to the strain with the lowest cell density to 50 ml. Bacteria were harvested by a centrifugation step (10 min, 4°C, 27,000 x g) and subsequently the pellet resuspended in 5 ml PBS containing 1 tablet Mini, EDTA-free Protease Inhibitor Cocktail (Roche) per 10 ml and 100 µg/ml gentamycin. Cells were lyzed using a French press (Thermo Scientific) and 18,000 psi pressure. After another centrifugation step (60 min, 4°C, 27,000 x g) the supernatant was sterilized using a filter with a pore size of 0.2 µm. The lysates were diluted 1:10, 1:50, 1:250 and 1:1,250 with culture medium and given onto the cells for 48 h. After the incubation, the actin cytoskeleton and nuclei were stained (2.2.2.6).

2.2.2.6 Visualization of the actin cytoskeleton

The actin cytoskeleton was stained to determine the impact of CNF_Y on the polymerization dynamic after different incubation times. For this purpose, cells were treated with FITC conjugated phalloidin.

Therefore, cells were seeded one day prior to treatment with a density of 1.7 x 10^4 cells/well in a microslide 8 well plate (ibidi). Cells were washed once with PBS and treated for 24 h with recombinant CNF_Y or 48 h with bacteria lysate. After incubation, the cells were washed three times with PBS and fixed with 4% Paraformaldehyde (PFA) for 10 min at room temperature. Subsequently, the cells were washed three times with PBS (each time 5 min) and permealized using 0.1% Triton X-100 (in PBS) for 5 min at room temperature. After the following washing steps (3 x 5 min), cells were stained for 1 - 3 h at room temperature in the dark, using Phalloidin-FITC (0.5 µg/ml in PBS). Cells were then washed (3 x 5 min) and the nuclei stained with DAPI (1 µg/ml in 1 x TBST) for 3 min at room temperature in the dark. After 3 additional washing steps (3 x 5 min), the cells were visualized using a fluorescence microscope (Axiovert II with Axiocam HR, Zeiss, Germany) and the AxioVision program (Zeiss, Germany) or stored at 4°C in the dark.

2.2.2.7 Rho/Rac/Cdc42 activation assay

To determine whether there is a concentration dependency of CNF_Y or an impact of YopE on the activation of the three small Rho-GTPases, RhoA, Rac1 and Cdc42 activation assays were carried out. To test the activation of Rac1 and Cdc42 a Rac1/Cdc42 Activation Assay Combo Kit of Cell Biolabs was used, whereas the activation of RhoA was tested using the Rho Activation Assay Kit 17-294 of Millipore, following the manufacturer instructions.

For the assays, the murine macrophage cell lines J774A.1 or RAW264.7 or the human epithelial cell line HEp-2 were seeded two days prior to treatment on 1 well plates (Fischer Scientific) with a concentration of 2 x 10^6 cells/well. At least 20 h before toxin treatment, cells were washed once in PBS and further incubated in starving medium (without FCS).

For evaluating activation levels' dependency on CNF_Y, cells were washed once with PBS and incubated with different concentrations of the recombinant CNF_Y toxin (1 nM, 10 nM, and 25 nM) for 3 h at 37°C in starving medium.

To test the impact of YopE on the activation of the three Rho-GTPases, the murine macrophages RAW264.7 were infected after toxin treatment (25 nM) with either YPIII (wild-type) or YP275 (Δ*yopE*). To this purpose, yersiniae were grown overnight at 37°C, washed once with PBS and adjusted to an OD_{600} of 1. For infection, the cells were washed once with PBS and the bacteria, diluted in the starving medium to an MOI of 100, were given onto the cells. Infection took place for 20 min at 37°C.

The activation assay is based on the use of Rhotekin RBD or PAK PBD agarose beads. When active (GTP-bound form), RhoA is specifically binding to the Rho-binding domain (RBD) of Rhotekin, whereas active Rac1 and Cdc42 specifically bind to the p21-binding domain (PBD) of the p21-activated protein kinase (PAK) to control downstream signaling cascades. Figure 2.2.1 scematically shows the principle of the Rac1/Cdc42 Activation Assay Combo Kit. The experiment was carried out according to the manufacturers protocols as shortly described below.

Cells were lyzed using the supplemented buffer of the kits. Subsequently protein loading controls were taken and the remaining lysates were incubated with Rhotekin RBD or PAK PBD agarose beads to isolate the active forms of RhoA, Rac1 or Cdc42. Isolated active forms of the GTPases and protein loading controls were then loaded onto SDS-PAGE and detected with specific antibodies via western blot (2.2.4.5).

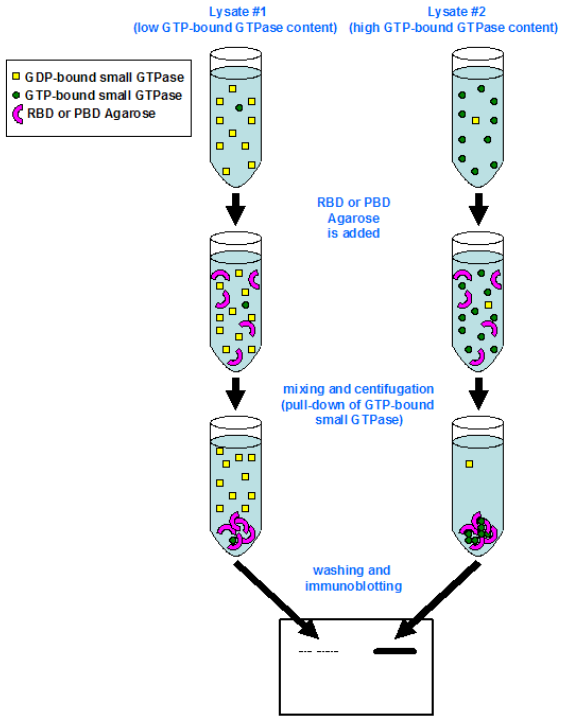

Figure 2.2.1: Principle of the Rho GTPase activation assay.
RhoA/Rac1/Cdc42 Activation Assay Combo Kit (Cell Biolabs, San Diego, CA, USA).

2.2.2.8 TEER (Trans Epithelial Electrical Resistance) measurement

To test a possible influence of the toxin CNF_Y on the intestinal epithelial cell monolyer, the transwell system of Corning Life Sciences was used. Therefore, the Transwell® (see Figure 2.2.2) with 3.0 µm Pore Polycarbonate Membrane Insert was moisted at least 1 h before seeding of the cells. In order to do this, 800 µl medium was given to the basolateral side and 100 µl to the apical side of the insert.

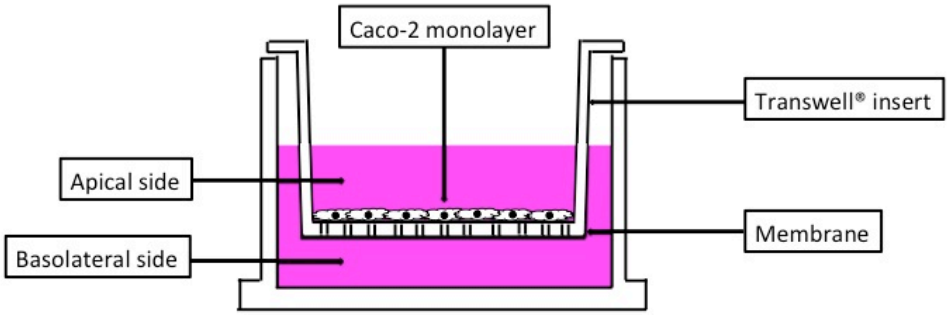

Figure 2.2.2: Scheme of the Transwell® culture chamber.

The Caco-2 cells were seeded apical (2.2.2.1.1 & 2.2.2.2) with a concentration of 1,5 x 10^5 cells/insert in 100 µl (in total 200 µl). A change of the medium (apical & basolateral) was performed every second day. The cells were seeded 21 - 29 days before the treatment to ensure the formation of a confluent monolayer. In order to test the confluency, the TEER was measured repeatedly with an epithelial Voltohmmeter (World Precision Instruments Inc.).

The Caco-2 monolayer was treated basolateral with the recombinant toxin or apically infected with *Yersinia* strains. For the toxin treatment, CNF_Y (10 nM) was given to the basolateral side of the membrane in fresh medium. The TEER was measured before treatment and subsequently every second hour. For the infection, bacteria were grown overnight at 25°C and adjusted to an OD_{600} of 0.5. Approximately 1 x 10^6 bacteria/well were given apical onto the monolayer in binding buffer. The TEER was measured before infection and was subsequently determined every hour.

2.2.2.9 Yop delivery assay *in vitro*

The Yop delivery assay was carried out to detect differences in the Yop translocation pattern into eukaryotic cells due to CNF_Y activity. The Yop delivery was measured with three different techniques (see below). Visualization and quantification of Yop translocated cells were carried out with the LiveBLAzer-FRET B/G Loading Kit from Life Technologies (Bla-reporter assay), whereas the detection of the translocated Yop proteins in the cells was carried out with antibodies against the proteins.

The general principle of the *bla*-reporter assay is based on the translocation of β-lactamase fusion proteins into the eukaryotic cell (see Figure 2.2.3). In this study, a *yopE-bla* fusion construct was used which is translocated with the T3SS. Hence, eukaryotic cells were infected with different *Y. pseudotuberculosis* strains harbouring the gene for the fusion-protein. After an infection/translocation period of 1 h, the cells were stained with the dye CCF4-AM. The dye gets trapped due to the activity of esterases in the living cells, which appear green fluorescent after excitation with 409 nm wavelength. If the fusion-protein is translocated, the β-lactamase is able to cleave the dye, leading to blue fluorescent cells after excitation with 409 nm wavelength.

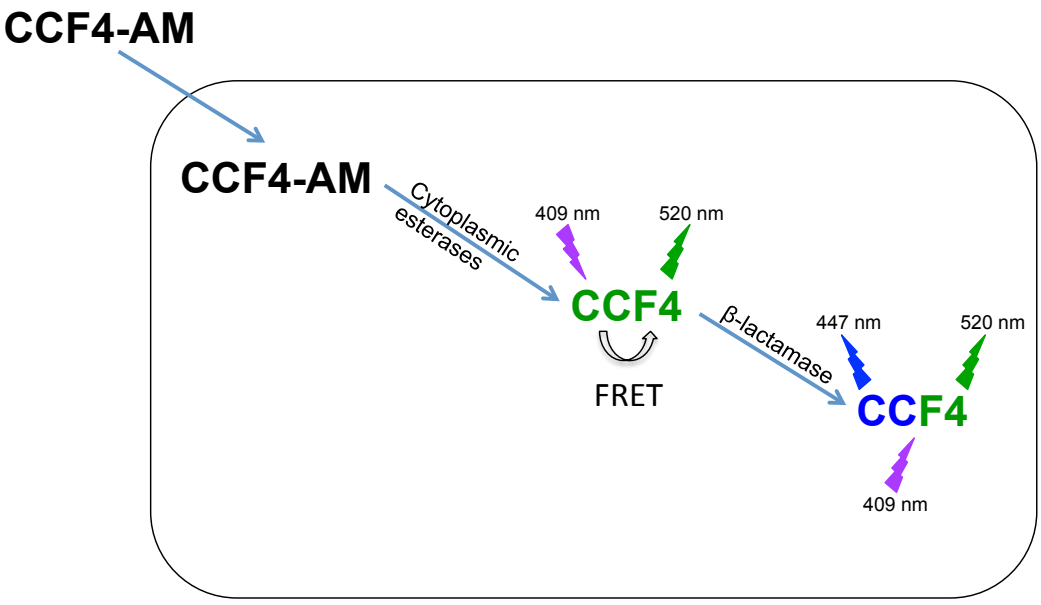

Figure 2.2.3: Principle of the *bla*-reporter assay.
The dye CCF4-AM is trapped in the cell by cytoplasmic esterases. After excitation with 409 nm wavelength, all living cells appear green fluorescent. All cells with translocated β-lactamase (YopE- β-lactamase in this study) appear blue fluorescent due to the cleavage of the dye.

2.2.2.9.1 Microscopy of Yop delivery

The microscopic Yop delivery assay was performed as described previously (Marketon *et al.*, 2005). Therefore, 5 x 10^4 cells/well (µ-slide, ibidi) of HEp-2, Caco-2, RAW264.7 or J774A.1 cells were seeded one day prior to infection.

At the day of infection, the cells were washed once with PBS and pretreated with 25 nM of the recombinant CNF_Y (3 µg/ml), exoenzyme C3 transferase from *Clostridium botulinum* (CT04, Cytoskeleton. Inc) (0.5 µg/ml, 1 µg/ml), *Clostridium difficile* toxin TcdBF (85 ng/ml, 250 ng/ml) (Huelsenbeck *et al.*, 2007a) or the same amount of PBS in serum free medium for 2 - 3 h at 37°C.

For infection, overnight cultures of the strains YPIII, YP173, YP174 or YP217 were washed once with PBS and adjusted to an OD_{600} of 1. The infection dose was at MOI of 10 and was carried out for 1 h at 37°C. To facilitate the interaction between eukaryotic cells and bacteria, the yersiniae were centrifuged onto the cells (5 min, RT, 172 x g). After infection the cells were washed three times and dyed with CCF4-AM using the LiveBLAzer-FRET B/G Loading Kit from Life Technologies for 90 min at RT, according to the manufacturers protocol. The Yop translocation was visualized with a fluorescence microscope (Axiovert II with Axiocam HR, Zeiss, Germany), using the AxioVision program (Zeiss, Germany).

2.2.2.9.2 Flow cytometry of Yop delivery

To determine a possible influence of CNF_Y on the Yop delivery rate into *Y. pseudotuberculosis* infected eukaryotic cells, a Yop delivery assay with subsequent flow cytometry analysis was performed. Hence, eukaryotic cells were infected with *Y. pseudotuberculosis* strains harbouring a *yopE-bla* fusion.

For quantification of the amount of cells translocated with the yop proteins, infected and stained cells were acquired with a LSR Fortessa cell analyzer (BD Bioscience). Therefore, 1 x 10^6 HEp-2 or J774A.1 cells/well (6-well plate, TPP) were seeded one day prior to infection.

At the day of infection, the cells were washed once with PBS and preincubated with the toxin CNF_Y (25 nM/ 3 µg/ml) or an equal amount of PBS for 3 h at 37°C. For infection, overnight cultures (37°C) of the strains YPIII, YP173, YP174 or YP217 were washed once with PBS and adjusted to an OD_{600} of 1. The infection dose was an MOI of 10 and was carried out in binding buffer for 1 h at 37°C. To facilitate the interaction between

eukaryotic cells and bacteria, the yersiniae were centrifuged onto the cells (5 min, RT, 172 x g). Subsequently, the cells were washed once with PBS and detached from the cell culture plate. Therefore, HEp-2 cells were treated with 500 µl trypsin-EDTA for 5 min. The reaction was stopped by the addition of 4.5 ml medium containing 7.5% NCS. J774A.1 macrophages were detached by scraping the cells off the tissue culture plate. After detachement, the cells were resuspended in 1 ml medium and centrifuged for 5 min at 400 x g. The supernatant was removed completely and the cell pellet resuspended in 200 µl of the CCF4-AM staining solution (according to the manufacturers protocol) and transfered into a non-coated 96-well microtiter plate. Throughout the staining period (90 min), the cells were shaken with a microplate shaker (PMS-1000, Grant bio) at 400 rpm. Subsequently, the cells were transferred into Matrix™ Blank and Alphanumeric Storage Tubes (Thermo Scientific) and acquired with the flow cytometer. Acquired data were then analyzed with FlowJo software (Treestar).

2.2.2.9.3 Western blot of Yop delivery

To compare the translocated Yop proteins in the eukaryotic cells after infection with YPIII (wt) or the *yopE* mutant strain (YP275), a specific antibody against all Yop proteins was used for western blot analysis. Therefore, 2 x 10^5 RAW264.7 cells/well were seeded one day prior to infection onto 24-well tissue culture plates.

At the day of infection, the cells were washed once with PBS and incubated with 25 nM recombinant CNF_Y or the equal amount of PBS for 3 h at 37°C. For infection, overnight cultures (37°C) of YPIII, YP275 and YP101 were washed once with PBS and adjusted to an OD_{600} of 1. The eukaryotic cells were infected with an MOI of 100 in binding buffer. To facilitate the interaction between eukaryotic cells and bacteria, the *Yersinia* were centrifuged onto the cells (5 min, RT, 172 x g). One hour post infection (37°C), the cells were washed twice with PBS and incubated for another hour with gentamycin containing binding buffer (50 µg/ml). After elimination of the extracellular bacteria, the cells were washed three times with PBS and resuspended in 100 µl 3 x SDS sample buffer. The lyzed cells were heated for 5 min at 95°C and 10 µl loaded onto a 12% SDS polyacrylamide gel. After separation on the gel, proteins were blotted onto a nitrocellulose membrane and the intracellular Yops were visualized with an antiserum directed against all secreted Yops (α-all Yop) (see 2.2.4.5). Subsequently, the membrane was stripped and reprobed with a pan-actin antibody as loading control.

2.2.3 Molecular biological methods

2.2.3.1 Measuring of DNA concentration

The measurement of the DNA concentration and purity was performed photometric with a NanoDrop spectrophotometer (PeqLab), using the optical density of the solution (OD_{260}, OD_{280}). Here, an OD_{260} of 1 corresponds to a dsDNA concentration of 50 µg/ml. To eliminate potential impurities, the ratio of OD_{260} to OD_{280} was calculated. A value of 1.8 represents a solution with high purity, whereas DNA solutions contaminated with proteins possess significant lower OD_{260}/OD_{280} values.

2.2.3.2 Polymerase chain reaction (PCR)

The PCR was used to amplify specific DNA fragments with heat stable DNA polymerases (e.g. *Taq*) and was carried out after Innis & Gelfand (1990). The annealing temperature is dependent on the used oligonucleotides (length, sequence) and was calculated (see Suggs *et al.*, 1981) and tested by a gradient PCR. The elongation time and temperature are dependent on the used polymerase and the size of the DNA fragment, which needs to be amplified.

Because of its proof reading activity, the Phusion® High-Fidelity DNA polymerase was mainly used to amplify DNA. The screening of positive clones was accomplished by the Mango*Taq*™ polymerase, which contains a coloured loading dye for gel electrophoresis. The LongAmp® *Taq* DNA polymerase was preferentially used to amplify long DNA fragments. PCR reaction compounds were mixed according to the manufacturers protocol in 20 - 25 µl aliquots. Fragments were amplified in a T3000 Thermocycler (PeqLab), an Eppendorf Master cycler or an Eppendorf gradient cycler.

2.2.3.3 Agarose gel electrophoresis

The agarose gel electrophoresis is used for separation of DNA fragments according to their molecular weights and was carried out in horizontal electrophoresis chambers after Sambrook *et al.* (1989). The agarose gels contained 0.8 - 2% agarose, which was heated in 1 x TAE buffer. The same buffer was used as running buffer in the chamber. DNA samples were mixed with 6 x loading dye, applied onto the gel and seperated electrophoretically at 90 - 110 V for 45 - 60 min. Using ethidiumbromide, the DNA was stained for 10 - 20 min, detected with UV light, and documented with the camera of the

gel documentation system (Gel Doc^{TM}, Bio-Rad). Molecular weigths were detected on the basis of the DNA size standard *Gene Ruler DNA Ladder Mix* (see Figure 2.2.4).

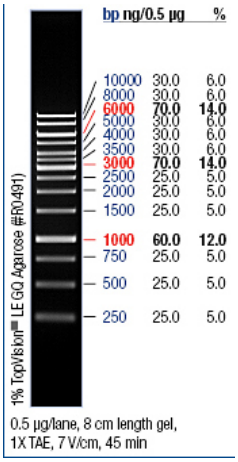

Figure 2.2.4: Gene Ruler DNA Ladder Mix (Thermo Scientific).

2.2.3.4 Plasmid DNA isolation

5 - 7 ml LB medium supplemented with antibiotics were inoculated with solid colonies of *E. coli* and incubated with agitation overnight at 37°C. The plasmid isolation was performed with the „*QIAprep®Spin Miniprep Kit*" (QIAGEN) according to the manufacturers protocol. Isolated plasmids were eluted with 50 µl H_2O_{dest}.

2.2.3.5 Genomic DNA isolation

For preparation of genomic DNA of *Yersinia*, bacteria were grown overnight at 25°C. 200 µl of the culture was mixed with 200 µl phenol/chloroform and centrifuged for 2 min (14,000 x g). The supernatant was transfered into a new tube and the DNA precipitated with 4 volumes of 100% ethanol. After centrifugation for 20 min (14,000 x g), the DNA was washed twice in 70% ethanol and the dried pellet resuspended in EB buffer. The concentration of the precipated genomic DNA was determined and adjusted to 100 ng/µl. The DNA was stored at 4°C and used for DNA amplification.

2.2.3.6 DNA extraction

For the isolation of DNA fragments out of agarose gels, the „*MinElute Gel Extraction Kit*" (QIAGEN) was used. The band was cut out of the gel under UV light and eluted according to the manufacturers protocol. The DNA was eluted in 50 µl H_2O_{dest}.

2.2.3.7 Purification of PCR fragments

For purification of PCR fragments, the „*QiAquick PCR Purification Kit*" (QIAGEN) was used. The purification was carried out according to the manufacturers protocol and for elution of the fragments 50 µl H_2O_{dest} was used.

2.2.3.8 Restriction digestion of DNA

For the restriction of plasmid DNA or PCR products, different restriction enzymes were used. These endonucleases possess the feature to target dsDNA at specific recognition sites. This reaction normally leads to the formation of „sticky ends", needed for the insertion of DNA fragments, which were treated with the same enzymes. The digestion was done according to the manufacturers protocol (New England Biolabs) with the appropriate buffer and if necessary 1 - 10 units of the enzymes were used depending on the reaction mix. The restriction took place for 3 - 12 h at 37°C. Heat inactivation was performed for 20 min at 65°C, when suitable. Subsequently, the digested DNA was loaded and extracted of an agarose gel.

2.2.3.9 Dephosphorylation

To prevent religation of the digested plasmid, the DNA fragments were treated with the antarctic phosphatase prior to ligation. In this reaction the 5' end of the restriction site is dephosphorylated with 1 - 3 µl of the phosphatase in the reaction mix for 1 h at 37°C.

2.2.3.10 Ligation

A ligation is used to insertion a DNA fragment into a plasmid. Hence both the fragment and the plasmid were digested with the same restriction endonucleases. Ligation was proceeded according to manufacturers protocol with 1 - 3 µl T_4-DNA-ligase and the appropriate buffer for 3 h at room temperature or overnight at 4°C in the dark. The ligase is catalyzing the formation of phosphodiester bonds.

2.2.3.11 DNA sequencing

Sequencing of constructed plasmids or PCR products was performed by the Department of Genome Analysis at the Helmholtz Centre for Infection Research.

2.2.3.12 Construction of plasmids

2.2.3.12.1 Construction of CNF_Y overexpressing plasmid

For the overexpression and purification of the toxin CNF_Y, the plasmid pJNS01 (*cnfY*$_{his6}$) was constructed. Therefore, the gene *cnfY* (*ypk_2615*) from the genomic DNA of *Y. pseudotuberculosis* YPIII was cloned into the commercial vector pET28a (Novagen). The gene *cnfY* was amplified with the primers II794/II795 and integrated into the *Xho*I/*Nhe*I sites of pET28a (see Table 2.8), which harbours a His tag sited at the N-terminus of *cnfY*. Clones were selected on LB agar plates containing kanamycin and tested by sequencing and test restriction digest (for general cloning procedure see chapters above).

2.2.3.12.2 Construction of mutagenesis plasmids

To achieve the genomic replacement of specific genes, mutagenesis plasmids were constructed. For the construction of the plasmid pJNS05 (containing *cnfY*::Kan^R mutation) and the plasmid pJNS13 (containing *yopE*::Kan^R), first the kanamycin resistance gene was amplified, using the *kan* primers (I661/I662) and plasmid pACYC177 as template. Next, *Y. pseudotuberculosis* YPIII genomic DNA or virulence plasmid DNA was used as a template to amplify 500-bp regions flanking the target gene *cnfY* or *yopE* up- and down- stream. The upstream fragment of *cnfY* or *yopE* was amplified using the primers III710/715 or V553/V554, respectively. The reverse primers contained 20 nucleotides at the 5'-end, which are homologous to the start of the kanamycin resistance gene. The downstream fragment of *cnfY* or *yopE* was amplified with the primers III712/III714 or V555/V556, respectively. The forward primers contained 20 nucleotides at the 3'-end, which are homologous to the end of the kanamycin resistance gene.

A fusion-PCR reaction was performed with the corresponding forward primer and the reverse primer using the upstream and downstream PCR products of the target genes and the kanamycin gene fragment as templates. The fragments were digested using *Sac*I and cloned into the suicide vector pAKH3. The transformants were selected on LB agar plates containing kanamycin and tested by sequencing and tesT restriction (for general cloning procedure see chapters above).

2.2.3.12.3 Construction of reporter gene fusion plasmids

For the construction of the *cnfY* promoter fusion with *gfpmut3.1*, the DNA upstream of *cnfY* (525 bp) was amplified from the genomic DNA of *Y. pseudotuberculosis* YPIII with the primers II896/II898. The fragment was integrated into the *BamHI/SalI* restriction site of pFU58. The transformants (pJNS03) were selected on LB agar plates supplemented with carbenicilin and tested by sequencing and restriction (for general cloning procedure see chapters above).

2.2.3.12.4 Others

For the complementation of the strain YP147 (Δ*cnfY*), the plasmid pJNS10 was constructed. This plasmid contains the *cnfY* gene under control of its own promoter.

For the construction, the vector pFU234 of the pFU series (Uliczka *et al.*, 2011) was used. First, the antibiotic resistance cassette was exchanged from kanamycin to carbenicilin, using the restriction sites *XhoI* and *SacI* to obtain the vector pJNS09. Next, a PCR fragment was amplified (P_{cnfY}-*cnfY*) with the primers II896/IV16 from the chromosomal DNA of *Y. pseudotuberculosis* YPIII. The fragment was integrated into the *BamHI/NotI* sites of pJNS09. The transformants were selected on LB agar plates containing carbenicilin. To confirm the positive clones, the inserted fragment was sequenced and restricted. As a control for the complementation experiments a vector containg only the ori SC101* and the antibiotic resistance cassette was constructed. Hence, the vector pJNS09 was restricted with the enzyme *AatII* and religated to obtain the plasmid pJNS11.

For easy western blot detection of the CNF_Y toxin without an appropriate antibody against CNF_Y, the *cnfY* gene with a C-terminal His tag was constructed. Therefore, the fragment P_{cnfY}-$cnfY_{his6}$ was amplified from the chromosomal DNA of *Y. pseudotuberculosis* YPIII using the primers II896/IV474 and integrated into the *BamHI/NotI* of pJNS09. The transformants were selected on LB agar plates containing carbenicillin. To confirm the positive clones, the inserted fragment was sequenced and restricted (for general cloning procedure see chapters above).

2.2.3.13 Construction of mutant strains

Different mutant strains were generated to identify functions of the deleted genes. For the construction procedure of the mutagenesis plasmids see 2.2.3.12.2. Mutants were genereated by homologous recombination as described previously (Nagel *et al.*, 2001).

For construction of the mutant strains YP147, YP188 and YP298, the plasmid pJNS05 was integrated via conjugation into the *cnfY* locus of YPIII, YP147 and YP101, respectively. The mutant strain YP275 was generated using the plasmid pJNS13. Chromosomal integration of the fragments was selected by plating on *Yersinia* agar plates supplemented with kanamycin and carbenicillin. Excision of the plasmid including the *cnfY* or *yopE* allele was obtained by plating of the strain on 10% sucrose and was analyzed by PCR and DNA sequencing. To verify the deletion of *cnfY* or *yopE*, different PCR reactions were carried out, using the primer pairs II371/II372, III711/III713, III727/II895, III711/III680 and III713/III681 for Δ*cnfY* and V557/V558, V553/III680 and V556/III681 for Δ*yopE*. To further test a new constructed Δ*cnfY* mutant, a multinucleation assay (2.2.2.5) and/or a western blot (2.2.4.5) against CNF_Y were performed. To further test the Δ*yopE* mutant, a western blot (2.2.4.5) against all Yop proteins was performed.

The strain YP217 was constructed by chromosomal integration of the YopE-β-lactamase (ETEM) fusion plasmid pSR47s-E-TEM1 into the *yopE* locus. Because the plasmid pSR47s-E-TEM1 also harbours a kanamycin resistance cassette, the resistance cassette of the YP147 strain needed to be removed first. In order to do so, the vector pCP20 was transformed electricallay into the strain. The transformants were inoculated in BHI medium and grown overnight at 37°C to remove the *kan* gene. At the next day, the overnight culture was diluted 1:10 in BHI and incubated for 1 h at 42°C to remove the remaining vector. Subsequently, the bacteria were plated on LB agar plates. The clones were tested for growth on kanamycin and carbenicillin. The bacteria not able to grow on the two antibiotics formed the mutant YP216. The following integration of *yopE-TEM1* was obtained through conjugation of *E. coli* K-12 strain S17λpir pSR47s-E-TEM1 with the *Y. pseudotuberculosis* strain as described previously (Harmon *et al.*, 2010). To verify the mutant a PCR was carried out with the primers V439/II306.

To obtain the mutant strain YP150, the YP147 was cured of the virulence plasmid pYV (see 2.2.1.5). The mutant was verified by PCR using the primers II371/II372.

For construction of the other mutant strains used in this study, see Schweer *et al.*, 2013.

2.2.3.14 Production of electrocompetent *Yersinia*

For the production of electrocompetent *Yersinia*, 20 ml BHI medium were inoculated 1:50 with an overnight culture and grown at 25°C to exponential growth phase (OD_{600} 0.5 - 0.8). After centrifugation for 15 min at 4°C (2,755 x g), the bacteria pellet was

resuspended in 2 ml ice-cold H_2O_{dest} and subsequently centrifuged for 2 min at 4°C (7,500 x g). The bacteria were resuspended in 2 ml ice-cold transformation buffer, centrifuged for 2 min at 4°C (7,500 x g), resuspended in 120 µl transformation buffer, and directly used for transformation (2.2.3.16).

2.2.3.15 Production of chemocompetent *E. coli*

Chemocompetent *E. coli* were produced using the rubidium chloride method. Hence, 200 ml LB medium were inoculated 1:100 with an overnight culture and supplemented with 4 ml $MgSO_4$ (20 mM). The culture was grown at 37°C to exponential growth phase (OD_{600} 0.5 - 0.8). Subsequently, the cells were centrifuged for 8 min at 4°C (2,755 x g) and the pellet resuspended in 80 ml TFB1 buffer. The suspension was incubated for 10 min on ice and centrifuged again for 8 min at 4°C (2,755 x g). Next, the pellet was resuspended in 8 ml ice-cold TFB2 buffer. After an incubation period of 45 min on ice, 100 µl aliquots of bacteria were transferred into tubes and stored at -40°C.

2.2.3.16 Electro transformation in *Yersinia*

For transformation of plasmid DNA in *Yersinia*, 40 µl electrocompetent cells were mixed wit 2 - 6 µl plasmid-DNA and transfered into a cold 2 mm cuvette (PeqLab). The electroporation was accomplished at 2.5 kV, 25 µF and 200 W with an elctroporator (GenePulser II, Bio-Rad). The bacteria were immediately taken up in 1 ml SOC medium without antibiotic for phenotypic expression (2 h, 25°C, 550 rpm). Next, the bacteria were grown on LB agar plates supplemented with antibiotics for selection of transformants for two days at 25°C.

2.2.3.17 Chemical transformation in *E. coli*

For the chemical transformation of plasmid DNA in *E. coli*, 100 µl aliquots of competent cells were thawed on ice and subsequently mixed with 1 - 15 µl plasmid-DNA or a ligation mix. After an incubation period of 30 min on ice, a heat shock at 42°C for 2 min and an incubation for 2 min at 4°C on ice, the bacteria were diluted in 500 µl LB medium. The cells were incubated at 37°C for 60 min at 550 rpm for phenotypic expression. The selection of the transformants was accomplished on LB agar plates supplemented with antibiotics.

2.2.4 Biochemical methods

2.2.4.1 Preparation of whole cell extracts

For the preparation of whole cell extracts, the OD_{600} was measured to calculate the correct buffer amount (see below) and 1 ml of the bacterial culture centrifuged for 5 min at 14,000 x g. The pellet was resuspended in 3 x SDS sample buffer (150 µl = OD_{600} 3) and heated at 95°C for 5 min. Subsequently, the samples were treated with 0.2 µl benzonase (5 - 5.8 U) for 1 h at 37°C and loaded onto a SDS polyacrylamid gel or stored at -20°C.

2.2.4.2 Protein precipitation (TCA)

To precipitate the proteins of the supernatant of a bacterial culture, TCA was used for denaturation. Therefore, the *Yersinia* were grown 3 h, 7 h or overnight at 37°C or 25°C and subsequently the OD_{600} was determined and adjusted to 45 ml with an OD_{600} of 1. After harvesting the bacteria by a centrifugation step (10 min, 4°C, 27,000 x g), the supernatant was sterilized with a 0.2 µm filter. To precipitate the proteins of the supernatant, 5 ml of 100% TCA was added. Incubation took place for 30 min on ice and the denatured proteins were harvested by centrifugation (10 min, 4°C, 27,000 x g). After discarding the supernatant, the pellet was resuspended in 4 ml Aceto-SDS and incubated for 20 min on ice. Subsequently, the mixture was centrifuged again (10 min, 4°C, 27,000 x g) and the pellet washed with 500 µl aceton. After another centrifugation step (10 min, 4°C, 27,000 x g) the pellet was dried and resuspended in 50 µl 3 x SDS sample buffer. After heating for 5 min at 95°C, the samples were separated on 10% SDS polyacrylamide gels. A western blot was carried out with antibodies against CNF_Y or a His tag to make the secreted proteins visible.

2.2.4.3 SDS polyacrylamide gel electrophoresis (SDS-PAGE)

The SDS-PAGE was performed as described previously (Laemmli, 1970). This method consists of a denaturating discontinuous electrophoresis separating proteins according to their molecular weight. The SDS and β-mercaptoethanol containing sample buffer denatures the native proteins by destroying non-covalent bondings and disulfide bridges. The different pH-values of the stacking- and running-gel lead to a discontinuous electrophoresis.

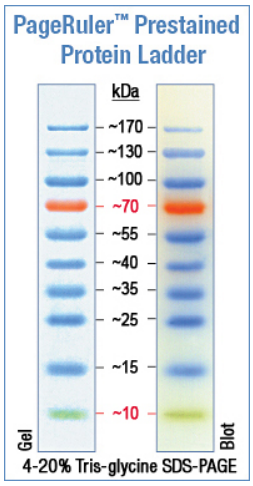

Figure 2.2.5: ***PageRulerTM Prestained Protein Ladder*** **(Fermentas).**

The samples were heated, prior to loading, for 5 min at 95°C and centrifuged for 5 min at 14,000 x g. 5 - 25 µl of the samples and 5 µl of the *PageRulerTM Prestained Protein Ladder* (see Figure 2.2.5) were used. The electrophoresis of the 10 - 15% gels was carried out at 130 V with SDS running buffer for 60 - 90 min. Gels were either stained in Coomassie staining solution (2.2.4.4) or blotted onto a polyvinylidene fluoride (PVDF) membrane (2.2.4.5).

Table 2.11: Composition of 0.75 mm SDS-gels (Sambrook *et al.*, 1989)

Component	10% running gel (2x)	12% running gel (2x)	15% running gel (2x)	Stacking gel (4x)
H_2O_{dest}	4.2 ml	3.5 ml	2.5 ml	6.5 ml
30% Acryl/bisacrylamide	3.3 ml	4.0 ml	5 ml	1.1 ml
Running gel buffer	2.5 ml	2.5 ml	2.5 ml	-
Stacking gel buffer	-	-	-	2.5 ml
TEMED	25 µl	25 µl	25 µl	25 µl
APS (10%)	100 µl	100 µl	100 µl	100 µl

2.2.4.4 Coomassie staining

The Coomassie staining method was used to stain all proteins separated by a SDS polyacrylamide gel (Diezel *et al.*, 1972). After electrophoresis, the gels were stained with agitation for 1 h at RT in the Coomassie staining solution. The destaining was carried out by agitation for 2 x 30 min in 10% acetic acid at RT.

2.2.4.5 Western blot

To specifically detect proteins, western blot analysis were carried out as described previously (Towbin *et al.*, 1979). Therefore, proteins were separated with a SDS-PAGE and transfered electrophoretic onto an Immobion PVDF membrane (Millipore). The membrane was activated previously for 10 - 15 sec in methanol. Subsequently, the activated membrane and the gel were enclosed in between two equlibrated (transblot buffer) sponges and Whatman paper and adjusted in the blotting chamber. The assembly was carried out according to the manufacturer's protocol (Mini-protean II western blot system, Bio-Rad). After transferring the proteins for 1 h at 100 V in precooled transblot buffer, the membrane was blocked, to avoid unspecific binding, for 1 h at RT or overnight at 4°C. Therefore, the membrane was agitated in TBSTB or TBSTM. After blocking, the membrane was incubated under agitation with the primary antibody for immuno-detection (diluted in TBSTB/TBSTM, see Table 2.5) of a specific protein for 1 - 5 h at RT or overnight at 4°C, according to the manufacturer's protocol. Subsequently, the membrane was wasched three times in TBST for 10 min under agitation. The secondary antibody conjugated to horseradish peroxidase (HRP), was added to the membrane (diluted in TBSTB/TBSTM) and incubated for 1 h at RT or overnight at 4°C under agitation. After three washing steps, for 10 min in TBST, the blot was developed using the Western Lightning ECL II Kit (Perkin Elmer) and documented with the chemi documentation system (Bio-Rad).

2.2.4.6 Stripping of the membrane

To remove antibodies from a membrane to detect additional proteins on it, the membrane was stripped. Therefore, the membrane was washed once in TBST after developing and stripped under agitation at RT for 5 - 15 min in Restore Plus Western Blot Stripping Buffer (Thermo Scientific) according to the manufacturer's protocol. After stripping the membrane, it was washed three times for 10 min in TBST and blocked again. Subsequently, new antibody probing on the membrane could be performed.

2.2.4.7 Purification of CNF_Y-His_6

For overexpression of CNF_Y, *E. coli* strain BL21λDE3 was transformed with the *cnfY* expression plasmid pJNS01. The bacteria were grown at 37°C in 500 ml LB medium supplemented with kanamycin, to an OD_{600} of 0.6. Subsequently, the P_{lac}-driven expression was induced upon addition of 250 µM IPTG. Further incubation took place at 17°C overnight at 200 rpm. After harvesting the bacteria by centrifugation (10 min, 4°C, 27,000 x g), the pellet was resuspended in 20 ml lysis buffer. Subsequently, the bacteria were lyzed with a French press (18,000 psi) and centrifuged for 90 min with 27,000 x g at 4°C. The supernatant was sterilized using a 0.2 µm filter.

The purification was performed by an affinity chromatography with 1.5 ml Ni-NTA agarose (Qiagen). Therefore, the agarose was transferred into a gravity chromatography column (Bio-Rad) and washed once with washing buffer. The sterile supernatant was inserted into the column to let the His tag conjugated CNF_Y bind. Subsequently, the supernatant with unbound proteins run out of the column and the agarose was washed with three column volumes of washing buffer. To elute the bound protein, 8 ml elution buffer 1 followed by 8 ml elution buffer 2 were added to the column and collected in 8 fractions. Samples of each fraction were loaded onto a SDS-PAGE and detected with Coomassie staining solution (2.2.4.4). Fractions containing the recombinant protein were pooled.

To get rid of the imidazol contained in the elution buffers, a buffer exchange against PBS was performed, using an Amicon (Millipore), which excludes proteins smaller than 100 kDa. The Amicon was used according to the manufacturer's protocol and the protein washed three times with each 10 ml PBS. After exchanging the buffer and concentrating the protein to 1.5 ml 10 µl of the protein was mixed with 5 µl of 3 x SDS sample buffer and boiled at 95°C for 5 min. The sample was loaded on 2 SDS polyacrylamide gels (5 µl/gel) and one gel was stained with Coomassie staining solution, the other used for western blot analysis with a anti His primary antibody (see 2.2.4.5).

To measure the concentration of the purified toxin, a Bradford assay was performed with the Coomassie Reagent Protein Assay Kit (Pierce), according to the manufacturer's protocol. Therefore, the protein was measured undiluted and diluted 1:10 and 1:100 in duplicates. 250 µl of the Coomassie reagent was added to each sample and incubated for 10 min at RT. The absorption was measured in an iMark Microplate Absorbance Reader (Bio-Rad) at wavelength 595 nm. Subsequently, the protein was aliquoted and

frozen at -20°C. To test the activity of the recombinant toxin a multinucleation assay was performed (see 2.2.2.5).

2.2.4.8 Polyclonal antibodies against CNF_Y of *Y. pseudotuberculosis*

Polyclonal antibodies against CNF_Y were generated in a rabbit (Davids Biotechnology) by injection of 0.2 - 0.6 mg purified recombinant CNF_Y (see 2.2.4.7). The toxin was heat inactivated for 30 min at 70°C prior to injection. For purification, the serum was specifically purified by affinity chromatography (see below). As a negative control for the polyclonal antibodies, pre-immune serum of the rabbit was used.

2.2.4.8.1 Specific purification of polyclonal CNF_Y antibody

To specifically purify the CNF_Y antibody of the rabbit serum, an affinity chromatography with CnBr activated sepharose 4B was performed. Therefore, approximately 1.5 mg of the recombinant CNF_Y protein (see 2.2.4.7) were diluted in 4 ml PBS. Subsequently, the PBS was exchanged with an Amicon (>100 kDa) against 4 ml coupling buffer and stored at 4°C before addition to the activated sepharose.

To activate the CnBr sepharose, 0.5 g were taken up in 10 ml 1 mM HCl and transferred onto a filter on a suction filter. The sepharose was washed on the filter first for 15 min with 200 ml 1 mM HCl and second with 10 ml coupling buffer. Subsequently, the sepharose was transferred into a 50 ml falcon tube with 5 ml coupling buffer.

To couple the prepared protein to the activated sepharose, the protein was given to the sepharose and incubated under agitation for 2 h at RT. After incubation, the mixture was transferred onto a polypropylene column and the sepharose was sedimented. The flow through was collected and prepared for a SDS-PAGE with 3 x SDS sample buffer (see 2.2.4.3). Uncoupled protein was removed by washing the sepharose with 2.5 ml coupling buffer. Using 1 M freshly prepared ethanolamine (pH 8) the remaining binding sites of the sepharose were blocked under agitation for 2 h at RT. Therefore, the column was filled completely with ethanolamine and sealed with parafilm. Subsequently, the sepharose was washed 3 times with 2.5 ml acetate buffer, 3 times with 2.5 ml neutralizing buffer and 3 times with 2.5 ml PBS.

To couple the antibodies with the antigen, 10 ml serum (see 2.2.4.8) were given to the coupled sepharose onto the polypropylene column. The column was sealed with parafilm and the sepharose incubated with the serum under agitation overnight at 4°C. The flow through was collected and prepared for a SDS-PAGE with 3 x SDS sample

buffer (see 2.2.4.3). To remove uncoupled antibodies, the sepharose was washed 10 times with 10 ml PBS and once with 10 ml 0.1 M glycine (pH 3) to remove the weakly coupled antibodies.

To elute the CNF_Y antibody, the sepharose was treated 5 times with 1.5 ml elution buffer to obtain 5 elution fractions. Each fraction was neutralized by the addition of 0.6 ml 1 M Tris-HCl (pH 8). SDS samples of each fraction were prepared with 3 x SDS sample buffer and the remaining aliquots were stored at -20°C. A SDS-PAGE with following Coomassie staining of the collected samples (see 2.2.4.3 & 2.2.4.4) was carried out. Additionally, to test the specificity of the purified antibody in the different elution fractions western blot analyses (see 2.2.4.5) were performed.

2.2.4.9 Expression analysis of P_{cnfY}::*lacZ* β-galactosidase assay

For expression analyses of the *cnf*$_Y$ gene the vector pJNS04 was used. This vector harbours a transcriptional fusion of the *cnf*$_Y$ promoter region and the *lacZ* gene. The β-galactosidase cleaves the substrate ONPG, which leads to the formation of nitrophenol. The yellow colour of the substance was measured using an ELISA-reader (OD_{420}), to calculate the specific enzyme activity.

The measurement of three independent cultures in triplicate was performed as described previously (Nagel *et al.*, 2001). Therefore, the bacteria were grown overnight at 25°C or 37°C. Subsequently, the culture was used to inoculate fresh medium 1:50 to let the bacteria grow to exponential or early stationary phase.

The OD_{600} of all samples of the three growth phases was determined. Next, 200 µl of the 1:10 diluted samples were transferred into glas tubes (duplicate). Lysis of the bacteria was performed by adding 0.1% SDS-solution, two drops of chloroform and incubation for 10 min at RT. After addition of 1.8 ml Z-buffer, the reaction was started with 400 µl ONPG. When the samples turned yellow, the reaction was stopped by a change in pH with 1 ml Na_2CO_3 (1 M). The stopping time was noted and each sample was measured in duplicate.

The activities were calculated as follows: β-galactosidase activity $OD_{420} \cdot 6.75\ OD_{600}^{-1} \cdot \Delta t\ (min)^{-1} \cdot vol\ (ml)^{-1}$. (6.75: extinction coefficient of cleaved ONPG in [µmol/min/mg protein])

2.2.5 Mouse experiments

Female BALB/c mice between 6- and 8-weeks old were purchased from Janvier (Saint Berthevin Cedex, France) and housed under specific pathogen-free conditions according to GV-SOLAS (German Recommendations of the Society for Laboratory Animal Science) and FELASA (Federation of Laboratory Animal Science Associations) recommendations in the animal facility of the Helmholtz Centre for Infection Research, Braunschweig. The animal protocol was approved by the „Niedersächsisches Landesamt für Verbraucherschutz und Lebensmittelsicherheit“: animal licensing committee permission no. 33.9.42502-04-055/09 and 33.9.42502-04-12/0907. Animals were handled with appropriate care and welfare, and all efforts were made to minimize suffering.

2.2.5.1 Oral infection

The infection of mice with *Y. pseudotuberculosis* was performed orally to mimic the natural route of infection. After starving the mice overnight, the bacteria were introduced directly into the stomach of the mouse, using a syringe with a gavage needle.

Therefore, the bacteria were grown overnight in 50 ml LB liquid culture at 25°C. Subsequently, 20 ml bacterial culture was mixed with 30 ml PBS to wash the bacteria and centrifuged 10 min with 2,755 x g at RT. The pellet was resuspended in 50 ml PBS and centrifuged again for 10 min with 2,755 x g at RT. After resuspension of the bacterial pellet in 10 ml PBS, the OD_{600} was measured and adjusted to the required OD_{600}. For infection 200 µl of the bacterial suspension was used.

In order to determine the infection dose, 1:10 serial dilutions of the bacteria were plated on LB agar plates and the colony forming units (CFU) were counted.

2.2.5.2 *In vivo* expression analysis

To determine the expression level of the *cnfY* gene *in vivo*, the plasmids pJNS02 or pJNS03 were used. Both plasmids harbour a transcriptional fusion of the *cnfY* promoter region with a reporter system (P_{cnfY}::*luxCDABE* & P_{cnfY}::*gfpmut3.1*, respectively).

2.2.5.2.1 *In vivo* imaging system (IVIS)

To detect the *cnfY* gene expression during the course of infection, the *Y. pseudotuberculosis* wild-type strain YPIII, harbouring the vector pJNS02 or the empty vector pFU54, were used. About 2 x 10^8 luminescent bacteria were used for oral infection (see 2.2.5.1). The expression was monitored over a period of 5 days. For imaging, the mice were anesthesized with isoflurane and the bacterial infection was followed daily using the IVIS Lumina system (Xenogen).

To ensure maintenance of the plasmid during the course of infection, an organ burden experiment was performed (see 2.2.5.5). Therefore, the bacteria were isolated from the small intestine, colon, caecum, MLNs, spleen and liver and tested for the presence of the plasmid five days post infection by plating on LB agar plates with or without antibiotics.

2.2.5.2.2 Cryosections

To detect the *cnfY* gene expression on single cell level in the different organs, cryosections have been prepared. Therefore, the *Y. pseudotuberculosis* wild-type strain YPIII, harbouring the vectors pJNS03 and pFU228 (P_{gapA}::*dsRed2*), were used. With this system it was possible to detect all bacteria under the microscope with DsRed and the ones expressing the *cnfY* gene with GFP. About 2 x 10^8 bacteria were used for oral infection (see 2.2.5.1). After five days the mice were sacrificed by CO_2 asphyxiation. For cryosections, the small intestine, colon, caecum, MLNs, spleen and liver were frozen in Tissue-Tek OCT freezing medium (Sakura Finetek) on dry ice. Sections of 6 - 10 mm were prepared using a Zeiss cryostat Hyrax C50, mounted on SuperFrost Plus slides (Thermo Scientific) and stored at -20°C. The samples were air-dried at RT in the dark, fixed for 10 min in ice-cold acetone and washed twice with PBS.

Nuclei in the fixed tissue were stained with 49,6-diamidino-2-phenylindole (DAPI). Therefore, a drop of Roti-Mount FluorCare MIT DAPI (Roth) was used per sample. The sample was coated with a cover slip, which was fixed with nail polish and stored at 4°C or directly used for microscopy. The visualization was performed with a fluorescence microscope (Axiovert II with Axiocam HR, Zeiss, Germany) using the AxioVision program (Zeiss, Germany).

2.2.5.3 Histology

For histological analysis of the infected organs, mice were infected orally with approximately 2 x 10^8 bacteria (see 2.2.5.1) for 3 or 6 days. After sacrificing the mice via CO_2 asphyxiation, the MLNs, spleen, liver, ileum, caecum and colon were prepared according to standard histology procedures. The organs were fixed in 4% neutrally buffered formaldehyde for 24 to 48 h, embedded in paraffin and 3 µm sections stained with hematoxylin-eosin (H & E). Organs of three to four mice per group were blindly analyzed by a histopathologist. Sections were evaluated by light microscopy blinded to the experimental groups. Dr. Marina Pils of the Mouse Pathology unit of the Helmholtz Centre for Infection Research performed the embedding, staining and microscopy.

2.2.5.4 Survival

Survival experiments were carried out to test the virulence of different *Y. pseudotuberculosis* strains. Therefore, groups of 10 mice were infected orally with approximately 2 x 10^9 bacteria of each strain. The infected mice were monitored every day for 14 days to record the survival rate, the body weight and health status. With a weight loss over 20%, in comparison to the baseline weight, mice were sacrificed and recorded as dead.

2.2.5.5 Organ burden

Organ burden experiments were performed to determine the bacterial load in the different organs affected in the infection route. Groups of 7 - 10 animals were orally infected with approximately 2 x 10^8 bacteria of different *Y. pseudotuberculosis* strains (YPIII, YP147 (Δ*cnfY*), YP12 (pYV^-), YP150 (pYV^- Δ*cnfY*), YP101 (Δ*yscS*) or YP298 (Δ*yscS* Δ*cnfY*)). At specific time points after infection, mice were euthanized by CO_2 asphyxiation. The Peyer's patches (PP), small intestine, caecum, MLNs, liver and spleen were prepared (for Flow cytometry + Organ burden experiments of spleen, MLNs and PP, see 2.2.5.6). The ileum and caecum were first rinsed in PBS and then incubated in PBS supplemented with gentamycin (50 µg/ml) for 30 min on ice to kill the extracellular bacteria. In order to remove the gentamycin, the small intestine and caecum were washed with PBS. Subsequently, all organs were weighed, transferred into falcon tubes with 2 - 5 ml PBS and homogenized in PBS at 30,000 rpm for 30 sec, using a Polytron PT 2100 homogenizer (Kinematica, Switzerland). To determine the bacterial load of the organs 50 µl of serial 1:10 dilutions of the homogenates were plated on LB agar plates

with and without antibiotics. The CFU were determined and calculated as CFU per g organ/tissue.

2.2.5.6 Flow cytometry (measurement of immune response)

To analyze the immune response triggered upon infection with different *Y. pseudotuberculosis* strains (wild-type strain YPIII in comparison to YP147 (Δ*cnfY*), YP12 (pYV$^-$), YP101 (Δ*yscS*), YP150 (pYV$^-$ Δ*cnfY*) or YP298 (Δ*yscS* Δ*cnfY*)), an antibody staining with subsequent flow cytometry analysis was performed. Therefore, groups of 5 - 8 mice were orally infected with approximately 2 x 10^8 bacteria. 3 or 28 days after infection mice were euthanized with CO_2 asphyxiation and PP, MLNs and spleen were isolated.

2.2.5.6.1 Preparation of single cell suspensions

After preparing the organs, the spleen weight was determined. Single cell suspensions were generated in PBS by pressing the spleen cells through a 100 µm cell strainer (Falcon) and the MLNs and PP through a 30 µm cell strainer with the stamp of a syringe. For isolation of spleen cells, the cell strainer was moistened with 1 ml FACS buffer and washed twice with 4 ml PBS. The cell strainer for MLNs and PP were moistened with 0.5 ml FACS buffer and washed twice with 1 ml FACS buffer. Organ burden samples were transferred into 15 ml falcon tubes (3 ml for spleen) or U-bottom tubes (100 µl PP sample + 900 µl PBS & 200 µl MLNs sample + 800 µl PBS) for homogenizing and plating (2.2.5.5). The remaining splenocytes for flow cytometry were treated with 1 ml erythrolysis buffer for 3 min at RT to eliminate the erythrocytes. By adding 10 ml FACS buffer, the lysis was stopped.

All samples were centrifuged for 8 min with 400 x g at 4°C. Subsequently, the cell pellets were resuspended in 1 ml FACS buffer. The spleen samples were transferred onto a 30 µm cell strainer, which was subsequently washed with 1 ml FACS buffer.

Next, the cell number was determined. Therefore, 20 µl of the cell suspension was diluted 1:25 with propidium iodide (PI). The cell counting was performed with an Accuri C6 flow cytometer (BD Bioscience). Amounts of 1 - 2.5 x 10^6 cells were transferred into Matrix™ Blank and Alphanumeric Storage Tube (Thermo Scientific).

2.2.5.6.2 Staining of immune cells

The aliquoted cell samples were washed twice by addition of 750 µl PBS and centrifugation for 3 min with 400 x g at 4°C. Subsequently, the supernatant was removed and the cell pellet resuspended in 200 µl Live/dead staining solution (Invitrogen; Live/dead Fixable Blue Dead Cell Stain Kit, UV excitation) to exclude dead cells from the analysis. After staining in the dark for 30 min on ice, the cells were washed once with 750 µl FACS-buffer. The supernatant was removed after centrifugation (3 min; 400 x g; 4°C) and blocking of FcγR and IgG was performed by addition of 50 µl CD16/CD32 (BioXCell; anti-mouse CD16/CD32) and ratIgG (Jackson ImmunoResearch; ChromPure Rat IgG, whole molecule) antibodies for 15 min on ice. By addition of 50 µl of the antibody mix (in FACS buffer) the cellular surface markers of either lymphoid or myeloid cells were stained for 15 min on ice in the dark. The following antibodies were used: CD3-APC, CD4-PerCP-Cy5.5, CD8-eFluor450, CD335-PerCP-Cy5.5, CD11b-PacificBlue, CD19-Biotin, CD45R-PerCP-Cy5.5, F4/80-PE, CD11c-APCeFluor780, CD19-FITC, CD49b-Biotin and Ly6C-APC. All antibodies were titrated for optimal staining conditions. The stained cells were washed twice with 750 µl FACS-buffer and subsequent centrifugation (3 min; 400 x g; 4°C).

Further, biotin-conjugated antibodies were treated with 100 µl streptavidin-FITC for 15 min on ice. After washing the samples twice with 750 µl FACS-buffer (3 min; 400 x g; 4°C) the cells were fixed by the addition of 200 µl Fix/Perm buffer (Foxp3 Staining Buffer Set; eBioscience) for 30 min on ice in the dark. Subsequently, 800 µl Perm buffer were added and the cells were centrifuged for 5 min with 450 x g at 4°C. The supernatant was removed and the cells resuspended in 150 µl FACS-buffer. Next, the cells were stored at 4°C or directly loaded into a LSR Fortessa cell analyzer (BD Bioscience). The acquired data were analyzed with FlowJo software (Treestar).

2.2.5.7 Yop delivery assay during mouse infection

To detect differences in the Yop translocation rates during mouse infection with or without CNF_Y, Yop delivery assays were performed. Therefore, groups of 5 to 8 mice were infected orally (see 2.2.5.1) with approximately 2 x 10^9 bacteria of strain YPIII-ETEM (YP173) and the isogenic *cnfY* mutant YP147-ETEM (YP217). As negative controls for Yop translocation, groups of 2 mice were infected with the same amount of wild-type YPIII or YP101-ETEM (YP174) bacteria. After three days, the mice were sacrificed via CO_2 asphyxiation. The lymphatic organs PP, MLNs and spleen were

isolated, single cell suspensions were prepared, samples for organ burden were taken, erythrocytes of the spleen eliminated and cells counted (see 2.2.5.6.1).

For the flow cytometry analysis, 1 x 10^6 cells were transferred into Matrix™ Blank and Alphanumeric Storage Tubes (Thermo Scientific) and centrifuged for 3 min with 400 x g, 15.4 r and 4°C. The supernatant was removed and FcγR blocked using CD16/CD32 antibody diluted in FACS buffer for 15 min at 4°C. By the addition of a biotin-conjugated antibody against CD19, the immune cells were stained first for 15 min at 4°C. Subsequently, the antibody solutions (in FACS buffer) for different surface marker for the innate immune cell panel or T cell panel were added. The staining incubation time was 20 min at 4°C with the following antibodies: Streptavidin-PerCP-Cy5.5, CD11c-APC, CD11c-PE-Cy7, Gr1-A700, CD3-PE, CD4-APC-Cy7, CD3-PE-Cy7, NKp46-PE and CD25-APC. The samples were washed twice with 750 µl FACS buffer, with a centrifugation step of 3 min with 400 x g, and 4°C in between.

To label the Yop translocated cells, the LiveBLAzer-FRET B/G Loading Kit (Life Technologies) was used with 1 µg/ml CCF4-AM for 1 hour at RT in the presence of 1.5 mM probenecid (Sigma) and 50 µg/ml gentamycin, according to the manufacturer's protocol. The cell subsets were defined as: B cells ($CD19^+$ $CD3^-$), T cells ($CD19^-$ $CD3^+$), NK cells ($CD19^-$ $CD3^-$ $NKp46^+$), neutrophils ($CD19^-$ $CD3^-$ $CD49b^-$ $Ly6G^+$ $CD11b^+$), macrophages/monocytes ($CD19^-$ $CD3^-$ $CD49b^-$ $Ly6G^-$ $CD11b^+$) and DCs ($CD19^-$ $CD3^-$ $CD49b^-$ $Ly\text{-}6G^-$ $B220^-$ $F4/80^-$ $CD11c^+$). A LSR Fortessa cell analyzer (BD Bioscience) was used to acquire the data. Data were analyzed with FlowJo software (Treestar) using unstained cells, YPIII infected and YP174 infected cells as negative controls.

2.2.5.8 Measurement of secreted cytokines

To measure the cytokine release in uninfected, YPIII- or YP147-infected mice, serum samples were prepared. Therefore, mice were infected orally with approximately 2 x 10^8 bacteria (see 2.2.5.1) for 3 days.

2.2.5.8.1 Serum preparation

After sacrificing the mice via CO_2 asphyxiation, heart blood was taken immediately with an insulin syringe. The blood samples were incubated for 30 min - 3 h at RT. After clotting of the blood, samples were centrifuged at RT for 8 min with 2,300 x g. Subsequently, the supernatant was transfered into new Eppendorf tubes, centrifuged and transferred again into new Eppendorf tubes. The prepared serum samples were stored at -80°C.

2.2.5.8.2 Luminex

To measure the cytokine concentrations in the serum, the MILLIPLEX MAP Mouse Cytokine/Chemokine Magnetic Bead Panel - Premixed 32 Plex - Immunology Multiplex Assay Kit from Millipore was used. The following cytokines were analyzed: Eotaxin, G-CSF, GM-CSF, IFN-γ, IL-10, IL-12 (p40), IL-12 (p70), IL-13, IL-15, IL-17, IL-1α, IL-1β, IL-2, IL-3, IL-4, IL-5, IL-6, IL-7, IL-9, IP-10, KC-like, LIF, LIX, M-CSF, MCP-1, MIG, MIP-1α, MIP-1β, MIP-2, RANTES, TNF-α and VEGF.

Therefore, the prepared serum samples were thawed on ice and processed for the measurement. The assay was performed according to the manufacturers protocol using the Luminex® detection system for the readout. This system is able to quantify multiple cytokine levels simultaneously.

3 Results

The wild-type strain YPIII of *Y. pseudotuberculosis* produces the cytotoxic necrotizing factor *cnfY*, which displays a sequence identity of about 65% (Lockman *et al.*, 2002) to its homolog *cnf1* of uropathogenic *E. coli* or *E. coli* K1 strains (Caprioli *et al.*, 1984). These toxins constitutively activate small Rho-GTPases, thereby inducing rearrangements of the actin cytoskeleton and thus the formation of stress fibres, filopodia or lamellipodia. Upon intoxication with CNFs, the eukaryotic cells become rigid and lose their ability to divide. This leads to the formation of multinucleated giant cells (Caprioli *et al.*, 1984; Lockman *et al.*, 2002). Previous studies with CNF_Y indicated that an intoxication of epithelial, as well as of neuronal cells, selectively activated the small Rho-GTPase RhoA (Hoffmann *et al.*, 2004).

So far, only little is known about the expression of *cnfY* and the impact of the toxin-induced Rho-GTPase activation on the virulence of *Y. pseudotuberculosis*. These points are addressed below.

3.1 Expression and secretion pattern of *cnfY*/CNF_Y

A functional *cnfY* gene is encoded by a few pathogenic *Y. pseudotuberculosis* isolates. Many *Yersinia* strains harbour mutations over the whole gene, including the *Y. pestis* strain CO92 (Lockman *et al.*, 2002). Expression of *cnfY* was tested in the wild-type strain *Y. pseudotuberculosis* YPIII.

3.1.1 The CNF_Y toxin is highly expressed and secreted under host-relevant conditions

For the *in vitro* expression analysis of the *cnfY* gene, a transcriptional promoter fusion of *cnfY* with the *lacZ* (β-galactosidase) gene was used (pJNS04). The *cnfY* expression was measured at three different growth phases, the exponential (3 h), the early stationary (7 h), and the late stationary phase (14 h) at 25°C and 37°C (see Figure 3.1.1). A low *cnfY* expression could be detected at 25°C, but the highest expression level was in the late stationary phase at 37°C, which best resembles conditions in the host.

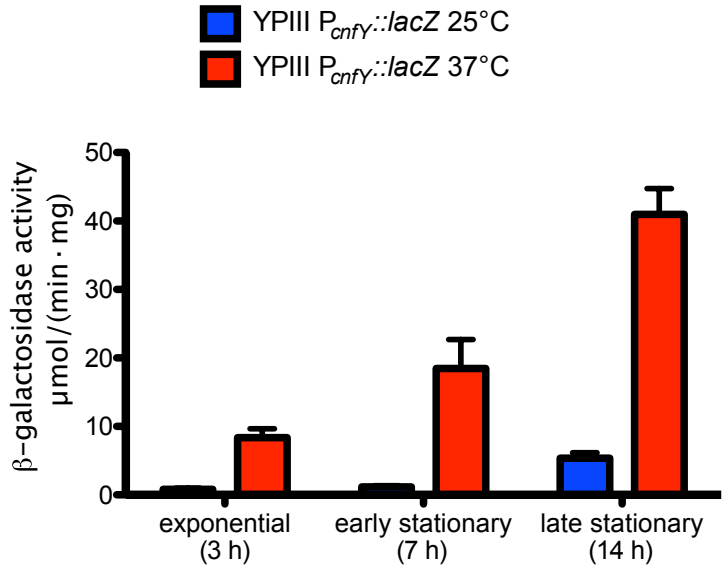

Figure 3.1.1: The highest expression of *cnfY in vitro* was detected at 37°C in the late stationary growth phase.

Y. pseudotuberucosis YPIII, harbouring the plasmid pJNS04 (P$_{cnfY}$::*lacZ*), was grown in LB medium at 25°C or 37°C to exponential (3 h), early stationary (7 h) and late stationary (14 h) growth phase. The β-galactosidase activity was determined from three independent cultures in triplicate.

Subsequently, the secretion level of the toxin was examined. Therefore, *Y. pseudotuberculosis* YPIII was incubated at 25°C or 37°C to the exponential (3 h), the early stationary (7 h) and the late stationary (14 h) growth phase. Next, the sterilized supernatants were precipitated and analyzed on a western blot, using a CNF$_Y$ specific antiserum (see Figure 3.1.2). The secretion of CNF$_Y$ resembles the expression pattern of *cnfY* with the highest secretion detectable at 37°C in the late stationary phase.

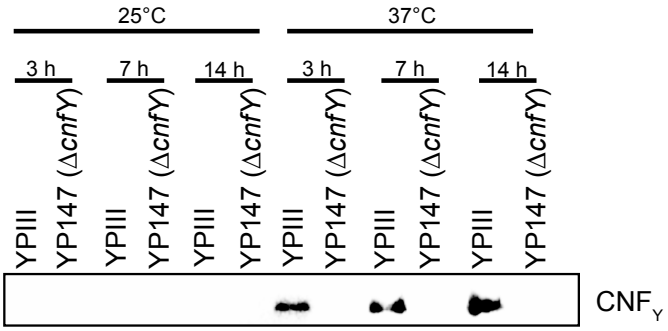

Figure 3.1.2: The highest secretion level of CNF$_Y$ *in vitro* was detected at 37°C in the late stationary growth phase.

Y. pseudotuberculosis YPIII and YP147 (Δ*cnfY*) were grown in LB medium at 25°C or 37°C to exponential (3 h), early stationary (7 h) and late stationary (14 h) growth phase. The supernatant was sterilized and precipitated. CNF$_Y$ was detected by western blot analysis with a specific CNF$_Y$ (~115 kDa) antibody.

Subsequently, the nutrient-dependent expression of *cnfY* was tested. To this purpose, bacteria were grown to the late stationary phase at 37°C in different minimal- and complex-culture media (see Figure 3.1.3, other tested conditions not shown). The expression of *cnfY* was significantly higher in the complex media, especially in brain-heart-infusion (BHI) in comparison to the minimal-media MMA and RPMI in which the expression was as low as at 25°C in LB medium.

In summary, the expression of *cnfY* is growth phase-, temperature-, and nutrient-dependent, suggesting a predominant expression during late stages of the infection.

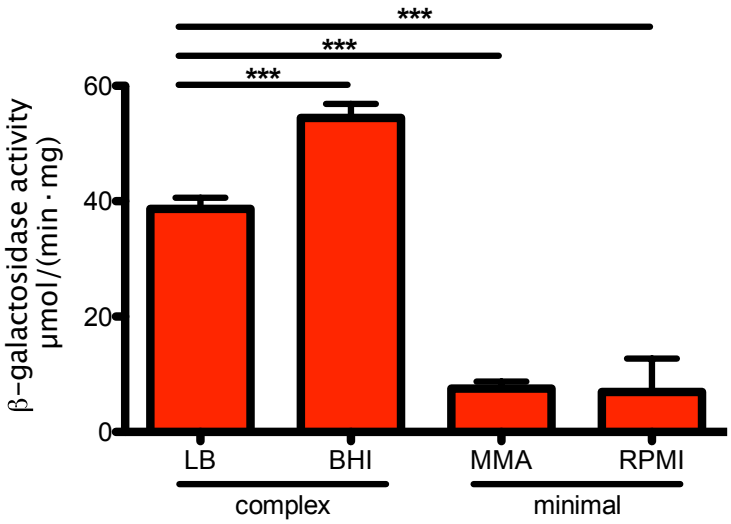

Figure 3.1.3: The *cnfY* expression is dependent on nutrient availability.
Y. pseudotuberucosis YPIII, harbouring the plasmid pJNS04 (P_{cnfY}::*lacZ*), was grown in complex (LB or BHI) or in minimal (MMA or RPMI) media at 37°C to the late stationary (14 h) growth phase. The β-galactosidase activity was determined from three independent cultures in triplicate. The asterisks indicate significant differences of β-galactosidase activities at the tested conditions calculated with an unpaired Student's t-test. The expression in different media differed significantly from expression in LB medium, *** (P<0.001).

3.1.2 The *cnfY* gene expression is controlled by virulence regulators

Due to the similarities in the expression conditions with the other known virulence genes, different regulatory factors have been tested for their influence on the *cnfY* expression or secretion. Hence, mutant strains lacking different virulence regulators have been used to measure the *cnfY* expression at the most relevant conditions at 37°C in the exponential, early stationary, and late stationary growth phases.

Previous data already showed an influence of the *Yersinia* modulator A (YmoA) as a repressor of CNF_Y at 25°C (J. Schweer, Master-thesis). YmoA has been shown before

as being important for controlling the expression of late virulence genes, like the Yop effector proteins, by inhibiting the transcription of *lcrF* (Böhme *et al.*, 2012). However, previous data also showed no *cnfY* expression dependency on the presence of the virulence plasmid, coding for *lcrF* (J. Schweer, Master-thesis).

Furthermore, the secretion of CNF_Y in a mutant strain lacking the virulence plasmid was examined. *Y. pseudotuberculosis* YPIII, the mutant YP12 pYV$^-$, and the *cnfY* mutant strain were incubated at 37°C overnight. Next, the sterilized supernatants were precipitated and analyzed on a western blot, using a CNF_Y specific antiserum for the toxin-detection (see Figure 3.1.4). No virulence plasmid-dependent secretion of CNF_Y could be detected. Taken together, these data suggest that the *cnfY* expression is repressed by YmoA like the Yop proteins, but independently from the plasmid encoded transcriptional activator LcrF. Additionally, CNF_Y is not secreted via the type three secretion system (T3SS).

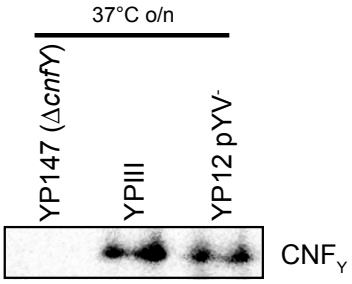

Figure 3.1.4: The CNF_Y secretion is independently from the virulence plasmid pYV.
Y. pseudotuberculosis YPIII, YP12 pYV$^-$, and YP147 (Δ*cnfY*) were grown overnight in LB medium at 37°C. The supernatant was sterilized and precipitated. CNF_Y was detected by western blot analysis with a specific CNF_Y (~115 kDa) antibody.

Additional regulators of known virulence genes were tested, the ferric uptake regulator (Fur) and the cyclic AMP receptor protein (Crp). Hence, *Y. pseudotuberculosis* strains YPIII, YP89 (Δ*crp*), and YP105 (Δ*fur*), all harbouring the plasmid pJNS04 (P_{cnfY}::*lacZ*), were incubated at 37°C to exponential (3 h), early stationary (7 h), and late stationary (14 h) growth phase. Figure 3.1.5 shows the expression of *cnfY* in the *fur*- and the *crp*-mutant strains. The deletion of the iron assimilation regulator Fur seems to have no impact on the expression of *cnfY* (also at 25°C, data not shown), whereas Crp appears to upregulate the expression of *cnfY* at 37°C, specifically in the late stationary phase. Crp is known to have an influence on the carbon storage regulator (Csr) system, which is in turn involved in the expression of InvA (Heroven *et al.*, 2012). Taken together, *cnfY*

is regulated by factors, which are also involved in the regulation of different virulence factors, e.g. the *invA* gene.

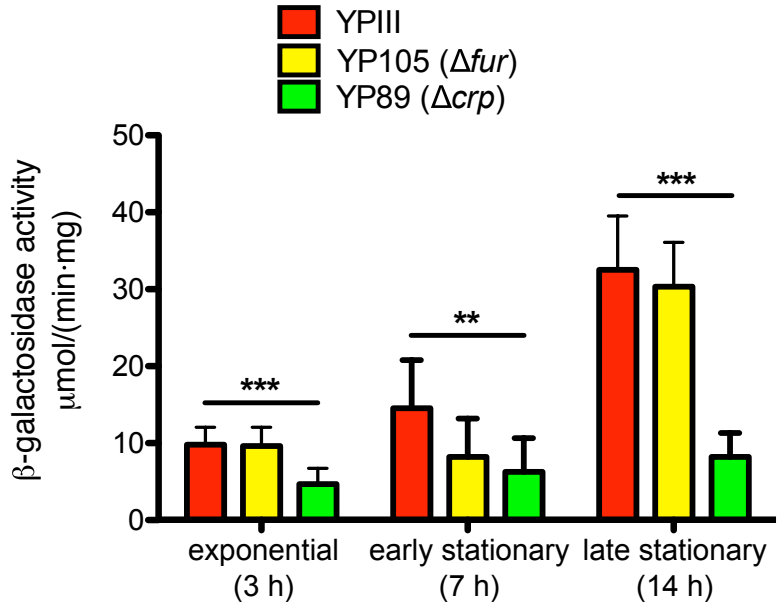

Figure 3.1.5: The *cnfY* expression is dependent on Crp, but not on Fur at 37°C.
Y. pseudotuberucosis YPIII, YP89 (Δ*crp*) and YP105 (Δ*fur*), harbouring the plasmid pJNS04 (P_{cnfY}::*lacZ*), were grown in LB medium at 37°C to exponential (3 h), early stationary (7 h), and late stationary (14 h) growth phase. The β-galactosidase activity was determined from three independent cultures in triplicate. The asterisks indicate significant differences of β-galactosidase activities at the tested conditions calculated with an unpaired Student's t-test. The expression in a *crp* mutant differed significantly from expression in the wild-type with **(P<0.01) and *** (P<0.001).

3.1.3 The *cnfY* gene is highly expressed *in vivo* during the whole infection route

Due to the high expression level of *cnfY in vitro*, a transcriptional *cnfY* promoter fusion with the luciferase operon (P_{cnfY}::*luxCDABE*) was used to detect the *cnfY* expression in the mouse model. The expression of the toxin during the course of infection was followed to determine time points and organs at/in which *cnfY* is expressed and possibly important for the infection.

To this purpose, groups of 3 - 5 BALB/c mice were infected orally with 3 x 10^8 bacteria of *Y. pseudotuberculosis* YPIII, carrying the P_{cnfY}::*luxCDABE* promoter fusion plasmid (pJNS02). The luciferase activity due to *cnfY* expression was measured using the *in vivo* imaging system (IVIS), which measures the bioluminescent signal. The expression was followed during the course of infection over six days (see Figure 3.1.6). As a negative

control for the basal expression level of the luciferase, mice were infected with bacteria harbouring an empty vector (pFU54), carrying the luciferase operon without the *cnfY* promoter. In these mice, no bioluminescent signal was detected (data not shown).

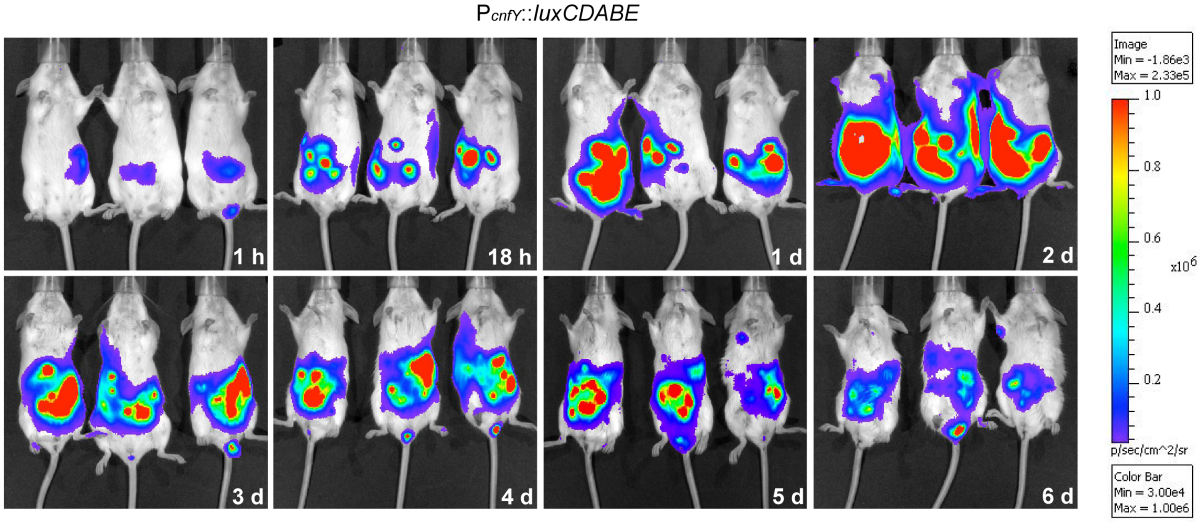

Figure 3.1.6: The highest *cnfY* expression *in vivo* was detectable two days post infection.
Groups of 3 - 5 BALB/c mice were infected orally with 3 x 10^8 bacteria of *Y. pseudotuberculosis* YPIII, harbouring the plasmid pJNS02 (P_{cnfY}::*luxCDABE*). At indicated time points, the mice were anesthesized and the bioluminescence was detected with a CCD camera of the *in vivo* imaging system (IVIS) on the ventral site. Mice were infected with three independent bacterial cultures. The figure is representative for two independent experiments.

The overall expression level of *cnfY in vivo* during the entire course of infection was very strong. Already one hour after infection, a small bioluminescent signal was visible in the abdominal part of the anesthesized mice. The highest expression was detectable after two days in the gut and gut-related tissues. The toxin was expressed during infection up to six days. However, due to the overall high expression, it was impossible to differentiate between the different tissues (see Figure 3.1.6).

In order to test the expression of *cnfY* at a single cell level in the organs, cryosections were prepared. Hence, groups of 3 BALB/c mice were infected for three or five days with approximately 2 x 10^8 *Y. pseudotuberculosis* wild-type bacteria, carrying two plasmids, coding for a constitutive P_{gapA}::*dsred2* reporter construct (pFU228) and a compatible P_{cnfY}::$gfp_{mut3.1}$ transcriptional fusion (pJNS03). The small intestine, caecum, colon, mesenteric lymph nodes (MLNs), spleen, and liver were analyzed. The infected tissues were screened for bacterial microcolonies under the fluorescent microscope by the expression of *dsred2* and subsequently tested for $gfp_{mut3.1}$-expression. Figure 3.1.7 shows the colonization and the expression of *cnfY* in the Peyer's patches (PP), caecum,

MLNs, spleen, and liver five days post infection. The *cnfY* gene is equally expressed in all tested organs, leading to the conclusion that CNF_Y is needed throughout the whole infection route.

In summary, *cnfY* is highly expressed *in vivo* during the entire infection and shows no organ dependency in its expression.

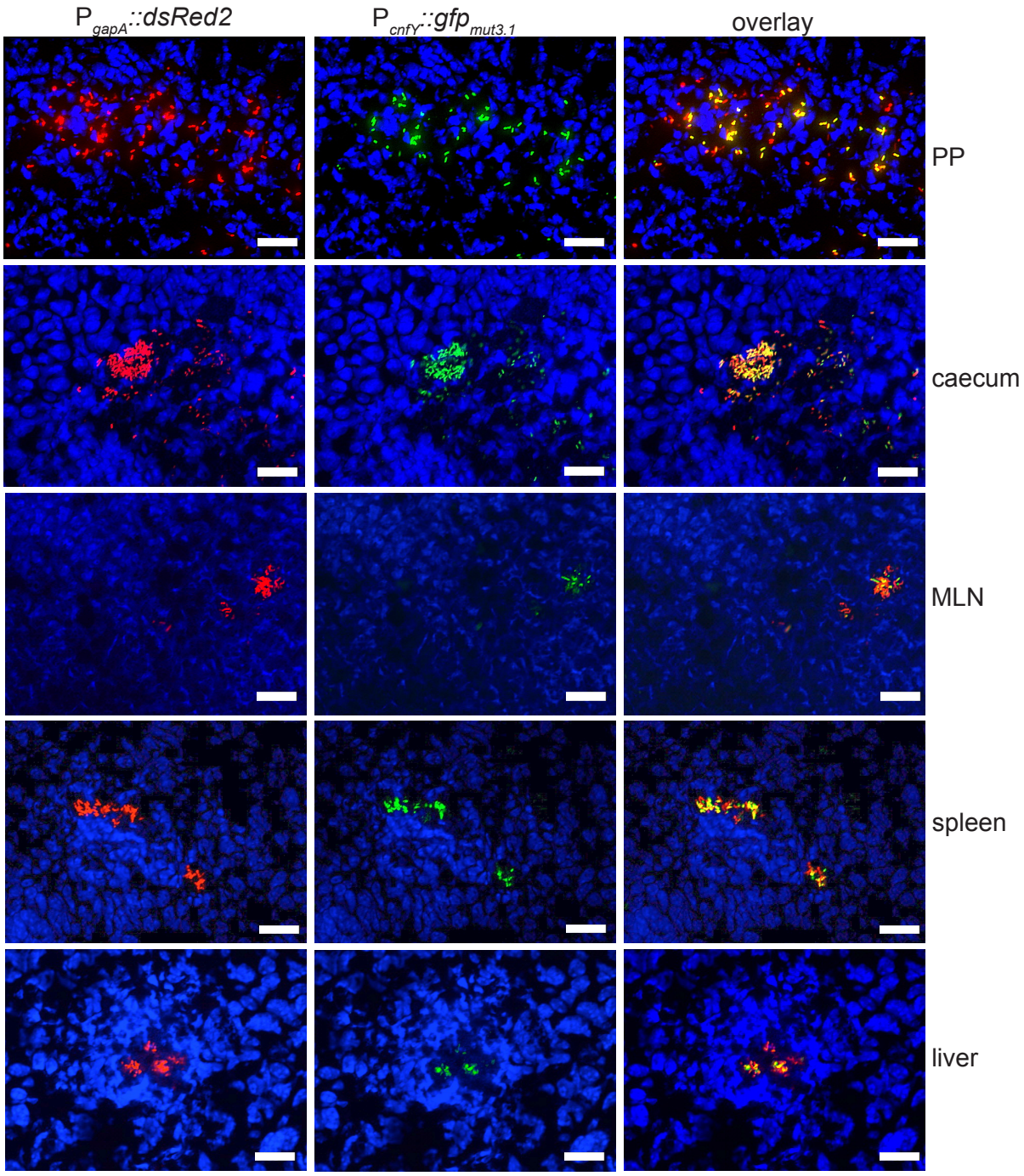

Figure 3.1.7: The *cnfY* expression is not organ-specific.
Groups of 3 BALB/c mice were infected orally with 2 x 10^8 bacteria of *Y. pseudotuberculosis* YPIII, harbouring the plasmids pJNS03 (P_{cnfY}::*gfp*$_{mut3.1}$) and pFU228 (P_{gapA}::*dsRed2*). Five days post infection, the mice were sacrificed and the small intestine, caecum, MLNs, spleen, and liver isolated. Cryosections

(6 μm) have been prepared and analyzed by fluorescence microscopy. Sections were screened for bacteria expressing the reporter protein DsRed2 and subsequently analyzed for *cnfY* expression by monitoring GFPmut3.1 fluorescence. White bars indicate 20 μm.

3.2 CNF_Y activates the small Rho-GTPases and alters the cell morphology

The *E. coli* homolog of CNF_Y, CNF_1 was shown to lead to the activation of the three small Rho-GTPases Rac1, Cdc42 and RhoA, whereas CNF_Y was shown to preferably activate the small Rho-GTPase RhoA in epithelial cells (Hoffmann *et al.*, 2004).

Given the high expression and secretion of the toxin (see 3.1) in *Y. pseudotuberculosis* YPIII, the CNF_Y function was further analyzed to investigate if the produced toxin was also active. To test the activity of the toxin directly produced by YPIII, the bacteria were grown overnight at 37°C to induce the highest expression and secretion of the toxin. Sterilized supernatants of bacterial lysates of the strains YPIII and YP147 (Δ*cnfY*) were given onto human epithelial cells (HEp-2) and incubated for 48 hours. The polymerized actin cytoskeleton and the nuclei of the cells were stained with FITC-conjugated pholloidin and DAPI, respectively and visualized via fluorescent microscopy. Multinucleation and formation of giant cells, which is exclusively attributed to the CNF_Y activity showed that CNF_Y is active (see Figure 3.2.1, complementation experiments not shown).

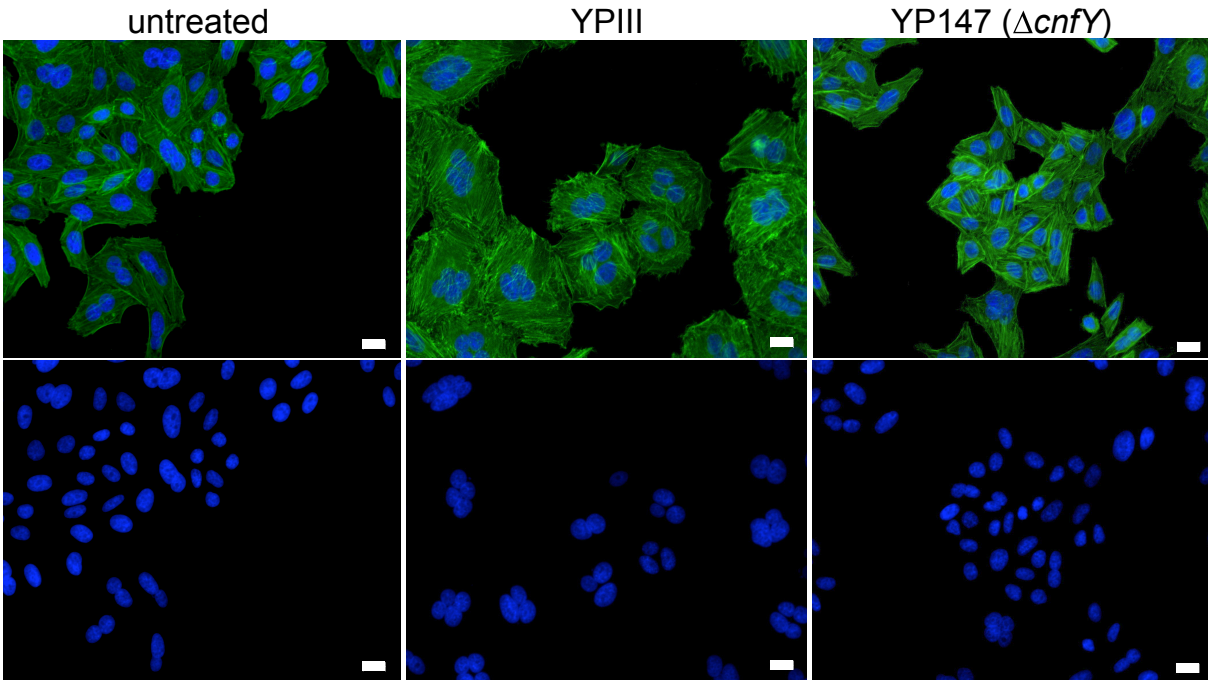

Figure 3.2.1: Incubation of epithelial cells with sterilized *Y. pseudotuberculosis* YPIII lysate leads to the formation of multinucleated giant cells.

Y. pseudotuberculosis YPIII and YP147 (Δ*cnfY*) were grown overnight at 37°C. The bacterial whole cell extract was lyzed, centrifuged and the sterilized supernatant incubated on human epithelial HEp-2 cells for 48 h. The nuclei were stained with DAPI (blue) and the F-actin with FITC-conjugated phalloidin. White bars indicate 20 μm.

Due to the high expression of *cnfY in vivo*, it was hypothesized that CNF_Y could play a relevant role for the virulence of *Y. pseudotuberculosis* wild-type YPIII, most likely by interfering with the immune cells and preventing the bacteria-elimination. To test the effect of CNF_Y on cultured cells, the recombinant toxin was purified. Because the innate immune cells form the first line of defence against a *Yersinia* infection, the effect of CNF_Y on murine macrophages was tested. The macrophage cell line J774A.1 with or without the induction of maturation to fully active macrophages by phorbol myristate acetate (PMA/ 48 h) was intoxicated with CNF_Y (10 nM) for 24 hours (see Figure 3.2.2). The polymerized actin cytoskeleton and nuclei of the cells were stained and visualized by fluorescent microscopy.

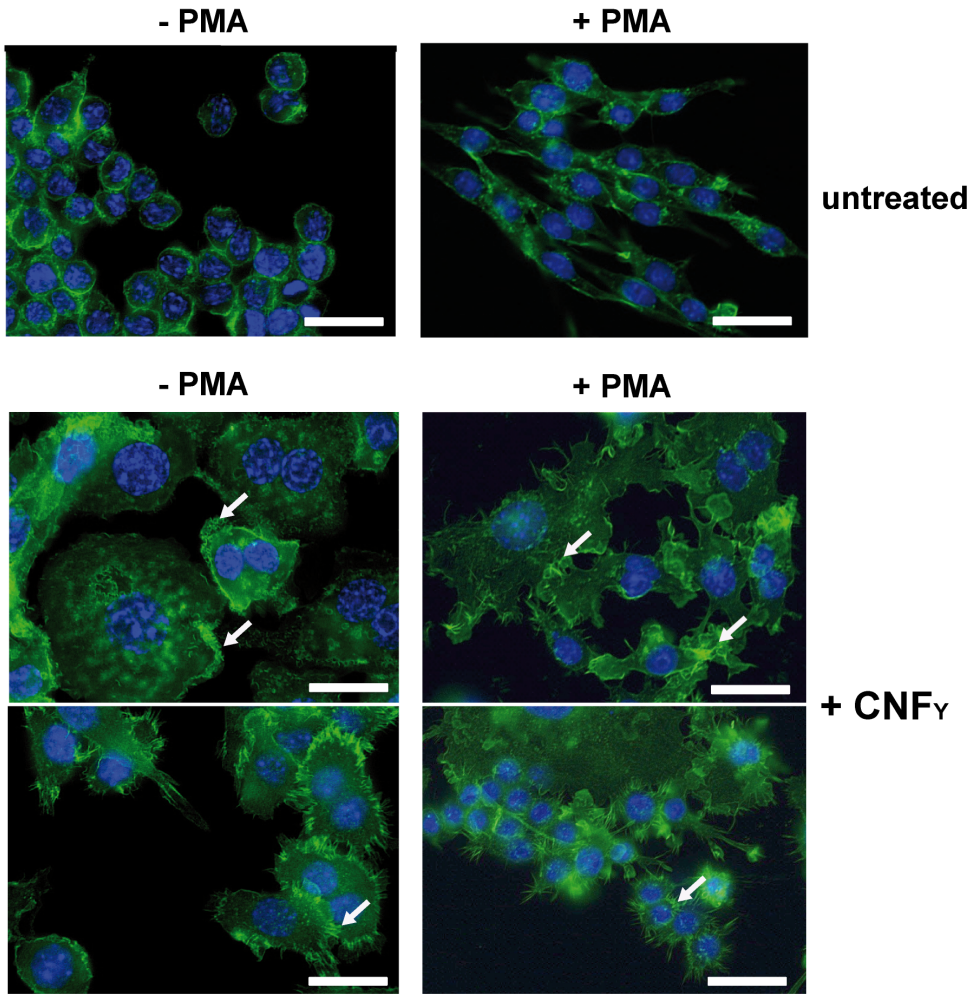

Figure 3.2.2: CNF_Y induces the formation of filopodia, lamellipodia and stress fibres of mature and immature murine macrophages.
Unstimulated (-PMA) or stimulated (+ PMA/48 h) murine macrophages J774A.1 were treated with 10 nM recombinant CNF_Y or the same amount of PBS for 24 h. Nuclei were stained with DAPI (blue), F-actin with FITC-conjugated phalloidin. Arrows show membrane ruffles, filopodia and stress fibres induced by CNF_Y intoxication. White bars indicate 20 μm.

No difference in the effect of CNF_Y on immature or mature macrophages regarding the cellular shape could be observed. However, the cells formed filopodia, lamellipodia and stress fibres, indicating the activation of the three Rho-GTPases Rac1, Cdc42 and RhoA. Subsequent Rho-GTPase activation assays of the three GTPases in the macrophages J774A.1 and the epithelial cells HEp-2 showed that CNF_Y, incubated for three hours on the cells, induces the activation of the tested GTPases (see Figure 3.2.3). The activation pattern as well as the whole GTPase contents varied, depending on the concentration of the toxin.

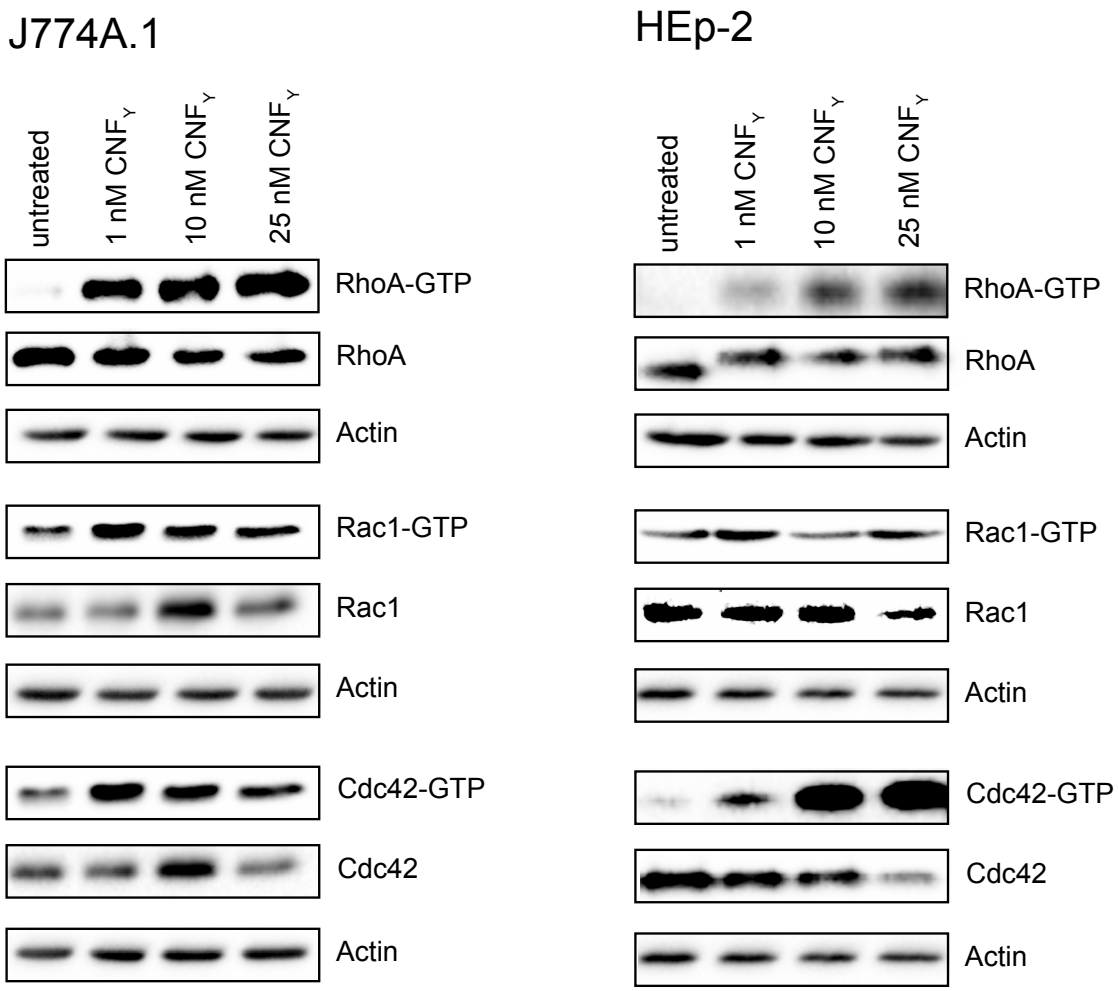

Figure 3.2.3: CNF_Y intoxication leads to the activation of the three small Rho-GTPases RhoA, Rac1 and Cdc42 in murine macrophages and human epithelial cells.
J774A.1 macrophages and HEp-2 epithelial cells were treated with 1, 10 or 25 nM recombinant CNF_Y or the same amount of PBS for 3 h. Cells were lyzed and aliquots taken for western blot analysis of total protein contents. The rest of the samples was used to isolate the activated GTPases Rac1-/Cdc42-GTP or RhoA-GTP using PAK1- or rhotekin-coupled beads, respectively. Using specific antibodies against RhoA (24 kDa), Rac1 (21 kDa) and Cdc42 (25 kDa), the activated and total protein contents of the lysates could be detected. As a loading control actin (45 kDa) was detected with a specific antibody.

The lowest concentration of 1 nM CNF_Y was sufficient to activate especially RhoA, but also Rac1 and Cdc42 in the macrophages, whereas the HEp-2 cells do not seem to be as susceptible to the CNF_Y treatment as macrophages. For the HEp-2 cells, a distinct activation of RhoA and Cdc42 is only detectable at concentrations of 10 nM and 25 nM. However, the basal activation level of Rac1 seems to be quite high in both cell lines. A RhoA shift due to the deamidation of a conserved glutamine is already clearly visible with 1 nM toxin in the HEp-2 cells, whereas it is not detectable even at higher CNF_Y concentrations in the treated J774A.1 cells. Additionally, Rac1 but predominantly Cdc42

seem to be degraded with higher CNF_Y concentrations in the HEp-2 cells, which was shown before for RhoA upon CNF_1 treatment (Doye *et al.*, 2002).

Taken together, CNF_Y treatment at these specific conditions leads to the activation of the three Rho-GTPases RhoA, Rac1 and Cdc42 in the tested cell lines. Very low concentrations are sufficient to activate the GTPases in J774A.1 cells, whereas higher concentrations of CNF_Y are needed to achieve an equal activation level in HEp-2 cells.

3.3 Impact of CNF_Y on the virulence of *Y. pseudotuberculosis*

Due to the overall high expression of *cnfY* and the impact on the cell morphology and Rho-GTPase activation state, it was essential to determine a possible impact of CNF_Y during the course of infection in the mouse model. To this purpose, a *cnfY* mutant strain was constructed by exchanging the functional *cnfY* gene against the kanamycin resistance gene.

3.3.1 CNF_Y is crucial for the virulence of *Y. pseudotuberculosis*

To evaluate the contribution of CNF_Y during infection with *Y. pseudotuberculosis* YPIII, a mouse survival experiment was conducted. Groups of 10 BALB/c mice were infected orally with *Y. pseudotuberculosis* wild-type or the *cnfY* mutant strain YP147 both harbouring either a complementation plasmid carrying the *cnfY* gene under control of its own promoter (pJNS10) or the empty vector (pJNS11).

A lethal infection dosis (2×10^9 bacteria/mouse) was used and mice were monitored day-to-day for a period of 14 days for their body weight and general appearance, e.g. rough fur. Mice with less than 80% of their start-up weight were recorded as dead and the date of death was noted. Figure 3.3.1 shows the survival (A) and the body weight curves (B) of the mice.

The wild-type strain infected mice developed severe symptoms of disease with a fast weight reduction and succumbed within six days post infection. Oppositely, all mice infected with the *cnfY* mutant strain survived and displayed only mild symptoms of disease until day five or six when they started recovering and regaining weight. The effect of the *cnfY* loss could be reverted by introducing the complementation plasmid pJNS10 (P_{cnfY}::*cnfY*, ori SC101*). Even a minimal reduction in the average survival time of the mice, approximately by one day (not significant), was detected probably because of a slight overexpression of the toxin.

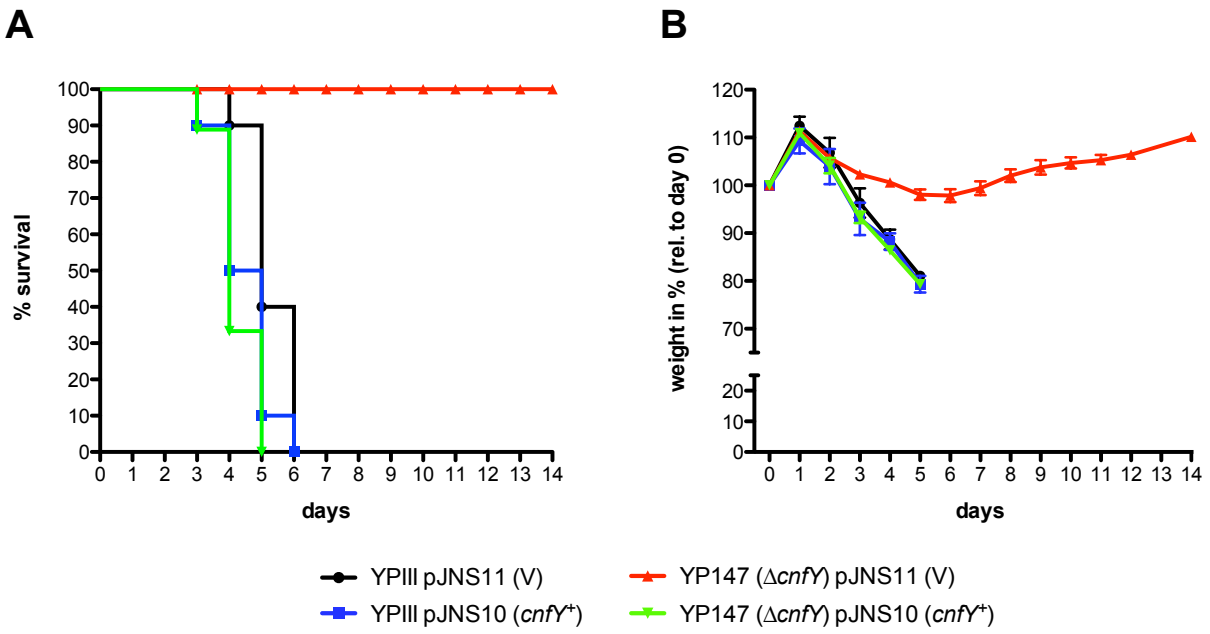

Figure 3.3.1: The *cnfY* mutant strain is avirulent in a mouse survival experiment, yet causes body weight reductions of mice up to five days post infection.
Groups of 10 BALB/c mice were infected orally with 2 x 10^9 bacteria of *Y. pseudotuberculosis* YPIII pJNS11 (empty vector), YP147 (Δ*cnfY*) pJNS11 (empty vector), YPIII pJNS10 (*cnfY*$^+$; complementation plasmid) or YP147 (Δ*cnfY*) pJNS10 (*cnfY*$^+$; complementation plasmid). Two independent experiments were performed. (A) Survival of infected mice was monitored for 14 days. (B) Body weight of infected mice was recorded for 14 days. Mice with a weight reduction over 20% were sacrificed and noted as dead.

Due to a defect in the allele of *phoP*, *Y. pseudotuberculosis* YPIII is not able to replicate in macrophages, unlike other *Y. pseudotuberculosis* strains (Grabenstein *et al.*, 2004). To rule out the possibility that the effect of CNF_Y on the virulence might only be visible in a *phoP*-deficient derivative with an overall lower pathogenicity, the defective *phoP* allele was exchanged against the functional *phoP* of *Y. pseudotuberculosis* IP32953 enabling the YPIII strain to replicate within macrophages. Groups of 10 BALB/c mice were infected orally with 2 x 10^9 bacteria of the *phoP*$^+$ YPIII strain (YP149) and the *phoP*$^+$ YPIII strain without *cnfY* (YP188). Survival and body weight of the mice were recorded as described above. All mice infected with the *phoP*$^+$ strain died within five days post infection, whereas 80% of the mice infected with the corresponding *cnfY* mutant strain survived and regained weight six days post infection (see Figure 3.3.2).

In summary, the activity of CNF_Y is highly important for the pathogenicity of *Y. pseudotuberculosis* YPIII, independently of the presence of a functional *phoP*. Loss of CNF_Y renders the *Y. pseudotuberculosis* YPIII strain avirulent.

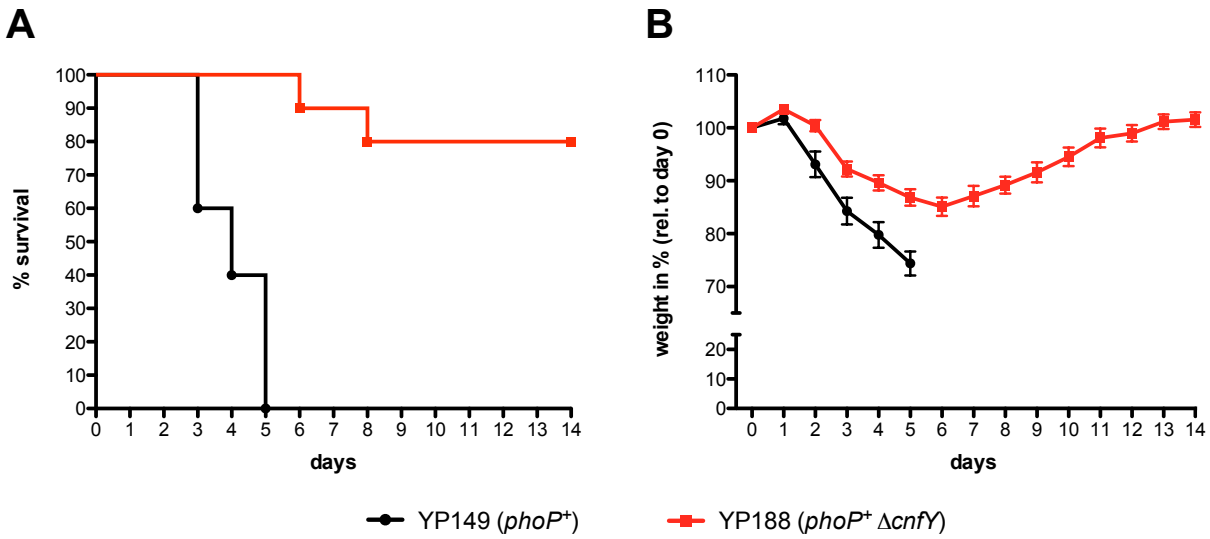

Figure 3.3.2: The introduction of a functional *phoP*$^+$ into *Y. pseudotuberculosis* YPIII does not change the impact of CNF$_Y$ on virulence significantly.
Groups of 10 BALB/c mice were infected orally with 2 x 10^9 bacteria of *Y. pseudotuberculosis* YP149 (*phoP*$^+$) or YP188 (*phoP*$^+$ Δ*cnfY*). (A) Survival of infected mice was monitored for 14 days. (B) Body weight of infected mice was recorded for 14 days. Mice with a weight reduction over 20% were sacrificed and noted as dead.

3.3.1.1 CNF$_Y$ is crucial for efficient colonization of mesenteric lymph nodes and the systemic organs

CNF$_Y$ seems to be crucial for the virulence of *Y. pseudotuberculosis*, as described above. To determine the stages during the infection in which CNF$_Y$ might be particularly relevant, oral infection experiments have been performed to detect the bacterial loads in the different organs during the infection process. Hence, groups of 5 BALB/c mice were infected orally with 2 x 10^8 bacteria and sacrificed after different time points (1 - 7 days). Small intestine, caecum, PP, MLNs, spleen, and liver were isolated, homogenized and dilutions of the homogenates were plated to determine the bacterial numbers per gram tissue.

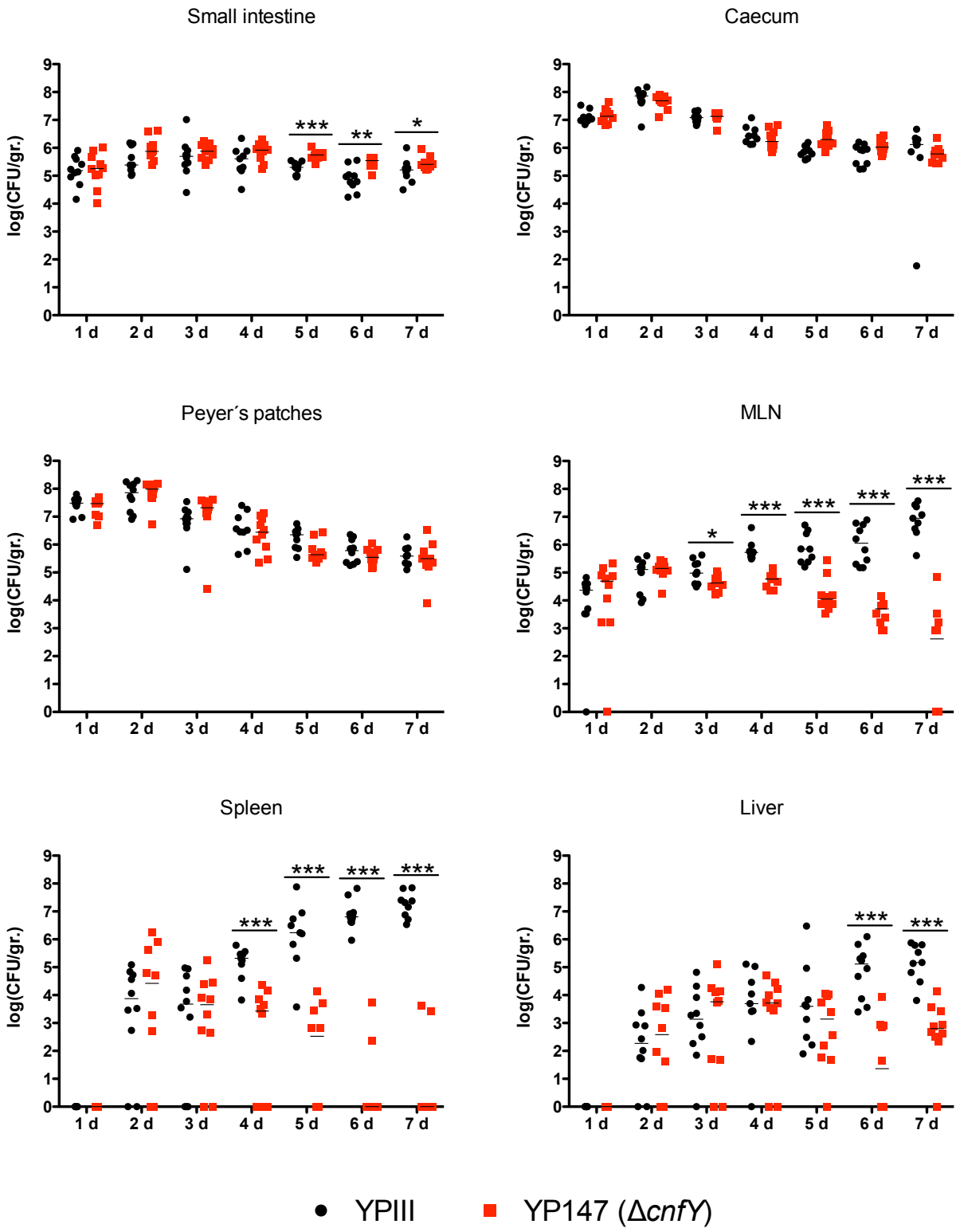

Figure 3.3.3: The loss of *cnfY* leads to clearance of *Yersinia* in MLNs, spleen and liver in the later infection phase.

Groups of 5 BALB/c mice were infected orally with 2 x 10^8 bacteria of *Y. pseudotuberculosis* YPIII or YP147 (Δ*cnfY*). At 1 - 7 days post infection, mice were sacrificed and the organs (small intestine, PP, caecum, MLNs, spleen, and liver) isolated. Homogenized organs were plated and the bacterial load (CFU) per gram tissue determined. The figure displays results of two independent experiments. For statistical analysis, a Mann-Whitney test was applied to determine significant differences in bacterial colonization of

the organs between YPIII- and YP147 (Δ*cnfY*)-infected mice. Asterisks indicate the significances, with * (P<0.05), ** (P<0.01) and *** (P<0.001).

Figure 3.3.3 depicts the bacterial loads at different infection periods in the organs. No difference in the colonization ability in caecum and PP between the two strains was detected. Surprisingly, at day five to seven a slightly higher amount of the *cnfY* mutant bacteria could be reisolated from the small intestine. This was probably due to shortening of the gut (a sign of inflammation; see below). The *cnfY* mutant strain is able to colonize the MLNs up to two days post infection, however after three days, the mutant strain seems to be cleared out of this tissue, whereas the wild-type strain is able to replicate therein. The clearance of the mutant strain out of the MLNs is even more pronounced four to seven days post infection. Clearance of the *cnfY* mutant is also visible in the systemic organs spleen and liver, starting at day four or five post infection. These data suggest that CNF_Y might be more important in the late infection phase for the colonization of the MLNs, spleen, and liver. With the loss of CNF_Y, *Y. pseudotuberculosis* YPIII is no longer able to colonize the host sufficiently to induce a severe infection.

In addition to the differences in colonization of the systemic organs spleen and liver, these organs displayed macroscopic differences such as size and colour during infection. The spleen of mice infected with the wild-type strain shrinked and displayed a pale red colour, whereas the spleens of the mice infected with the *cnfY* mutant strain enlarged (see Figure 3.3.4 A) and were intensely red coloured over time (data not shown). Also the livers of mice infected with the strain YPIII were less red and shrinked, whereas the livers of the mice infected with the *cnfY* mutant were deep red, but showed no difference in their weights (see Figure 3.3.4 B). Additionally, the gut lengths of the mice infected with the two strains differed significantly. The small intestine of mice infected with the wild-type strain was significantly shorter after six to seven days post infection, a sign of severe inflammation as the intestinal length correlates to inflammation (see Figure 3.3.4 C). This indicates that CNF_Y is not only affecting the colonization of the systemic organs by YPIII, but also induces a different intestinal inflammation despite similar bacterial amounts.

In summary, CNF_Y seems to induce severe inflammation in the gut and leads to the shrinking of the systemic organs spleen and liver, in which CNF_Y seems to be important for the bacterial colonization.

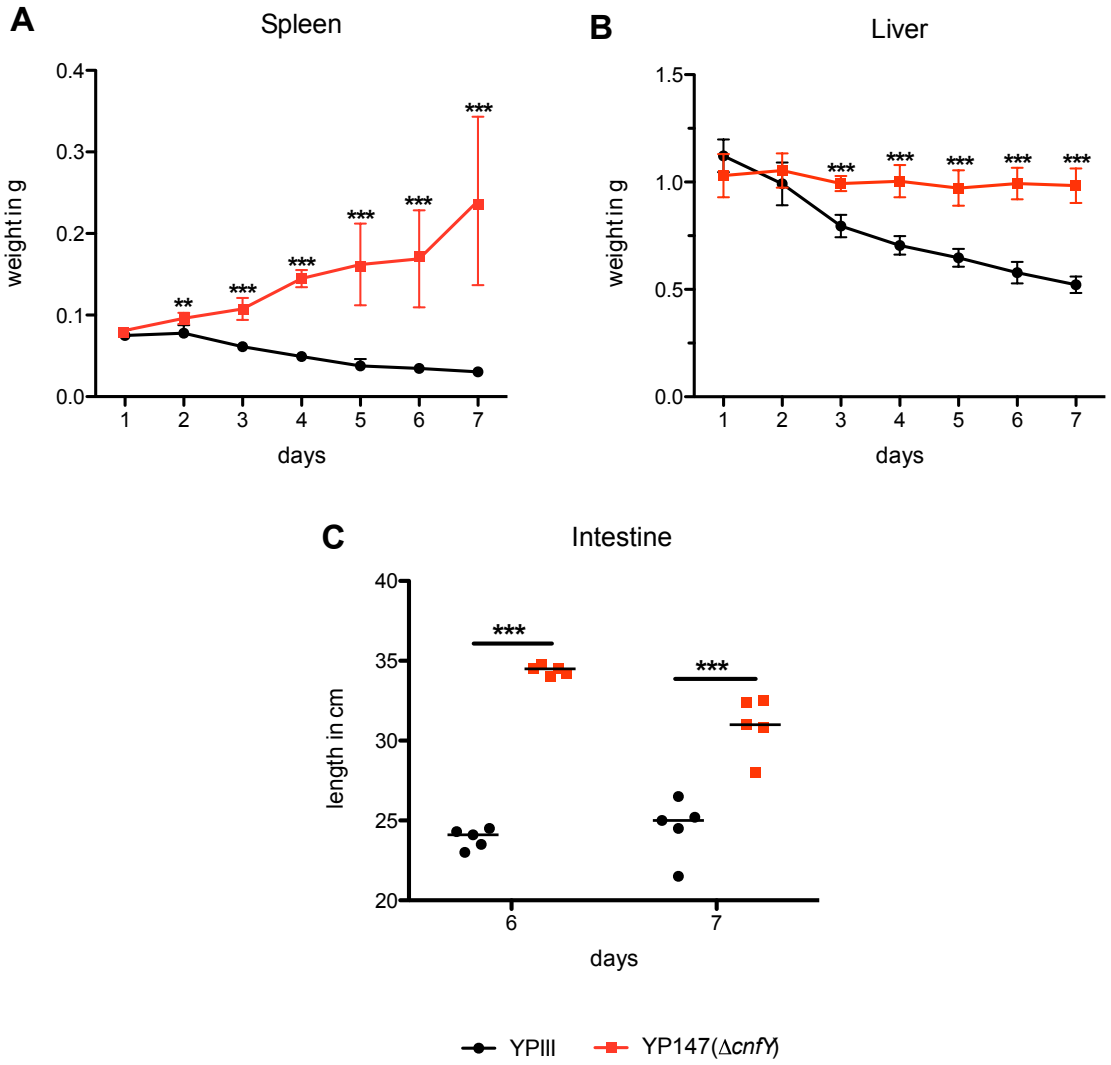

Figure 3.3.4: CNF_Y induces shrinkage of spleen and liver and shortening of the gut length of infected mice.

Groups of 5 BALB/c mice were infected orally with 2 x 10^8 bacteria of *Y. pseudotuberculosis* YPIII or YP147 (Δ*cnfY*). Mice were sacrificed and the organs (small intestine, spleen, and liver) isolated. Figure A and B display results of two independent experiments, figure C of one experiment. (A) Spleen and (B) liver weights were monitored each day up to seven days post infection. (C) Lengths of intestines were determined 6 and 7 days after infection. For statistical analysis, a Mann-Whitney test was applied to determine significant differences between the tissues of YPIII- and YP147 (Δ*cnfY*)-infected mice. Asterisks indicate the significances, with ** (P<0.01) and *** (P<0.001).

3.3.2 CNF_Y leads to highly inflamed tissues

As mentioned above, the infection with *Y. pseudotuberculosis* wild-type or the *cnfY* mutant leads to differences in the overall appearance of the isolated organs. To analyze the impact on the different tissues, histopathological analysis of the small intestine, caecum, colon, MLNs, spleen, and liver was performed. Groups of 3 BALB/c mice were infected orally with 2 x 10^8 bacteria for three or six days, the organs were isolated and embedded in formaldehyd. The sections were stained with hematoxylin-eosin (H & E) and blindly evaluated. The histopathological analysis was performed by Dr. Marina C. Pils of the „Mouse Pathology, Animal Experimental Unit“ of the Helmholtz Centre for Infection Research.

The overall inflammation of the examined tissues of YPIII infected mice was significantly higher in comparison to the tissue of the mice infected with the *cnfY* mutant strain. The inflammatory response was especially evident in the gut and the spleens of the animals. The intestinal inflammation was most pronounced in the ileum and the caecum in both groups.

Figure 3.3.5 shows microscopic pictures of the small intestine and the spleen of YPIII- and YP147 (Δ*cnfY*)-infected or untreated mice six days post infection. The ileum of the mice infected with the wild-type strain was overall severely inflamed with disrupted villi and a thickened lamina propria (see Figure 3.3.5 A/ B). However, the inflammation of the ileum of YP147 (Δ*cnfY*)-infected mice was locally restricted with the formation of multifocal lesions characterized by the presence of inflammatory cells from the muscular layer up to the epithelial cells (see Figure 3.3.5 A/B). The inflammation in these spots led to an enlargement of the villi length, due to epithelial cell hyperplasia (increased proliferation), but did not affect the flanking tissue.

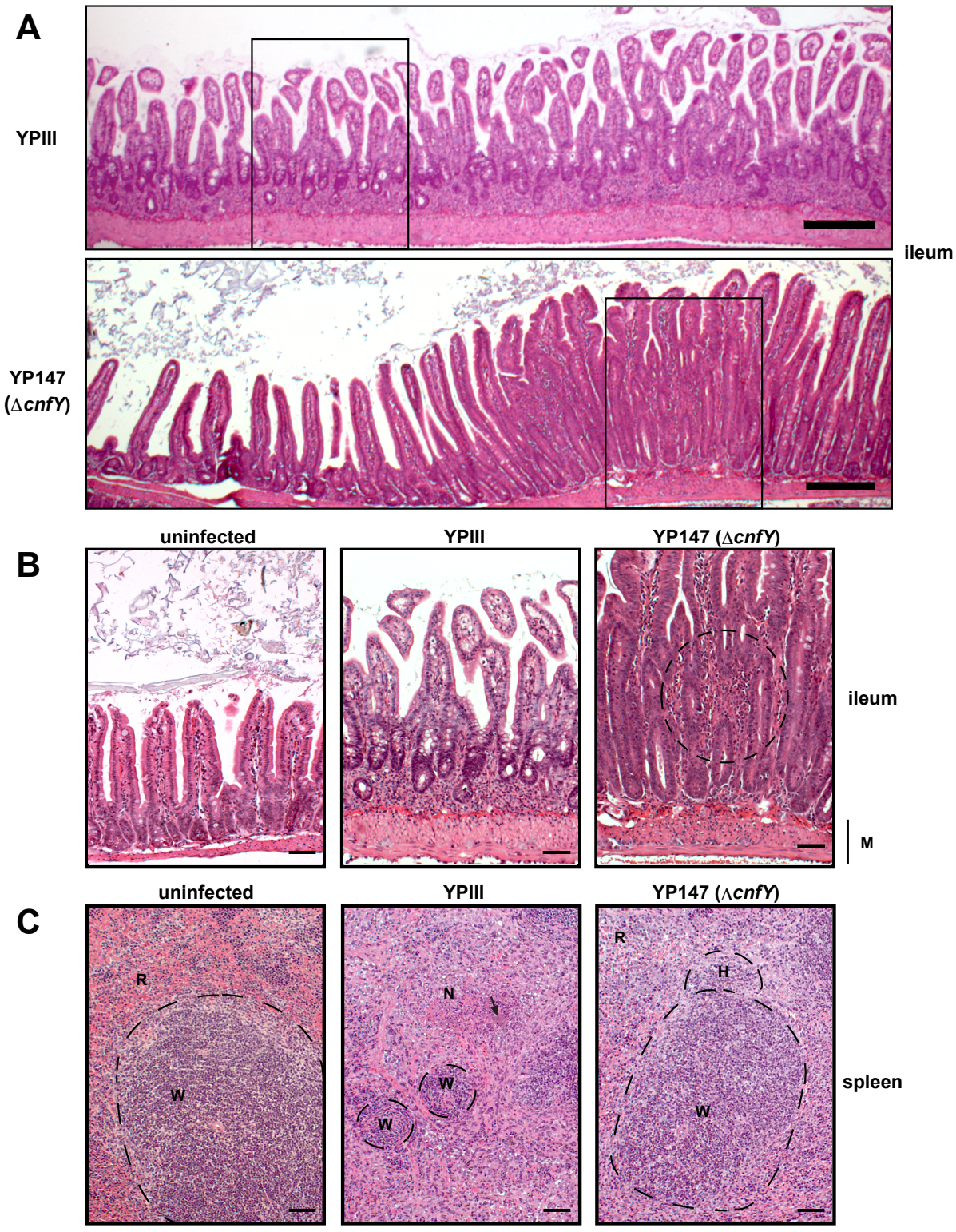

Figure 3.3.5: CNF_Y leads to a highly inflamed intestine and necrosis in the spleen.
Groups of 3 BALB/c mice were infected orally with 2 x 10^8 bacteria of *Y. pseudotuberculosis* YPIII or YP147 (Δ*cnfY*). Mice were sacrificed six days post infection, organs (ileum and spleen) isolated and sections stained with H & E. (A) Representative light microscopic picture of an ileum of YPIII- and YP147 (Δ*cnfY*)-infected animals. YPIII induces diffuse invasion of inflammatory cells into the lamina propria. YP147 (Δ*cnfY*) induces invasion of inflammatory cells into the lamina propria at occasional inflammatory areas. Black bar represents 200 µm. Boxes indicate magnified areas shown in figure B. (B) Representative light microscopic pictures of an ileum of an uninfected mouse, the magnified ileum of a YPIII-infected

mouse, and the magnified ileum of a YP147 (Δ*cnfY*)-infected mouse, showing an occasional inflammatory area. The circle indicates focal invasion of inflammatory cells. Black bar represents 50 µm. (C) Representative light microscopic picture of a spleen of an uninfected mouse, of a YPIII-infected mouse with splenic atrophy and a bacterial microcolony surrounded by necrosis, and of a YP147 (Δ*cnfY*)-infected mouse, showing hyperplasia of the white pulp and activated lymphoid follicle. Bar represents 50 µm. Arrow indicates bacterial foci. W: white pulp (dashed line); N: necrosis; H: hyperplasia; R: red pulp; M: muscularis mucosa.

In the spleens of mice infected with the *cnfY* mutant strain, no bacterial microcolonies (diffuse patches of bacteria) could be detected under the light microscope with the H & E staining three or six days post infection. However, in prepared cryosections with fluorescent YP147 (Δ*cnfY*) bacteria harbouring a constitutively expressed *dsred2* reporter gene (pFU228), few microcolonies could also be detected in the spleen three days post infection (see Figure S1). Most spleens of YPIII-infected mice in contrast contained many bacterial microcolonies, already visible in the H & E stained spleen sections six days post infection (see Figure 3.3.5 C). In addition to the higher amounts of bacteria, the inflammation in these spleens was more severe in comparison to the spleens of YP147 (Δ*cnfY*)-infected animals and showed areas of multifocal necrosis. The bacteria in the spleens of YPIII-infected mice resulted in necrotizing splenitis leading to splenic atrophy with marked depletion of the white pulp. However, the spleens of YP147 (Δ*cnfY*)-infected mice only displayed mild hyperplasia of the white pulp and an influx of red blood cells (erythropiesis) (see Figure 3.3.5 C). Nevertheless, necrotic areas could also be detected in the livers infected with YPIII (data not shown).

In summary, CNF_Y leads to a severe, wide-spread inflammation in the gut particularly in the ileum. This enables the bacteria to effectively colonize the spleen, and causes necrosis in the systemic organs spleen and liver.

3.3.3 CNF_Y triggers the release of multiple proinflammatory cytokines

Due to the inflammatory response visible in the histopathological analysis, the serum cytokine response triggered upon an infection of mice with YPIII or YP147 (Δ*cnfY*) in comparison to untreated mice, was measured. Hence, groups of 5 BALB/c mice were infected orally with 2 x 10^8 bacteria, heart blood was taken, the serum prepared, and the level of released cytokines (eotaxin, G-CSF, GM-CSF, IFN-γ, IL-10, IL-12 (p40), IL-12 (p70), IL-13, IL-15, IL-17, IL-1α, IL-1β, IL-2, IL-3, IL-4, IL-5, IL-6, IL-7, IL-9, IP-10, KC-like, LIF, LIX, M-CSF, MCP-1, MIG, MIP-1α, MIP-1β, MIP-2, RANTES, TNF-α and

VEGF) was measured by an immunology multiplex assay, measured with the Luminex® detection system.

Figure 3.3.6 represents the released proinflammatory cytokines in the serum, which showed different levels upon infection with the two strains (eotaxin, tumor necrosis factor-α (TNF-α), macrophage inflammatory protein-1β (MIP-1β), interleukin 6 (IL-6), granulocyte macrophage colony-stimulating factor (GM-CSF), and IL-12 (p40)).

The secretion was generally higher upon infection with the wild-type strain YPIII, indicating a severe inflammation when CNF_Y is present, thus supporting the histopathological data (see above). The GM-CSF median concentration in the serum of YPIII-infected mice was 1.1 times higher compared to YP147 (Δ*cnfY*)-infected animals. This cytokine is secreted by different immune cells, e.g. macrophages or NK cells and increases the inflammation by stimulating the production of further immune cells (e.g. neutrophils) and the maturation of monocytes to macrophages and DCs (Shi *et al.*, 2006). The IL-12 (p40) median concentration in the serum of YPIII-infected mice was 1.5 times higher in comparison to YP147 (Δ*cnfY*)-infected animals. IL-12 (p40) is a subunit of IL-12 and mainly produced by DCs and macrophages. It induces the production of cytokines from NK cells and T cells, enhances the cytotoxic activity of NK cells, and stimulates cytotoxic T cell proliferation (Trinchieri, 1995). The median concentration of TNF-α in the serum of YPIII-infected mice was also 1.5 times higher when compared to YP147 (Δ*cnfY*)-infected animals. TNF-α is primarily produced by macrophages, but also by T cells and results in the activation of neutrophils and further proinflammatory responses (Gifford & Flick, 1987).

The median concentration of the chemokine eotaxin was 2 times higher in the serum of YPIII-infected mice in comparison to YP147 (Δ*cnfY*)-infected animals. Different cell types, but mainly fibroblasts produce eotaxin in response to allergic stimuli or parasites, leading to the recruitment of eosinophils (Griffiths-Johnson *et al.*, 1993; Jose *et al.*, 1994). The median concentration of MIP-1β in the serum of YPIII-infected mice was also increased twofoldly in comparison to YP147 (Δ*cnfY*)-infected animals. MIP-1β is a chemokine secreted by macrophages, which activates inflammatory responses, resulting in the secretion of IL-6 or TNF-α (Sherry *et al.*, 1988). However, the most significant changes were detected in the concentration measured for the IL-6. A median concentration in the serum of YPIII-infected mice, which was 4 times higher in comparison to YP147 (Δ*cnfY*)-infected animals could be detected. IL-6 plays a cruicial

role in the transition from innate to adaptive immune response and is mainly produced by macrophages, but also by T cells and endothelial cells (Jones, 2005).

In summary, these data suggest that CNF_Y leads to the secretion of proinflammatory cytokines and induces an increased inflammation in the host.

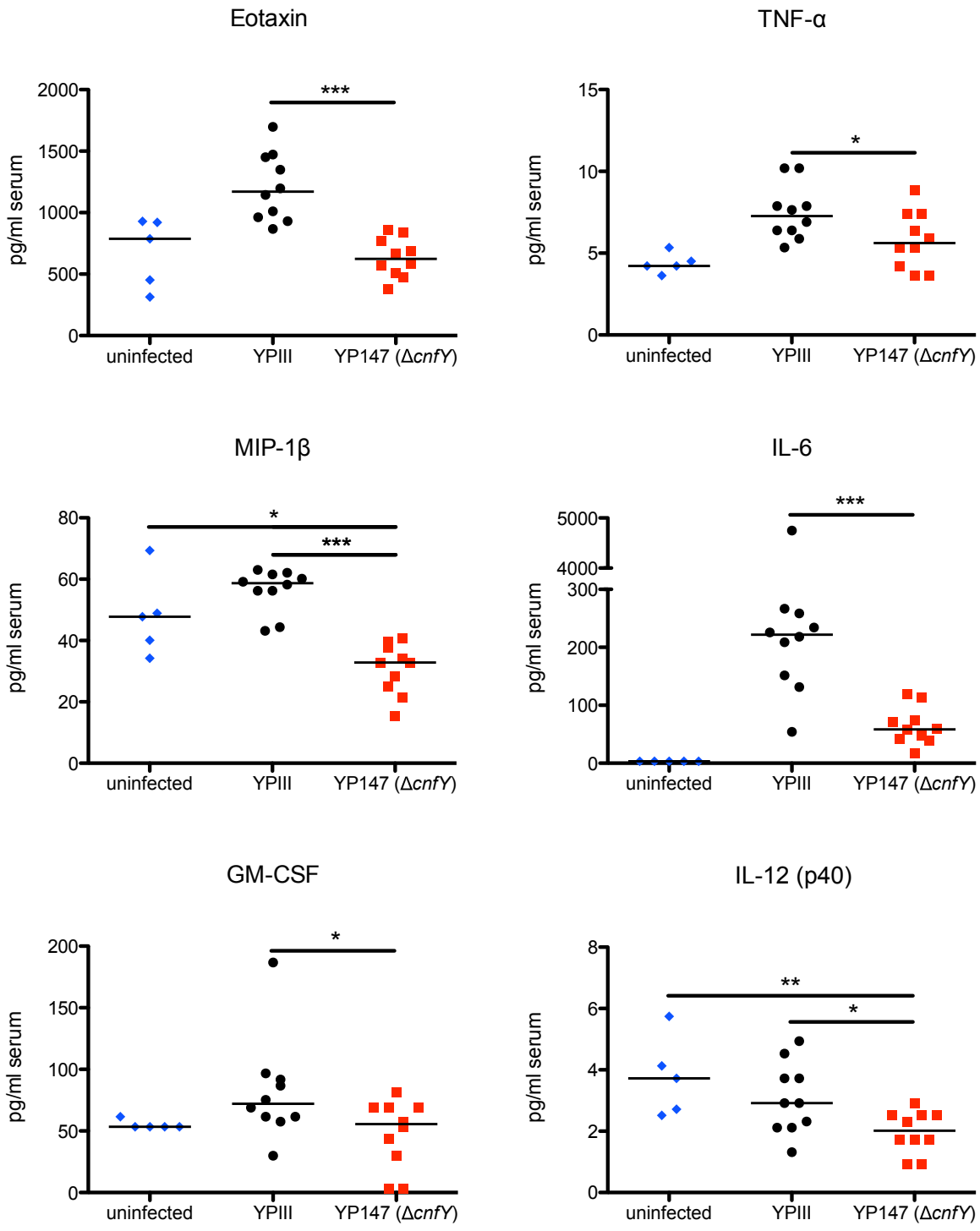

Figure 3.3.6: CNF_Y induces higher proinflammatory cytokine levels in the serum of infected mice.

Groups of 5 BALB/c mice were infected orally with 2 x 10^8 bacteria of *Y. pseudotuberculosis* YPIII or YP147 (Δ*cnfY*). Three days after infection, mice were sacrificed and serum prepared. A quantitative cytokine (eotaxin, TNF-α, MIP-1β, IL-6, GM-CSF, and IL-12 (p40)) analysis was performed. Scatter dot plots show the median of two independent experiments. For statistical analysis, a Mann-Whitney test was applied to determine significant differences in the serum cytokine levels between YPIII-infected, YP147 (Δ*cnfY*)-infected or uninfected mice. Asterisks indicate the significances, with * (P<0.05), ** (P<0.01) and *** (P<0.001).

3.3.4 CNF_Y modulates the host immune response

The differences in the colonizing abilities of the strains in the MLNs, spleen and liver and the harsh influx of proinflammatory cytokines due to the infection with YPIII led to the assumption that the triggered immune response in the lymphatic tissues PP, MLNs, and spleen could differ. These experiments have been performed in cooperation with Jörn Pezoldt of the group „Experimental Immunology“ led by Prof. Dr. Jochen Hühn, of the Helmholtz Centre for Infection Research. Due to preliminary data for infection periods of three and six days (data not shown), a period of three days was chosen for the analysis. These preliminary data suggested that the immune response is already altered at the shorter time point at which the bacterial loads are still quite similar. Furthermore, the health status of mice infected for six days is already severely reduced.

Hence, groups of 5 - 6 BALB/c mice were infected orally with approximately 2 x 10^8 bacteria of *Y. pseudotuberculosis* per mouse. After three days, the PP, MLNs or spleens were isolated, the prepared cell suspensions stained with fluorescently labeled antibodies for different immune cells (neutrophils, macrophages/monocytes, dendritic cells, $CD3^+$ T cells, $CD4^+$ T cells, $CD8^+$ T cells, and B cells) and analyzed by multi-colour flow cytometry. Two different panels of antibodies were used to identify the different cell populations (see Figure S2).

Figure 3.3.7 shows the amounts of isolated neutrophils ($CD11b^+Ly6G^+$), macrophages/monocytes ($CD11b^+Ly6G^-$), DCs ($CD11c^+$), NK cells ($NKp46^+$), B cells ($CD19^+$), and T cells ($CD3^+$) of the different tissues. The innate immune response in the PP was triggered upon infection with both strains, but almost no change in the adaptive immune response was detectable (see Figure 3.3.7 A). Despite the unchanged colonizing abilities of the two strains in the PP, the measured quantities of infiltrated neutrophils differed significantly. The infection with YPIII led to a 100-fold higher amount of neutrophils, whereas the infection with YP147 (Δ*cnfY*) only induced a 40-fold higher influx in comparison to the steady state level of neutrophils in the PP of untreated mice.

Within three days, the numbers of the *cnfY* mutant strain began to decrease in the MLNs, whereas the wild-type strain was able to replicate. Figure 3.3.7 B shows the corresponding immune response in the MLNs. An overall increase of innate as well as adaptive immune cells was detected due to the infections. However, no drastic differences between the strains were visible. Nevertheless, slightly higher amounts of macrophages/monocytes upon infection with YPIII and of T cells upon infection with YP147 (Δ*cnfY*) were detected.

The colonization of the spleen up to day three post infection does not differ significantly between the two strains, yet the immune cell contents show drastic differences (see Figure 3.3.7 C). Already after three days, all tested immune cell populations were significantly decreased upon infection with YPIII, in accordance with the shrinking of the spleen and the necrotic spots in the histopathological analysis. The most significant reduction was visible in the innate immune cell contents. Particularly macrophages, monocytes, and NK cells, were significantly reduced (approximately 15-fold) in comparison to the cell populations in the spleens of untreated animals. This effect was less pronounced in the neutrophil, DC, T cell, and B cell populations.

On the other hand, a significant increase of the immune cells predominantly of neutrophils and macrophages/monocytes, was detectable in mice infected with the *cnfY* mutant. These data are also consistent with the differences in the spleen weight, the histopathological analysis, and the fast clearance of the mutant strain of this tissue after triggering the immune response. Necrosis in the spleen induced by YPIII infection and splenomegaly induced by YP147 (Δ*cnfY*) infection, resulted in significant differences in the overall cell counts for this organ between the groups. Hence, the percentages of populations also for PP and MLNs were determined to test a possible effect of CNF_Y on the steady-state level of a specific cell population. CNF_Y seems not to affect the steady-state level of the cell populations in the PP and MLNs (see Figure S3 A + B). However, a significant expansion of neutrophils and macrophages/monocytes could be detected in the YP147 (Δ*cnfY*)-infected spleens (see Figure S3 C).

Taken together, the measured immune response in the PP and MLNs, the histopathological data of the gut, and the increased secretion of proinflammatory cytokines in the serum suggest that CNF_Y leads to an enhanced inflammatory response. Furthermore, the measured immune response and the histopathological data of the

spleen strongly suggest that CNF_Y reduces an influx and/or leads to a rapid cell death of the infiltrating immune cells.

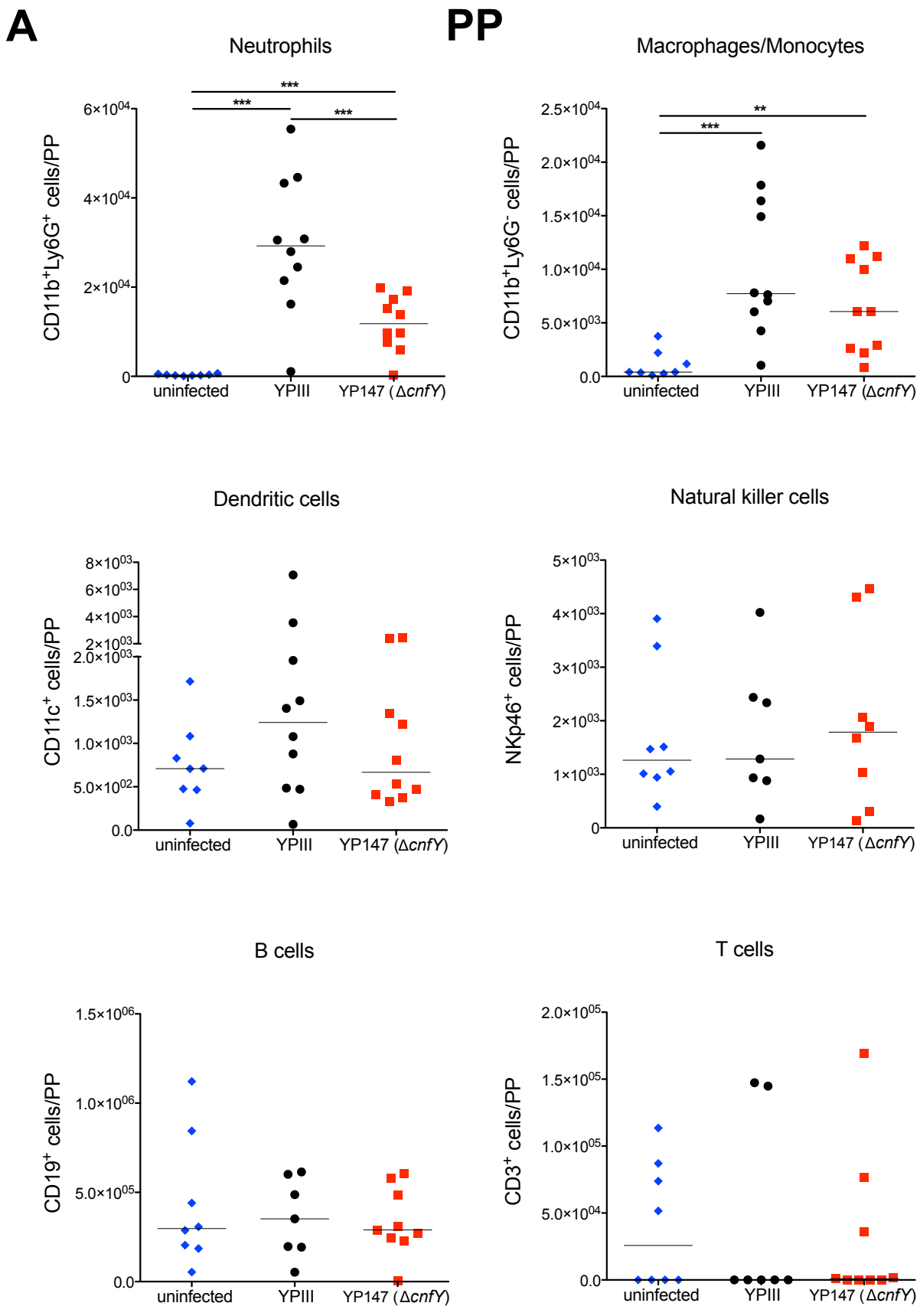

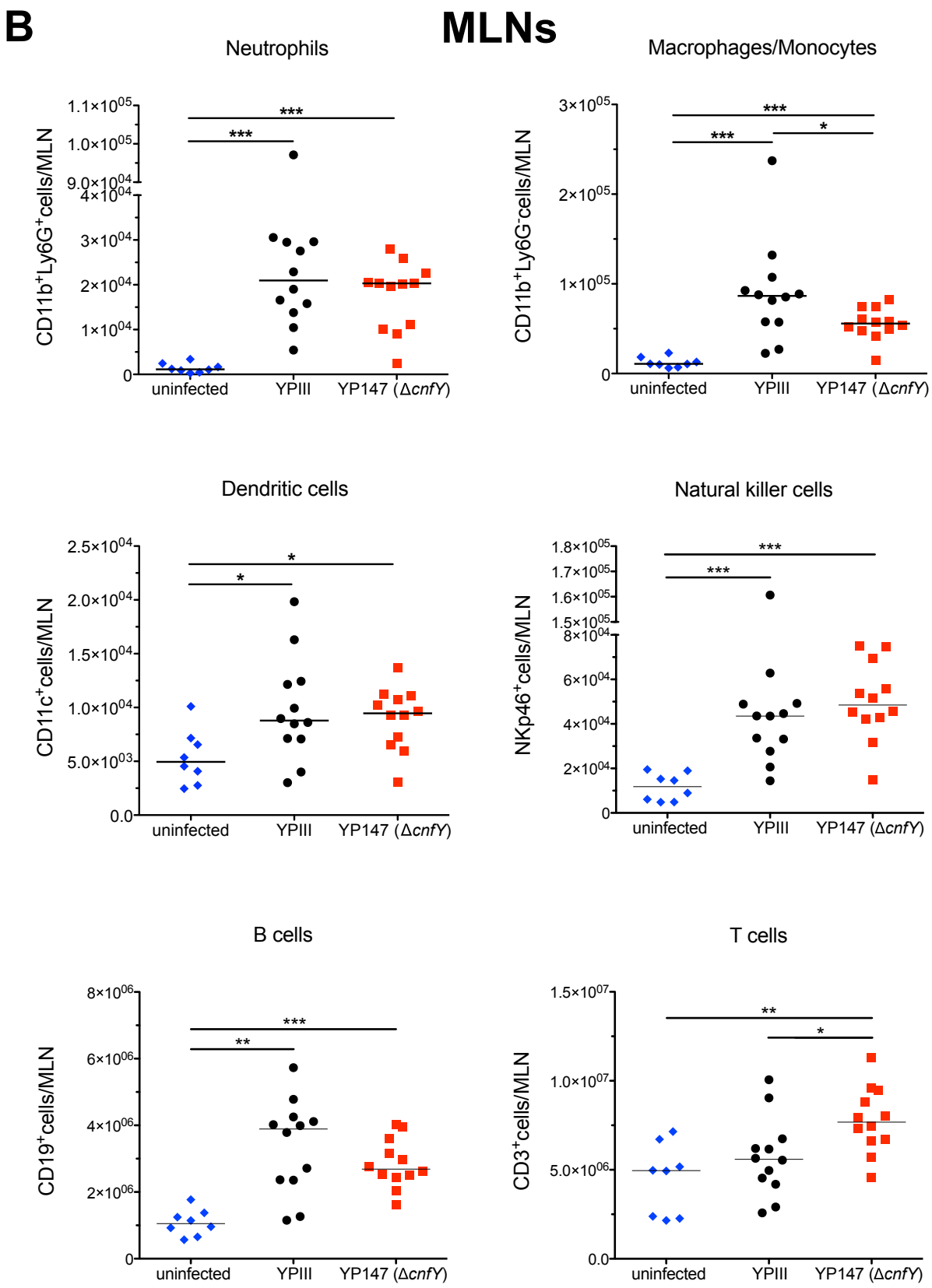
B
MLNs
Neutrophils
CD11b+Ly6G+cells/MLN
1.1×10^05
1.0×10^05
9.0×10^04
4×10^04
3×10^04
2×10^04
1×10^04
0
***
***
uninfected
YPIII
YP147 (ΔcnfY)
Macrophages/Monocytes
CD11b+Ly6G-cells/MLN
3×10^05
2×10^05
1×10^05
0
***
***
*
uninfected
YPIII
YP147 (ΔcnfY)
Dendritic cells
CD11c+cells/MLN
2.5×10^04
2.0×10^04
1.5×10^04
1.0×10^04
5.0×10^03
0.0
*
*
uninfected
YPIII
YP147 (ΔcnfY)
Natural killer cells
NKp46+cells/MLN
1.8×10^05
1.7×10^05
1.6×10^05
1.5×10^05
8×10^04
6×10^04
4×10^04
2×10^04
0
***
***
uninfected
YPIII
YP147 (ΔcnfY)
B cells
CD19+cells/MLN
8×10^06
6×10^06
4×10^06
2×10^06
0
***
**
uninfected
YPIII
YP147 (ΔcnfY)
T cells
CD3+cells/MLN
1.5×10^07
1.0×10^07
5.0×10^06
0.0
**
*
uninfected
YPIII
YP147 (ΔcnfY)

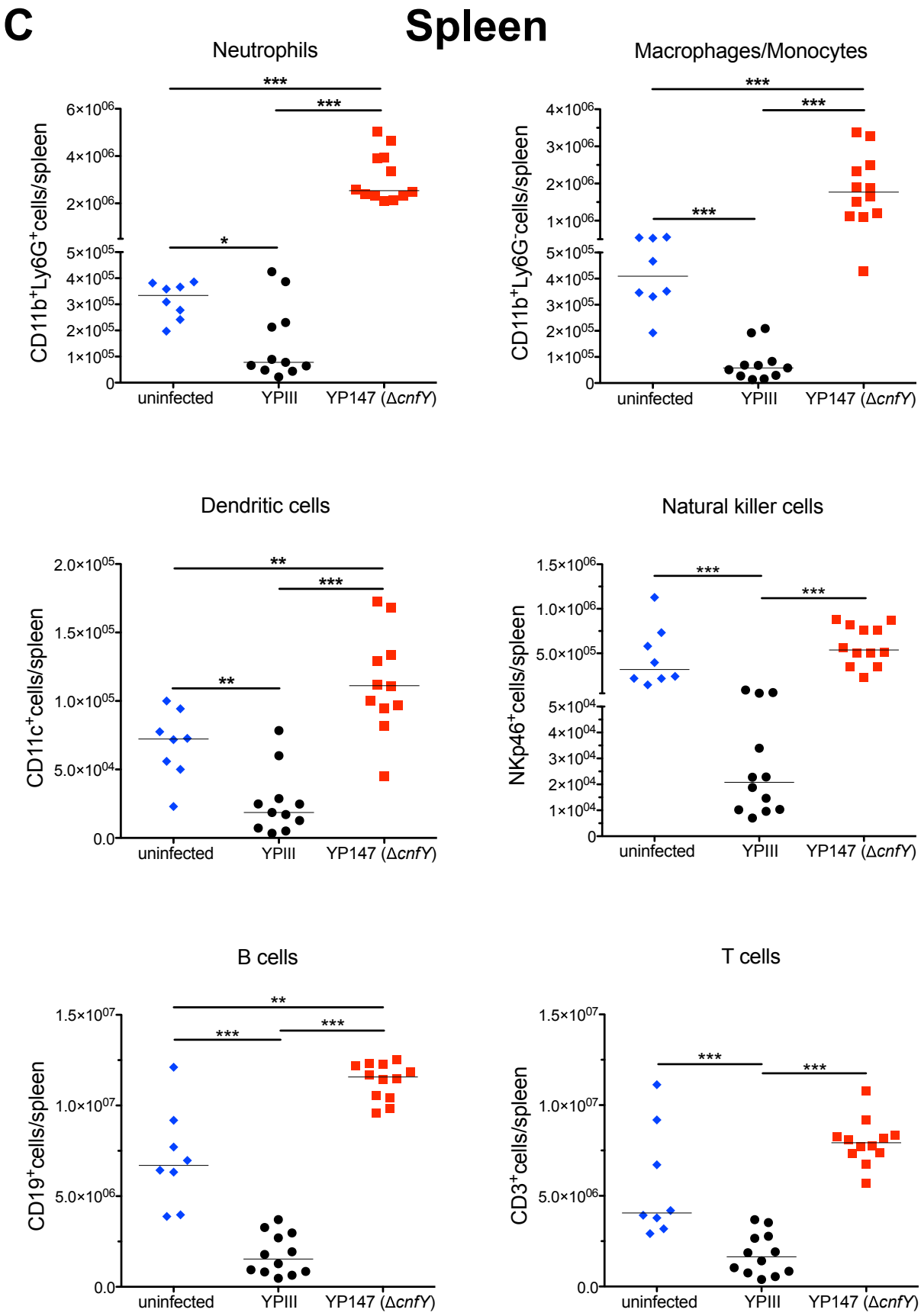

Figure 3.3.7: CNF_Y modulates the host immune response and leads to depletion of immune cells.
Groups of 5 - 6 BALB/c mice were infected orally with 2 x 10^8 bacteria of *Y. pseudotuberculosis* YPIII or YP147 (Δ*cnfY*). Three days after infection, mice were sacrificed and organs (PP, MLNs, and spleen)

isolated. Prepared cell suspensions were stained with fluorescently labeled antibodies to detect the different immune cells with flow cytometry: neutrophils ($CD11b^+/Ly6G^+$), macrophages/monocytes ($CD11b^+Ly6G^-$), DCs ($CD11c^+$), NK cells ($NKp46^+$), B cells ($CD19^+$), and T cells ($CD3^+$). Data plotted on the y axis indicate the cell numbers isolated from uninfected, YPIII-infected of YP147 (Δ*cnfY*)-infected organs. Scatter dot plots show the median of two independent experiments for (A) PP, (B) MLNs, and (C) spleen. For statistical analysis, a Mann-Whitney test was applied to determine significant differences in the numbers of indicated cell types in the whole organ between YPIII-infected, YP147 (Δ*cnfY*)-infected or uninfected mice. Asterisks indicate the significances, with * ($P<0.05$), ** ($P<0.01$) and *** ($P<0.001$).

3.3.5 CNF_Y influence on Yop delivery

Previous infection experiments showed that loss of CNF_Y leads to a clearance of the bacteria from the MLNs, spleen, and liver and avirulence of *Y. pseudotuberculosis* YPIII. Similar effects after oral mouse infections have been reported for YPIII (1) without the virulence plasmid and thus without the T3SS and the Yop effector proteins, (2) with multiple *yop* gene deletions, and (3) without the transcriptional regulator LcrF, a regulator of the T3SS and the Yop effector proteins (Böhme *et al.*, 2012; Logsdon & Mecsas, 2003). Furthermore, a *Y. pestis yopM* mutant strain induced an influx of neutrophils into the spleens of infected mice, whereas the wild-type strain caused a decrease of this cell type, similar to the effects observed in this study (Kerschen *et al.*, 2004; Ye *et al.*, 2009). Moreover, the Yop effector protein YopJ was demonstrated to induce the cell death of professional phagocytes (Monack *et al.*, 1997; Zheng *et al.*, 2011).

These data suggested an interaction or control of the CNF_Y toxin with the Yop machinery during the course of infection. Furthermore, it was recently shown that Rho activation leads to enhanced Yop delivery (Mejía *et al.*, 2008). Therefore, it was hypothesized that the CNF_Y toxin might influence Yop translocation into the innate immune cells by activation of the small Rho-GTPases (Blumenthal *et al.*, 2007; Hoffmann *et al.*, 2004).

3.3.5.1 CNF_Y enhances the Yop delivery into eukaryotic cells

Due to the known impact of CNF_Y on the actin cytoskeleton and the Rho-GTPases of human epithelial cells (see 3.2), these cells were tested for the Yop delivery. Generally, the Yop secretion *in vitro* under secretion inducing conditions did not differ between the wild-type and the *cnfY* mutant strain (data not shown).

In order to test the Yop delivery by *Y. pseudotuberculosis* YPIII into eukaryotic cells, different strains harbouring a YopE-β-lactamase reporter fusion were employed (Harmon *et al.*, 2010). These strains were YP173 (YPIII-ETEM), YP174 (YP101 (Δ*yscS*)-ETEM), and YP217 (YP147 (Δ*cnfY*)-ETEM). Tested cells were stained with the dye CCF4-AM, consisting of coumarin and fluorescein conjugated by a lactam ring. This dye is trapped inside the living cells by estarases and fluoresces green after excitation. After translocation of the YopE β-lactamase fusion protein, the β-lactam ring of the dye is cleaved resulting in a fluorescent shift from green to blue, which allows the detection of Yop translocated cells (Gao *et al.*, 2003; Zlokarnik *et al.*, 1998).

Two approaches were followed to detect the stained translocated cells *in vitro*, (1) visualization and counting with the fluorescent microscope and (2) analysis of translocated cells by flow cytometry. To test the Yop delivery into eukaryotic cells, the cells were either pretreated with the recombinant CNF_Y toxin (25 nM) or the same amount of PBS for three hours. Cells were subsequently infected with an MOI 10 of the strains YPIII/YP147 (Δ*cnfY*) (both without the Yop-β-lactamase reporter fusion as negative controls), YP173 (YPIII-ETEM), YP174 (YP101 (Δ*yscS*)-ETEM) (without functional T3SS; additional negative control), and YP217 (YP147 (Δ*cnfY*)-ETEM) grown at 37°C overnight to achieve a high production of CNF_Y.

No blue cells were detectable in the control groups: untreated, YPIII, YP147 (Δ*cnfY*) or YP174 (YP101 (Δ*yscS*)-ETEM) treated cells. However, a high amount of cells infected with YP173 (YPIII-ETEM) without CNF_Y pretreatment appeared blue, indicating high translocation rates of the YopE-β-lactamase reporter fusion (see Figure 3.3.8 A, B). In contrast, an infection with YP217 (YP147 (Δ*cnfY*)-ETEM) led to significantly reduced levels of Yop delivery, indicating an impact of CNF_Y on Yop delivery. Additional pretreatment of the cells with recombinant CNF_Y led to an even higher translocation rate after infection with both strains. Nevertheless, a significantly higher amount of blue cells was still detectable due to infection with YP173 (YPIII-ETEM), compared to YP217

(YP147 (Δ*cnfY*)-ETEM). In conclusion, Yop translocation into eukaryotic cells is enhanced by the CNF_Y activity.

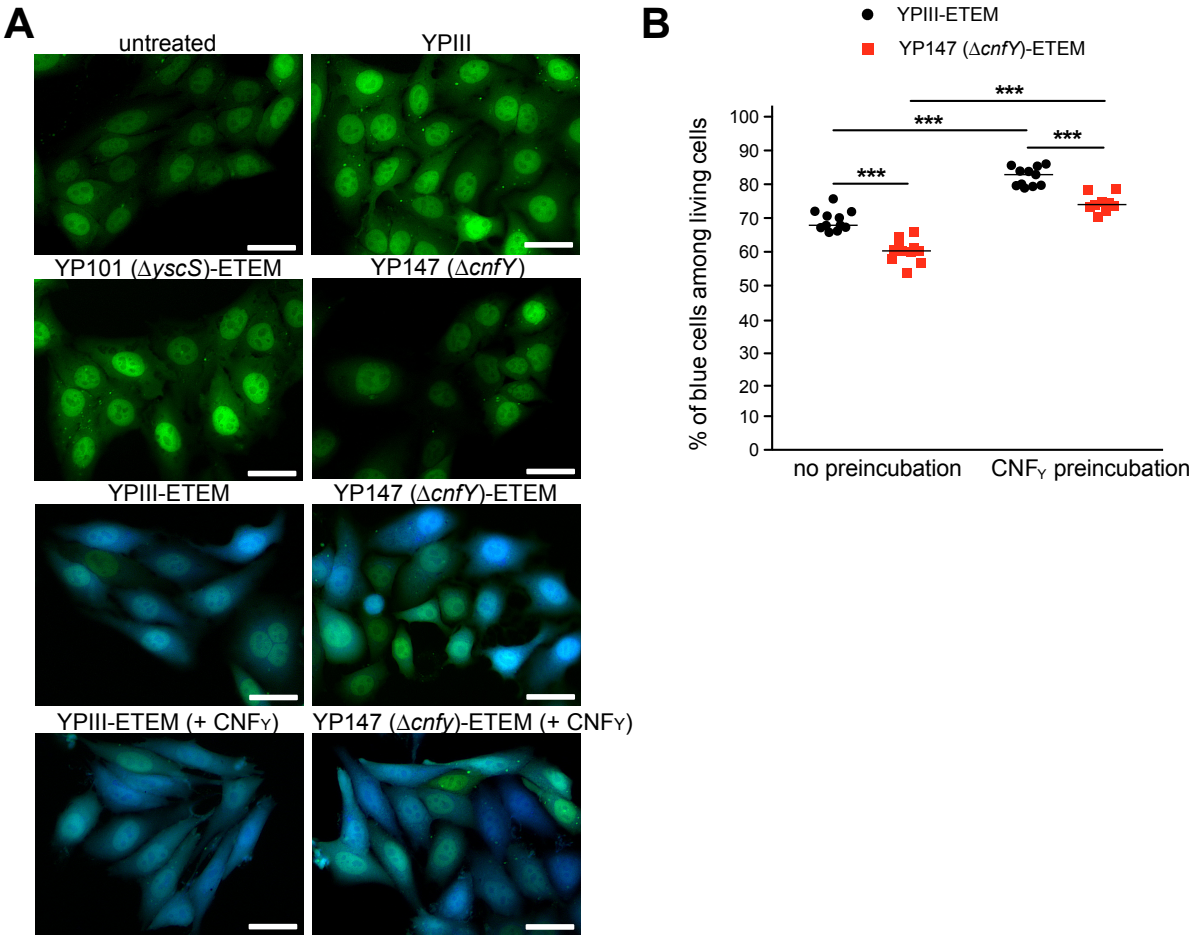

Figure 3.3.8: CNF_Y enhances Yop delivery into human epithelial cells.
Bacteria were pregrown for infection overnight at 37°C to induce the CNF_Y secretion. The human epithelial cells HEp-2 were treated with 25 nM recombinant CNF_Y or the same amount of PBS for 3 h prior infection for 1 h with *Y. pseudotuberculosis* YPIII-ETEM (YP173), YP147 (Δ*cnfY*)-ETEM (YP217), YPIII, YP101 (Δ*yscS*)-ETEM (YP174) or YP147 (Δ*cnfY*), using an MOI of 10. Cells were labeled with the dye CCF4-AM and analyzed: (A) Fluorescent microscopy of the HEp-2 cells. All living cells appear green fluorescent, all Yop translocated cells appear blue fluorescent after excitation. Microscopic pictures are representative for three independent experiments of 3 wells. White bars indicate 20 μm. + CNF_Y indicates preincubation with the toxin. (B) Flow cytometry of the HEp-2 cells. Scatter dot plot represents the median of two independent experiments with 5 - 6 samples. For statistical analysis, a Mann-Whitney test was applied to determine significant differences in the numbers of translocated cells between YPIII-ETEM- and YP147 (Δ*cnfY*)-ETEM-infected cells with or without CNF_Y pretreatment. Asterisks indicate the significances, with *** (P<0.001). ETEM: *yopE-bla*-expressed β-lactamase.

3.3.5.1.1 Activation of Rho is crucial for enhanced Yop delivery

The innate immune cells are known to be the main targets of the T3SS and the Yop effector proteins *in vivo* (Durand *et al.*, 2010). Hence, murine macrophages (J774A.1 and RAW246.7) were tested for the effect of CNF_Y on Yop delivery. Cells were pretreated two hours with recombinant CNF_Y (3 μg/ml (25 nM)) or the same amount of PBS. The subsequent infection was performed with an MOI of 10 with the strain YP173 (YPIII-ETEM) grown overnight at 37°C to increase the expression of CNF_Y. Blue and green cells were counted from fluorescent microscopic pictures. CNF_Y had a boosting effect on the Yop delivery also on the phagocytes, indicating a possible impact of CNF_Y on the innate immune cells *in vivo* (see Figure 3.3.9).

In addition, the Rho-GTPase responsible for the higher translocation rate induced by CNF_Y was determined. Previous publications showed that activation of Rac1 by YadA or invasin is required for the *Yersinia* uptake into epithelial cells (Wong & Isberg, 2005). However, the bacterial internalization as well as the Rac1 activation was not necessary to promote the Yop translocation into HeLa cells by *Y. pseudotuberculosis* (Mejía *et al.*, 2008). These data prompted the hypothesis that CNF_Y might induce the enhanced Yop delivery especially via RhoA activation. Hence, Rho-GTPase interacting bacterial toxins were used to specifically inhibit the different GTPases. For this purpose J774A.1 or RAW264.7 macrophages were pretreated two hours with (1) the C3 toxin (0.5 μg/ml, 1 μgml) of *C. botulinum* an ADP-ribosylating protein that specifically inhibits RhoA, B and C or (2) the toxin B (85 ng/ml, 250 ng/ml) from variant *C. difficile* serotype F strain 1470 (TcdBF), which specifically inhibits Rac, but not RhoA/B/C (Aktories & Hall, 1989; Huelsenbeck *et al.*, 2007b).

The toxin treated cells displayed typical actin cytoskeletal rearrangements and morphological changes, with no associated cell death (data not shown). Figure 3.3.9 shows the translocation rate into the macrophages after treatment with the different toxins. The RhoA/B/C inhibitor C3 led to a significantly diminished Yop translocation into the macrophages already at the lowest toxin concentration, particularly in the J774A.1 macrophages. However, even at high concentrations the Rac inhibitory toxin TcdBF had no effect on the amount of blue cells.

Taken together, these data indicate that the toxin CNF_Y enhances the Yop delivery into murine macrophages. The process leading to this boost seems to be mainly dependent on RhoA activation in the professional phagocytes, rather than Rac1.

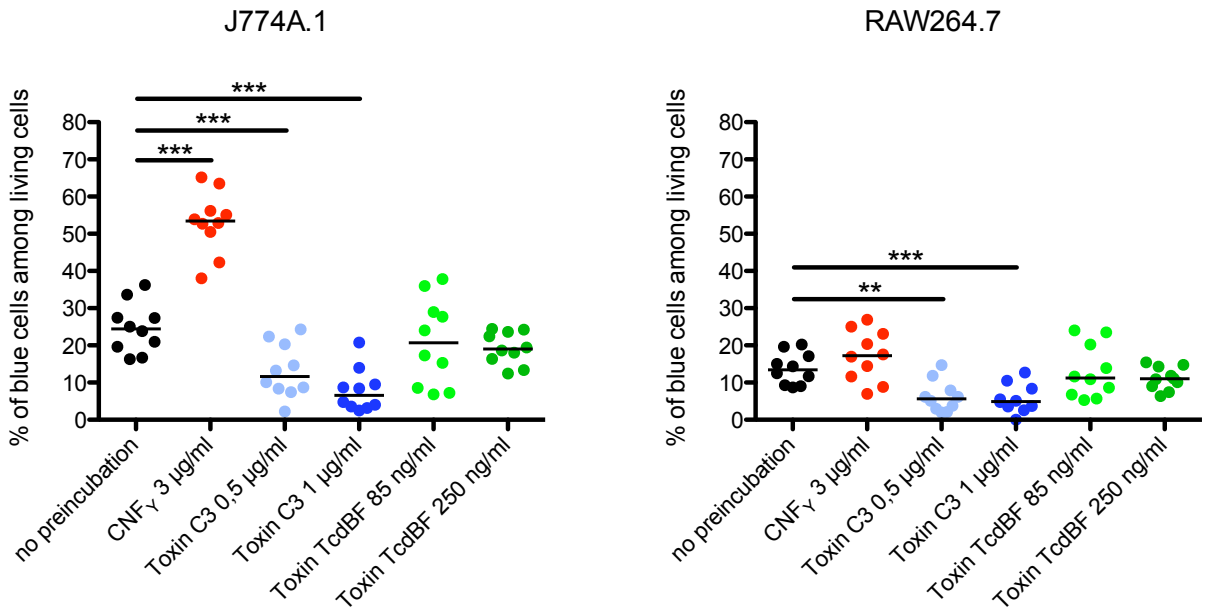

Figure 3.3.9: CNF_Y enhanced Yop delivery into murine macrophages is dependent on RhoA activation.

Bacteria were pregrown for infection overnight at 37°C to induce the CNF_Y secretion. The murine macrophages J774A.1 and RAW264.7 were untreated or treated with Rho-GTPase modifying toxins: recombinant CNF_Y (3 µg/ml (25 nM)), toxin C3 of *C. botulinum* (0.5 µg/ml/ 1 µg/ml) or toxin TcdBF of *C. difficile* (85 ng/ml/ 250 ng/ml) for 2 h prior infection for 1 h with *Y. pseudotuberculosis* YPIII-ETEM (YP173), YPIII or YP101 (Δ*yscS*)-ETEM (YP174), using an MOI of 10. Cells were labeled with the dye CCF4-AM and analyzed for percentage of blue (translocated) cells among green (living) cells. Scatter dot plot represents the median of three independent experiments with 3 samples. For statistical analysis, a Mann-Whitney test was applied to determine significant differences in the numbers of translocated cells between cells without pretreatment and toxin (CNF_Y, C3 or TcdBF)-treated cells. Asterisks indicate the significances, with ** (P<0,01) and *** (P<0.001).

3.3.5.2 YopE is not strong enough to counteract CNF_Y

It is known that YopE of *Y. pseudotuberculosis* YPIII is a GTPase-activating protein (GAP) mainly targeting Rac1 and RhoA. Thus, it can be considered a counterplayer of CNF_Y. The function of YopE seems to be important for the regulation of Yop translocation and modulation of host defences (Aili *et al.*, 2002, 2006; Black & Bliska, 2000; Songsungthong *et al.*, 2010).

This raised the question whether YopE and CNF_Y interact or compete in Rho-GTPase activation and Yop delivery. To test the ability of YopE to counteract the activity of CNF_Y, a *yopE* mutant strain was constructed. This strain was tested for its influence on RhoA/Rac1-GTP levels and for differences in the Yop translocation into murine macrophages with or without CNF_Y pretreatment.

For this purpose, murine macrophages were treated with recombinant CNF_Y (25 nM) or the same amount of PBS for three hours and subsequently infected with an MOI of 100 with *Y. pseudotuberculosis* wild-type YPIII or the *yopE* mutant YP275 or left uninfected. The bacteria were grown at 37°C overnight to induce a high amount of CNF_Y and to mimic the situation prior to host cell contact.

The uninfected cells without CNF_Y pretreatment showed low activation levels of the tested GTPases (GTP-bound) (see Figure 3.3.10 A). Upon treatment with the toxin, a higher amount of activated RhoA/Rac1 could be detected as indicated by the ratio of GTP-bound to GDP-bound forms. As indicated by the RhoA-GTP/RhoA ratio, macrophages infected with a *yopE* mutant strain with or without CNF_Y pretreatment show a slightly increased level of the GTP-bound form in comparison to wild-type-infected cells. However, Rac1-GTP levels seem to be unaffected or only minimally affected by the translocation of YopE.

Since RhoA was demonstrated to be mainly responsible for the CNF_Y-induced enhanced Yop delivery and YopE is supposed to counteract the activation, the ability of YopE to act against CNF_Y in terms of Yop translocation was evaluated. In order to test this, murine macrophages were pretreated with recombinant CNF_Y (25 nM) or the same amount of PBS for three hours and infected with the bacteria YPIII or YP275 (Δ*yopE*) grown at 37°C overnight (MOI 100). The translocated Yop proteins were detected with an anti-serum directed against all Yop proteins. The ratios of the respective Yop to the actin control were calculated. As a negative control, cells were infected with a *yscS* mutant strain (YP101), unable to form a functional T3SS. However, loss of YopE had no or only a slight stimulatory effect on the translocation of YopD and YopH independently of the pretreatment with CNF_Y (see Figure 3.3.10 B). Thus, the intracellular GAP activity of YopE seems to be insufficient to efficiently counteract CNF_Y under the tested conditions, as indicated by the slightly higher activation of the GTPases and the higher amount of translocated Yop proteins when YopE is absent.

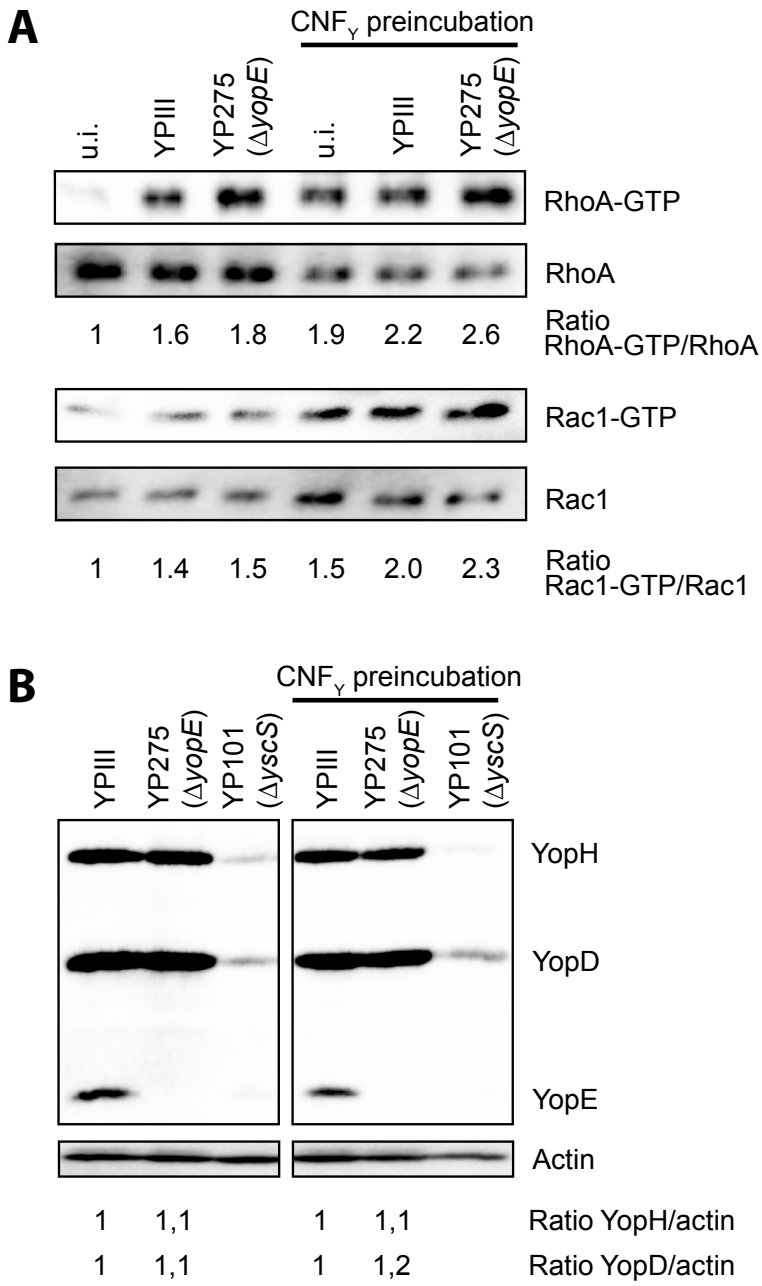

Figure 3.3.10: Deletion of YopE induces slightly higher amounts of RhoA/Rac1-GTP and leads to a minimal increase in Yop delivery.

Murine macrophages RAW264.7 were incubated with 25 nM recombinant CNF_Y or the same amount of PBS for 3 h prior to infection with an MOI 100. Bacteria were pregrown for infection at 37°C overnight. (A) Infection for 20 min was performed with *Y. pseudotuberculosis* strains YPIII or YP275 (Δ*yopE*) and PBS as negative control. Cells were lyzed and aliquots taken for western blot analysis. The rest of the samples was used to isolate the activated GTPases Rac1-GTP or RhoA-GTP using PAK1- or rhotekin-coupled beads, respectively. Using specific antibodies against RhoA (24 kDa) and Rac1 (21 kDa), the activated form and total amount of the proteins in the lysates could be detected. (B) Infection was performed for 1 h with *Y. pseudotuberculosis* YPIII, YP275 (Δ*yopE*) or YP101 (Δ*yscS*). Cells were lyzed and taken for western blot analysis, using an antiserum directed against all secreted Yops (α-Yop). Strain YP101 (Δ*yscS*) represents the negative control to rule out permeabilization of the membrane in the detergent solubility assay. A western blot analysis with a specific antibody directed against actin was used as loading control.

3.3.5.3 CNF_Y enhances Yop delivery *in vivo*

Due to the significant differences in the Yop translocation efficiency between the *Y. pseudotuberculosis* wild-type strain and a *cnfY* mutant strain *in vitro*, further *in vivo* analyses were performed. Former publications already reported that *Y. pseudotuberculosis* selectively targets the Yop injection into professional phagocytes of the PP, MLNs and spleen during the oral infection route (Durand *et al.*, 2010).

The following experiments were performed in cooperation with Dr. Devesha Kulkarni, formerly in the group „Experimental Immunology“ led by Prof. Dr. Jochen Hühn, of the Helmholtz Centre for Infection Research.

To analyze a possible influence of CNF_Y on the YopE-β-lactamase delivery during the infection process, groups of 6 - 8 BALB/c mice were infected orally with 2 x 10^9 bacteria of the strains YP173 (YPIII-ETEM) or YP217 (YP147 (Δ*cnfY*)-ETEM), and as negative controls with the strains YPIII and YP174 (YP101 (Δ*yscS*)-ETEM). Three days post infection, the mice were sacrificed, PP, MLNs and spleen isolated and the cells of single suspensions stained with fluorescently conjugated antibodies and the dye CCF4-AM. Before the staining, aliquots were removed for detection of the bacterial load in the different organs. The stained cells were acquired using a multi-colour flow cytometer and the Yop translocation into the different immune cell subsets ($Gr1^+CD11b^+$ neutrophils, $CD11^+$ macrophages, $CD11c^+$ DCs, $NKp46^+$ NK cells, $CD19^+$ B cells and $CD3^+$ T cells) was analyzed (see Figure S4).

The percentage of translocated (blue) cells among all living (green) cells was calculated. The PP contained overall the highest rate of translocated cells of the tested lymphatic tissues. The PP of mice infected with the strain YP173 (YPIII-ETEM) contained 4.5% of blue cells among the living cells (see Figure S5 A). In contrast to that, the PP of YP217 (YP147 (Δ*cnfY*)-ETEM)-infected mice only contained around 1.5% of blue cells among the living ones.

Because of the differences between the strains in bacterial colonization of the different organs, the data were additionally normalized to the bacterial load in the different organ/tissue (see Figure 3.3.11). The normalization is based on the assumption that the bacteria are infecting the different cells with the same MOI, but this is unknown. However, the *cnfY* mutant strain is significantly less able to translocate the Yop proteins into the cells of the PP, MLNs and spleen (see Figure 3.3.11 A; Figure S5 A).

These data indicate that CNF_Y enhances the Yop delivery also *in vivo*, yet the question remained if one cell subset is affected more frequently in the MLNs and spleen. Generally, the Yop proteins of *Y. pseudotuberculosis* targeted all the analyzed immune cells with a higher efficiency in the presence of CNF_Y (see Figure 3.3.11 B, Figure S5 B). Nevertheless, neutrophils in the MLNs and spleen showed a higher percentage of translocated cells, indicating a more frequently targeting of this cell type by the T3SS in these tissues. However, also macrophages, DCs and NK cells showed distinct blue/translocated populations, particularly in comparison to the T cells in both organs and the B cells in the spleen. These findings are in full agreement with former studies, which showed that YopH of *Y. pseudotuberculosis* IP2666 was concentrated in neutrophils, macrophages and DCs of the MLNs and spleen (Durand *et al.*, 2010).

The most significant reduction of Yop translocation was found for the cells of the MLNs in the absence of CNF_Y (except for NK cells). However, significantly less translocation due to the loss of CNF_Y was also detectable for neutrophils, B cells, and T cells in the spleen (see Figure 3.3.11 B). Additionally, lower percentages of Yop translocated cells were measured for macrophages and NK cells in the absence of CNF_Y (see Figure S5 B). However, a slight reduction of the translocation rates due to the loss of *cnfY* was visible with all the tested cell subsets.

Considering that *Y. pseudotuberculosis* induces host cell death (Bergsbaken & Cookson, 2007) and CNF_Y in particular seems to be involved in formation of necrotic spots in the spleen (see 3.3.2), it can be speculated that the amount of Yop translocated immune cells is probably higher in the presence of CNF_Y. In summary, CNF_Y enhances Yop delivery into host immune cells *in vivo*, in particular into professional phagocytes and thereby plays a significant role during infection of *Y. pseudotuberculosis* YPIII.

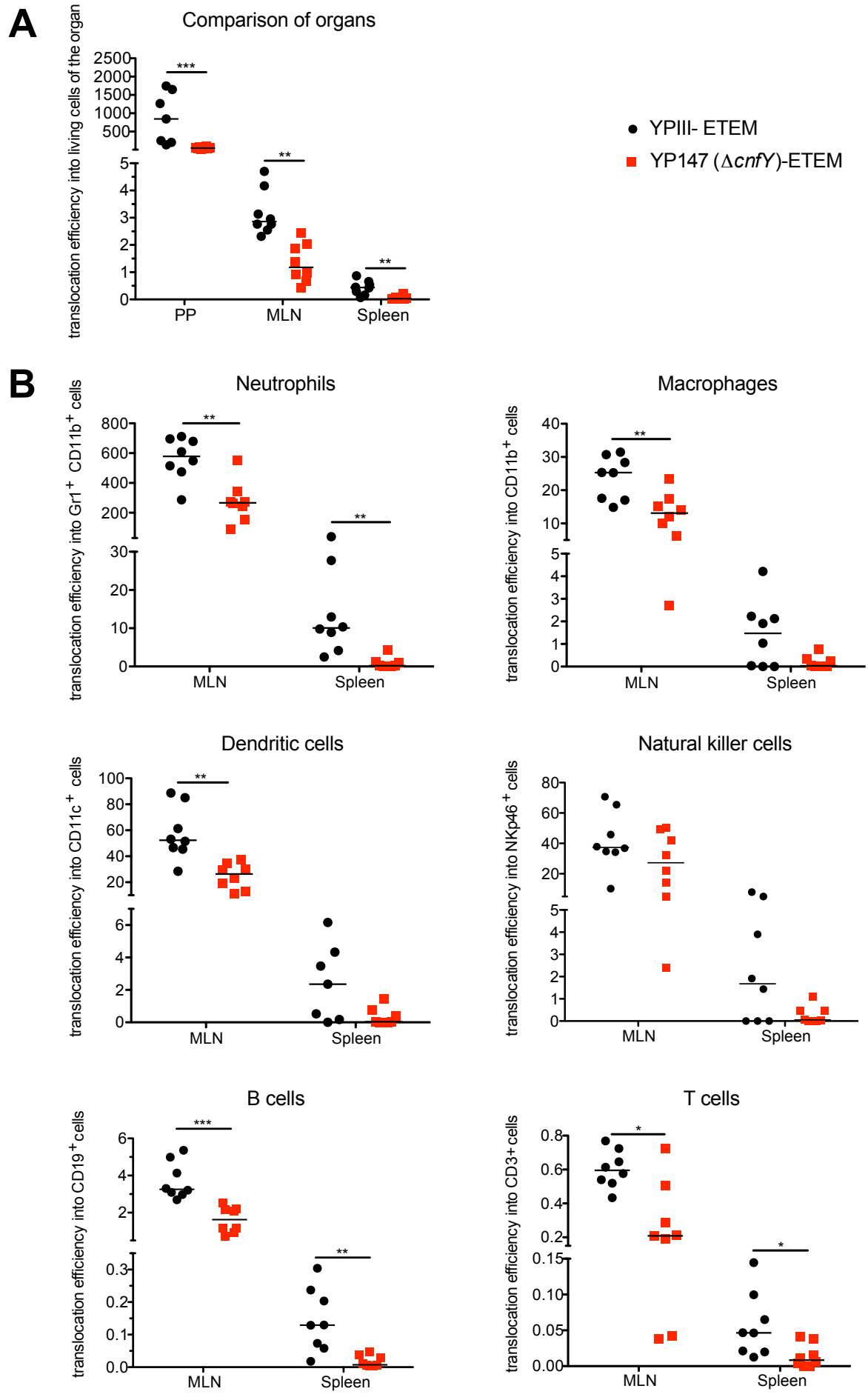
A
Comparison of organs
translocation efficiency into living cells of the organ
PP
MLN
Spleen
YPIII- ETEM
YP147 (ΔcnfY)-ETEM
B
Neutrophils
translocation efficiency into Gr1+ CD11b+ cells
Macrophages
translocation efficiency into CD11b+ cells
Dendritic cells
translocation efficiency into CD11c+ cells
Natural killer cells
translocation efficiency into NKp46+ cells
B cells
translocation efficiency into CD19+ cells
T cells
translocation efficiency into CD3+ cells
MLN
Spleen

Figure 3.3.11: Deletion of *cnfY* diminishes Yop delivery predominantly into neutrophils, macrophages and DCs in PP, MLNs and spleen *in vivo*.
Groups of 6 - 8 BALB/c mice were infected orally with 2 x 10^9 bacteria of *Y. pseudotuberculosis* YPIII-ETEM (YP173), YP147 (Δ*cnfY*)-ETEM (YP217), YPIII or YP101 (Δ*yscS*)-ETEM (YP174). Three days after infection, mice were sacrificed and the organs (PP, MLNs, and spleen) isolated. Prepared cell suspensions were stained with fluorescently labeled antibodies to detect the different immune cells with flow cytometry: neutrophils ($Gr1^+/CD11b^+$), macrophages ($CD11b^+$), DCs ($CD11c^+$), NK cells ($NKp46^+$), B cells ($CD19^+$), and T cells ($CD3^+$). Subsequently, cells were additionally dyed using CCF4-AM. The percentage of blue cells was analyzed by multi-colour flow cytometry of two independent experiments (see also Figure S5). Bacterial loads of the organs of 8 mice have been determined in parallel. These data were used for normalization to determine the Yop translocation efficiency. (A) Yop translocation efficiency into living cells of PP, MLNs, and spleen of mice infected with YPIII-ETEM (YP173) or YP147 (Δ*cnfY*)-ETEM (YP217) is illustrated. (B) Yop translocation efficiency into different living immune cell subsets of MLNs and spleen of mice infected with YPIII-ETEM (YP173) or YP147 (Δ*cnfY*)-ETEM (YP217) is illustrated. For statistical analysis, a Mann-Whitney test was applied to determine significant differences in translocation efficiency in (A) the different organs and (B) cell types between YPIII-ETEM (YP173)- and YP147 (Δ*cnfY*)-ETEM (YP217)-infected mice. Asterisks indicate the significances, with * ($P<0.05$), ** ($P<0.01$) and *** ($P<0.001$).

3.3.6 Yop delivery-independent CNF_Y function

To test whether CNF_Y has an impact on the virulence of *Y. pseudotuberculosis* YPIII besides its influence on Yop delivery, further analyses were performed. For this purpose, a *yscS* single and a *yscS cnfY* double mutant strain were used. These strains lack the ability to translocate the Yop effector proteins due to the loss of the essential T3SS injectisome component YscS. Hence, an additional function of CNF_Y independently of the T3SS and the Yop effector proteins could be displayed with these strains. In order to test potential differences, the bacterial loads in the organs, the histopathology of the infected tissues, and the triggered immune response were analyzed three days post infection. This time-point was chosen to ensure bacterial colonization, considering that a mutant without the T3SS lacks the main defence mechanism against the host immune system and is rapidly eradicated.

3.3.6.1 Additional loss of *cnfY* in a *yscS* mutant leads to a efficient colonization of the gut

Organ burden experiments have been performed for the analysis of the bacterial loads in the different organs important in the enteropathogenic *Yersinia* infection route. Former studies already revealed that the pathogenicity of the *Yersinia* species is massively diminished without the virulence plasmid and thus the T3SS and the Yop effector proteins. These mutant bacteria are no longer able to reach the systemic organs liver and spleen (Cornelis *et al.*, 1998; Straley *et al.*, 1993).

In order to test the bacterial colonization of the organs three days post infection, groups of 5 BALB/c mice were infected orally with 2 x 10^8 bacteria of the strains YPIII, YP147 (Δ*cnfY*), YP101 (Δ*yscS*) or YP298 (Δ*yscS* Δ*cnfY*). The mice were sacrificed, the organs (small intestine, PP, caecum, colon, MLNs, spleen, and liver) isolated, and the organ homogenates plated to determine the colony forming units (CFU) per gram tissue.

Figure 3.3.12 shows the bacterial loads of the different organs. The data for the systemic organs spleen and liver are not plotted because no bacteria of the strains YP101 (Δ*yscS*) and YP298 (Δ*yscS* Δ*cnfY*) could be reisolated (data not shown). Similar amounts of all strains could be detected in the MLNs, whereas high variations between the strains were visible in the different intestinal tissues. Both bacterial strains without YscS are not able to colonize the gut as efficiently as the wild-type and the *cnfY* mutant bacteria. Interestingly, the double mutant strain YP298 (Δ*yscS* Δ*cnfY*) is significantly more able to colonize especially the small intestine, caecum, and colon compared to the *yscS* single mutant strain. To exclude growth deficiencies/differences between the different strains, growth of the strains was monitored at 25°C and 37°C, but no differences in the bacterial growth *in vitro* were detectable (data not shown). These data indicate that the functional CNF_Y toxin in the absence/loss of the T3SS function is disadvantageous for the pathogen. Expression of a non-functional CNF_Y toxin or deletions in the gene could be beneficial for *Y. pseudotuberculosis* to prevent inflammation and tissue damage.

In summary, the bacteria without a functional T3SS are less able to colonize the intestinal parts, show only slight differences in the colonization of the MLNs, and are not able to reach the underlying organs spleen and liver. Further, secretion of the CNF_Y toxin seems to reduce colonization of the bacteria in the intestinal tissues in the absence of a functional T3SS. In the MLNs, however, the additional loss of CNF_Y to YscS does not alter the colonizing ability of the bacteria.

Small intestine

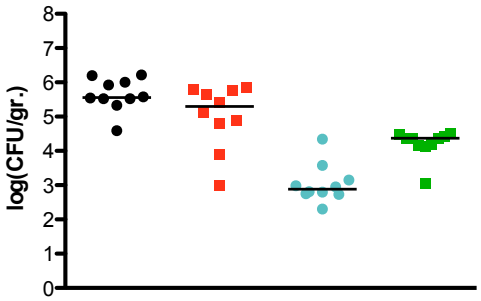

	YPIII	YP147 (Δ*cnfY*)	YP101 (Δ*yscS*)
YP298 (Δ*yscS* Δ*cnfY*)	***	*	***
YP101 (Δ*yscS*)	***	***	
YP147 (Δ*cnfY*)	n.s.		

Peyer's patches

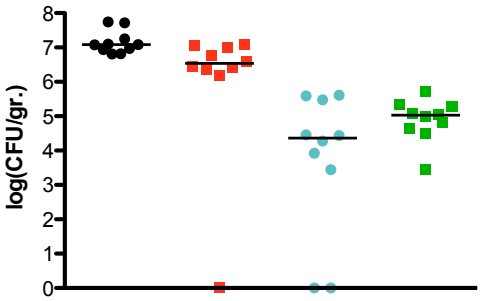

	YPIII	YP147 (Δ*cnfY*)	YP101 (Δ*yscS*)
YP298 (Δ*yscS* Δ*cnfY*)	***	**	n.s.
YP101 (Δ*yscS*)	***	**	
YP147 (Δ*cnfY*)	**		

Caecum

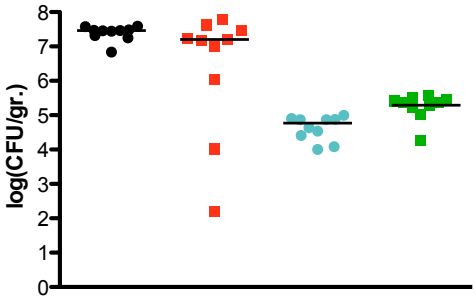

	YPIII	YP147 (Δ*cnfY*)	YP101 (Δ*yscS*)
YP298 (Δ*yscS* Δ*cnfY*)	***	*	***
YP101 (Δ*yscS*)	***	*	
YP147 (Δ*cnfY*)	n.s.		

Colon

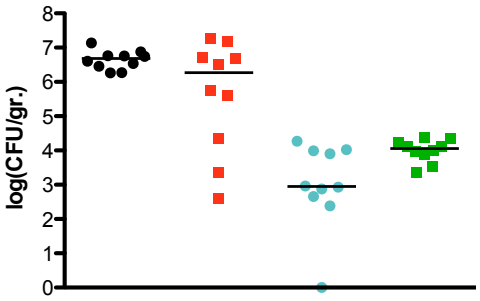

	YPIII	YP147 (Δ*cnfY*)	YP101 (Δ*yscS*)
YP298 (Δ*yscS* Δ*cnfY*)	***	*	*
YP101 (Δ*yscS*)	***	**	
YP147 (Δ*cnfY*)	n.s.		

MLN

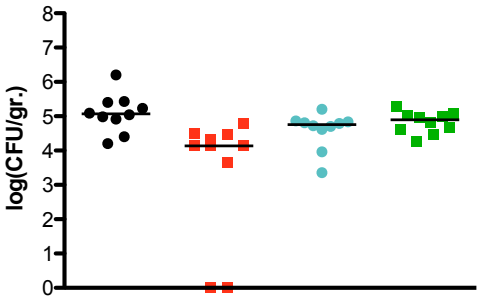

	YPIII	YP147 (Δ*cnfY*)	YP101 (Δ*yscS*)
YP298 (Δ*yscS* Δ*cnfY*)	n.s.	**	n.s.
YP101 (Δ*yscS*)	*	*	
YP147 (Δ*cnfY*)	**		

- YPIII
- YP147 (Δ*cnfY*)
- YP101 (Δ*yscS*)
- YP298 (Δ*yscS* Δ*cnfY*)

Figure 3.3.12: Deletion of *yscS* reduces colonization of intestinal tissues, whereby a *yscS cnfY* double mutant strain more efficiently colonizes the intestinal tract than a *yscS* single mutant.
Groups of 5 BALB/c mice were infected orally with 2 x 10^8 bacteria of *Y. pseudotuberculosis* YPIII, YP101 (Δ*yscS*), YP147 (Δ*cnfY*) or YP298 (Δ*yscS* Δ*cnfY*). Three days after infection, mice were sacrificed and the organs (small intestine, PP, caecum, colon, MLNs, spleen, and liver) were isolated. Homogenized organs were plated and the bacterial load (CFU) per gram tissue determined. The figure displays results of two independent experiments. For statistical analysis, a Mann-Whitney test was applied to determine significant differences in bacterial colonization of the organs between YPIII-, YP101 (Δ*yscS*)-, YP147 (Δ*cnfY*)-, and YP298 (Δ*yscS* Δ*cnfY*)-infected mice. Asterisks in tables below the graphs indicate the significances, with * (P<0.05), ** (P<0.01) and *** (P<0.001). n.s.: no significance

3.3.6.2 CNF_Y causes slight inflammation in the intestine independent of the Yop machinery

The organ burden experiments revealed differences in the colonizing abilities between the tested strains YP101 (Δ*yscS*) and YP298 (Δ*yscS* Δ*cnfY*) (see 3.3.6.1). Interestingly, the additional loss of *cnfY* in the *yscS* mutant led to higher bacterial colonization rates in the intestinal parts. To further analyze the infection, a histopathological analysis was performed by Dr. Marina C. Pils of the „Mouse Pathology, Animal Experimental Unit“ of the Helmholtz Centre for Infection Research.

Hence, groups of 4 BALB/c mice were infected orally with 2 x 10^8 bacteria, YPIII, YP147 (Δ*cnfY*), YP101 (Δ*yscS*) or YP298 (Δ*yscS* Δ*cnfY*) for three days. Subsequently, the mice were sacrificed, the organs isolated, embedded in formaldehyde, the sections stained with H & E, and evaluated blindly. Only minor differences in the histopathology of the different tissues between YP101 (ΔyscS)- and YP298 (ΔyscS ΔcnfY)-infected mice could be detected in the intestine, particularly in the ileum and caecum already three days after infection.

Figure 3.3.13 shows representative pictures of the ileum of infected mice. The YPIII infection caused a severe diffuse ileitis already visible after three days of infection, which was observed before in mice infected for six days (see 3.3.2 for details). The infection with the *cnfY* mutant strain caused a moderate granulomatous ulcerative ileitis and inflammation (neutrophilic invasion) in the PP, restricted to focal areas (observed before after six days of infection; see 3.3.2 for details).

However, the *yscS* mutant strain induced only mild epithelial hyperplasia in the intestinal epithelium (extension of villi), whereas no alterations could be observed after infection with the double mutant strain YP298 (Δ*yscS* Δ*cnfY*) when compared with uninfected mice (see Figure 3.3.13, scale). In summary, CNF_Y causes a slight inflammation in the

intestine. However, the inflammation is much less severe compared to strains expressing a functional T3SS machinery.

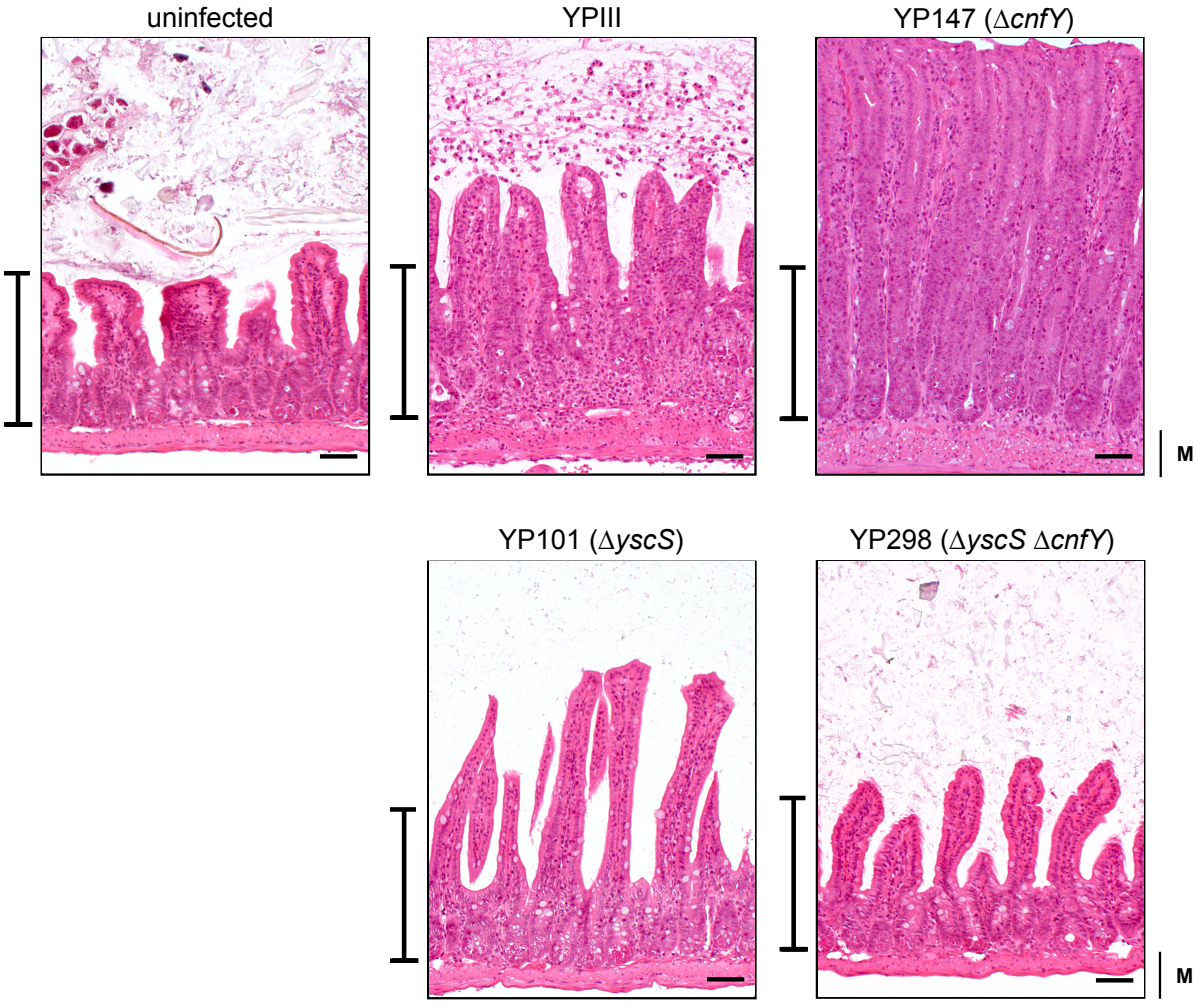

Figure 3.3.13: CNF_Y induces slight inflammation in the ileum independent of the T3SS.
Groups of 4 BALB/c mice were infected orally with 2 x 10^8 bacteria of *Y. pseudotuberculosis* YPIII, YP147 (Δ*cnfY*), YP101 (Δ*yscS*) or YP298 (Δ*yscS* Δ*cnfY*). Mice were sacrificed three days post infection, the ileum isolated and sections stained with H & E. The figure shows representative light microscopic pictures of an ileum of a YPIII- , YP147 (Δ*cnfY*)-, YP101 (Δ*yscS*)- or YP298 (Δ*yscS* Δ*cnfY*)-infected or uninfected animal. YPIII induced severe diffuse neutrophilic ileitis. YP147 (Δ*cnfY*) induced a moderate focal ileitis and epithelial hyperplasia. YP101 (Δ*yscS*) induced mild to moderate epithelial hyperplasia. YP298 (Δ*yscS* Δ*cnfY*) induced no alteration of the ileum. Black bar represents 50 µm. M: muscularis mucosa; Scale: villi length of uninfected control.

3.3.6.3 Loss of *cnfY* in a Δ*yscS* mutant causes no significant alteration of the immune response

Loss of *cnfY* in an *yscS* mutant strain led to slightly, but not significantly higher colonization rates of this mutant strain in the PP, but no alteration in colonization of the MLNs. The growth curves *in vitro* showed no differences in the growth of the bacterial strains, which suggested a change in the triggered immune response especially in the PP. Potential differences in the immune responses exclusively attributed to CNF_Y should be analyzed. The PP, MLNs, and spleen were examined because these lymphatic tissues are the main sites for initiation of an immune response against enteric *Yersinia* infections.

Hence, groups of 5 BALB/c mice were infected orally with 2 x 10^8 bacteria, YPIII, YP147 (Δ*cnfY*), YP101 (Δ*yscS*) or YP298 (Δ*yscS* Δ*cnfY*) for three days. The mice were sacrificed, the organs PP, MLNs and spleen isolated, and single cell suspensions prepared. Cells were stained with fluorescently labeled antibodies to stain the different immune cells (neutrophils, macrophages, DCs, monocytes, NK cells, $CD3^+$ T cells, $CD4^+$ T cells, $CD8^+$ T cells, and $CD19^+$ B cells) and analyzed by multi-colour flow cytometry (see Figure S6 B). Figure 3.3.14 shows the amounts of isolated neutrophils ($CD11b^+Ly6G^+$), macrophages ($F4/80^{hi}$), DCs ($CD11c^+$), and monocytes ($Ly6C^+CD11b^+$) of the different tissues.

The strains YPIII and YP147 (Δ*cnfY*) were able to colonize the PP more efficiently in comparison to the strains YP101 (Δ*yscS*) or YP298 (Δ*yscS* Δ*cnfY*). The double mutant could even be detected with slightly, but not significant higher amounts than the *yscS* single mutant (see Figure 3.3.12). However, the triggered innate immune response showed no differences as a result to the infection with the two *yscS* mutant strains YP101 (Δ*yscS*) or YP298 (Δ*yscS* Δ*cnfY*) in the PP (see Figure 3.3.14 A). A slight influx of neutrophils and monocytes could be detected in response to the infection with the *yscS* single and *yscS cnfY* double mutant strains, yet the influx of these cell types upon infection with the *cnfY* mutant strain was significantly higher. However, the highest influx of innate immune cells was detectable after infection with the wild-type strain harbouring both, YscS and CNF_Y.

The bacterial numbers in the MLNs did differ only minorly between the four strains (see Figure 3.3.12). However, the infection with the wild-type strain caused generally a higher influx of all tested innate immune cells into the MLNs (see Figure 3.3.14 B). The loss of

cnfY, *yscS* or both *yscS* and *cnfY* led to significantly reduced amounts of neutrophils, macrophages, DCs, and monocytes. Again, no significant differences in the amounts of the tested immune cells were measured between an *yscS* and a *yscS cnfY* double mutant strain. Nevertheless, the innate immune response to a mutant strain without *yscS* or both *yscS* and *cnfY* does not or only slightly differ from the response caused by the infection with YP147 (Δ*cnfY*), indicating that the functional T3SS machinery and CNF_Y combined lead to a changed immune response in the MLNs.

In general, only slightly higher amounts of neutrophils and macrophages could be detected upon infection with the *cnfY* mutant, the *yscS* mutant or the *yscS cnfY* double mutant strain in comparison to the amounts in the MLNs of untreated mice. These data indicate that all the analyzed mutant strains are less attacked by the immune system in the MLNs compared to YPIII. It can be assumed that neither CNF_Y nor YscS (the Yop delivery) are exclusively responsible for the induction of the immune response in the MLNs, and a fine-tuned concerted function is needed to trigger Yop translocation and resulting effects on the immune system.

YP101 (Δ*yscS*) and YP298 (Δ*yscS* Δ*cnfY*) bacteria could not be reisolated out of the spleens of infected mice (see Figure 3.3.12). In agreement with this result, no significant differences in the immune reaction could be detected between the strains. However, overall slightly lower amounts of neutrophils, macrophages and monocytes and an even significant lower amount of DCs could be detected upon infection with YP298 (Δ*yscS* Δ*cnfY*) in contrast to an YP101 (Δ*yscS*) infection. The YP147 (Δ*cnfY*) bacteria in contrast are able to colonize the spleen up to day three and induce a harsh influx predominantly of neutrophils and monocytes. In the wild-type the amounts are diminished, indicating that the combined activity of YscS and CNF_Y is needed. In summary, YscS but not CNF_Y is needed for the initial colonization of the spleen, but the concerted activity of YscS and CNF_Y seems to be important for defending the bacteria against the host immune system to remain in this tissue, probably by enhancing the Yop delivery machinery.

Taken together, these data indicate that the major influence of CNF_Y *in vivo* appears to be the enhancement of Yop delivery.

A PP

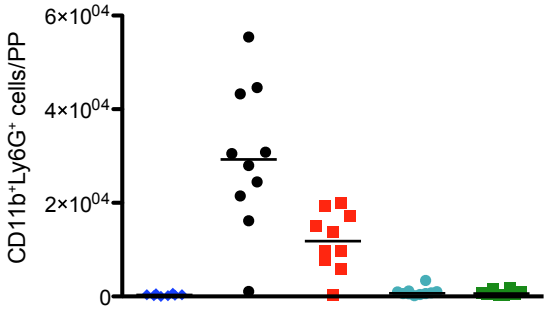

	un-infected	YPIII	YP147 (Δ*cnfY*)	YP101 (Δ*yscS*)
YP298 (Δ*yscS* Δ*cnfY*)	*	***	**	n.s.
YP101 (Δ*yscS*)	*	***	**	
YP147 (Δ*cnfY*)	***	**		
YPIII	***			

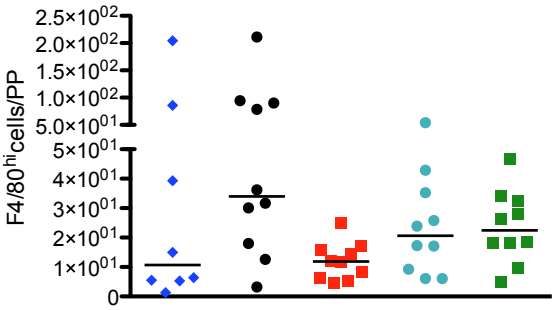

	un-infected	YPIII	YP147 (Δ*cnfY*)	YP101 (Δ*yscS*)
YP298 (Δ*yscS* Δ*cnfY*)	n.s.	n.s.	*	n.s.
YP101 (Δ*yscS*)	n.s.	n.s.	n.s.	
YP147 (Δ*cnfY*)	n.s.	**		
YPIII	n.s.			

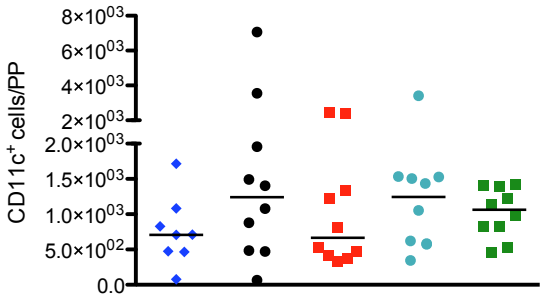

	un-infected	YPIII	YP147 (Δ*cnfY*)	YP101 (Δ*yscS*)
YP298 (Δ*yscS* Δ*cnfY*)	n.s.	n.s.	n.s.	n.s.
YP101 (Δ*yscS*)	n.s.	n.s.	n.s.	
YP147 (Δ*cnfY*)	n.s.	n.s.		
YPIII	n.s.			

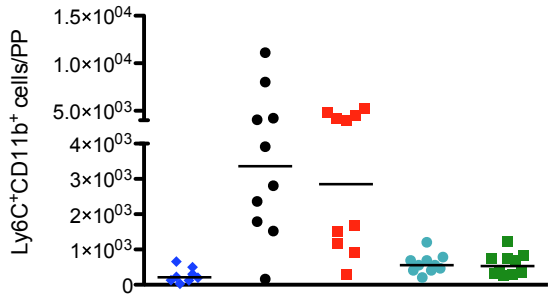

	un-infected	YPIII	YP147 (Δ*cnfY*)	YP101 (Δ*yscS*)
YP298 (Δ*yscS* Δ*cnfY*)	*	**	**	n.s.
YP101 (Δ*yscS*)	*	**	**	
YP147 (Δ*cnfY*)	***	n.s.		
YPIII	***			

◆ uninfected ● YPIII ● YP101 (Δ*yscS*)
■ YP147 (Δ*cnfY*) ■ YP298 (Δ*yscS* Δ*cnfY*)

B **MLNs**

Neutrophils

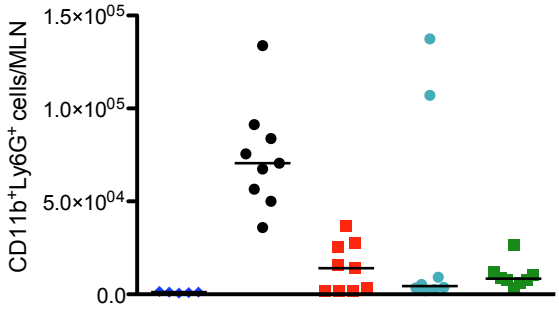

	un-infected	YPIII	YP147 (Δ*cnfY*)	YP101 (Δ*yscS*)
YP298 (Δ*yscS* Δ*cnfY*)	**	***	n.s.	n.s.
YP101 (Δ*yscS*)	**	n.s.	n.s.	
YP147 (Δ*cnfY*)	**	***		
YPIII	***			

Macrophages

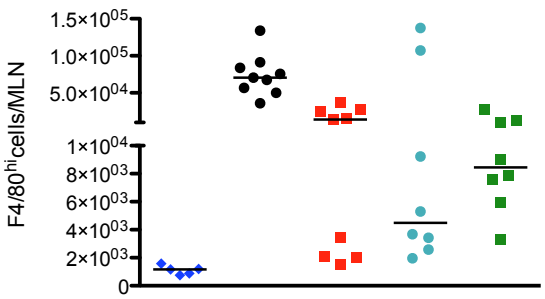

	un-infected	YPIII	YP147 (Δ*cnfY*)	YP101 (Δ*yscS*)
YP298 (Δ*yscS* Δ*cnfY*)	**	***	n.s.	n.s.
YP101 (Δ*yscS*)	**	n.s.	n.s.	
YP147 (Δ*cnfY*)	**	***		
YPIII	***			

Dendritic cells

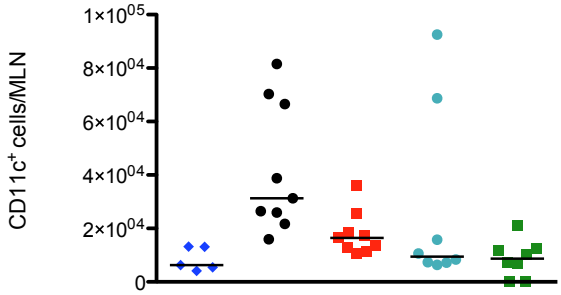

	un-infected	YPIII	YP147 (Δ*cnfY*)	YP101 (Δ*yscS*)
YP298 (Δ*yscS* Δ*cnfY*)	n.s.	***	*	n.s.
YP101 (Δ*yscS*)	n.s.	n.s.	n.s.	
YP147 (Δ*cnfY*)	*	**		
YPIII	***			

Monocytes

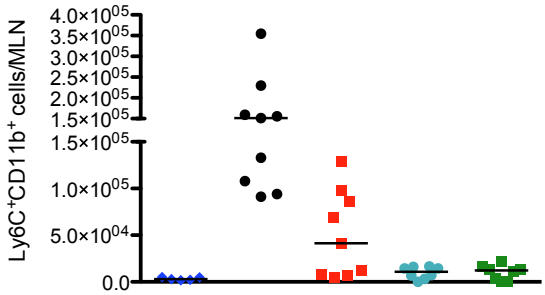

	un-infected	YPIII	YP147 (Δ*cnfY*)	YP101 (Δ*yscS*)
YP298 (Δ*yscS* Δ*cnfY*)	n.s.	***	n.s.	n.s.
YP101 (Δ*yscS*)	n.s.	***	n.s.	
YP147 (Δ*cnfY*)	**	***		
YPIII	***			

◆ uninfected ● YPIII ● YP101 (Δ*yscS*)
■ YP147 (Δ*cnfY*) ■ YP298 (Δ*yscS* Δ*cnfY*)

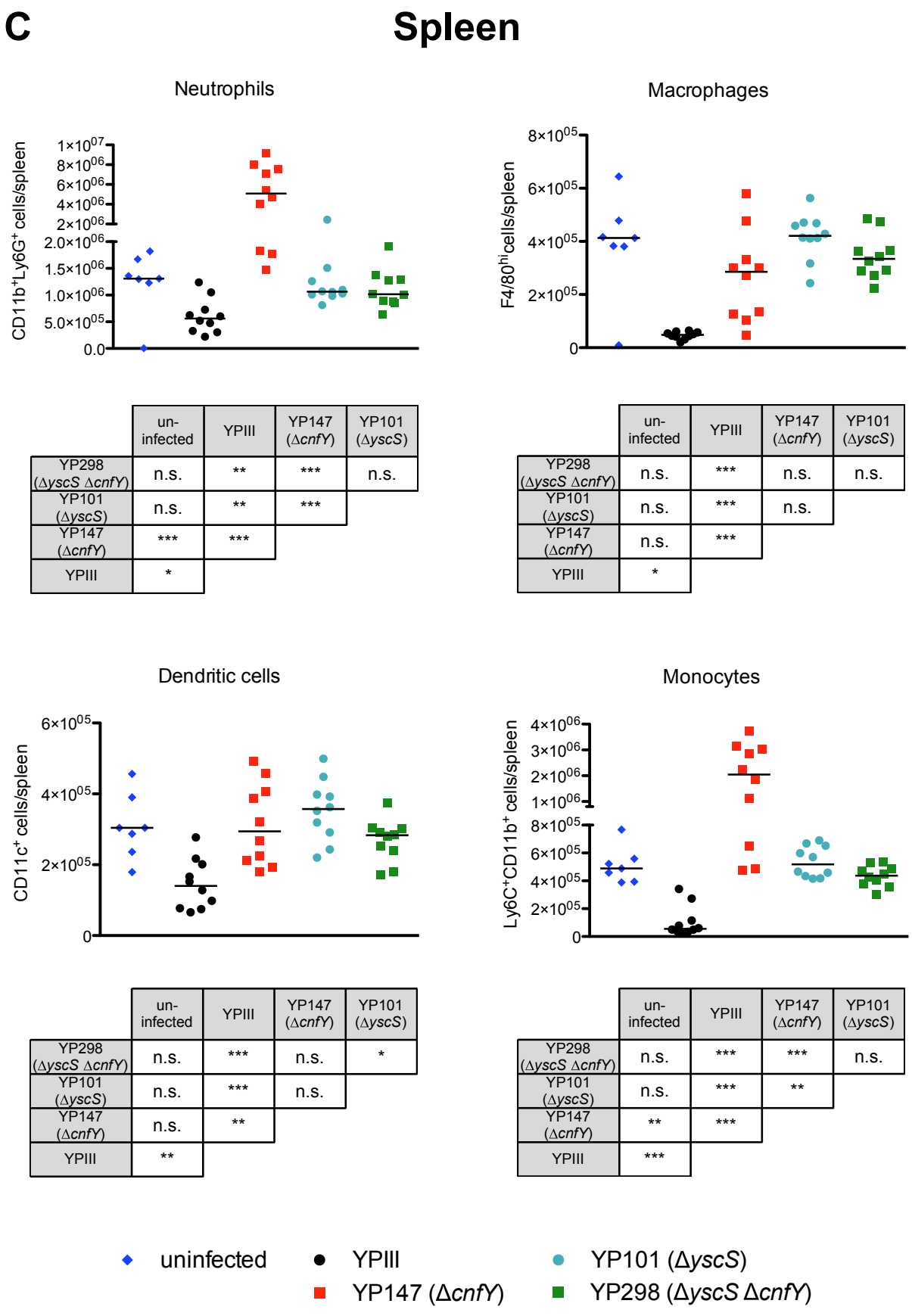

	un-infected	YPIII	YP147 (ΔcnfY)	YP101 (ΔyscS)
YP298 (ΔyscS ΔcnfY)	n.s.	**	***	n.s.
YP101 (ΔyscS)	n.s.	**	***	
YP147 (ΔcnfY)	***	***		
YPIII	*			

	un-infected	YPIII	YP147 (ΔcnfY)	YP101 (ΔyscS)
YP298 (ΔyscS ΔcnfY)	n.s.	***	n.s.	n.s.
YP101 (ΔyscS)	n.s.	***	n.s.	
YP147 (ΔcnfY)	n.s.	***		
YPIII	*			

	un-infected	YPIII	YP147 (ΔcnfY)	YP101 (ΔyscS)
YP298 (ΔyscS ΔcnfY)	n.s.	***	n.s.	*
YP101 (ΔyscS)	n.s.	***	n.s.	
YP147 (ΔcnfY)	n.s.	**		
YPIII	**			

	un-infected	YPIII	YP147 (ΔcnfY)	YP101 (ΔyscS)
YP298 (ΔyscS ΔcnfY)	n.s.	***	***	n.s.
YP101 (ΔyscS)	n.s.	***	**	
YP147 (ΔcnfY)	**	***		
YPIII	***			

Figure 3.3.14: Additional loss of *cnfY* in a Δ*yscS* mutant does not change the triggered immune response.

Groups of 5 BALB/c mice were infected orally with 2 x 10^8 bacteria of *Y. pseudotuberculosis* YPIII, YP101 (Δ*yscS*), YP147 (Δ*cnfY*) or YP298 (Δ*yscS* Δ*cnfY*). Three days after infection, mice were sacrificed and organs (PP, MLNs, and spleen) were isolated. Prepared cell suspensions were stained with fluorescently labeled antibodies to detect the different immune cells with flow cytometry: neutrophils ($CD11b^+/Ly6G^+$), macrophages ($F4/80^{hi}$), DCs ($CD11c^+$), and monocytes ($Ly6C^+CD11b^+$). Data plotted on the y axis indicate the cell numbers isolated from uninfected, YPIII-, YP101 (Δ*yscS*)-, YP147 (Δ*cnfY*)-, and YP298 (Δ*yscS* Δ*cnfY*)-infected organs. Scatter dot plots show the median of two independent experiments for (A) PP, (B) MLNs, and (C) spleen. For statistical analysis, a Mann-Whitney test was applied to determine significant differences in the numbers of indicated cell types in the whole organ between YPIII-, YP101 (Δ*yscS*)-, YP147 (Δ*cnfY*)-, YP298 (Δ*yscS* Δ*cnfY*)-infected or uninfected mice. Asterisks in the tables below the graphs indicate the significances, with * (P<0.05), ** (P<0.01) and *** (P<0.001).

3.3.6.4 Proteins of the virulence plasmid decrease the membrane integrity

Previous studies of the CNF_Y homolog of *E. coli*, CNF_1 revealed a strong increase of the membrane permeability of epithelial cells due to RhoA activation by CNF_1 (Schlegel *et al.*, 2011). Since CNF_Y is known to mainly activate RhoA in epithelial cells (Hoffmann *et al.*, 2004), the influence of CNF_Y on membrane permeability was tested.

For this purpose, Caco-2 cells were cultivated on a membrane until a polarized monolayer was formed (see 2.2.2.8). The cell monolayer was infected apically with 3 x 10^6 bacteria of YPIII, YP147 (Δ*cnfY*), YP12 pYV^- or YP150 pYV^- (Δ*cnfY*) for 8 hours. Every hour and prior to infection, the trans epithelial electrical resistance (TEER) and thus the membrane integrity was determined. After 8 hours, the pH increased in the presence of bacteria, making a reliable measurement impossible.

As visible in Figure 3.3.15 A, the strains containing the virulence plasmid YPIII and YP147 (Δ*cnfY*) and thus a functional Yop delivery machinery, caused a fast destruction of the epithelial membrane, starting already two hours post infection. The monolayers infected with the strains YP12 pYV^- or YP150 pYV^- (Δ*cnfY*) lacking the virulence plasmid stayed intact over 8 hours. These data suggest that the factors encoded on the virulence plasmid of *Y. pseudotuberculosis* YPIII diminish the membrane integrity.

To test whether CNF_Y acts independently of other bacterial factors (e.g. the Yops), the recombinant toxin (50 nM) was used to intoxicate the cells basolaterally. The TEER was measured prior treatment and every second hour up to 22 hours (see Figure 3.3.15 B). At a TEER value lower than 80% of the starting point, the membrane becomes leaky (permeability threshold) and is termed as permeable. These data show a slight impact of CNF_Y on the membrane permeability, starting after four hours. However, this impact is not as significant as the one of the virulence plasmid-encoded factors.

In summary, CNF_Y seems to decrease the membrane integrity when applied in high concentrations. However, the T3SS and Yop effector proteins seem to play a predominant role in disrupting the membrane function.

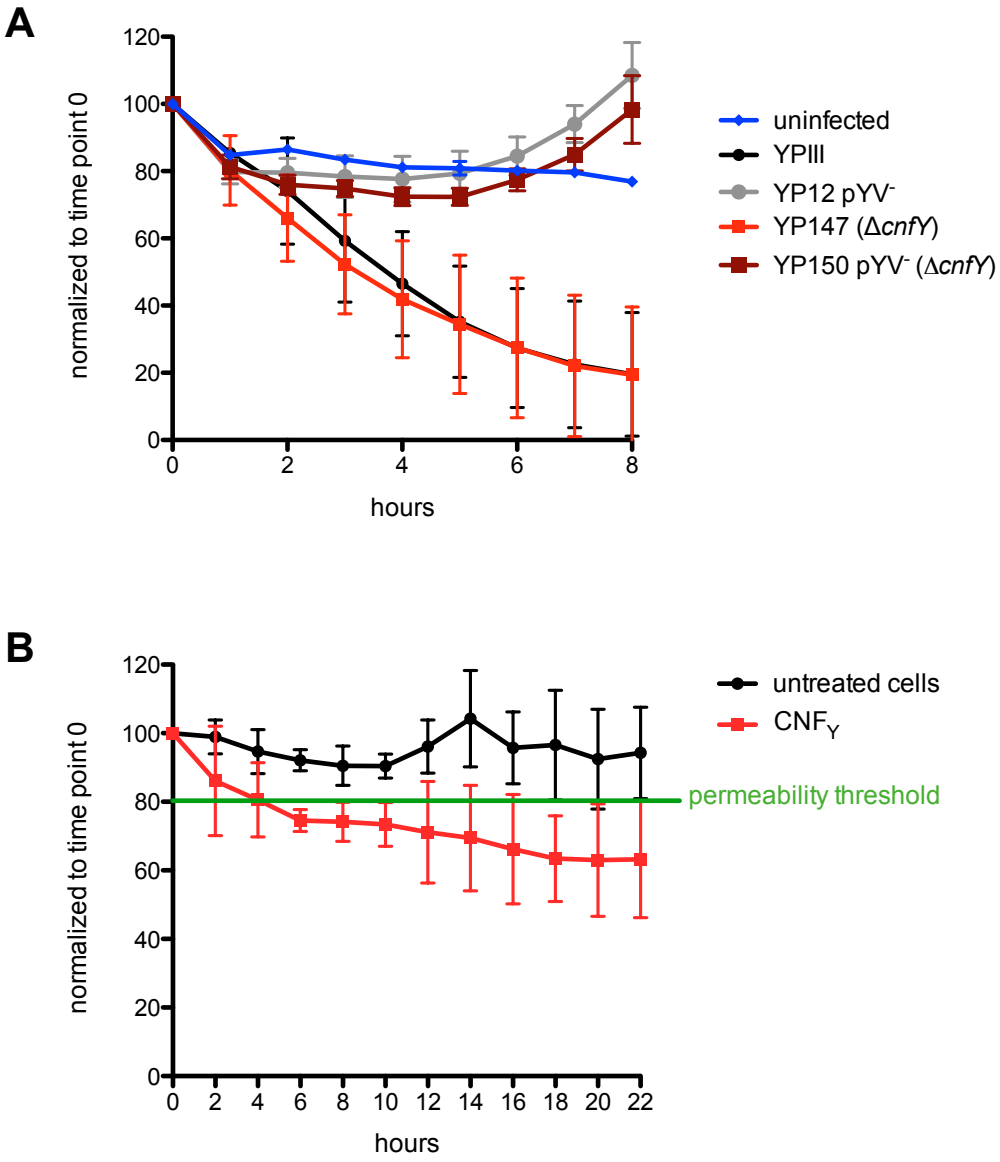

Figure 3.3.15: Proteins of the virulence plasmid lead to destruction of an epithelial membrane, whereas CNF_Y only causes a slight increase in membrane permeability.

Caco-2 cells were cultivated on a membrane till a dense monolayer was formed. (A) Bacteria were grown overnight at 25°C. Cells on the membrane stayed uninfected or were infected apical with approximately 3 x 10^6 bacteria of *Y. pseudotuberculosis* YPIII, YP12 pYV$^-$, YP147 (Δ*cnfY*) or YP150 pYV$^-$ (Δ*cnfY*). Graph represents data of three independent experiments with each 2 wells normalized to time point 0. The trans epithelial electrical resistance (TEER) was measured 8 hours every hour. (B) Cells were treated basolaterally with 50 nM recombinant CNF_Y or the same amount of PBS over 22 hours. Graph represents data of three independent experiments with each 2 wells normalized to time point 0. TEER was measured every second hour. Green line indicates at which point the epithelial membrane starts being permeable.

3.4 CNF_Y leads to long-term changes of the host immune system

Previous data suggested that the *cnfY* mutant strain is able to colonize the caecum and to some extent also the PP over long periods after an oral infection (14, 28 and 80 days; data not shown). In order to test if avirulent *Yersinia* mutant strains (YP12 pYV^-, YP147 (Δ*cnfY*) or YP150 pYV^- (Δ*cnfY*)) possess different colonization abilities and induce different immune responses, long-term infections were performed for 28 days. Such experiments should allow to determine a possible effect of CNF_Y, independently from the virulence plasmid (no Yop machinery). Since YPIII-infected mice would not survive long-term infections, the wild-type strain was not included in this experiment. The immune response in the PP, MLNs, and spleen was measured because these are the lymphatic tissues in which an immune response against *Yersinia* is expected.

Groups of 5 BALB/c mice were infected orally with 2 x 10^8 bacteria. At day 28, the mice were sacrificed, the organs (small intestine, PP, caecum, colon, MLNs, spleen, and liver) were isolated and single cell suspensions were prepared of PP, MLNs and spleen and aliquots were taken to determine the bacterial load. Furthermore, single cell suspensions were stained with fluorescently labeled antibodies to detect different immune cells (neutrophils, macrophages, DCs, monocytes, NK cells, $CD3^+$ T cells, $CD4^+$ T cells, $CD8^+$ T cells, and $CD19^+$ B cells) and analyzed with multi-colour flow cytometry (see Figure S6).

Neither YP12 pYV^- nor YP150 pYV^- (Δ*cnfY*) bacteria could be reisolated of the examined tissues, maybe due to the high detection limit. However, the *cnfY* mutant strain could be detected in the caecum in 7 out of 9 mice (see Figure 3.4.1 A). The spleen weights of untreated mice still differed slightly from YP12 pYV^--infected and significantly from the YP147 (Δ*cnfY*)- and YP150 pYV^- (Δ*cnfY*)-infected mice, thus indicating long-lasting changes in this organ (see Figure 3.4.1 B).

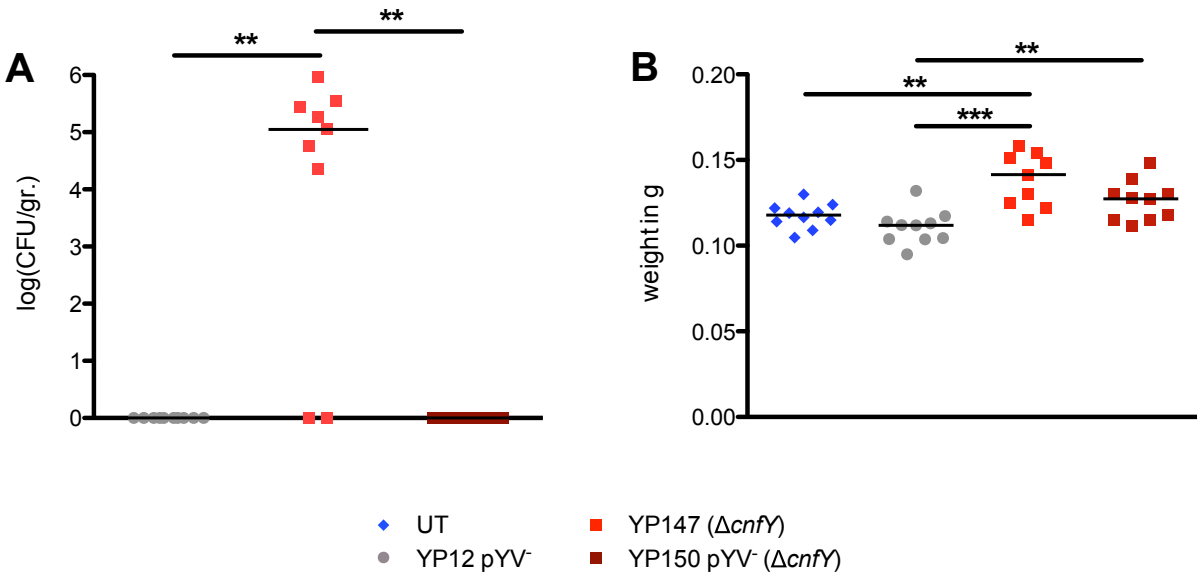

Figure 3.4.1: Only the *cnfY* mutant strain could be reisolated of the caecum 28 days post infection, yet the spleen weights still differ after infection with YP12 pYV$^-$, YP147 (Δ*cnfY*) or YP150 pYV$^-$ (Δ*cnfY*).

Groups of 5 BALB/c mice were infected orally with 2 x 10^8 bacteria of *Y. pseudotuberculosis* YP12 pYV$^-$, YP147 (Δ*cnfY*) or YP150 pYV$^-$ (Δ*cnfY*) or the same amount of PBS. 28 days after infection, mice were sacrificed and the organs were isolated. An YPIII-infection control was not included since mice would not survive a long-term infection. (A) Homogenized organs were plated and the bacterial load (CFU) per gram of the tissue determined. The figure displays the results of two independent experiments of the caecum. No bacteria could be reisolated of the other tested organs (small intestine, PP, colon, MLNs, spleen, and liver). (B) Spleen weights were determined in two independent experiments. For statistical analysis, a Mann-Whitney test was applied to determine significant differences in (A) bacterial colonization in the caecum and (B) spleen weights between YP12 pYV$^-$-, YP147 (Δ*cnfY*)-, YP150 pYV$^-$ (Δ*cnfY*)-infected or uninfected mice. Asterisks indicate the significances, with ** (P<0.01) and *** (P<0.001).

Figure 3.4.2 represents the flow cytometry analysis of the organs PP, MLNs and spleen for the immune cells neutrophils (CD11b$^+$Ly6G$^+$), macrophages (F4/80^{hi}), DCs (CD11c$^+$), monocytes (Ly6C$^+$CD11b$^+$), NK cells (NKp46$^+$), T cells (CD3$^+$), and B cells (CD19$^+$).

Analysis of the immune cell composition of the PP highlighted an ongoing immune response after infection with the three different strains in comparison to uninfected PP (see Figure 3.4.2 A). Significant differences could be measured for the DCs, monocytes, NK cells, T cells, and B cells without detectable bacterial numbers in this organ.

Also the MLNs showed differences in their immune cell composition after a long-term infection without measurable bacterial numbers. Significantly higher amounts of neutrophils, monocytes, NK cells, and B cells could be detected upon infection with YP12 pYV$^-$ and YP147 (Δ*cnfY*) (see Figure 3.4.2 B). In addition, significantly higher amounts of macrophages and DCs could be detected upon infection with YP12 pYV$^-$, indicating an even stronger immune response due to infection with YP12 pYV$^-$ than with

YP147 (Δ*cnfY*). However, a long-term infection with the strain YP150 pYV$^-$ (Δ*cnfY*) only led to increased levels of NK cells, T cells, and B cells in comparison to the levels in uninfected MLNs, and thus a very mild remodulation of the immune compartment. In summary, no bacteria could be detected in the MLNs after a long-term infection with the three strains. Yet, significantly increased amounts of most tested immune cells could be measured 28 days after infection with YP12 pYV$^-$ - the strain harbouring the toxin - when compared to uninfected MLNs.

As indicated by the differences in the spleen weights the mutant strains seem to have different impacts on the spleen (see Figure 3.4.1 B). However, an infection with the strains YP147 (Δ*cnfY*) and YP150 pYV$^-$ (Δ*cnfY*) did not or only slightly alter the immune cell contents in the spleen (see Figure 3.4.2 C). An infection with the strain YP12 pYV$^-$ in contrast led to significantly lower amounts of all tested immune cells, except for T cells and B cells in comparison to the contents of uninfected, YP147 (Δ*cnfY*)- or YP150 pYV$^-$ (Δ*cnfY*)-infected spleens. These data strongly indicate that CNF_Y affects innate immune cell contents in the spleen independent of the T3SS machinery.

In summary, these strains (YP12 pYV$^-$, YP147 (Δ*cnfY*), YP150 pYV$^-$ (Δ*cnfY*)) affect the immune system of the host over long periods after an infection without detectable bacterial numbers in the intestinal tissues (except for the caecum of YP147 (Δ*cnfY*)-infected mice), MLNs, and organs. Additionally, CNF_Y seems to be able to diminish the immune cell numbers in the spleen, independently from the virulence plasmid.

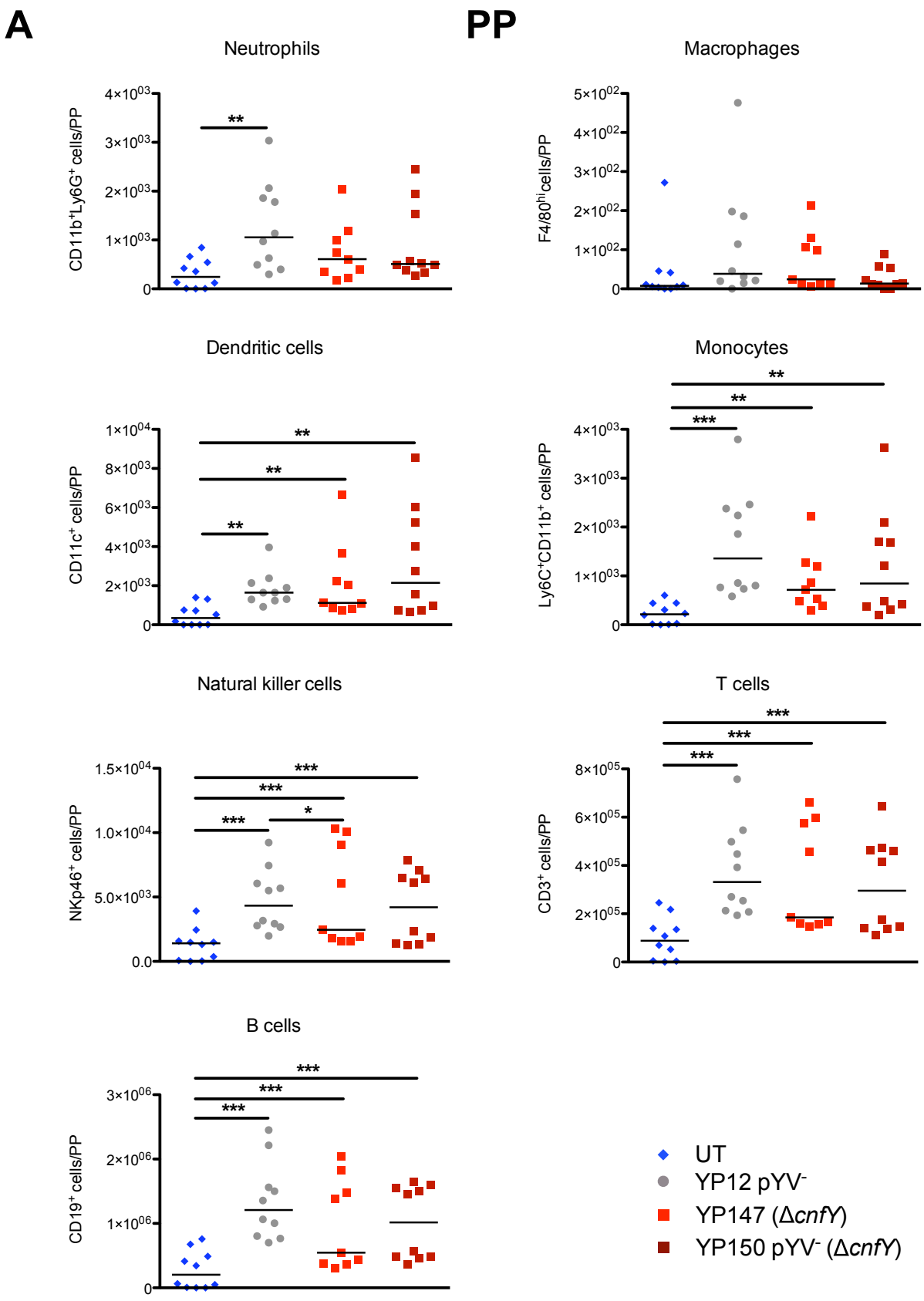
A
PP
Neutrophils
CD11b+Ly6G+ cells/PP
Macrophages
F4/80hi cells/PP
Dendritic cells
CD11c+ cells/PP
Monocytes
Ly6C+CD11b+ cells/PP
Natural killer cells
NKp46+ cells/PP
T cells
CD3+ cells/PP
B cells
CD19+ cells/PP
UT
YP12 pYV-
YP147 (ΔcnfY)
YP150 pYV- (ΔcnfY)

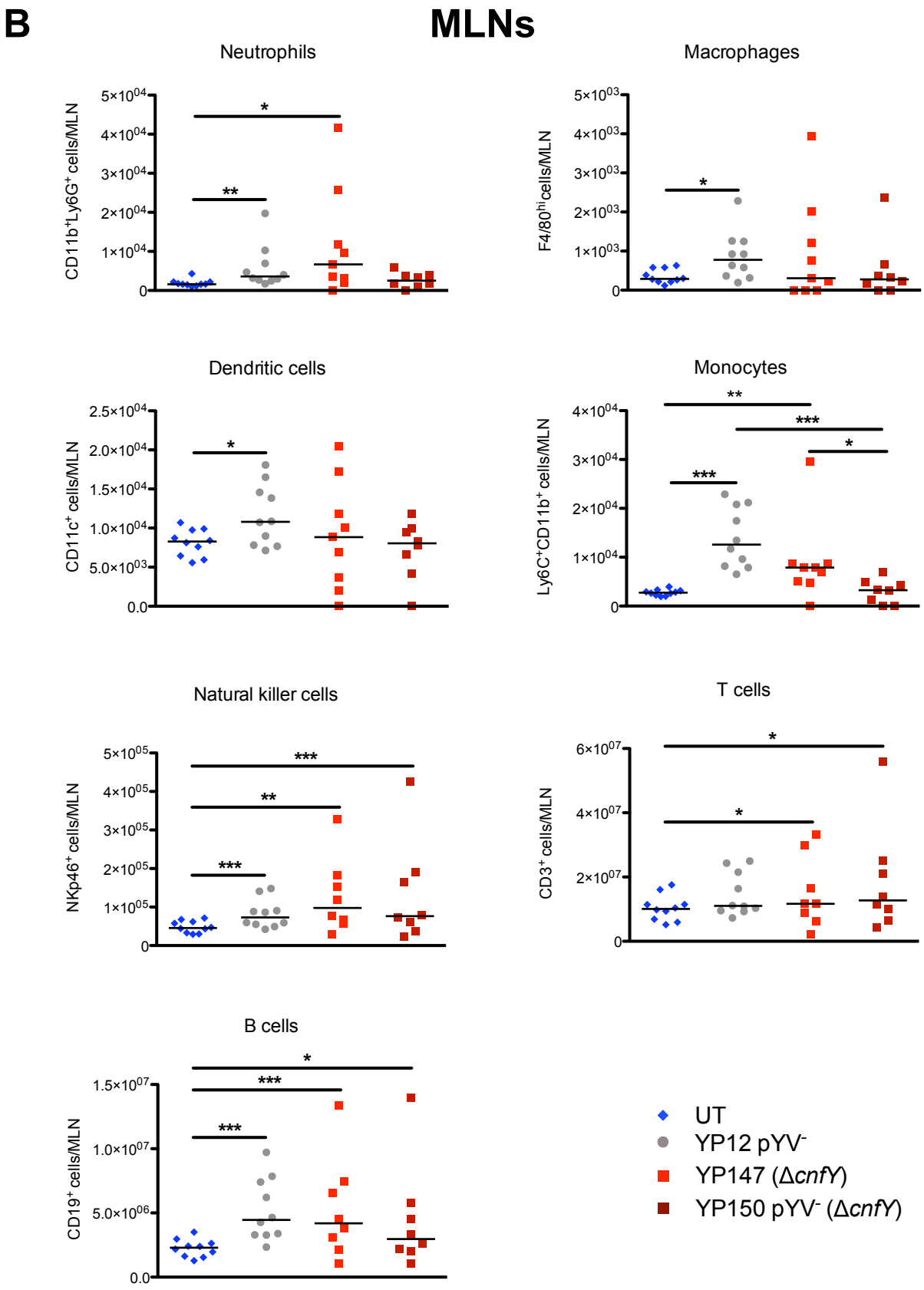
B
MLNs
Neutrophils
CD11b+Ly6G+ cells/MLN
Macrophages
F4/80hi cells/MLN
Dendritic cells
CD11c+ cells/MLN
Monocytes
Ly6C+CD11b+ cells/MLN
Natural killer cells
NKp46+ cells/MLN
T cells
CD3+ cells/MLN
B cells
CD19+ cells/MLN
UT
YP12 pYV-
YP147 (ΔcnfY)
YP150 pYV- (ΔcnfY)

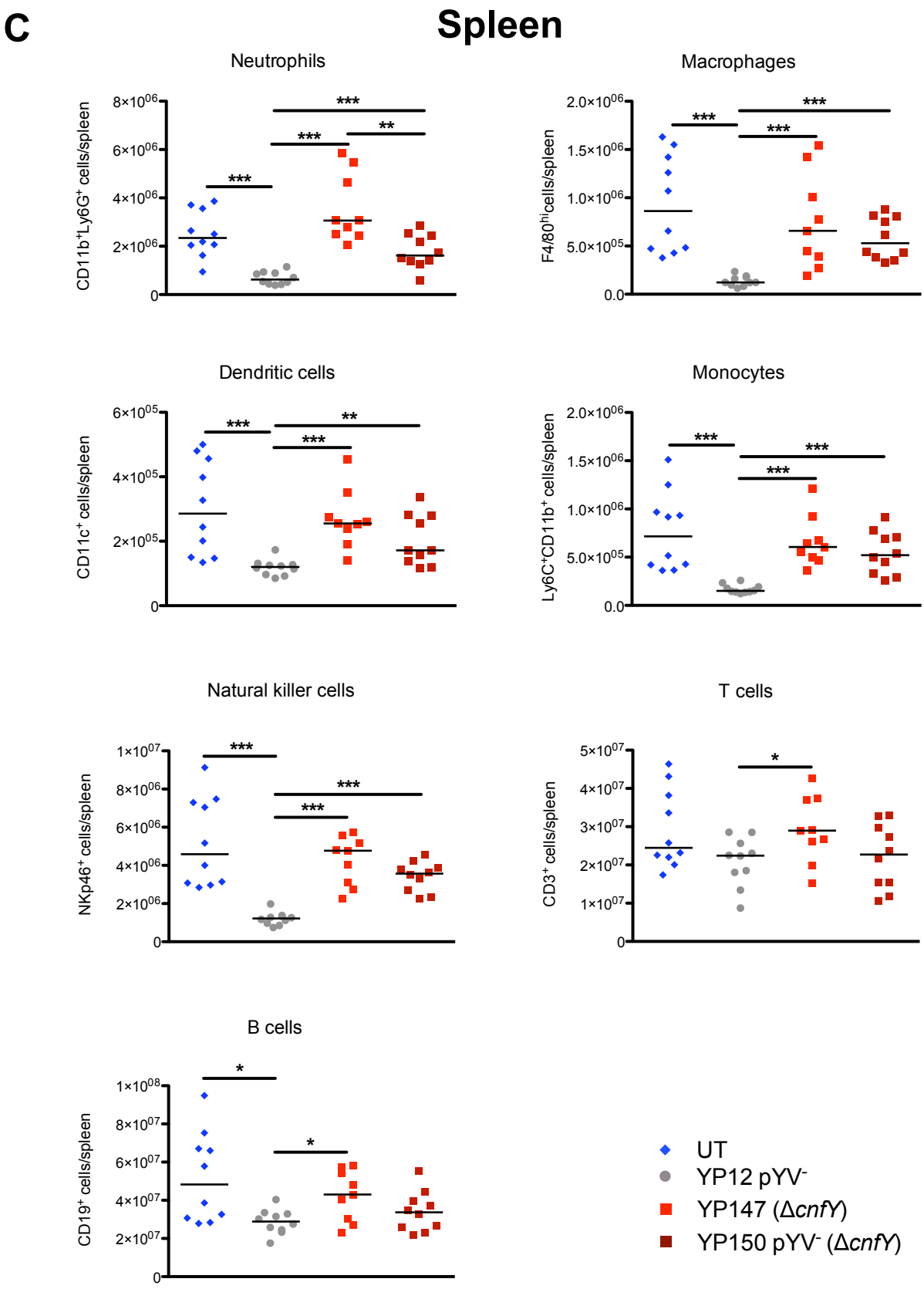

Figure 3.4.2: CNF_Y induced reduction of immune cell numbers in the spleen is independently from the virulence plasmid and still detectable 28 days post infection.

Groups of 5 BALB/c mice were infected orally with 2 x 10^8 bacteria of *Y. pseudotuberculosis* YP12 pYV$^-$, YP147 (Δ*cnfY*) or YP150 pYV$^-$ (Δ*cnfY*) or the same amount of PBS. 28 days after infection, mice were sacrificed and organs (PP, MLNs, and spleen) were isolated. Prepared cell suspensions were stained with fluorescently labeled antibodies to detect the different immune cells with flow cytometry: neutrophils

($CD11b^+/Ly6G^+$), macrophages ($F4/80^{hi}$), DCs ($CD11c^+$), monocytes ($Ly6C^+CD11b^+$), NK cells ($NKp46^+$), T cells ($CD3^+$), and B cells ($CD19^+$). Data plotted on the y axis indicate the cell numbers isolated from uninfected, YP12 pYV$^-$-, YP147 (Δ*cnfY*)- or YP150 pYV$^-$ (Δ*cnfY*)-infected organs. Scatter dot plots show the median of two independent experiments for (A) PP, (B) MLNs, and (C) spleen. For statistical analysis, a Mann-Whitney test was applied to determine significant differences in the numbers of indicated cell types in the whole organ between YP12 pYV$^-$-, YP147 (Δ*cnfY*)-, YP150 pYV$^-$ (Δ*cnfY*)-infected or uninfected mice. Asterisks indicate the significances, with * ($P<0.05$), ** ($P<0.01$) and *** ($P<0.001$).

4 Discussion

The small Rho-GTPases are involved in different cellular processes, like the cell cycle progression, genetic information processing, organization of the cytoskeleton, and different host defence mechanisms (Etienne-Manneville & Hall, 2002; Lemonnier *et al.*, 2007). Particularly the actin cytoskeleton plays a crucial role in bacterial pathogenesis, e.g. phagocytosis of pathogens. Different bacteria have evolved toxins and effector proteins targeting the small Rho-GTPases which enable them (1) to prevent their phagocytosis by macrophages, (2) to induce their phagocytosis into non-phagocytic cells or (3) to disrupt the epithelial barrier to reach the underlying tissue (Bhavsar *et al.*, 2007; Cossart & Toledo-Arana, 2008; Gouin *et al.*, 2005).

This study investigates the function of the Rho-GTPase-activating toxin CNF_Y, produced by the clinical isolate *Y. pseudotuberculosis* YPIII (Lockman *et al.*, 2002). The molecular mechanism by which the toxin modulates cellular pathways and the cell morphology has already been addressed by several studies. However, the CNF_Y role in the pathogenesis of *Y. pseudotuberculosis* has not yet been dissected. To shed light upon this topic, the regulation of the *cnfY* expression, the molecular function, and particularly the impact of a *cnfY* deletion on the virulence of YPIII in a mouse gastrointestinal infection model were investigated.

4.1 CNF_Y is present at infection relevant conditions

The significance of CNF_Y for the pathogenesis of *Y. pseudotuberculosis* YPIII was initially studied by the expression and secretion profile of the toxin *in vitro* as well as *in vivo*. Not much was known about the expression conditions of *cnfY*. It was previously shown that *cnfY* expression is not regulated by temperature, the growth phase or calcium (Lockman *et al.*, 2002). However, this study tested broth supernatant and bacteria-free lysates on epithelial cells for CNF_Y activity by monitoring the formation of multinucleated, giant cells.

Here, promoter fusions (P_{cnfY}*::lacZ*) were used to measure the expression of the toxin, which give more detailed information about the expression conditions. It could be demonstrated that *cnfY* is predominantly expressed at 37°C during late stationary growth phase in nutrient rich media. Hence, the expression is temperature-, growth phase-, and nutrient-dependent, i.e. *cnfY* is expressed under similar conditions to other virulence genes, e.g. the virulence-plasmid encoded *yops* or *yadA* (Cornelis & Wolf-

Watz, 1997). This supported the assumption that CNF_Y could be an additional virulence factor for *Y. pseudotuberculosis* YPIII, since 37°C and a nutrient rich environment are conditions found in the intestinal tract of the host. Furthermore, the expression *in vitro* as well as *in vivo* in all tested organs of the infection route was distinct and leads to the assumption that the toxin is active throughout the whole infection process in the different organs. Additionally, the high secretion level of CNF_Y at 37°C suggests that a high concentration of the toxin is needed in the infection process for an adequate effect in the host.

Additionally, the *cnfY* expression has been tested in dependence of different global virulence regulators crucial for temperature- or nutrient-dependent regulation of virulence gene expression in *Y. pseudotuberculosis*. The *cnfY* expression was independent of the ferric uptake regulator (Fur), indicating that CNF_Y synthesis does not depend on the iron concentration in the surrounding of the bacteria. Oppositely, Crp (cAMP receptor protein) activated the *cnfY* expression at the tested conditions, as *cnfY* is significantly less expressed in a *crp* mutant strain at 37°C in nutrient rich medium. The Crp protein controls the transcription of a variety of genes, e.g. *invA* of *Y. pseudotuberculosis*, and operons of the family *Enterobacteriaceae*, depending on carbon sources in the surrounding (Saier, 1998; Zheng *et al.* 2004; Heroven *et al.* 2012). Hence, Crp probably regulates the *cnfY* expression in response of the nutrients in the surrounding.

Previous data also revealed that *cnfY* expression is controlled by the *Yersinia* modulator A (YmoA) (J. Schweer, Master-thesis). The nucleoid-associated protein YmoA is an important modulator involved in different thermo-regulated virulence gene expressions, linking early and late virulence phases (Cornelis *et al.*, 1991). The expression of *cnfY* was repressed by YmoA at 25°C, particularly in the stationary growth phase, similarly to other late virulence genes like the *yops* (Böhme, 2010; Cornelis *et al.*, 1991), indicating that *cnfY* is co-expressed with the *yops* in the late virulence phase *in vivo*.

Since different virulence-relevant factors are often regulated and encoded by the *Yersinia* virulence plasmid pYV (*yadA*, *yops*, and T3SS), the influence of pYV on the expression and secretion of CNF_Y was tested. The data showed neither a virulence plasmid-dependent expression, nor secretion of the toxin. Hence, the plasmid encoded global virulence regulator LcrF, crucial for *yop* expression (Böhme *et al.*, 2012; Lambert

de Rouvroit *et al.*, 1992), plays no role in regulation of the toxin expression at the tested conditions.

Furthermore, the CNF_Y secretion is independent of the virulence plasmid-encoded T3SS. The homologous toxin CNF_1 of *E. coli*, was shown to be secreted by outer membrane vesicles (OMVs) (Davis *et al.*, 2006). This could also be the case for CNF_Y, enabling the toxin to be transported over long distances in the host - independent of the bacteria - to prime the eukaryotic cells before these cells encounter the yersiniae. Nevertheless, a recent work by Kolodziejek *et al.* indicated that *Y. pseudotuberculosis* might not produce OMVs, whereas *Y. pestis* was shown to secrete membrane vesicles at the experimental conditions (Kolodziejek *et al.*, 2013). These data and the sequence-identity to *cnf1* of only around 65% - also in the signal peptide region - suggest an OMV-independent secretion mechanism for CNF_Y. Moreover, the CNF_Y toxin does not harbour a conserved signal sequence at its N-terminus, suggesting a secretion mechanism different from other well described mechanisms.

A recent study of the typhoid toxin from *Salmonella* Typhi - also an A-B toxin - described a bacteriophage endolysin-like N-acetyl-β-D-muramidase, now termed as typhoid toxin secretion A (TtsA), which is essential for secretion of the typoid toxin (Hodak & Galán, 2013). Endolysins are used by bacteriophages for lysis of the bacterial host to release the replicated phages. These peptides are secreted through the inner bacterial membrane and are able to cleave the peptidoglycan of the host (Borysowski *et al.*, 2006; Young, 2002). The secretion of the endolysins is established by holins, small pore forming membrane proteins (Young, 1992, 2002). TtsA contains unique amino acids at the predicted peptidoglycan-binding domain and thus is probably a secretion mechanism newly evolved from bacteria (Hodak & Galán, 2013). Database research at the National Center for Biotechnology Information (NCBI) revealed that also *Y. pseudotuberculosis* YPIII harbours homologous proteins to bacteriophage holins and endolysins in its genome. It can be speculated that the CNF_Y toxin is secreted via a similar pathway as the typhoid toxin of *S.* Typhi.

4.2 CNF_Y constitutively activates the small Rho-GTPases Rac1, Cdc42, and RhoA and causes inflammation

The Rho-GTPases are known to be the target of different virulence factors of pathogenic bacteria. Over 30 bacterial molecules directly or indirectly interacting with the GTPases were described (Symons & Settleman, 2000). All these factors help to ensure a successful infection of the pathogen. The CNF_Y toxin of *Y. pseudotuberculosis* YPIII is a Rho-GTPase constitutively activating toxin. In the present study, it was shown that intoxication of macrophages and epithelial cells with CNF_Y under the tested conditions led to the activation of the three small Rho-GTPases Rac1, RhoA, and Cdc42, whereby the macrophages were more susceptible to the treatment than the epithelial cells. The activation in macrophages was accompanied by high contents of actin stress fibres, formation of filopodia, and lamellipodia, and additionally the formation of giant, multinucleated cells. Previous studies with epithelial cells already demonstrated that CNF intoxication leads to the inhibition of cytokinesis, mainly by activation of RhoA (Falzano *et al.*, 2006; Huelsenbeck *et al.*, 2009). Thus, the cells lose their ability to divide, whereas mitosis continues (Caprioli *et al.*, 1984; Knust *et al.*, 2009).

It was described previously that CNF_Y is able to interact with the three GTPases Rac1, Cdc42, and RhoA. Yet, it was shown to predominantly activate RhoA in intoxicated epithelial cells (Hoffmann *et al.*, 2004; Lockman *et al.*, 2002). However, a recent study also observed CNF_Y-mediated activation of Rac1 and Cdc42 additionally to RhoA, consistent with the data presented in this study (Wolters *et al.*, 2013). Explanations for these variations in activation of the GTPases could be the intoxication periods, the toxin concentrations, and/or the employed cell lines in which CNFs may display different selectivity (e.g. different cellular receptors) and/or efficiency. As demonstrated for macrophages and epithelial cells, eukaryotic cells display a different susceptibility to the toxin treatment. Nevertheless, the Rho-GTPase activation pattern induced by CNF_Y changes over time with a generally more distinct RhoA activation level over Rac1 and Cdc42 two hours after toxin addition (Wolters *et al.*, 2013). Taken together these data suggest that CNF_Y might induce RhoA predominantly at early time points and/or with low toxin concentrations, which are probably found in the host (see also 4.4).

Since these three GTPases are known to influence the activation state among each other, most probably depending on the requirement, the initial RhoA activation could also result in activation/blocking of the other GTPases. The exploitation of this interaction

between the GTPases by enteropathogenic yersiniae was described before. For instance, the activation of Rac1 by invasin is needed for the β_1-integrin mediated invasion of *Yersinia*, which in turn inhibits RhoA activation. This interaction is needed, because RhoA was shown to block the β_1-integrin-mediated invasion (Alrutz *et al.*, 2001; Wong *et al.*, 2006).

CNF_Y-induced changes in the activation pattern of the GTPases with different concentrations, incubation periods, and susceptibilities of the cells could be an advantage for the bacteria in the host, e.g. to induce/inhibit their cellular uptake. Previous studies demonstrated that phagocytes preferentially take up opsonised particles mostly by RhoA-, but also Rac-, and Cdc42-dependent pathways (Caron & Hall, 1998; Cox *et al.*, 1997), which might also be activated by CNF_Y. Additionally, CNF_1 was shown to exploit the ubiquitin-proteasome machinery to eliminate the constitutively active GTPases and thus facilitate the invasion of the bacteria into the host cells (Doye *et al.*, 2002). Furthermore, it has been reported that YPIII can initially survive in macrophages (Grabenstein *et al.*, 2004), prompting the hypothesis that the bacteria might use these phagocytes as vehicles to reach underlying tissues without being attacked by the immune system. This suggests a possible advantage for those bacteria carrying the Rho-GTPase activating CNF_Y toxin to induce their cellular uptake to reach the underlying tissue.

4.3 CNF_Y is crucial for virulence of *Y. pseudotuberculosis* YPIII

The high expression levels of *cnfY* and its regulation by known virulence regulators suggested a function for CNF_Y during the course of infection. The role of CNF_Y was tested in the mouse model with an isogenic *cnfY* mutant strain. With the loss of *cnfY*, the bacterium *Y. pseudotuberculosis* was unable to cause a severe disease. Similar effects were published for uropathogenic *E. coli* strains, showing attenuated virulence in urinary tract infections with the loss of CNF_1 in a mouse model (Rippere-Lampe *et al.*, 2001a).

Additionally, a homolog to the catalytic domain of CNF_1 and thus also of CNF_Y, the toxin BPSL1549 (now termed *Burkholderia* lethal factor 1) of *B. pseudomallei*, is crucial for the virulence of this bacterium in a mouse model. This factor is a cytotoxin, which deamidates the glutamine of a translational factor and thereby inhibits translation (Cruz-Migoni *et al.*, 2011). These data display the importance of each individual bacterial toxin for their parental strain, as the deletion of one factor renders the bacterium avirulent. In general, such a dramatic influence on virulence by the loss of one single gene has only

been observed for important virulence genes or regulators of *Yersinia*: (1) with the absence of the global *yop* expression regulator LcrF (Böhme *et al.*, 2012) or (2) when different *yop* genes are deleted (Logsdon & Mecsas, 2003).

It is relevant to note that YopT (Viboud & Bliska, 2001), and the response regulator PhoP (Grabenstein *et al.*, 2004) are not expressed in the CNF_Y^+ *Y. pseudotuberculosis* strain YPIII, indicating that different strains may exert virulence through alternative mechanisms. The *cnfY* gene is only active in few *Y. pseudotuberculosis* strains. Large deletions over the whole gene in other *Y. pseudotuberculosis* as well as *Y. pestis* strains are frequently found. As the toxin is flanked by a transposase it can be assumed that this gene has been acquired from other bacterial strains (Lockman *et al.*, 2002). Presumably the strains with deletions in the *cnfY* gene did not utilise the gene and/or had even a disadvantage in their colonisation/persistence in the host by the toxin.

Yet, the clinical *Y. pseudotuberculosis* isolate YPIII was shown to be strongly attenuated in its virulence without the toxin. Due to mutations in the *phoP* gene, this strain is not able to replicate in macrophages (Grabenstein *et al.*, 2004). Other *Y. pseudotbuerculosis* strains display a strongly attenuated virulence upon inactivation of PhoP (Fisher *et al.*, 2007; Grabenstein *et al.*, 2004; Oyston *et al.*, 2000). However, YPIII retains its virulence despite an unfunctional PhoP, which might be attributed to the activity of CNF_Y. Furthermore, a $phoP^+$ mutant of YPIII used in this study was also shown to lose its virulence without the functional *cnfY*, indicating a significant role for CNF_Y during *Y. pseudotuberculosis* YPIII infection independent of PhoP.

One strain harbouring both the *cnfY* gene and the functional *phoP* was already identified, namely *Y. pseudotuberculosis* IP2666 (Pujol & Bliska, 2003). This strain was shown to be able to replicate within macrophages (Grabenstein *et al.*, 2004). Additionally, it was demonstrated that the wild-type strain IP2666 seems to be slightly more virulent than the wild-type strain YPIII (McCoy *et al.*, 2010). Thus, it can be hypothesized that the presence of both functional genes might be an advantage for this strain. However, this hypothesis is rather speculative as the two *Y. pseudotuberculosis* strains probably display several other differences.

Studies addressing the dissemination ability of *Y. pseudotuberculosis* YPIII to deeper tissues revealed a strong impact of the toxin in the colonization of the MLNs, spleen, and liver. The *cnfY* mutant bacteria were still able to reach the underlying tissue, but could not persist for longer than three to five days after infection. This phenomenon was also

observed with different *yop* single mutant strains, e.g. *yopE* or *yopH* (Logsdon & Mecsas, 2003), indicating a similar function for CNF_Y in defending the bacteria against the immune system. The wild-type bacteria in contrast were able to replicate and led ultimately to the death of infected animals.

Moreover, compared to YPIII the *cnfY* mutant strain did not induce the same release of proinflammatory cytokines into the serum of infected animals, resulting in a significantly lower inflammatory response. Particularly eotaxin, a chemokine involved in processes of allergic inflammation, was secreted in significantly higher amounts upon infection with YPIII, compared to the YP147 (Δ*cnfY*) infection. This cytokine was demonstrated to prime the production of reactive oxygen species (ROS) from eosinophils (Honda & Chihara, 1999), a process associated with cell- or tissue-damage (Bergamini *et al.*, 2004). Interestingly, this reaction was inhibited by the pertussis toxin of *Bordetella pertussis*, an A-B toxin blocking the activation of GTPases probably involved in the eosinophil activation signal transduction (Honda & Chihara, 1999). Hence, this toxin exerts counteracting activities to CNF_Y.

Data of this work showed that *Y. pseudotuberculosis* wild-type, which was demonstrated to be able to persist in the systemic organs, induces eotaxin secretion into the serum. Furthermore, recruitment of eosinophils into the gastrointestinal tract and PP by eotaxin was described (Mishra *et al.*, 2000). It can be assumed that YPIII primes the production of ROS by eosinophils, leading to subsequent dramatic tissue damage in the infected animals probably mainly in the intestine. Further, CNF_Y could enhance the production of ROS by activating GTPases involved in signaling pathways of the eosinophil activation. This hypothesis is in accordance with the histopathological analysis and the immune cell composition in the different infected tissues. These revealed a strong CNF_Y involvement in the acute inflammatory response and host tissue damage during infection. Former studies of *cnf1* uropathogenic *E. coli* deletion mutant strains revealed similar effects after mouse infection, using urinary tract and prostatitis infection models by subcutaneous injection (Rippere-Lampe *et al.*, 2001a, b). It was shown that CNF_1 leads to highly inflamed bladders or prostates of the animals.

Notably the caecum and ileum of infected mice displayed severe signs of diffuse inflammation due to CNF_Y with disrupted villi, thickened lamina propria, and resulting shortened gut lengths. With the loss of CNF_Y the intestinal inflammation of mice was restricted to small foci and reversible, whereas with CNF_Y the inflammation is more

generalized. Similar impacts on the intestine of mice have been found with *S. enterica* serovar Typhimurium (*S.* Typhimurium) infections, revealing an advantage for these bacteria in the inflamed gut to compete with the intestinal microbiota, thus enhancing the growth of *Salmonella* in the gut lumen (Stecher *et al.*, 2007; Winter *et al.*, 2010). *S.* Typhimurium was demonstrated to being able to metabolize ethanolamine, provided by the host, which enables the bacterium to avoid competition with the microbiota, regarding nutrients (Thiennimitr *et al.*, 2011). *Yersinia* might also be able to metabolize substances produced in the inflamed gut, which the bacteria of the microbiota can not metabolize.

Additionally, it was shown that *S.* Typhimurium exploits the inflammatory response (primarily of neutrophils), which results in disruption of the microbiota and the intestinal barrier, to reach the underlying tissues (Winter *et al.*, 2010). Hence, it can be hypothesized that the CNF_Y induced intestinal inflammation promotes the migration of the yersiniae through the gut by the disruption of the intestinal barrier.

The decreased immune cell content in the *Y. pseudotuberculosis* wild-type infected spleens compared to the *cnfY* mutant suggests an induction of apoptosis of immune cells in the presence of the toxin CNF_Y: the histopathologic evaluation underlined this assumption, as the necrotic spots in this organ were not seen after infection with the *cnfY* mutant strain. In YPIII infected spleens, cell death led to atrophy of the organ, displayed by shrinking and less red coloring, whereas infection with the *cnfY* mutant led to hyperplasia of the white pulp (contains mainly lymphocytes) indicating a triggered immune response, which is also displayed by splenomegaly.

4.4 CNF_Y functions as a Yop delivery enhancer

Professional phagocytes are preferentially targeted by the Yop effector proteins of *Yersinia* (Durand *et al.*, 2010). Since these cell types were shown to be mostly affected by CNF_Y, testing the differences in Yop delivery rates into the immune cells caused by CNF_Y presence was consequential. Furthermore, it was observed that a selective modulation of RhoA activity by *Y. pseudotuberculosis* (e.g. by the binding of InvA to the β_1-integrins or signals triggered by the YopB/D translocon) leads to cellular changes, controlling the T3SS pore formation and Yop translocation (Mejía *et al.*, 2008).

As discussed above, the CNF_Y intoxication of eukaryotic cell lines predominantly induces the activation of RhoA. Overall significantly higher translocation rates due to CNF_Y could

be detected in tested epithelial cells and macrophages. This is consistent with a recently published study in which CNF_Y preincubation enhances the Yop delivery of a CNF_Y-negative *Y. enterocolitica* strain (Wolters *et al.*, 2013). Wolters *et al.* were able to demonstrate that mostly CNF_Y-induced Rac1 activation is responsible for higher Yop translocation by *Y. enterocolitica* (CNF_Y^- strain).

Contrary to that, CNF_Y induced Yop translocation by *Y. pseudotuberculosis* into macrophages was diminished after treatment with the Rho inhibitor C3-transferase of *C. botulinum*, yet was unaffected by the Rac1 inhibitor TcdBF of *C. difficile* even at high concentrations in this study. This demonstrated that the activation of RhoA by CNF_Y is essential to enhance Yop translocation of *Y. pseudotuberculosis* into macrophages. This is consistent with the study of Mejía *et al.*, which showed that mostly RhoA controls the pore formation of the T3SS (Mejía *et al.*, 2008). These discrepancies in between the study of Wolters *et al.* and this current study regarding the impact of the different GTPases on Yop delivery could be due to differences in the experimental setups, likely the differences between the species *Y. pseudotuberculosis* and *Y. enterocolitica*. Factors causing these discrepancies might be differences in the YadA/InvA-promoted signaling events, in Yop protein abundance (e.g. the RhoA-inactivating YopT does not exist in YPIII), and in the regulation of Yop delivery by Rho-GTPases.

Furthermore, CNF_Y influence on Yop translocation rates was observed for all cells of the lymphatic tissues PP, MLNs, and spleen *in vivo*. Less Yop delivery into the different immune cells - mostly into phagocytes - was measured after infection with the *cnfY* mutant strain, especially in the MLNs. Translocation rates into the splenocytes would probably differ more significantly between YPIII- and YP147 (Δ*cnfY*)-infected animals. However, it was shown that the YPIII infection causes necrosis and particularly reduced amounts of phagocytic cells in the spleen, resulting in overall lower numbers of living cells. As professional phagocytes are preferentially attacked by the Yop proteins (Durand *et al.*, 2010) and some of these proteins cause cellular death (see 4.4.1) (Viboud & Bliska, 2005) identification of less Yop translocated cells could result since only living cells were analyzed. Taken together, CNF_Y enhances Yop translocation by activation of Rho-GTPases, which is crucial for defence of *Y. pseudotuberculosis* YPIII against the immune system in this mouse infection model.

4.4.1 CNF_Y causes inflammation and increased cellular death

Gastrointestinal infections with enteropathogenic *Yersinia* lead to a biphasic inflammatory process. Initially, the bacteria are able to replicate, adhere to, and transmigrate through the gut epithelial layer accompanied only by a slight antibacterial defence response with little inflammation, e.g. IL-8 expression by epithelial cells. Subsequently, an acute influx and activation of phagocytes, cytokine production and tissue damage occurs (Autenrieth *et al.*, 1993b; Dube *et al.*, 2001, 2004). The invading yersiniae are recognized at first due to their LPS by Toll-like receptor 4 (TLR4) of naïve host macrophages. This initiates the production of proinflammatory cytokines by activation of the mitogen-activated protein kinase (MAPK) and NF-κB (Haase *et al.*, 2003; Zhang & Bliska, 2003). YopJ was shown to inhibit the activation of MAPK and NF-κB after translocation into the eukaryotic cell, inducing an apoptotic signaling pathway, which includes the activation of initiator caspase-8 and the executioner caspase-3, -7, and -9 (Bergsbaken & Cookson, 2009; Philip & Brodsky, 2012; Zhang *et al.*, 2005).

A *yopJ* mutant strain was observed to be deficient in spreading from PP to other lymphoid tissues (Monack *et al.*, 1998) similar to the effect of a *cnfY* deletion mutant. Hence, both YopJ and CNF_Y are needed for the efficient systemic dissemination after oral infection. Moreover, the wild-type *Yersinia* infection was shown to induce apoptosis of macrophages in the spleen (Monack *et al.*, 1998). YopJ seems to be mainly responsible for elimination of the immune cells in this organ and thereby decreases the triggered immune response against *Yersinia*. However, since CNF_Y enhances Yop delivery predominantly into the innate immune cells, a higher amount of YopJ is also released into the cells and probably causes increased apoptosis. This effect is presumably displayed by the shrinking of the spleen and the decreased immune cell contents after infection with YPIII. Apoptotic macrophages are eliminated by other phagocytes, triggering the production of anti-inflammatory cytokines like IL-10 and TGF-β (Fink & Cookson, 2005; Savill *et al.*, 2002).

Since CNF_Y seems to enhance the apoptotic cell death of macrophages, the bacteria might be less attacked by these cells and subsequently are able to replicate uncontrollably. This would result in even higher CNF_Y secretion, higher Yop translocation, and thus increased amounts of apoptotic cells. Generally, the apoptotic cell death is non-inflammatory, yet it is probably not completely immunologically silent particularly not if the amount of apoptotic cells increases significantly, e.g. phagocytosis

of apoptotic cells can prime other immunological responses like the activation of cytotoxic $CD8^+$ T cells (Philip & Brodsky, 2012). During the process of the *Yersinia* infection, the contents of activated macrophages increase, whereas the contents of naïve macrophages decrease. Moreover, the infection induces cell death of naïve macrophages by apoptotic pathways, while it induces cell death of mature macrophages by proinflammatory pyroptosis (Bergsbaken & Cookson, 2007). Pyroptosis occurs due to activation of a multiprotein complex, the inflammasome, a platform for the autoprocessing and activation of the cysteine protease caspase-1. *Yersinia* was shown to induce caspase-1 activation and thus initiates pyroptosis by LPS, the T3SS, and the translocated YopJ (Brodsky *et al.*, 2010; Philip & Brodsky, 2012; Zheng *et al.*, 2011). The activation of caspase-1 induces the secretion of proinflammatory cytokines like IL-1α, IL-1β, and IL-18, which causes the cell death (Bergsbaken & Cookson, 2007).

The induction of the proinflammatory cell death (pyroptosis) is associated with the later infection phase of *Yersinia*. It is indeed very likely that CNF_Y promotes cell death of activated phagocytes by pyroptosis in the spleen. In this study, necrotic spots were observed in spleens of YPIII-, but not of Δ*cnfY*-infected animals six days after infection. Additionally, the wild-type strain induced a harsh release of proinflammatory cytokines (TNF-α, IL-6, GM-CSF, and IL-12 (p40)) into the serum and caused severe inflammation of the intestine, especially the ileum and caecum. Moreover, CNF_Y was shown to manipulate the immune cell contents in the spleen. Particularly macrophage-, monocyte-, and neutrophil-amounts were significantly diminished three days post infection. On the other hand, an infection with the *cnfY* mutant strain resulted in a harsh influx of phagocytes into the spleen (in comparison to spleens of uninfected mice) and induces only minor inflammation, which strongly suggests that the increased translocation of YopJ into phagocytes in the presence of CNF_Y stimulates proinflammatory cell death in the spleen during later stages of the infection.

Particularly striking was the effect of CNF_Y on the NK cell contents in the spleen, which were significantly decreased when compared to the amounts in uninfected spleens. This reduction could either be caused by induced cell death or by migration of the NK cells from the spleen into other tissues. A deletion mutant of *cnfY* in contrast led to no or even slightly increased amounts of these cells in the spleen when compared to uninfected mice. Furthermore, no differences in the amounts of NK cells could be detected in the PP and MLNs between YPIII- and Δ*cnfY*-infected animals. Hence, CNF_Y seems to contribute to NK cell reduction in the spleen at this stage of the infection, by enhancing

cell death. A similar effect was observed with a *yopM* deficient *Y. pestis* mutant, which failed to decrease the global NK cell levels, whereas the wild-type strain led to a depletion of these cells (Kerschen *et al.*, 2004). Hence, CNF_Y seems to enhance the NK cell depletion by inducing a higher YopM translocation. These data propose that CNF_Y secretion results in death of immune cells allowing an uncontrollably replication of the bacteria, which in turn secrete higher CNF_Y amounts.

The secreted toxin leads to the activation of the small Rho-GTPases as mentioned above. It was recently reported that the effector SopE of *Salmonella*, which also activates Rac1 and Cdc42, triggered the NOD1 pathway (Keestra *et al.*, 2013). NOD1 is a pattern recognition receptor sensing cytosolic microbial products (similar to NOD2), which monitors the activation states of the three small Rho-GTPases RhoA, Rac1, and Cdc42. Hence, the activation of the GTPases induced NOD1 signaling pathways, resulting in the RIP2-mediated triggering of the nuclear factor κB (NF-κB)-dependent proinflammatory responses (Keestra *et al.*, 2013). Additional to that, all three Rho-GTPases were previously shown to activate the NF-κB pathway, but particularly CNF_1-activated Rac1 has been reported to induce the NF-κB activation (Boyer *et al.*, 2004). CNF_1 leads to the clustering of the NF-κB inhibitor IκBα and components of the IκBα E3-ubiquitin ligase into formed membrane ruffles. This indicates a similar effect for CNF_Y, leading to even higher inflammatory responses, activation of phagocytes, and tissue damage. This would in turn presumably enable the bacteria to spread to the underlying tissues and additionally lead to the release of nutrients through the cell death.

4.4.2 YopE exerts counteracting effects to CNF_Y

Since CNF_Y was shown to enhance the Yop delivery by activating the small Rho-GTPases, also Yop proteins with counteracting effects on the GTPases are translocated more frequently (YopE, YopA/O, and YopT). Particularly YopE, a GTPase-activating protein (GAP), leading to the inactivation of the GTPases, seems to act as a counterplayer for CNF_Y. YopE was previously shown to inhibit the Yop delivery by inactivation of RhoA and Rac1. Additionally, a *yopE* mutant strain was observed to cause increased translocation rates into epithelial cells compared to the wild-type (Aili *et al.*, 2002, 2006, 2008; Songsungthong *et al.*, 2010; Wong & Isberg, 2005). Thus, YopE acts as a regulator for the Yop delivery, like an intracellular control system, which measures and adjusts the amount of translocated Yop proteins during infection. A study

of the effector YopJ demonstrated the importance for a tight regulation of the Yop delivery in the oral mouse infection: a higher YopJ translocation results in raised cytotoxicity rates of phagocytes, yet leads to a decreased virulence of *Y. pseudotuberculosis*, as does the complete loss of YopJ (Brodsky & Medzhitov, 2008). The YopJ hyper-secretion or deletion resulted in reduced proinflammatory cytokine levels in the serum of infected mice (e.g. TNF-α or IL-6), similar to the effect of an infection with the *cnfY* mutant strain observed in this study. It was hypothesized that the secretion of proinflammatory cytokines induced by the wild-type bacteria promotes tissue damage, which in turn would enable the bacteria to spread to deeper tissues (Brodsky & Medzhitov, 2008). Since the mutant strains did not induce the same inflammatory response like the wild-type, this could result in disadvantages in dissemination of the bacteria.

In this study it was demonstrated that the absence of *yopE* in a *Y. pseudotuberculosis* infection did not or only slightly increased the Rac1- or RhoA-GTP levels or the amount of translocated Yop proteins into murine macrophages with or without CNF_Y pretreatment. This indicates that although YopE possesses counteracting activities compared to CNF_Y, it is not strong enough to antagonize CNF_Y intracellularly in murine macrophages at the tested conditions *in vitro*. A recently published study is supporting this observation, as it shows that none of the Rho-GTPase interacting Yop effector proteins (YopE, YopO, and YopT) were able to reduce the effect of CNF_Y on Yop delivery of *Y. enterocolitica* into human epithelial cells (Wolters *et al.*, 2013).

However, the Yop secretion is dependent on contact with eukaryotic host cells *in vivo* and calcium depletion *in vitro* (Forsberg *et al.*, 1987, 1994; Goguen *et al.*, 1984; Pettersson *et al.*, 1996). Since CNF_Y was shown to be secreted at infection relevant conditions, it can be assumed that CNF_Y is priming the eukaryotic cells - most likely the professional phagocytes - by constitutively activating the Rho-GTPases, resulting in higher Yop delivery rates. However, it can be hypothesized that if sufficient counteracting Yop effectors (especially YopE) are translocated, the translocation is diminished, most likely to prevent proinflammatory cell death and thus the triggering of an increased inflammatory response (Aili *et al.*, 2008). Nevertheless, counteraction of CNF_Y by other cell functions cannot be excluded, e.g. the enhancement of deamidation and subsequent ubiquitin-dependent degradation of the activated GTPases, as it was observed after CNF_1 intoxication (Doye *et al.*, 2002).

4.4.3 Schematic model of CNF_Y-enhanced Yop delivery

The results of this study highlight for the first time a dominant role of CNF_Y during the course of an oral *Y. pseudotuberculosis* YPIII infection. Based on these data, a basic model of the CNF_Y-enhanced Yop delivery can be proposed (see Figure 4.4.1).

To the current knowledge, CNF_Y is starting a cascade, resulting in the proinflammatory cell death pyroptosis and additional proinflammatory responses. In the first step during the early phase of the infection process, the secreted toxin is endocytosed by infiltrating innate immune cells (e.g. neutrophils, macrophages, DCs). The catalytic domain of CNF_Y is secreted into the cytosol of the phagocytes in a pH-dependent manner and activates the Rho-GTPases, in particular RhoA, by deamidation. The constitutive activation of the GTPases induces actin-polymerization, leading to enhanced Yop delivery into the host cell. The translocated Yop effector proteins counteract the innate and adaptive immune responses by inhibition of the invading immune cells and the subsequent induction of apoptosis. In parallel, the bacteria can replicate uncontrollably, leading to the secretion of even higher CNF_Y amounts. The resulting enhanced activation of the Rho-GTPases triggers proinflammatory responses like the NOD1-RIP2 (NF-κB) signaling pathway. Hence, the *Yersinia* infection increases the numbers of activated macrophages. The interaction of the bacteria with these cells results in the proinflammatory cell death pyroptosis, inducing a strong inflammation and necrosis of the infected tissues during later phases of the infection.

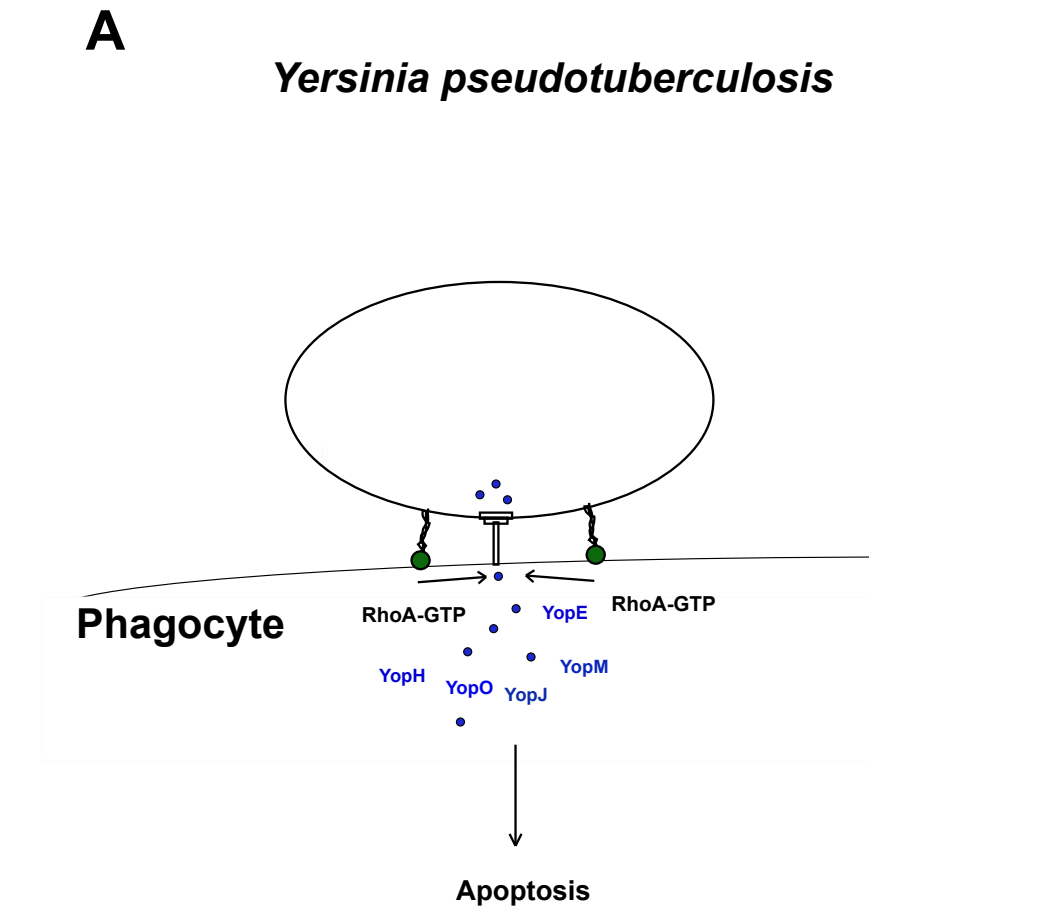
A
Yersinia pseudotuberculosis
Phagocyte
RhoA-GTP
YopE
RhoA-GTP
YopH
YopO
YopJ
YopM
Apoptosis

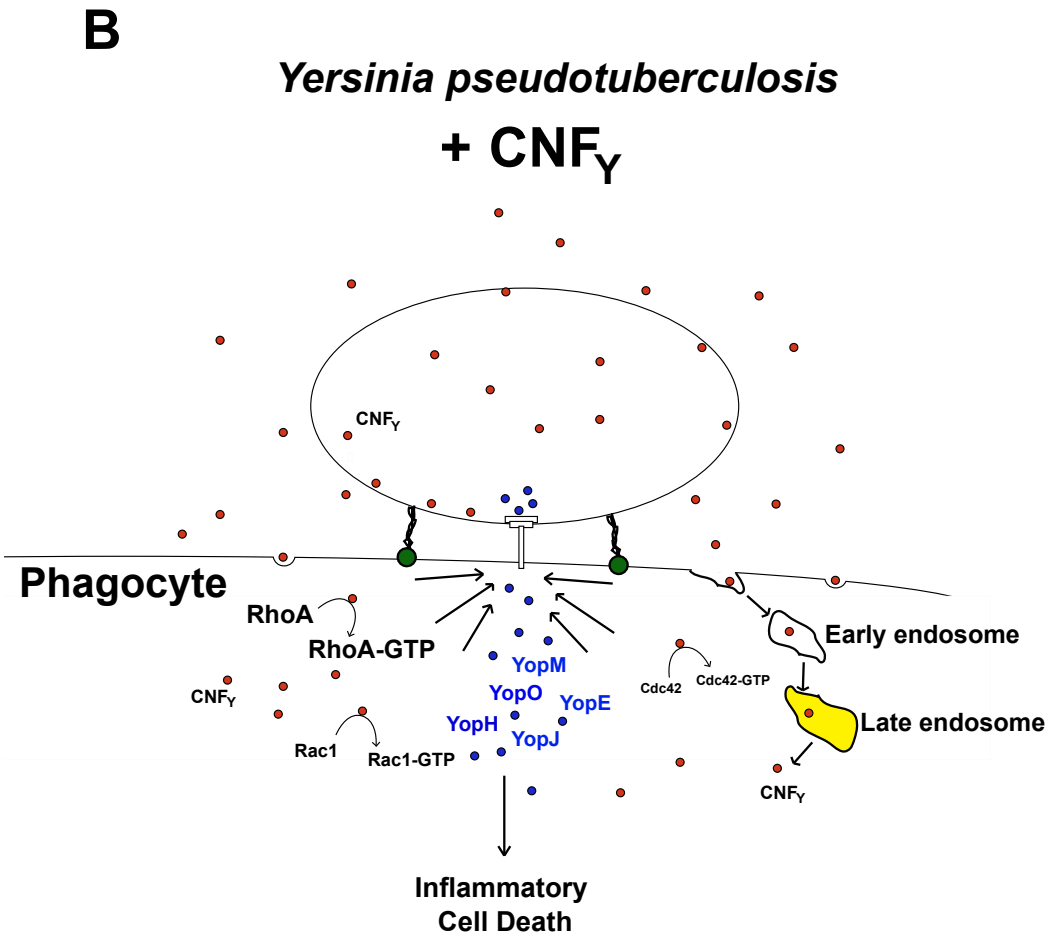
B
Yersinia pseudotuberculosis
+ CNFY
CNFY
Phagocyte
RhoA
RhoA-GTP
CNFY
Rac1
Rac1-GTP
YopM
YopO
YopE
YopH
YopJ
Cdc42
Cdc42-GTP
Early endosome
Late endosome
CNFY
Inflammatory
Cell Death

Figure 4.4.1: Proposed model of CNF_Y-enhanced Yop delivery.
(A) Adhesion of *Y. pseudotuberculosis* to macrophages induces activation of RhoA, resulting in actin polymerization, which in turn leads to Yop delivery into the phagocyte by the T3SS. The translocated Yop effector proteins inhibit the phagocytosis and induce YopJ-mediated apoptotic cell death. (B) CNF_Y-producing *Y. pseudotuberculosis* strains secrete the toxin prior or parallel to the interaction with the macrophage. CNF_Y is internalized, most likely by receptor-mediated endocytosis, into early endosomes. Due to acidification of the early endosomes, maturation to late endosomes occurs. The catalytic domain of CNF_Y is translocated across the membrane of the endosome via its translocation domain. The toxin deamidates the small Rho-GTPases RhoA over Rac1, and Cdc42 and renders them constitutively active. The activation results in enhanced Yop delivery and subsequent cell death. The Rho-GTPase activation was demonstrated to promote pore formation of the T3SS, probably leading to caspase-1 activation (Brodsky *et al.*, 2010; Mejía *et al.*, 2008). Additionally, the induced cell death may lead to increased proinflammatory immune responses, resulting in raised levels of activated macrophages and the *Yersinia*-triggered activation of caspase-1 (Bergsbaken & Cookson, 2007). This activation induces the release of proinflammatory cytokines and the proinflammatory cell death pyroptosis. Meanwhile, the bacteria replicate and the CNF_Y levels increase, resulting in enhanced activation of the Rho-GTPases and thus increased inflammatory pyroptosis.

4.5 CNF_Y exerts a minor impact on the epithelial layer permeability

An important factor for the host to prevent penetration or dissemination of bacteria is the maintenance of the intestinal epithelial barrier function. Different actin cytoskeleton-modifying bacterial toxins are known to destroy this barrier, like the GTPase inactivating (glycosylation) toxin A of *C. difficile*, which causes severe inflammatory enterocolitis and diarrhea (Hecht *et al.*, 1988; Shen, 2012; Triadafilopoulos *et al.*, 1987). Similar effects were observed in the histopathological analysis of the small intestine after YPIII infections in this study.

The intoxication of a monolayer with the CNF_1 toxin of *E. coli* leads to the disruption of the barrier function mostly by the constitutive activation of RhoA, which affects the tight junction integrity (Schlegel *et al.*, 2011). Since CNF_Y was shown to predominantly activate RhoA, it was assumed that this toxin exerts an even stronger impact on the cell-cell contact of the monolayer than CNF_1, thus enabling the bacteria to pass through the epithelial layer without the M-cells (paracytosis). Additionally, CNF_Y was demonstrated to decrease the endothelial barrier integrity (Baumer *et al.*, 2008), possibly enabling the bacteria to cross the endothelial layer of the blood vessels. However, incubation of an epithelial monolayer of Caco-2 cells with the CNF_Y toxin revealed only a slight increase in permeability, shown by the measurement of the trans epithelial electrical resistance (TEER). This barrier breakdown was not as harsh as the disruption caused by the

proteins of the virulence plasmid (coding for T3SS and the Yop effector proteins), indicating a significant role for these proteins to facilitate the transmigration of the yersiniae across membranes in the host. Consistent with this assumption, it was recently shown that the virulence plasmid and particularly YopJ are needed to disrupt the intestinal barrier integrity *in vivo*. YopJ was shown to be able to subvert the NOD2/RICK/TAK1 pathway, activate caspase-1, and induce the secretion of IL-1β in the PP, thus increasing the epithelial barrier permeability (Jung *et al.*, 2012; Meinzer *et al.*, 2012). These results strongly suggest that CNF_Y induces the disruption of the intestinal epithelial membrane by enhancing the delivery of YopJ. This would promote the dissemination of *Yersinia* by exploiting the mucosal inflammatory response.

4.6 CNF_Y activity is detrimental to *Y. pseudotuberculosis* without activated T3SS

To detect an additional function of CNF_Y besides the enhancement of Yop delivery during the course of infection, mutant strains without a functional T3SS were tested for colonizing abilities, histopathological changes, and the host immune response in both, the presence and absence of CNF_Y.

It was observed that a functional T3SS of *Y. pseudotuberculosis* YPIII is crucial to efficiently colonize the gastrointestinal tract, as the bacteria without a functional T3SS are significantly less able to colonize. This is consistent with previous studies demonstrating that mutations in different genes encoding components of the T3SS lead to non-efficient colonization of the gastrointestinal tract (Mecsas *et al.*, 2001). The mutant strains without the functional T3SS colonized the MLNs with equal amounts as the wild-type strain. It was described before that *Y. pseudotuberculosis* has a tropism for B cell and T cell zones in the MLNs, which seems to protect wild-type bacteria as well as T3SS mutant bacteria from the infiltrating phagocytes (Balada-Llasat & Mecsas, 2006).

However, three days post infection the exclusive loss of either the functional T3SS (Δ*yscS*) or *cnfY* had no significant impact on the colonization of the MLNs by the bacteria in comparison to the colonization by the wild-type. Yet, decreased amounts of neutrophils and monocytes were detected after infection with either the *cnfY* or the *yscS* mutant strain in comparison to the amounts in the MLNs of YPIII-infected animals. This leads to the assumption that neither CNF_Y nor the Yop machinery alone induce the increase of immune cells normally detected in the YPIII infection. Hence, it can be

hypothesized that the concerted presence of the Yop machinery and CNF_Y (e.g. by enhancing the Yop delivery) is responsible for the higher contents of neutrophils and monocytes in the MLNs. Yet, the *cnfY* mutant strain is in the long-term probably more efficient in defending the immune system, due to the Yop proteins that are translocated.

Moreover, the *yscS* mutant strain failed to reach the systemic organs spleen and liver, indicating that the Yop machinery is essential for *Y. pseudotuberculosis* YPIII to spread. Contrary to that, the *cnfY* mutant strain was able to colonize the spleen and liver, but was cleared rapidly. Hence, the Yop machinery is crucial to reach the systemic organs, whereas the Yop translocation enhancement of CNF_Y is presumably essential for *Y. pseudotuberculosis* YPIII to efficiently colonize these organs.

Interestingly, the double mutant strain without *cnfY* and *yscS* was able to colonize the gastrointestinal tract better than the *yscS* single mutant strain, particularly the small intestine and the caecum. Thus, CNF_Y seems to be a disadvantage for those bacteria without a functional T3SS or under conditions in which the T3SS is not fully active. Former studies showed a decreased ability of single *yop* mutant strains to colonize the intestine and PP when co-infected with the wild-type strain, compared to single infections of the mutants (Logsdon & Mecsas, 2003, 2006). Regarding the *yop* mutant strains, their reduced ability to colonize is due to the inflammation of the gastrointestinal tract induced by the co-infected wild-type. Hence, immune cells (e.g. neutrophils) infiltrate and lead to the reduction of the mutant bacteria, as these bacteria are less able/unable to withstand the immune response.

Since CNF_Y was shown before to be immunogenic (Mou *et al.*, 2012), it can be assumed that this toxin is leading to an infiltration of innate immune cells into the intestine. This attraction of immune cells would eradicate the bacteria, as the functional T3SS is missing. Additionally, CNF_1 of *E. coli* has been shown to activate NF-κB by the constitutively activation of Rac1, which is causing inflammation (Boyer *et al.*, 2004). CNF_Y could induce similar effects, since it was also shown to activate Rac1. Hence, CNF_Y could induce inflammatory responses by activating NF-κB pathways. This assumption was supported by the histopathological analysis, which displayed that the ileum of mice infected with the mutant without a functional T3SS, but CNF_Y showed sites of inflammation, whereas the ileum of mice infected with the double mutant strain ($YscS^-$, CNF_Y^-) was not inflamed and appeared like the uninfected control group. This supports the hypothesis that CNF_Y induces inflammation in the host's intestine, resulting in a

faster eradication of the single mutant strain without a functional T3SS compared to the double mutant strain without the toxin and the T3SS.

Slightly higher amounts of the double mutant bacteria without the functional T3SS and CNF_Y in comparison to the single mutant without a functional T3SS were reisolated of the PP. However, the differences in inflammation seen in the histopathological analysis of the ileum were not displayed in the analysis of the immune response in the PP. No significant differences in the recruitment of immune cells could be detected upon infection. Reasons therefore could be that the (1) differences are too minor to detect or (2) the time point of investigation three days after infection is too early.

4.6.1 CNF_Y causes long-lasting modulation of the immune cell contents in the spleen

The detected bacterial loads of the *cnfY* mutant strain in the different organs indicated the necessity of CNF_Y for the effective colonization of the underlying tissues MLNs, spleen, and liver by *Y. pseudotuberculosis* YPIII. However, no difference could be detected between YPIII and a *cnfY* mutant in the colonization of the gut and gut-related tissues up to seven days after infection. So far, not much is known about persistence and long-term influence on the immune system after infection of mice with avirulent/low virulent *Yersinia* strains. A long-range infection with a *cnfY* mutant strain, a pYV-negative strain (e.g. without the T3SS and the Yop effector proteins), and a *cnfY*, pYV-negative mutant strain was performed in this study to measure a possible exclusive long-term effect of CNF_Y.

The *cnfY* mutant strain could be reisolated of the caecum (not of the other tissues) of infected mice 28 days post infection. The pYV-negative mutant strains - with or without *cnfY* - were initially able to colonize, but could not persist over 28 days in the caecum. Hence, not *cnfY* but the virulence plasmid encoded genes are crucial for the persistence of the bacteria in detectable amounts over long time periods in the host's intestine.

Increased levels of the immune cells DCs, monocytes, NK cells, T cells, and B cells could be measured in the PP of mice infected with the different strains (pYV^- CNF_Y^+, pYV^+ CNF_Y^- and pYV^- CNF_Y^-) in comparison to uninfected mice. Yet, the measured immune responses showed no significant differences among the strains. These data indicated an ongoing immune reaction even though no bacteria were detectable in this tissue.

However, the infection with the different avirulent/low virulent *Yersinia* strains resulted in different immune responses in the MLNs and spleens of the infected mice over a long period of infection. The MLNs contained slightly increased amounts of the immune cells upon infection with all tested strains (pYV$^-$ CNF$_Y^+$, pYV$^+$ CNF$_Y^-$ and pYV$^-$ CNF$_Y^-$) when compared to uninfected MLNs. However, the increase of the immune cells (neutrophils, macrophages, DCs, monocytes, NK cells, and B cells) was most significant in the presence of CNF$_Y$ and absence of the T3SS/Yop machinery. This leads to the hypothesis that CNF$_Y$ could be immunogenic and has a long-term influence on the immune system independent of the T3SS machinery. The hypothesis is supported by a study, where the CNF$_Y$ toxin of *Y. pseudotuberculosis* was administered subcutaneously to vaccinate mice. This vaccination entails immunity against a subsequent *Y. pseudotuberculosis* aerosol mouse infection (Mou *et al.*, 2012).

Since the splenic structure is mostly altered over long time periods, the spleen weights were recorded 28 days post infection to detect possible changes caused by necrosis or infiltrating immune cells. Significant differences in the spleen weights of uninfected and infected animals could be detected in the long-term infection. These data showed that the infection of mice with the strain harbouring CNF$_Y$ but not pYV caused slightly reduced spleen weights, whereas the infection with the strain harbouring pYV but not CNF$_Y$ caused significantly increased spleen weights, when compared to the spleen weights of uninfected mice. The spleen weights of mice infected with the double mutant, without pYV and CNF$_Y$, were significantly increased when compared to mice infected with the mutant harbouring CNF$_Y$, but not the Yop machinery. These effects could either be due to (1) long-term changes of the splenic structure by the secreted toxin or effectors, (2) an initially/ongoing infiltration of immune cells or (3) a bacterial colonization of the spleen below the detection limit.

Most strikingly, CNF$_Y$ seems to diminish the amount of immune cells in the spleen, as the infection with the strain carrying *cnfY* but not the virulence plasmid resulted in significantly reduced immune cells (neutrophils, macrophages, DCs, monocytes, NK cells, and B cells) 28 days post infection. This effect was not detected upon infection with the strains without the toxin, no matter whether the virulence plasmid (CNF$_Y^-$ pYV$^{+/-}$) was present, proposing that the toxin caused the decreased amount of immune cells. Moreover, F4/80^{hi} macrophages are resident macrophages of the spleen (Lloyd *et al.*, 2008), thus CNF$_Y$ seems to eliminate the immune cells independently from the Yop machinery. Furthermore, the virulence plasmid of *Y. pseudotuberculosis* is crucial to

infect the systemic organs spleen and liver in the oral infection process (Balada-Llasat & Mecsas, 2006). Hence, the bacteria with CNF_Y, but without pYV are not able to reach the spleen, yet were shown to decrease the amount of residential immune cells in this organ, indicating that CNF_Y reaches the spleen independently from the presence of the bacteria.

The toxin circulation could be via the blood, as it is described for other secreted bacterial toxins like the tetanus toxin of *C. tetani* (Schiavo *et al.*, 2000). As described above, the toxin is secreted by an unknown mechanism and is able to increase the endothelial barrier permeability (Baumer *et al.*, 2008), which could enable the toxin to enter the blood stream and circulate to the different tissues. It can be further hypothesized that the toxin induces the production of ROS, resulting in tissue damage. Additionally, data of this work indicate that CNF_Y is able to eliminate immune cells without the Yop delivery machinery. Since the homologous toxin CNF_1 of *E. coli* was shown to induce necrosis of rabbit skin when injected subcutaneously (Caprioli *et al.*, 1983), CNF_Y could have a similar effect in the spleen.

The loss of *cnfY* was shown to cause an influx of immune cells into the spleen of the infected animals, resulting in splenomegaly, which was still measurable after 28 days of infection. Another avirulent enteropathogenic *Yersinia* strain also induces splenomegaly upon infection (Ruiz-Bravo *et al.*, 2001). Further, it causes increased levels of $CD3^+$ T cells, $CD4^+$ helper T cells, $CD8^+$ cytotoxic T cells, and $CD11b^+$ phagocytic cells in the spleen, although the mice were not colonized, except for the feces. The phenomenon of fecal excretion without detectable bacteria colonization was described before for avirulent/low virulent enteropathogenic *Yersinia* strains (Kaneko & Hashimoto, 1983; Ricciardi *et al.*, 1978). This prolonged bacteria shedding could be due to residing bacteria in the intestinal lumen like shown for *L. monocytogenes*, which is residing in the mucus (Travier *et al.*, 2013). Hence, these residing bacteria could constantly stimulate the immune system, indicating a similar effect for the *cnfY* mutant strain, which is persisting in the caecum at least up to 28 days.

The infection with the avirulent *Y. enterocolitica* strain resulted in a resistance against a subsequent *Listeria monocytogenes* infection (Ruiz-Bravo *et al.*, 2001). Furthermore, another low virulent *Y. pseudotuberculosis* strain (IP32680, originated from hare infection), which was able to persist at least 14 days in the PP, the feces, and the MLNs of infected mice also induces immunity against *Y. pestis* infections (Blisnick *et al.*, 2008).

Moreover, a CNF_Y^+ *Y. pseudotuberculosis* strain (IP2666) without the virulence plasmid is able to induce 100% immunity against an oral *Y. pseudotuberculosis* infection, whereas it induces only 50% immunity against an intraperitoneal or intranasal infection with *Y. pseudotuberculosis*, when administered six weeks prior infection (Balada-Llasat *et al.*, 2007). Hence, it can be hypothesized that the tested avirulent/low virulent *Y. pseudotuberculosis* strains of this study (pYV^- CNF_Y^+, pYV^+ CNF_Y^- and pYV^- CNF_Y^-) could presumably also be applied as live attenuated vaccines as these were demonstrated to have long-term effects on the immune system.

However, the strain without the virulence plasmid, which secretes CNF_Y is probably not the best choice for a live attenuated vaccine, as it was shown to diminish the immune cell contents in the spleen. A *cnfY* mutant with the virulence plasmid also is probably not the best alternative because it still causes mild symptoms of disease at the early infection and is able to persist over long periods in the host. The latter could cause a chronic infection or ongoing reinfections. Taken together, the best option for a live attenuated vaccine against more virulent pathogens is probably the strain lacking both, the *cnfY* gene and pYV. This strain was shown to trigger the immune response in the PP and MLNs without causing symptoms of disease and to be unable to efficiently persist in the tissues as no detectable amounts of bacteria where found after long periods of infection.

5 Outlook

CNF_Y was demonstrated to be an important virulence factor for *Y. pseudotuberculosis* YPIII, as it diminishes the immune cell amounts in the spleen by enhancing the translocation of Yop effector proteins into professional phagocytes and to a lesser extent also independent of the virulence plasmid and the bacteria.

Further experiments could focus on the aspect of CNF_Y-induced inflammation. Extensive studies on the activation of the inflammasome and the induced signaling pathways could be conducted. In addition, intra-peritoneal or subcutaneous injection of the purified CNF_Y toxin would provide information about the transport mechanism of the toxin in the host and the consequences of intoxication - regardless of the Yop machinery and presence of the bacteria - for a better understanding of the mode of action of this toxin. Histopathological and immune response analyses of intoxicated mice should be performed.

Moreover, regulation of the *cnfY* expression, as well as the secretion mechanism of the toxin needs to be unravelled. Another important task for later studies would be to identify the cellular receptor of CNF_Y on the eukaryotic cells, in order to detect those cells preferably approached by the toxin.

Furthermore, the effects of long-term changes of the immune response caused by infections with different avirulent/low virulent *Y. pseudotuberculosis* strains (pYV^-, Δ*cnfY* or Δ*cnfY* pYV^-) could be evaluated. These strains might be suitable to apply as live attenuated vaccines. A subsequent reinfection with *Y. pseudotuberculosis* or other pathogenic bacteria would reveal if immunity was achieved. Furthermore, mechanisms of persistence and induction of chronic infection with long-term effects (e.g. arthritis) would be interesting to analyze.

A comparison regarding the *cnfY* expression pattern, and impact on the virulence of different *Y. pseudotuberculosis* wild-type strains (CNF_Y^+/CNF_Y^- & $PhoP^+$/$PhoP^-$) could provide some indications about advantages/disadvantages for the bacteria by harbouring the functional toxin gene. Mimicking a naturally occurring horizontal gene-transfer by bacteria, the *cnfY* gene could be integrated into the genome of other CNF_Y-negative pathogens. Possible effects for the pathogens could be examined, like an enhanced virulence and thus potentially resulting consequences for the population if a gene-transfer would occur naturally.

6 Summary

Several bacteria express various toxins to manipulate eukaryotic cells to their advantage. Some *Y. pseudotuberculosis* isolates produce the cytotoxic necrotizing factor CNF_Y, which constitutively activates small Rho-GTPases, important molecular switches regulating different cellular functions. However, the role of CNF_Y in host-pathogen interaction during infection was unknown.

Data of this study demonstrated that the *cnfY* gene of *Y. pseudotuberculosis* is temperature-, growth-phase-, and nutrient-dependently regulated and highly expressed in all lymphatic tissues of orally infected mice. Additionally, CNF_Y is secreted and induces rearrangements of the actin cytoskeleton and the formation of giant, multinucleated cells by activation of the GTPases RhoA, Rac1, and Cdc42 in epithelial cells and macrophages.

Moreover, the deletion of *cnfY* leads to an avirulent phenotype of *Y. pseudotuberculosis*. The *cnfY* mutant strain reaches the underlying tissues MLNs, spleen, and liver, but the infection is rapidly cleared three to five days post infection. Presence of CNF_Y stimulates an acute inflammatory response and induces the formation of necrotic areas in the lymphatic tissues. The secretion of CNF_Y resulted in a strong reduction of professional phagocytes and NK cells, especially in the spleen, whereas the loss of CNF_Y caused a strong influx of these cells, accompanied by rapid killing of the bacteria. Further, CNF_Y was shown to enhance Yop delivery, mostly by RhoA activation, into eukaryotic cells *in vitro* and during the course of infection. This resulted in an increased ability of the bacteria to defend themselve against the host immune system. Moreover, CNF_Y seems to play an additional role during late stages of the infection, as the toxin is sufficient to reduce immune cell contents in the spleen independent of the virulence plasmid even when the number of residing bacteria is very low.

In summary, the data of this study identified CNF_Y as an important Rho-GTPase-activating toxin, crucial for virulence of *Y. pseudotuberculosis* YPIII. This toxin is essential for the establishment of a successful infection and determines the severity of the associated disease by modulating the inflammatory response.

References

Abdel-Haq, N. M., Asmar, B. I., Abuhammour, W. M. & Brown, W. J. (2000). Yersinia enterocolitica infection in children. *Pediatr Infect Dis J* **19**, 954–958.

Achtman, M., Zurth, K., Morelli, G., Torrea, G., Guiyoule, A. & Carniel, E. (1999). Yersinia pestis, the cause of plague, is a recently emerged clone of Yersinia pseudotuberculosis. *Proc Natl Acad Sci U S A* **96**, 14043–14048.

Adamkiewicz, T. V, Berkovitch, M., Krishnan, C., Polsinelli, C., Kermack, D. & Olivieri, N. F. (1998). Infection due to Yersinia enterocolitica in a series of patients with beta-thalassemia: incidence and predisposing factors. *Clin Infect Dis* **27**, 1362–6.

Van Aelst, L. & D'Souza-Schorey, C. (1997). Rho GTPases and signaling networks. *Genes Dev* **11**, 2295–322.

Agrain, C., Sorg, I., Paroz, C. & Cornelis, G. R. (2005). Secretion of YscP from Yersinia enterocolitica is essential to control the length of the injectisome needle but not to change the type III secretion substrate specificity. *Mol Microbiol* **57**, 1415–1427.

Ahmadian, M. R., Wittinghofer, A. & Herrmann, C. (2002). Fluorescence methods in the study of small GTP-binding proteins. *Methods Mol Biol* **189**, 45–63.

Aili, M., Hallberg, B., Wolf-Watz, H. & Rosqvist, R. (2002). GAP activity of Yersinia YopE. *Methods Enzymol* **358**, 359–70.

Aili, M., Isaksson, E. L., Hallberg, B., Wolf-Watz, H. & Rosqvist, R. (2006). Functional analysis of the YopE GTPase-activating protein (GAP) activity of Yersinia pseudotuberculosis. *Cell Microbiol* **8**, 1020–33.

Aili, M., Isaksson, E. L., Carlsson, S. E., Wolf-Watz, H., Rosqvist, R. & Francis, M. S. (2008). Regulation of Yersinia Yop-effector delivery by translocated YopE. *Int J Med Microbiol* **298**, 183–92.

Aktories, K. & Hall, A. (1989). Botulinum ADP-ribosyltransferase C3: a new tool to study low molecular weight GTP-binding proteins. *Trends Pharmacol Sci* **10**, 415–8.

Aktories, K. (2011). Bacterial protein toxins that modify host regulatory GTPases. *Nat Rev Microbiol* **9**, 487–98.

Allaoui, A., Woestyn, S., Sluiters, C. & Cornelis, G. R. (1994). YscU, a Yersinia enterocolitica inner membrane protein involved in Yop secretion. *J Bacteriol* **176**, 4534–4542.

Allaoui, A., Schulte, R. & Cornelis, G. R. (1995). Mutational analysis of the Yersinia enterocolitica virC operon: characterization of yscE, F, G, I, J, K required for Yop secretion and yscH encoding YopR. *Mol Microbiol* **18**, 343–355.

Alrutz, M. A., Srivastava, A., Wong, K. W., D'Souza-Schorey, C., Tang, M., Ch'ng, L. E., Snapper, S. B. & Isberg, R. R. (2001). Efficient uptake of Yersinia pseudotuberculosis via integrin receptors involves a Rac1-Arp 2/3 pathway that bypasses N-WASP function. *Mol Microbiol* **42**, 689–703.

Augspach, A., List, J., Wolf, P., Bielek, H., Schwan, C., Elsässer-Beile, U., Aktories, K. & Schmidt, G. (2013). Activation of RhoA,B,C by Yersinia Cytotoxic Necrotizing Factor (CNFy) Induces Apoptosis in LNCaP Prostate Cancer Cells. *Toxins (Basel)* **5**, 2241–2257.

Autenrieth, I. B. & Firsching, R. (1996). Penetration of M cells and destruction of Peyer's patches by Yersinia enterocolitica: an ultrastructural and histological study. *J Med Microbiol* **44**, 285–94.

Autenrieth, I. B. & Heesemann, J. (1992). In vivo neutralization of tumor necrosis factor-alpha and interferon- gamma abrogates resistance to Yersinia enterocolitica infection in mice. *Med Microbiol Immunol* **181**, 333–338.

Autenrieth, I. B., Tingle, A., Reske-Kunz, A. & Heesemann, J. (1992). T lymphocytes mediate protection against Yersinia enterocolitica in mice: characterization of murine T-cell clones specific for Y. enterocolitica. *Infect Immun* **60**, 1140–1149.

Autenrieth, I. B., Vogel, U., Preger, S., Heymer, B. & Heesemann, J. (1993a). Experimental Yersinia enterocolitica infection in euthymic and T-cell- deficient athymic nude C57BL/6 mice: comparison of time course, histomorphology, and immune response. *Infect Immun* **61**, 2585–2595.

Autenrieth, I. B., Hantschmann, P., Heymer, B. & Heesemann, J. (1993b). Immunohistological characterization of the cellular immune response against Yersinia enterocolitica in mice: evidence for the involvement of T lymphocytes. *Immunobiology* **187**, 1–16.

Autenrieth, I. B., Kempf, V., Sprinz, T., Preger, S. & Schnell, A. (1996). Defense mechanisms in Peyer's patches and mesenteric lymph nodes against Yersinia enterocolitica involve integrins and cytokines. *Infect Immun* **64**, 1357–1368.

Balada-Llasat, J.-M. & Mecsas, J. (2006). Yersinia has a tropism for B and T cell zones of lymph nodes that is independent of the type III secretion system. *PLoS Pathog* **2**, e86 (D. A. Portnoy, Ed.). Public Library of Science.

Balada-Llasat, J.-M., Panilaitis, B., Kaplan, D. & Mecsas, J. (2007). Oral inoculation with Type III secretion mutants of Yersinia pseudotuberculosis provides protection from oral, intraperitoneal, or intranasal challenge with virulent Yersinia. *Vaccine* **25**, 1526–33.

Balligand, G., Laroche, Y. & Cornelis, G. (1985). Genetic analysis of virulence plasmid from a serogroup 9 Yersinia enterocolitica strain: role of outer membrane protein P1 in resistance to human serum and autoagglutination. *Infect Immun* **48**, 782–786.

Barbieri, J. T., Riese, M. J. & Aktories, K. (2002). Bacterial toxins that modify the actin cytoskeleton. *Annu Rev Cell Dev Biol* **18**, 315–44.

Barocchi, M. A., Masignani, V. & Rappuoli, R. (2005). Opinion: Cell entry machines: a common theme in nature? *Nat Rev Microbiol* **3**, 349–358.

Bartra, S. S., Styer, K. L., O'Bryant, D. M., Nilles, M. L., Hinnebusch, B. J., Aballay, A. & Plano, G. V. (2008). Resistance of Yersinia pestis to complement-dependent killing is mediated by the Ail outer membrane protein. *Infect Immun* **76**, 612–22.

Baumer, Y., Burger, S., Curry, F. E., Golenhofen, N., Drenckhahn, D. & Waschke, J. (2008). Differential role of Rho GTPases in endothelial barrier regulation dependent on endothelial cell origin. *Histochem Cell Biol* **129**, 179–91.

Bergamini, C., Gambetti, S., Dondi, A. & Cervellati, C. (2004). Oxygen, Reactive Oxygen Species and Tissue Damage. *Curr Pharm Des* **10**, 1611–1626. Bentham Science Publishers.

Bergsbaken, T. & Cookson, B. T. (2007). Macrophage activation redirects yersinia-infected host cell death from apoptosis to caspase-1-dependent pyroptosis. *PLoS Pathog* **3**, e161.

Bergsbaken, T. & Cookson, B. T. (2009). Innate immune response during Yersinia infection: critical modulation of cell death mechanisms through phagocyte activation. *J Leukoc Biol* **86**, 1153–8.

Beuscher, H. U., Rausch, U. P., Otterness, I. G. & Röllinghoff, M. (1992). Transition from interleukin 1 beta (IL-1 beta) to IL-1 alpha production during maturation of inflammatory macrophages in vivo. *J Exp Med* **175**, 1793–7.

Bhavsar, A. P., Guttman, J. A. & Finlay, B. B. (2007). Manipulation of host-cell pathways by bacterial pathogens. *Nature* **449**, 827–834.

Biedzka-Sarek, M., Salmenlinna, S., Gruber, M., Lupas, A. N., Meri, S. & Skurnik, M. (2008). Functional mapping of YadA- and Ail-mediated binding of human factor H to Yersinia enterocolitica serotype O:3. *Infect Immun* **76**, 5016–5027.

Björnfot, A.-C., Lavander, M., Forsberg, A. & Wolf-Watz, H. (2009). Autoproteolysis of YscU of Yersinia pseudotuberculosis is important for regulation of expression and secretion of Yop proteins. *J Bacteriol* **191**, 4259–67.

Black, D. S. & Bliska, J. B. (1997). Identification of p130Cas as a substrate of Yersinia YopH (Yop51), a bacterial protein tyrosine phosphatase that translocates into mammalian cells and targets focal adhesions. *EMBO J* **16**, 2730–2744.

Black, D. S. & Bliska, J. B. (2000). The RhoGAP activity of the Yersinia pseudotuberculosis cytotoxin YopE is required for antiphagocytic function and virulence. *Mol Microbiol* **37**, 515–527.

Blanco, J., Blanco, M., Alonso, M. P., Blanco, J. E., González, E. A. & Garabal, J. I. (1992). Characteristics of haemolytic Escherichia coli with particular reference to production of cytotoxic necrotizing factor type 1 (CNF1). *Res Microbiol* **143**, 869–78.

Blaylock, B., Riordan, K. E., Missiakas, D. M. & Schneewind, O. (2006). Characterization of the Yersinia enterocolitica type III secretion ATPase YscN and its regulator, YscL. *J Bacteriol* **188**, 3525–34.

Bliska, J. B., Guan, K. L., Dixon, J. E. & Falkow, S. (1991). Tyrosine phosphate hydrolysis of host proteins by an essential Yersinia virulence determinant. *Proc Natl Acad Sci U S A* **88**, 1187–1191.

Blisnick, T., Ave, P., Huerre, M., Carniel, E. & Demeure, C. E. (2008). Oral vaccination against bubonic plague using a live avirulent Yersinia pseudotuberculosis strain. *Infect Immun* **76**, 3808–16.

Blum, G., Falbo, V., Caprioli, A. & Hacker, J. (1995). Gene clusters encoding the cytotoxic necrotizing factor type 1, Prs-fimbriae and alpha-hemolysin form the pathogenicity island II of the uropathogenic Escherichia coli strain J96. *FEMS Microbiol Lett* **126**, 189–95.

Blumenthal, B., Hoffmann, C., Aktories, K., Backert, S. & Schmidt, G. (2007). The cytotoxic necrotizing factors from Yersinia pseudotuberculosis and from Escherichia coli bind to different cellular receptors but take the same route to the cytosol. *Infect Immun* **75**, 3344–53.

Böhme, K., Steinmann, R., Kortmann, J., Seekircher, S., Heroven, A. K., Berger, E., Pisano, F., Thiermann, T., Wolf-Watz, H. & other authors. **(2012).** Concerted actions of a thermo-labile regulator and a unique intergenic RNA thermosensor control Yersinia virulence. *PLoS Pathog* **8**, e1002518.

Böhme, K. (2010). *Identification and characterization of the regulatory factors and regulatory RNA elements controlling the expression of the primary invasion factors invasin and YadA in Yersinia pseudotuberculosis*. TU Braunschweig.

Bohn, E. & Autenrieth, I. B. (1996). IL-12 is essential for resistance against Yersinia enterocolitica by triggering IFN-gamma production in NK cells and CD4+ T cells. *J Immunol* **156**, 1458–1468.

Bolin, I., Norlander, I. & Wolf-Watz, H. (1982). Temperature-inducible outer membrane protein of Yersinia pseudotuberculosis and Yersinia enterocolitica is associated with the virulence plasmid. *Infect Immun* **37**, 506–512.

Bonacorsi, S. P., Clermont, O., Tinsley, C., Le Gall, I., Beaudoin, J. C., Elion, J., Nassif, X. & Bingen, E. (2000). Identification of regions of the Escherichia coli chromosome specific for neonatal meningitis-associated strains. *Infect Immun* **68**, 2096–101.

Boquet, P. & Lemichez, E. (2003). Bacterial virulence factors targeting Rho GTPases: parasitism or symbiosis? *Trends Cell Biol* **13**, 238–46.

Borysowski, J., Weber-Dabrowska, B. & Górski, A. (2006). Bacteriophage endolysins as a novel class of antibacterial agents. *Exp Biol Med (Maywood)* **231**, 366–77.

Boyer, L., Travaglione, S., Falzano, L., Gauthier, N. C., Popoff, M. R., Lemichez, E., Fiorentini, C. & Fabbri, A. (2004). Rac GTPase instructs nuclear factor-kappaB activation by conveying the SCF complex and IkBalpha to the ruffling membranes. *Mol Biol Cell* **15**, 1124–33.

Brenner, D. J., Steigerwalt, A. G., Falcao, D. P., Weaver, R. E. & Fanning, G. R. (1976). Characterization of Yersinia enterocolitica and Yersinia pseudotuberculosis by Deoxyribonucleic Acid Hybridization and by Biochemical Reactions. *Int J Syst Bacteriol* **26**, 180–194.

Brodsky, I. E. & Medzhitov, R. (2008). Reduced secretion of YopJ by Yersinia limits in vivo cell death but enhances bacterial virulence. *PLoS Pathog* **4**, e1000067.

Brodsky, I. E., Palm, N. W., Sadanand, S., Ryndak, M. B., Sutterwala, F. S., Flavell, R. A., Bliska, J. B. & Medzhitov, R. (2010). A Yersinia effector protein promotes virulence by preventing inflammasome recognition of the type III secretion system. *Cell Host Microbe* **7**, 376–87.

Brzostek, K., Raczkowska, A. & Zasada, A. (2003). The osmotic regulator OmpR is involved in the response of Yersinia enterocolitica O:9 to environmental stresses and survival within macrophages. *FEMS Microbiol Lett* **228**, 265–271.

Buetow, L., Flatau, G., Chiu, K., Boquet, P. & Ghosh, P. (2001). Structure of the Rho-activating domain of Escherichia coli cytotoxic necrotizing factor 1. *Nat Struct Biol* **8**, 584–8.

Bustelo, X. R., Sauzeau, V. & Berenjeno, I. M. (2007). GTP-binding proteins of the Rho/Rac family: regulation, effectors and functions in vivo. *Bioessays* **29**, 356–70.

Caprioli, A., Falbo, V., Roda, L. G., Ruggeri, F. M. & Zona, C. (1983). Partial purification and characterization of an escherichia coli toxic factor that induces morphological cell alterations. *Infect Immun* **39**, 1300–6.

Caprioli, A., Donelli, G., Falbo, V., Possenti, R., Roda, L. G., Roscetti, G. & Ruggeri, F. M. (1984). A cell division-active protein from E. coli. *Biochem Biophys Res Commun* **118**, 587–93.

Carniel, E., Autenrieth, I., Cornelis, G., Fukushima, H., Guinet, F., Isberg, R., Pham, J., Prentice, M., Simonet, M. & other authors. **(2006).** *The Prokaryotes* (M. Dworkin, S. Falkow, E. Rosenberg, K.-H. Schleifer & E. Stackebrandt, Eds.). Springer New York.

Caron, E. & Hall, A. (1998). Identification of two distinct mechanisms of phagocytosis controlled by different Rho GTPases. *Science* **282**, 1717–21.

Casadaban, M. J. & Cohen, S. N. (1980). Analysis of gene control signals by DNA fusion and cloning in Escherichia coli. *J Mol Biol* **138**, 179–207.

Cavanaugh, D. C. & Randall, R. (1959). The role of multiplication of Pasteurella pestis in mononuclear phagocytes in the pathogenesis of flea-borne plague. *J Immunol* **83**, 348–63.

Chain, P. S., Carniel, E., Larimer, F. W., Lamerdin, J., Stoutland, P. O., Regala, W. M., Georgescu, A. M., Vergez, L. M., Land, M. L. & other authors. **(2004).** Insights into the evolution of Yersinia pestis through whole-genome comparison with Yersinia pseudotuberculosis. *Proc Natl Acad Sci U S A* **101**, 13826–13831.

Chen, P. E., Cook, C., Stewart, A. C., Nagarajan, N., Sommer, D. D., Pop, M., Thomason, B., Thomason, M. P. K., Lentz, S. & other authors. **(2010).** Genomic characterization of the Yersinia genus. *Genome Biol* **11**, R1.

Chiu, H. Y., Flynn, D. M., Hoffbrand, A. V & Politis, D. (1986). Infection with Yersinia enterocolitica in patients with iron overload. *Br Med J (Clin Res Ed)* **292**, 97.

Le Clainche, C. & Carlier, M.-F. (2008). Regulation of actin assembly associated with protrusion and adhesion in cell migration. *Physiol Rev* **88**, 489–513.

Clark, M. A., Hirst, B. H. & Jepson, M. A. (1998). M-cell surface beta1 integrin expression and invasin-mediated targeting of Yersinia pseudotuberculosis to mouse Peyer's patch M cells. *Infect Immun* **66**, 1237–1243.

Conlan, J. W. (1997). Critical roles of neutrophils in host defense against experimental systemic infections of mice by Listeria monocytogenes, Salmonella typhimurium, and Yersinia enterocolitica. *Infect Immun* **65**, 630–5.

Contamin, S., Galmiche, A., Doye, A., Flatau, G., Benmerah, A. & Boquet, P. (2000). The p21 Rho-activating toxin cytotoxic necrotizing factor 1 is endocytosed by a clathrin-independent mechanism and enters the cytosol by an acidic-dependent membrane translocation step. *Mol Biol Cell* **11**, 1775–87.

Cornelis, G., Vanootegem, J. C. & Sluiters, C. (1987). Transcription of the yop regulon from Y. enterocolitica requires trans acting pYV and chromosomal genes. *Microb Pathog* **2**, 367–379.

Cornelis, G. R. (1998). The Yersinia Yop virulon, a bacterial system to subvert cells of the primary host defense. *Folia Microbiol (Praha)* **43**, 253–261.

Cornelis, G. R. (2002a). The Yersinia Ysc-Yop virulence apparatus. *Int J Med Microbiol* **291**, 455–462.

Cornelis, G. R. (2002b). Yersinia type III secretion: send in the effectors. *J Cell Biol* **158**, 401–408.

Cornelis, G. R. & Wolf-Watz, H. (1997). The Yersinia Yop virulon: a bacterial system for subverting eukaryotic cells. *Mol Microbiol* **23**, 861–867.

Cornelis, G. R., Sluiters, C., Delor, I., Geib, D., Kaniga, K., Lambert de Rouvroit, C., Sory, M. P., Vanooteghem, J. C. & Michiels, T. (1991). ymoA, a Yersinia enterocolitica chromosomal gene modulating the expression of virulence functions. *Mol Microbiol* **5**, 1023–1034.

Cornelis, G. R., Boland, A., Boyd, A. P., Geuijen, C., Iriarte, M., Neyt, C., Sory, M. P. & Stainier, I. (1998). The virulence plasmid of Yersinia, an antihost genome. *Microbiol Mol Biol Rev* **62**, 1315–1352.

Cossart, P. & Toledo-Arana, A. (2008). Listeria monocytogenes, a unique model in infection biology: an overview. *Microbes Infect* **10**, 1041–50.

Cox, D., Chang, P., Zhang, Q., Reddy, P. G., Bokoch, G. M. & Greenberg, S. (1997). Requirements for Both Rac1 and Cdc42 in Membrane Ruffling and Phagocytosis in Leukocytes. *J Exp Med* **186**, 1487–1494.

Cruz-Migoni, A., Hautbergue, G. M., Artymiuk, P. J., Baker, P. J., Bokori-Brown, M., Chang, C.-T., Dickman, M. J., Essex-Lopresti, A., Harding, S. V & other authors. **(2011).** A Burkholderia pseudomallei toxin inhibits helicase activity of translation factor eIF4A. *Science* **334**, 821–4.

Darwin, A. J. & Miller, V. L. (1999). Identification of Yersinia enterocolitica genes affecting survival in an animal host using signature-tagged transposon mutagenesis. *Mol Microbiol* **32**, 51–62.

Datsenko, K. A. & Wanner, B. L. (2000). One-step inactivation of chromosomal genes in Escherichia coli K-12 using PCR products. *Proc Natl Acad Sci U S A* **97**, 6640–6645.

Davis, J. M., Carvalho, H. M., Rasmussen, S. B. & O'Brien, A. D. (2006). Cytotoxic necrotizing factor type 1 delivered by outer membrane vesicles of uropathogenic Escherichia coli attenuates polymorphonuclear leukocyte antimicrobial activity and chemotaxis. *Infect Immun* **74**, 4401–8.

DerMardirossian, C., Schnelzer, A. & Bokoch, G. M. (2004). Phosphorylation of RhoGDI by Pak1 mediates dissociation of Rac GTPase. *Mol Cell* **15**, 117–27.

Dersch, P. & Isberg, R. R. (1999). A region of the Yersinia pseudotuberculosis invasin protein enhances integrin-mediated uptake into mammalian cells and promotes self-association. *EMBO J* **18**, 1199–1213.

Dersch, P. & Isberg, R. R. (2000). An immunoglobulin superfamily-like domain unique to the Yersinia pseudotuberculosis invasin protein is required for stimulation of bacterial uptake via integrin receptors. *Infect Immun* **68**, 2930–2938.

Dewoody, R. S., Merritt, P. M. & Marketon, M. M. (2013). Regulation of the Yersinia type III secretion system: traffic control. *Front Cell Infect Microbiol* **3**, 4.

Diepold, A., Amstutz, M., Abel, S., Sorg, I., Jenal, U. & Cornelis, G. R. (2010). Deciphering the assembly of the Yersinia type III secretion injectisome. *EMBO J* **29**, 1928–1940.

Diepold, A., Wiesand, U., Amstutz, M. & Cornelis, G. R. (2012). Assembly of the Yersinia injectisome: the missing pieces. *Mol Microbiol* **85**, 878–92.

Diezel, W., Kopperschläger, G. & Hofmann, E. (1972). An improved procedure for protein staining in polyacrylamide gels with a new type of Coomassie Brilliant Blue. *Anal Biochem* **48**, 617–20.

Doye, A., Mettouchi, A., Bossis, G., Clément, R., Buisson-Touati, C., Flatau, G., Gagnoux, L., Piechaczyk, M., Boquet, P. & Lemichez, E. (2002). CNF1 exploits the ubiquitin-proteasome machinery to restrict Rho GTPase activation for bacterial host cell invasion. *Cell* **111**, 553–64.

Dranoff, G. (2004). Cytokines in cancer pathogenesis and cancer therapy. *Nat Rev Cancer* **4**, 11–22.

Dube, P. (2009). Interaction of Yersinia with the gut: mechanisms of pathogenesis and immune evasion. *Curr Top Microbiol Immunol* **337**, 61–91.

Dube, P. H., Revell, P. A., Chaplin, D. D., Lorenz, R. G. & Miller, V. L. (2001). A role for IL-1 alpha in inducing pathologic inflammation during bacterial infection. *Proc Natl Acad Sci U S A* **98**, 10880–5.

Dube, P. H., Handley, S. A., Lewis, J. & Miller, V. L. (2004). Protective role of interleukin-6 during Yersinia enterocolitica infection is mediated through the modulation of inflammatory cytokines. *Infect Immun* **72**, 3561–3570.

Durand, E. A., Maldonado-Arocho, F. J., Castillo, C., Walsh, R. L. & Mecsas, J. (2010). The presence of professional phagocytes dictates the number of host cells targeted for Yop translocation during infection. *Cell Microbiol* **12**, 1064–82.

Eckmann, L., Kagnoff, M. F. & Fierer, J. (1995). Intestinal epithelial cells as watchdogs for the natural immune system. *Trends Microbiol* **3**, 118–120.

Edqvist, P. J., Olsson, J., Lavander, M., Sundberg, L., Forsberg, A., Wolf-Watz, H. & Lloyd, S. A. (2003). YscP and YscU regulate substrate specificity of the Yersinia type III secretion system. *J Bacteriol* **185**, 2259–66.

Eitel, J., Heise, T., Thiesen, U. & Dersch, P. (2005). Cell invasion and IL-8 production pathways initiated by YadA of Yersinia pseudotuberculosis require common signalling molecules (FAK, c-SRC, Ras) and distinct cell factors. *Cell Microbiol* **7**, 63–77.

Erfurth, S. E., Grobner, S., Kramer, U., Gunst, D. S., Soldanova, I., Schaller, M., Autenrieth, I. B. & Borgmann, S. (2004). Yersinia enterocolitica induces apoptosis and inhibits surface molecule expression and cytokine production in murine dendritic cells. *Infect Immun* **72**, 7045–7054.

Etienne-Manneville, S. & Hall, A. (2002). Rho GTPases in cell biology. *Nature* **420**, 629–635.

Fabbri, A., Gauthier, M. & Boquet, P. (1999). The 5' region of cnf1 harbours a translational regulatory mechanism for CNF1 synthesis and encodes the cell-binding domain of the toxin. *Mol Microbiol* **33**, 108–18.

Falnes, P. O. & Sandvig, K. (2000). Penetration of protein toxins into cells. *Curr Opin Cell Biol* **12**, 407–13.

Falzano, L., Fiorentini, C., Boquet, P. & Donelli, G. (1993a). Interaction of Escherichia coli cytotoxic necrotizing factor type 1 (CNF1) with cultured cells. *Cytotechnology* **11 Suppl 1**, S56–8.

Falzano, L., Fiorentini, C., Donelli, G., Michel, E., Kocks, C., Cossart, P., Cabanié, L., Oswald, E. & Boquet, P. (1993b). Induction of phagocytic behaviour in human epithelial cells by Escherichia coli cytotoxic necrotizing factor type 1. *Mol Microbiol* **9**, 1247–54.

Falzano, L., Filippini, P., Travaglione, S., Miraglia, A. G., Fabbri, A. & Fiorentini, C. (2006). Escherichia coli cytotoxic necrotizing factor 1 blocks cell cycle G2/M transition in uroepithelial cells. *Infect Immun* **74**, 3765–72.

Felek, S. & Krukonis, E. S. (2009). The Yersinia pestis Ail protein mediates binding and Yop delivery to host cells required for plague virulence. *Infect Immun* **77**, 825–836.

Fink, S. L. & Cookson, B. T. (2005). Apoptosis, pyroptosis, and necrosis: mechanistic description of dead and dying eukaryotic cells. *Infect Immun* **73**, 1907–16.

Finlay, B. B. & Cossart, P. (1997). Exploitation of mammalian host cell functions by bacterial pathogens. *Science (80-)* **276**, 718–725.

Fiorentini, C., Fabbri, A., Flatau, G., Donelli, G., Matarrese, P., Lemichez, E., Falzano, L. & Boquet, P. (1997). Escherichia coli cytotoxic necrotizing factor 1 (CNF1), a toxin that activates the Rho GTPase. *J Biol Chem* **272**, 19532–7.

Fiorentini, C., Falzano, L., Travaglione, S. & Fabbri, A. (2003). Hijacking Rho GTPases by protein toxins and apoptosis: molecular strategies of pathogenic bacteria. *Cell Death Differ* **10**, 147–52.

Fisher, M. L., Castillo, C. & Mecsas, J. (2007). Intranasal inoculation of mice with Yersinia pseudotuberculosis causes a lethal lung infection that is dependent on Yersinia outer proteins and PhoP. *Infect Immun* **75**, 429–42.

Flatau, G., Lemichez, E., Gauthier, M., Chardin, P., Paris, S., Fiorentini, C. & Boquet, P. (1997). Toxin-induced activation of the G protein p21 Rho by deamidation of glutamine. *Nature* **387**, 729–33.

Flügel, A., Schulze-Koops, H., Heesemann, J., Kuhn, K., Sorokin, L., Burkhardt, H., von der Mark, K. & Emmrich, F. (1994). Interaction of enteropathogenic Yersinia enterocolitica with complex basement membranes and the extracellular matrix proteins collagen type IV, laminin-1 and -2, and nidogen/entactin. *J Biol Chem* **269**, 29732–29738.

Fogh, J. & Trempe, G. (1975). New human tumor cell lines. *Hum Tumor Cells Vitr* 115–141.

Forsberg, A., Bölin, I., Norlander, L. & Wolf-Watz, H. (1987). Molecular cloning and expression of calcium-regulated, plasmid-coded proteins of Y. pseudotuberculosis. *Microb Pathog* **2**, 123–37.

Forsberg, A., Viitanen, A. M., Skurnik, M. & Wolf-Watz, H. (1991). The surface-located YopN protein is involved in calcium signal transduction in Yersinia pseudotuberculosis. *Mol Microbiol* **5**, 977–986.

Forsberg, A., Rosqvist, R. & Wolf-Watz, H. (1994). Regulation and polarized transfer of the Yersinia outer proteins (Yops) involved in antiphagocytosis. *Trends Microbiol* **2**, 14–19.

Fosse, J., Seegers, H. & Magras, C. (2009). Prevalence and risk factors for bacterial food-borne zoonotic hazards in slaughter pigs: a review. *Zoonoses Public Heal* **56**, 429–454.

Fredriksson-Ahomaa, M., Stolle, A., Siitonen, A. & Korkeala, H. (2006). Sporadic human Yersinia enterocolitica infections caused by bioserotype 4/O : 3 originate mainly from pigs. *J Med Microbiol* **55**, 747–749.

Fu, Y. & Galan, J. E. (1999). A Salmonella protein antagonizes Rac-1 and Cdc42 to mediate host-cell recovery after bacterial invasion. *Nature* **401**, 293–297.

Galan, J. E. (1994). Interactions of bacteria with non-phagocytic cells. *Cuur Opi Immunol* **6**, 590–595.

Galletta, B. J. & Cooper, J. A. (2009). Actin and endocytosis: mechanisms and phylogeny. *Curr Opin Cell Biol* **21**, 20–7.

Galyov, E. E., Hakansson, S., Forsberg, A. & Wolf-Watz, H. (1993). A secreted protein kinase of Yersinia pseudotuberculosis is an indispensable virulence determinant. *Nature* **361**, 730–732.

Gao, W., Xing, B., Tsien, R. Y. & Rao, J. (2003). Novel fluorogenic substrates for imaging beta-lactamase gene expression. *J Am Chem Soc* **125**, 11146–7.

Gerhard, R., Schmidt, G., Hofmann, F. & Aktories, K. (1998). Activation of Rho GTPases by Escherichia coli cytotoxic necrotizing factor 1 increases intestinal permeability in Caco-2 cells. *Infect Immun* **66**, 5125–31.

Gifford, G. E. & Flick, D. A. (1987). Natural production and release of tumour necrosis factor. *Ciba Found Symp* **131**, 3–20.

Goguen, J. D., Yother, J. & Straley, S. C. (1984). Genetic analysis of the low calcium response in Yersinia pestis mu d1(Ap lac) insertion mutants. *J Bacteriol* **160**, 842–8.

Gort, A. S. & Miller, V. L. (2000). Identification and characterization of Yersinia enterocolitica genes induced during systemic infection. *Infect Immun* **68**, 6633–6642.

Gouin, E., Welch, M. D. & Cossart, P. (2005). Actin-based motility of intracellular pathogens. *Curr Opin Microbiol* **8**, 35–45.

Grabenstein, J. P., Marceau, M., Pujol, C., Simonet, M. & Bliska, J. B. (2004). The response regulator PhoP of Yersinia pseudotuberculosis is important for replication in macrophages and for virulence. *Infect Immun* **72**, 4973–4984.

Griffiths-Johnson, D. A., Collins, P. D., Rossi, A. G., Jose, P. J. & Williams, T. J. (1993). The chemokine, eotaxin, activates guinea-pig eosinophils in vitro and causes their accumulation into the lung in vivo. *Biochem Biophys Res Commun* **197**, 1167–72.

Grosdent, N., Maridonneau-Parini, I., Sory, M. P. & Cornelis, G. R. (2002). Role of Yops and adhesins in resistance of Yersinia enterocolitica to phagocytosis. *Infect Immun* **70**, 4165–4176.

Grutzkau, A., Hanski, C., Hahn, H. & Riecken, E. O. (1990). Involvement of M cells in the bacterial invasion of Peyer's patches: a common mechanism shared by Yersinia enterocolitica and other enteroinvasive bacteria. *Gut* **31**, 1011–1015.

Guan, K. L. & Dixon, J. E. (1990). Protein tyrosine phosphatase activity of an essential virulence determinant in Yersinia. *Science* **249**, 553–6.

Haase, R., Kirschning, C. J., Sing, A., Schrottner, P., Fukase, K., Kusumoto, S., Wagner, H., Heesemann, J. & Ruckdeschel, K. (2003). A dominant role of Toll-like receptor 4 in the signaling of apoptosis in bacteria-faced macrophages. *J Immunol* **171**, 4294–4303.

Hakansson, S., Bergman, T., Vanooteghem, J. C., Cornelis, G. & Wolf-Watz, H. (1993). YopB and YopD constitute a novel class of Yersinia Yop proteins. *Infect Immun* **61**, 71–80.

Hakansson, S., Schesser, K., Persson, C., Galyov, E. E., Rosqvist, R., Homble, F. & Wolf-Watz, H. (1996a). The YopB protein of Yersinia pseudotuberculosis is essential for the translocation of Yop effector proteins across the target cell plasma membrane and displays a contact-dependent membrane disrupting activity. *EMBO J* **15**, 5812–5823.

Hakansson, S., Galyov, E. E., Rosqvist, R. & Wolf-Watz, H. (1996b). The Yersinia YpkA Ser/Thr kinase is translocated and subsequently targeted to the inner surface of the HeLa cell plasma membrane. *Mol Microbiol* **20**, 593–603.

Hanski, C., Kutschka, U., Schmoranzer, H. P., Naumann, M., Stallmach, A., Hahn, H., Menge, H. & Riecken, E. O. (1989). Immunohistochemical and electron microscopic study of interaction of Yersinia enterocolitica serotype O8 with intestinal mucosa during experimental enteritis. *Infect Immun* **57**, 673–678.

Harmon, D. E., Davis, A. J., Castillo, C. & Mecsas, J. (2010). Identification and characterization of small-molecule inhibitors of Yop translocation in Yersinia pseudotuberculosis. *Antimicrob Agents Chemother* **54**, 3241–3254.

Hecht, G., Pothoulakis, C., LaMont, J. T. & Madara, J. L. (1988). Clostridium difficile toxin A perturbs cytoskeletal structure and tight junction permeability of cultured human intestinal epithelial monolayers. *J Clin Invest* **82**, 1516–24.

Heesemann, J. (1994). Die Gattung Yersinia. Yersiniosen. In *Medizinische Mikrobiol*, pp. 425–436. Edited by B. ed. Berlin: Springer.

Heise, T. & Dersch, P. (2006). Identification of a domain in Yersinia virulence factor YadA that is crucial for extracellular matrix-specific cell adhesion and uptake. *Proc Natl Acad Sci U S A* **103**, 3375–3380.

Heroven, A. K., Bohme, K. & Dersch, P. (2012). The Csr/Rsm system of Yersinia and related pathogens: A post-transcriptional strategy for managing virulence. *RNA Biol* **9**.

Hinnebusch, B. J. (1997). Bubonic plague: a molecular genetic case history of the emergence of an infectious disease. *J Mol Med* **75**, 645–652.

Hinnebusch, B. J., Jarrett, C. O., Callison, J. A., Gardner, D., Buchanan, S. K. & Plano, G. V. (2011). Role of the Yersinia pestis Ail protein in preventing a protective polymorphonuclear leukocyte response during bubonic plague. *Infect Immun* **79**, 4984–9.

Hodak, H. & Galán, J. E. (2013). A Salmonella Typhi homologue of bacteriophage muramidases controls typhoid toxin secretion. *EMBO Rep* **14**, 95–102.

Hoe, N. P., Minion, F. C. & Goguen, J. D. (1992). Temperature sensing in Yersinia pestis: regulation of yopE transcription by lcrF. *J Bacteriol* **174**, 4275–4286.

Hoffmann, C. & Schmidt, G. (2004). CNF and DNT. *Rev Physiol Biochem Pharmacol* **152**, 49–63.

Hoffmann, C., Pop, M., Leemhuis, J., Schirmer, J., Aktories, K. & Schmidt, G. (2004). The Yersinia pseudotuberculosis cytotoxic necrotizing factor (CNFY) selectively activates RhoA. *J Biol Chem* **279**, 16026–16032.

Hofman, P., Le Negrate, G., Mograbi, B., Hofman, V., Brest, P., Alliana-Schmid, A., Flatau, G., Boquet, P. & Rossi, B. (2000). Escherichia coli cytotoxic necrotizing factor-1 (CNF-1) increases the adherence to epithelia and the oxidative burst of human polymorphonuclear leukocytes but decreases bacteria phagocytosis. *J Leukoc Biol* **68**, 522–8.

Hoiczyk, E. & Blobel, G. (2001). Polymerization of a single protein of the pathogen Yersinia enterocolitica into needles punctures eukaryotic cells. *Proc Natl Acad Sci U S A* **98**, 4669–4674.

Hoiczyk, E., Roggenkamp, A., Reichenbecher, M., Lupas, A. & Heesemann, J. (2000). Structure and sequence analysis of Yersinia YadA and Moraxella UspAs reveal a novel class of adhesins. *EMBO J* **19**, 5989–5999.

Holmstrom, A., Petterson, J., Rosqvist, R., Hakansson, S., Tafazoli, F., Fallman, M., Magnusson, K. E., Wolf-Watz, H. & Forsberg, A. (1997). YopK of Yersinia pseudotuberculosis controls translocation of Yop effectors across the eukaryotic cell membrane. *Mol Microbiol* **24**, 73–91.

Honda, K. & Chihara, J. (1999). Eosinophil activation by eotaxin--eotaxin primes the production of reactive oxygen species from eosinophils. *Allergy* **54**, 1262–9.

Hopkins, A. M., Walsh, S. V, Verkade, P., Boquet, P. & Nusrat, A. (2003). Constitutive activation of Rho proteins by CNF-1 influences tight junction structure and epithelial barrier function. *J Cell Sci* **116**, 725–742.

Huang, X.-Z. & Lindler, L. E. (2004). The pH 6 antigen is an antiphagocytic factor produced by Yersinia pestis independent of Yersinia outer proteins and capsule antigen. *Infect Immun* **72**, 7212–7219.

Huelsenbeck, J., Dreger, S. C., Gerhard, R., Fritz, G., Just, I. & Genth, H. (2007a). Upregulation of the immediate early gene product RhoB by exoenzyme C3 from Clostridium limosum and toxin B from Clostridium difficile. *Biochemistry* **46**, 4923–4931.

Huelsenbeck, J., Dreger, S., Gerhard, R., Barth, H., Just, I. & Genth, H. (2007b). Difference in the cytotoxic effects of toxin B from Clostridium difficile strain VPI 10463 and toxin B from variant Clostridium difficile strain 1470. *Infect Immun* **75**, 801–9.

Huelsenbeck, S. C., May, M., Schmidt, G. & Genth, H. (2009). Inhibition of cytokinesis by Clostridium difficile toxin B and cytotoxic necrotizing factors--reinforcing the critical role of RhoA in cytokinesis. *Cell Motil Cytoskeleton* **66**, 967–75.

Innis, M. & Gelfand, D. (1990). Optimization of PCRs. In *PCR Protoc A Guid to Methods Appl*, pp. 4–12.

Isberg, R. R. (1989). Mammalian cell adhesion functions and cellular penetration of enteropathogenic Yersinia species. *Mol Microbiol* **3**, 1449–1453.

Isberg, R. R. (1996). Uptake of enteropathogenic Yersinia by mammalian cells. *Curr Top Microbiol Immunol* **209**, 1–24.

Isberg, R. R. & Falkow, S. (1985). A single genetic locus encoded by Yersinia pseudotuberculosis permits invasion of cultured animal cells by Escherichia coli K-12. *Nature* **317**, 262–264.

Isberg, R. R. & Van Nhieu, G. T. (1994). Two mammalian cell internalization strategies used by pathogenic bacteria. *Annu Rev Genet* **28**, 395–422.

Isberg, R. R., Swain, A. & Falkow, S. (1988). Analysis of expression and thermoregulation of the Yersinia pseudotuberculosis inv gene with hybrid proteins. *Infect Immun* **56**, 2133–2138.

Jones, S. A. (2005). Directing Transition from Innate to Acquired Immunity: Defining a Role for IL-6. *J Immunol* **175**, 3463–3468. American Association of Immunologists.

Jose, P. J., Griffiths-Johnson, D. A., Collins, P. D., Walsh, D. T., Moqbel, R., Totty, N. F., Truong, O., Hsuan, J. J. & Williams, T. J. (1994). Eotaxin: a potent eosinophil chemoattractant cytokine detected in a guinea pig model of allergic airways inflammation. *J Exp Med* **179**, 881–7.

Journet, L., Agrain, C., Broz, P. & Cornelis, G. R. (2003). The needle length of bacterial injectisomes is determined by a molecular ruler. *Science (80-)* **302**, 1757–1760.

Jung, C., Hugot, J.-P. & Barreau, F. (2010). Peyer's Patches: The Immune Sensors of the Intestine. *Int J Inflam* **2010**, 823710.

Jung, C., Meinzer, U., Montcuquet, N., Thachil, E., Château, D., Thiébaut, R., Roy, M., Alnabhani, Z., Berrebi, D. & other authors. **(2012).** Yersinia pseudotuberculosis disrupts intestinal barrier integrity through hematopoietic TLR-2 signaling. *J Clin Invest* **122**, 2239–51.

Kampik, D., Schulte, R. & Autenrieth, I. B. (2000). Yersinia enterocolitica invasin protein triggers differential production of interleukin-1, interleukin-8, monocyte chemoattractant protein 1, granulocyte-macrophage colony-stimulating factor, and tumor necrosis factor alpha in epithelial cells: implicatio. *Infect Immun* **68**, 2484–92.

Kaneko, K. & Hashimoto, N. (1983). Fecal excretion associated with Ca2+ dependency of Yersinia enterocolitica O3 and O9 and Yersinia pseudotuberculosis in mice. *Microbiol Immunol* **27**, 199–202.

Kapatral, V. & Minnich, S. A. (1995). Co-ordinate, temperature-sensitive regulation of the three Yersinia enterocolitica flagellin genes. *Mol Microbiol* **17**, 49–56.

Keestra, A. M., Winter, M. G., Auburger, J. J., Frässle, S. P., Xavier, M. N., Winter, S. E., Kim, A., Poon, V., Ravesloot, M. M. & other authors. **(2013).** Manipulation of small Rho GTPases is a pathogen-induced process detected by NOD1. *Nature* **496**, 233–7.

Kerschen, E. J., Cohen, D. A., Kaplan, A. M. & Straley, S. C. (2004). The plague virulence protein YopM targets the innate immune response by causing a global depletion of NK cells. *Infect Immun* **72**, 4589–602.

Kim, K. J., Chung, J. W. & Kim, K. S. (2005). 67-kDa laminin receptor promotes internalization of cytotoxic necrotizing factor 1-expressing Escherichia coli K1 into human brain microvascular endothelial cells. *J Biol Chem* **280**, 1360–8.

Kirjavainen, V., Jarva, H., Biedzka-Sarek, M., Blom, A. M., Skurnik, M. & Meri, S. (2008). Yersinia enterocolitica serum resistance proteins YadA and Ail bind the complement regulator C4b-binding protein. *PLoS Pathog* **4**, e1000140.

Knust, Z. & Schmidt, G. (2010). Cytotoxic Necrotizing Factors (CNFs)−A Growing Toxin Family. *Toxins (Basel)*.

Knust, Z., Blumenthal, B., Aktories, K. & Schmidt, G. (2009). Cleavage of Escherichia coli cytotoxic necrotizing factor 1 is required for full biologic activity. *Infect Immun* **77**, 1835–41.

Kolodziejek, A. M., Sinclair, D. J., Seo, K. S., Schnider, D. R., Deobald, C. F., Rohde, H. N., Viall, A. K., Minnich, S. S., Hovde, C. J. & other authors. **(2007).** Phenotypic characterization of OmpX, an Ail homologue of Yersinia pestis KIM. *Microbiology* **153**, 2941–51.

Kolodziejek, A. M., Schnider, D. R., Rohde, H. N., Wojtowicz, A. J., Bohach, G. A., Minnich, S. A. & Hovde, C. J. (2010). Outer membrane protein X (Ail) contributes to Yersinia pestis virulence in pneumonic plague and its activity is dependent on the lipopolysaccharide core length. *Infect Immun* **78**, 5233–43.

Kolodziejek, A. M., Caplan, A. B., Bohach, G. A., Paszczynski, A. J., Minnich, S. A. & Hovde, C. J. (2013). Physiological levels of glucose induce membrane vesicle secretion and affect the lipid and protein composition of Yersinia pestis cell surfaces. *Appl Environ Microbiol* **79**, 4509–14.

Koster, M., Bitter, W., de Cock, H., Allaoui, A., Cornelis, G. R. & Tommassen, J. (1997). The outer membrane component, YscC, of the Yop secretion machinery of Yersinia enterocolitica forms a ring-shaped multimeric complex. *Mol Microbiol* **26**, 789–97.

Kouokam, J. C., Wai, S. N., Fällman, M., Dobrindt, U., Hacker, J. & Uhlin, B. E. (2006). Active cytotoxic necrotizing factor 1 associated with outer membrane vesicles from uropathogenic Escherichia coli. *Infect Immun* **74**, 2022–30.

Kubori, T., Sukhan, A., Aizawa, S. I. & Galán, J. E. (2000). Molecular characterization and assembly of the needle complex of the Salmonella typhimurium type III protein secretion system. *Proc Natl Acad Sci U S A* **97**, 10225–30.

Kudryashev, M., Stenta, M., Schmelz, S., Amstutz, M., Wiesand, U., Castaño-Díez, D., Degiacomi, M. T., Münnich, S., Bleck, C. K. & other authors. **(2013).** In situ structural analysis of the Yersinia enterocolitica injectisome. *Elife* **2**, e00792.

Laemmli, U. K. (1970). Cleavage of structural proteins during assembly of bacteriophage T4. *Nature* **227**, 680–685.

Lambert de Rouvroit, C., Sluiters, C. & Cornelis, G. R. (1992). Role of the transcriptional activator, VirF, and temperature in the expression of the pYV plasmid genes of Yersinia enterocolitica. *Mol Microbiol* **6**, 395–409.

Lamps, L. W. (2003). Pathology of food-borne infectious diseases of the gastrointestinal tract: an update. *Adv Anat Pathol* **10**, 319–327.

Lamps, L. W., Madhusudhan, K. T., Havens, J. M., Greenson, J. K., Bronner, M. P., Chiles, M. C., Dean, P. J. & Scott, M. A. (2003). Pathogenic Yersinia DNA is detected in bowel and mesenteric lymph nodes from patients with Crohn's disease. *Am J Surg Pathol* **27**, 220–227.

Landraud, L., Gauthier, M., Fosse, T. & Boquet, P. (2000). Frequency of Escherichia coli strains producing the cytotoxic necrotizing factor (CNF1) in nosocomial urinary tract infections. *Lett Appl Microbiol* **30**, 213–6.

Lavander, M., Sundberg, L., Edqvist, P. J., Lloyd, S. A., Wolf-Watz, H. & Forsberg, A. (2003). Characterisation of the type III secretion protein YscU in Yersinia pseudotuberculosis. YscU cleavage--dispensable for TTSS but essential for survival. *Adv Exp Med Biol* **529**, 109–12.

Lee, V. T., Anderson, D. M. & Schneewind, O. (1998). Targeting of Yersinia Yop proteins into the cytosol of HeLa cells: one-step translocation of YopE across bacterial and eukaryotic membranes is dependent on SycE chaperone. *Mol Microbiol* **28**, 593–601.

Leeuwen, F. N., Kain, H. E., Kammen, R. A., Michiels, F., Kranenburg, O. W. & Collard, J. G. (1997). The guanine nucleotide exchange factor Tiam1 affects neuronal morphology; opposing roles for the small GTPases Rac and Rho. *J Cell Biol* **139**, 797–807.

Lemaitre, N., Sebbane, F., Long, D. & Hinnebusch, B. J. (2006). Yersinia pestis YopJ suppresses tumor necrosis factor alpha induction and contributes to apoptosis of immune cells in the lymph node but is not required for virulence in a rat model of bubonic plague. *Infect Immun* **74**, 5126–5131.

Lemichez, E., Flatau, G., Bruzzone, M., Boquet, P. & Gauthier, M. (1997). Molecular localization of the Escherichia coli cytotoxic necrotizing factor CNF1 cell-binding and catalytic domains. *Mol Microbiol* **24**, 1061–70.

Lemonnier, M., Landraud, L. & Lemichez, E. (2007). Rho GTPase-activating bacterial toxins: from bacterial virulence regulation to eukaryotic cell biology. *FEMS Microbiol Rev* **31**, 515–34.

Linke, D., Riess, T., Autenrieth, I. B., Lupas, A. & Kempf, V. A. J. (2006). Trimeric autotransporter adhesins: variable structure, common function. *Trends Microbiol* **14**, 264–270.

Lloyd, C. M., Phillips, A. R. J., Cooper, G. J. S. & Dunbar, P. R. (2008). Three-colour fluorescence immunohistochemistry reveals the diversity of cells staining for macrophage markers in murine spleen and liver. *J Immunol Methods* **334**, 70–81.

Lockman, H. A., Gillespie, R. A., Baker, B. D. & Shakhnovich, E. (2002). Yersinia pseudotuberculosis produces a cytotoxic necrotizing factor. *Infect Immun* **70**, 2708–14.

Logsdon, L. K. & Mecsas, J. (2003). Requirement of the Yersinia pseudotuberculosis effectors YopH and YopE in colonization and persistence in intestinal and lymph tissues. *Infect Immun* **71**, 4595–607.

Logsdon, L. K. & Mecsas, J. (2006). The proinflammatory response induced by wild-type Yersinia pseudotuberculosis infection inhibits survival of yop mutants in the gastrointestinal tract and Peyer's patches. *Infect Immun* **74**, 1516–27.

Lynch, M., Painter, J., Woodruff, R. & Braden, C. (2006). Surveillance for foodborne-disease outbreaks - United States, 1998-2002. *Morb Mortal Wkly Rep* **55**, 1–42.

Madaule, P. & Axel, R. (1985). A novel ras-related gene family. *Cell* **41**, 31–40.

Manoil, C. & Beckwith, J. (1986). A genetic approach to analyzing membrane protein topology. *Science (80-)* **233**, 1403–1408.

Marketon, M. M., DePaolo, R. W., DeBord, K. L., Jabri, B. & Schneewind, O. (2005). Plague bacteria target immune cells during infection. *Science* **309**, 1739–1741.

Marlovits, T. C., Kubori, T., Lara-Tejero, M., Thomas, D., Unger, V. M. & Galan, J. E. (2006). Assembly of the inner rod determines needle length in the type III secretion injectisome. *Nature* **441**, 637–640.

Masuda, M., Betancourt, L., Matsuzawa, T., Kashimoto, T., Takao, T., Shimonishi, Y. & Horiguchi, Y. (2000). Activation of rho through a cross-link with polyamines catalyzed by Bordetella dermonecrotizing toxin. *EMBO J* **19**, 521–30.

May, M., Kolbe, T., Wang, T., Schmidt, G. & Genth, H. (2012). Increased Cell-Matrix Adhesion upon Constitutive Activation of Rho Proteins by Cytotoxic Necrotizing Factors from E. Coli and Y. Pseudotuberculosis. *J Signal Transduct* **2012**, 570183.

McCoy, M. W., Marré, M. L., Lesser, C. F. & Mecsas, J. (2010). The C-terminal tail of Yersinia pseudotuberculosis YopM is critical for interacting with RSK1 and for virulence. *Infect Immun* **78**, 2584–98.

McCrumb, F. R., Mercier, S., Robic, J., Bouillat, M., Smadel, J. E., Woodward, T. E. & Goodner, K. (1953). Chloramphenicol and terramycin in the treatment of pneumonic plague. *Am J Med* **14**, 284–293.

McDonald, C., Vacratsis, P. O., Bliska, J. B. & Dixon, J. E. (2003). The Yersinia virulence factor YopM forms a novel protein complex with two cellular kinases. *J Biol Chem* **278**, 18514–18523.

Mecsas, J., Bilis, I. & Falkow, S. (2001). Identification of attenuated Yersinia pseudotuberculosis strains and characterization of an orogastric infection in BALB/c mice on day 5 postinfection by signature-tagged mutagenesis. *Infect Immun* **69**, 2779–2787.

Meinzer, U., Barreau, F., Esmiol-Welterlin, S., Jung, C., Villard, C., Léger, T., Ben-Mkaddem, S., Berrebi, D., Dussaillant, M. & other authors. **(2012).** Yersinia pseudotuberculosis effector YopJ subverts the Nod2/RICK/TAK1 pathway and activates caspase-1 to induce intestinal barrier dysfunction. *Cell Host Microbe* **11**, 337–51.

Mejía, E., Bliska, J. B. & Viboud, G. I. (2008). Yersinia controls type III effector delivery into host cells by modulating Rho activity. *PLoS Pathog* **4**, e3.

Miller, J. H. (1992). *A short course in bacterial genetic: a laboratory manual and handbook for Escherichia coli and related bacteria* (C. S. H. Laboratories, Ed.). Cold Spring Habor, New York.

Miller, V. L. & Falkow, S. (1988). Evidence for two genetic loci in Yersinia enterocolitica that can promote invasion of epithelial cells. *Infect Immun* **56**, 1242–1248.

Mishra, A., Hogan, S. P., Brandt, E. B. & Rothenberg, M. E. (2000). Peyer's patch eosinophils: identification, characterization, and regulation by mucosal allergen exposure, interleukin-5, and eotaxin. *Blood* **96**, 1538–1544.

Monack, D. M., Mecsas, J., Ghori, N. & Falkow, S. (1997). Yersinia signals macrophages to undergo apoptosis and YopJ is necessary for this cell death. *Proc Natl Acad Sci U S A* **94**, 10385–10390.

Monack, D. M., Mecsas, J., Bouley, D. & Falkow, S. (1998). Yersinia-induced apoptosis in vivo aids in the establishment of a systemic infection of mice. *J Exp Med* **188**, 2127–37.

Mou, S., Cote, C. K. & Worsham, P. L. (2012). Cytotoxic necrotizing factor is an effective immunogen in a Yersinia pseudotuberculosis aerosol mouse model. *Adv Exp Med Biol* **954**, 179–81.

Mueller, C. A., Broz, P., Muller, S. A., Ringler, P., Erne-Brand, F., Sorg, I., Kuhn, M., Engel, A. & Cornelis, G. R. (2005). The V-antigen of Yersinia forms a distinct structure at the tip of injectisome needles. *Science (80-)* **310**, 674–676.

Mukherjee, S., Keitany, G., Li, Y., Wang, Y., Ball, H. L., Goldsmith, E. J. & Orth, K. (2006). Yersinia YopJ acetylates and inhibits kinase activation by blocking phosphorylation. *Science* **312**, 1211–4.

Nagel, G., Lahrz, A. & Dersch, P. (2001). Environmental control of invasin expression in Yersinia pseudotuberculosis is mediated by regulation of RovA, a transcriptional activator of the SlyA/Hor family. *Mol Microbiol* **41**, 1249–1269.

Naktin, J. & Beavis, K. G. (1999). Yersinia enterocolitica and Yersinia pseudotuberculosis. *Clin Lab Med* **19**, 523–36, vi.

Neutra, M. R., Mantis, N. J., Frey, A. & Giannasca, P. J. (1999). The composition and function of M cell apical membranes: implications for microbial pathogenesis. *Semin Immunol* **11**, 171–181.

Neyt, C. & Cornelis, G. R. (1999). Insertion of a Yop translocation pore into the macrophage plasma membrane by Yersinia enterocolitica: requirement for translocators YopB and YopD, but not LcrG. *Mol Microbiol* **33**, 971–981.

Neyt, C., Iriarte, M., Thi, V. H. & Cornelis, G. R. (1997). Virulence and arsenic resistance in Yersiniae. *J Bacteriol* **179**, 612–619.

Nobes, C. D. & Hall, A. (1995). Rho, rac, and cdc42 GTPases regulate the assembly of multimolecular focal complexes associated with actin stress fibers, lamellipodia, and filopodia. *Cell* **81**, 53–62.

Nomanbhoy, T. K., Erickson, J. W. & Cerione, R. A. (1999). Kinetics of Cdc42 membrane extraction by Rho-GDI monitored by real-time fluorescence resonance energy transfer. *Biochemistry* **38**, 1744–50.

Oyston, P. C., Dorrell, N., Williams, K., Li, S. R., Green, M., Titball, R. W. & Wren, B. W. (2000). The response regulator PhoP is important for survival under conditions of macrophage-induced stress and virulence in Yersinia pestis. *Infect Immun* **68**, 3419–25.

Parkhill, J., Wren, B. W., Thomson, N. R., Titball, R. W., Holden, M. T., Prentice, M. B., Sebaihia, M., James, K. D., Churcher, C. & other authors. **(2001).** Genome sequence of Yersinia pestis, the causative agent of plague. *Nature* **413**, 523–7.

Von Pawel-Rammingen, U., Telepnev, M. V, Schmidt, G., Aktories, K., Wolf-Watz, H. & Rosqvist, R. (2000). GAP activity of the Yersinia YopE cytotoxin specifically targets the Rho pathway: a mechanism for disruption of actin microfilament structure. *Mol Microbiol* **36**, 737–48.

Payne, P. L. & Straley, S. C. (1999). YscP of Yersinia pestis is a secreted component of the Yop secretion system. *J Bacteriol* **181**, 2852–62.

Pepe, J. C., Badger, J. L. & Miller, V. L. (1994). Growth phase and low pH affect the thermal regulation of the Yersinia enterocolitica inv gene. *Mol Microbiol* **11**, 123–135.

Persson, C., Carballeira, N., Wolf-Watz, H. & Fällman, M. (1997). The PTPase YopH inhibits uptake of Yersinia, tyrosine phosphorylation of p130Cas and FAK, and the associated accumulation of these proteins in peripheral focal adhesions. *EMBO J* **16**, 2307–18.

Pettersson, J., Nordfelth, R., Dubinina, E., Bergman, T., Gustafsson, M., Magnusson, K. E. & Wolf-Watz, H. (1996). Modulation of virulence factor expression by pathogen target cell contact. *Science* **273**, 1231–3.

Philip, N. H. & Brodsky, I. E. (2012). Cell death programs in Yersinia immunity and pathogenesis. *Front Cell Infect Microbiol* **2**, 149.

Pilz, D., Vocke, T., Heesemann, J. & Brade, V. (1992). Mechanism of YadA-mediated serum resistance of Yersinia enterocolitica serotype O3. *Infect Immun* **60**, 189–95.

Pollard, T. D. & Borisy, G. G. (2003). Cellular motility driven by assembly and disassembly of actin filaments. *Cell* **112**, 453–65.

Portnoy, D. A. & Falkow, S. (1981). Virulence-associated plasmids from Yersinia enterocolitica and Yersinia pestis. *J Bacteriol* **148**, 877–883.

Del Pozo, M. A., Kiosses, W. B., Alderson, N. B., Meller, N., Hahn, K. M. & Schwartz, M. A. (2002). Integrins regulate GTP-Rac localized effector interactions through dissociation of Rho-GDI. *Nat Cell Biol* **4**, 232–9.

Pujol, C. & Bliska, J. B. (2003). The ability to replicate in macrophages is conserved between Yersinia pestis and Yersinia pseudotuberculosis. *Infect Immun* **71**, 5892–9.

Pujol, C. & Bliska, J. B. (2005). Turning Yersinia pathogenesis outside in: subversion of macrophage function by intracellular yersiniae. *Clin Immunol* **114**, 216–226.

Quenee, L. E. & Schneewind, O. (2009). Plague vaccines and the molecular basis of immunity against Yersinia pestis. *Hum Vaccin* **5**, 817–823.

Ralph, P. & Nakoinz, I. (1977). Antibody-dependent killing of erythrocyte and tumor targets by macrophage-related cell lines: enhancement by PPD and LPS. *J Immunol* **119**, 950–954.

Ralph, P., Nakoinz, I. (1975). Phagocytosis and cytolysis by a macrophage tumour and its cloned cell line. *Nature* **257**, 393–4.

Revell, P. A. & Miller, V. L. (2001). Yersinia virulence: more than a plasmid. *FEMS Microbiol Lett* **205**, 159–164.

Ricciardi, I. D., Pearson, A. D., Suckling, W. G. & Klein, C. (1978). Long-term fecal excretion and resistance induced in mice infected with Yersinia enterocolitica. *Infect Immun* **21**, 342–344.

Riley, G. & Toma, S. (1989). Detection of pathogenic Yersinia enterocolitica by using congo red-magnesium oxalate agar medium. *J Clin Microbiol* **27**, 213–214.

Riordan, K. E. & Schneewind, O. (2008). YscU cleavage and the assembly of Yersinia type III secretion machine complexes. *Mol Microbiol* **68**, 1485–501.

Rippere-Lampe, K. E., O'Brien, A. D., Conran, R. & Lockman, H. A. (2001a). Mutation of the gene encoding cytotoxic necrotizing factor type 1 (cnf(1)) attenuates the virulence of uropathogenic Escherichia coli. *Infect Immun* **69**, 3954–64.

Rippere-Lampe, K. E., Lang, M., Ceri, H., Olson, M., Lockman, H. A. & O'Brien, A. D. (2001b). Cytotoxic necrotizing factor type 1-positive Escherichia coli causes increased inflammation and tissue damage to the prostate in a rat prostatitis model. *Infect Immun* **69**, 6515–9.

Rittinger, K., Walker, P. A., Eccleston, J. F., Smerdon, S. J. & Gamblin, S. J. (1997). Structure at 1.65 A of RhoA and its GTPase-activating protein in complex with a transition-state analogue. *Nature* **389**, 758–62.

Rosner, B. M., Stark, K. & Werber, D. (2010). Epidemiology of reported Yersinia enterocolitica infections in Germany, 2001-2008. *BMC Public Health* **10**, 337.

Rosqvist, R., Persson, C., Håkansson, S., Nordfeldt, R. & Wolf-Watz, H. (1995). Translocation of the Yersinia YopE and YopH virulence proteins into target cells is mediated by YopB and YopD. *Contrib Microbiol Immunol* **13**, 230–4.

Ross, J. A. & Plano, G. V. (2011). A C-terminal region of Yersinia pestis YscD binds the outer membrane secretin YscC. *J Bacteriol* **193**, 2276–89.

Rossman, K. L., Der, C. J. & Sondek, J. (2005). GEF means go: turning on RHO GTPases with guanine nucleotide-exchange factors. *Nat Rev Mol Cell Biol* **6**, 167–80.

Roux, E. & Yersin, A. (1888). Contribution à l'étude de la diphtérie. *Ann Inst Pasteur* **2**, 629–661.

Ruckdeschel, K., Deuretzbacher, A. & Haase, R. (2008). Crosstalk of signalling processes of innate immunity with Yersinia Yop effector functions. *Immunobiology* **213**, 261–9.

Ruiz-Bravo, A., Moreno, E. & Jiménez-Valera, M. (2001). Intestinal infection of BALB/c mice with Yersinia enterocolitica O9 causes major modifications in phenotype and functions of spleen cells. *Microbiology* **147**, 3165–9.

Saier, M. H. (1998). Multiple mechanisms controlling carbon metabolism in bacteria. *Biotechnol Bioeng* **58**, 170–4.

Sambrook, J., Fritsch, E. F. & Maniatis, T. (1989). *Molecular Cloning: A Laboratory Manual. New York*.

Savill, J., Dransfield, I., Gregory, C. & Haslett, C. (2002). A blast from the past: clearance of apoptotic cells regulates immune responses. *Nat Rev Immunol* **2**, 965–75.

Savin, C., Martin, L., Bouchier, C., Filali, S., Chenau, J., Zhou, Z., Becher, F., Fukushima, H., Thomson, N. R. & other authors. (2014). The Yersinia pseudotuberculosis complex: Characterization and delineation of a new species, Yersinia wautersii. *Int J Med Microbiol*.

Schiavo, G., Matteoli, M. & Montecucco, C. (2000). Neurotoxins Affecting Neuroexocytosis. *Physiol Rev* **80**, 717–766.

Schlegel, N., Meir, M., Spindler, V., Germer, C.-T. & Waschke, J. (2011). Differential role of Rho GTPases in intestinal epithelial barrier regulation in vitro. *J Cell Physiol* **226**, 1196–203.

Schmid, Y., Grassl, G. A., Bühler, O. T., Skurnik, M., Autenrieth, I. B. & Bohn, E. (2004). Yersinia enterocolitica adhesin A induces production of interleukin-8 in epithelial cells. *Infect Immun* **72**, 6780–6789.

Schmidt, G., Selzer, J., Lerm, M. & Aktories, K. (1998). The Rho-deamidating cytotoxic necrotizing factor 1 from Escherichia coli possesses transglutaminase activity. Cysteine 866 and histidine 881 are essential for enzyme activity. *J Biol Chem* **273**, 13669–74.

Schulte, R., Wattiau, P., Hartland, E. L., Robins-Browne, R. M. & Cornelis, G. R. (1996). Differential secretion of interleukin-8 by human epithelial cell lines upon entry of virulent or nonvirulent Yersinia enterocolitica. *Infect Immun* **64**, 2106–13.

Schweer, J., Kulkarni, D., Kochut, A., Pezoldt, J., Pisano, F., Pils, M. C., Genth, H., Huehn, J. & Dersch, P. (2013). The Cytotoxic Necrotizing Factor of Yersinia pseudotuberculosis (CNFY) Enhances Inflammation and Yop Delivery during Infection by Activation of Rho GTPases. *PLoS Pathog* **9**, e1003746.

Sebbane, F., Jarrett, C., Gardner, D., Long, D. & Hinnebusch, B. J. (2009). The Yersinia pestis caf1M1A1 fimbrial capsule operon promotes transmission by flea bite in a mouse model of bubonic plague. *Infect Immun* **77**, 1222–1229.

Shao, F., Merritt, P. M., Bao, Z., Innes, R. W. & Dixon, J. E. (2002). A Yersinia effector and a Pseudomonas avirulence protein define a family of cysteine proteases functioning in bacterial pathogenesis. *Cell* **109**, 575–88.

Shao, F., Vacratsis, P. O., Bao, Z., Bowers, K. E., Fierke, C. A. & Dixon, J. E. (2003). Biochemical characterization of the Yersinia YopT protease: cleavage site and recognition elements in Rho GTPases. *Proc Natl Acad Sci U S A* **100**, 904–9.

Shen, A. (2012). Clostridium difficile toxins: mediators of inflammation. *J Innate Immun* **4**, 149–58.

Sherry, B., Tekamp-Olson, P., Gallegos, C., Bauer, D., Davatelis, G., Wolpe, S. D., Masiarz, F., Coit, D. & Cerami, A. (1988). Resolution of the two components of macrophage inflammatory protein 1, and cloning and characterization of one of those components, macrophage inflammatory protein 1 beta. *J Exp Med* **168**, 2251–9.

Shi, Y., Liu, C. H., Roberts, A. I., Das, J., Xu, G., Ren, G., Zhang, Y., Zhang, L., Yuan, Z. R. & other authors. (2006). Granulocyte-macrophage colony-stimulating factor (GM-CSF) and T-cell responses: what we do and don't know. *Cell Res* **16**, 126–33.

Simon, R., Priefer, U. & Pühler, A. (1983). A Broad Host Range Mobilization System for *In Vivo* Genetic Engineering: Transposon Mutagenesis in Gram Negative Bacteria. *Bio/Technology* **1**, 784–791.

Skrzypek, E., Cowan, C. & Straley, S. C. (1998). Targeting of the Yersinia pestis YopM protein into HeLa cells and intracellular trafficking to the nucleus. *Mol Microbiol* **30**, 1051–65.

Songsungthong, W., Higgins, M. C., Rolán, H. G., Murphy, J. L. & Mecsas, J. (2010). ROS-inhibitory activity of YopE is required for full virulence of Yersinia in mice. *Cell Microbiol* **12**, 988–1001.

Sorg, I., Wagner, S., Amstutz, M., Müller, S. A., Broz, P., Lussi, Y., Engel, A. & Cornelis, G. R. (2007). YscU recognizes translocators as export substrates of the Yersinia injectisome. *EMBO J* **26**, 3015–24.

Spreter, T., Yip, C. K., Sanowar, S., André, I., Kimbrough, T. G., Vuckovic, M., Pfuetzner, R. A., Deng, W., Yu, A. C. & other authors. **(2009).** A conserved structural motif mediates formation of the periplasmic rings in the type III secretion system. *Nat Struct Mol Biol* **16**, 468–76.

Stainier, I., Bleves, S., Josenhans, C., Karmani, L., Kerbourch, C., Lambermont, I., Tötemeyer, S., Boyd, A. & Cornelis, G. R. (2000). YscP, a Yersinia protein required for Yop secretion that is surface exposed, and released in low Ca2+. *Mol Microbiol* **37**, 1005–18.

Stecher, B., Robbiani, R., Walker, A. W., Westendorf, A. M., Barthel, M., Kremer, M., Chaffron, S., Macpherson, A. J., Buer, J. & other authors. **(2007).** Salmonella enterica serovar typhimurium exploits inflammation to compete with the intestinal microbiota. *PLoS Biol* **5**, 2177–89.

Straley, S. C., Skrzypek, E., Plano, G. V & Bliska, J. B. (1993). Yops of Yersinia spp. pathogenic for humans. *Infect Immun* **61**, 3105–10.

Strobel, S. & Mowat, A. M. (1998). Immune responses to dietary antigens: oral tolerance. *Immunol Today* **19**, 173–81.

Studier, F. W. & Moffatt, B. A. (1986). Use of bacteriophage T7 RNA polymerase to direct selective high-level expression of cloned genes. *J Mol Biol* **189**, 113–130.

Suggs, S. V, Wallace, R. B., Hirose, T., Kawashima, E. H. & Itakura, K. (1981). Use of synthetic oligonucleotides as hybridization probes: isolation of cloned cDNA sequences for human beta 2-microglobulin. *Proc Natl Acad Sci U S A* **78**, 6613–6617.

Symons, M. & Settleman, J. (2000). Rho family GTPases: more than simple switches. *Trends Cell Biol* **10**, 415–9.

Tertti, R., Skurnik, M., Vartio, T. & Kuusela, P. (1992). Adhesion protein YadA of Yersinia species mediates binding of bacteria to fibronectin. *Infect Immun* **60**, 3021–4.

Thiennimitr, P., Winter, S. E., Winter, M. G., Xavier, M. N., Tolstikov, V., Huseby, D. L., Sterzenbach, T., Tsolis, R. M., Roth, J. R. & Bäumler, A. J. (2011). Intestinal inflammation allows Salmonella to use ethanolamine to compete with the microbiota. *Proc Natl Acad Sci U S A* **108**, 17480–5.

Thomson, N. R., Howard, S., Wren, B. W., Holden, M. T. G., Crossman, L., Challis, G. L., Churcher, C., Mungall, K., Brooks, K. & other authors. **(2006).** The complete genome sequence and comparative genome analysis of the high pathogenicity Yersinia enterocolitica strain 8081. *PLoS Genet* **2**, e206.

Toolan, H. (1954). Transplantable human neoplasms maintained in cortisone-treated laboratory animals: H.S. No. 1; H.Ep. No. 1; H.Ep. No. 2; H.Ep. No. 3; and H.Emb.Rh. No. 1. *Cancer Res* **14**, 660–6.

Tosello-Trampont, A.-C., Nakada-Tsukui, K. & Ravichandran, K. S. (2003). Engulfment of apoptotic cells is negatively regulated by Rho-mediated signaling. *J Biol Chem* **278**, 49911–9.

Towbin, H., Staehelin, T. & Gordon, J. (1979). Electrophoretic transfer of proteins from polyacrylamide gels to nitrocellulose sheets: procedure and some applications. *Proc Natl Acad Sci U S A* **76**, 4350–4354.

Tran Van Nhieu, G. & Isberg, R. R. (1993). Bacterial internalization mediated by beta 1 chain integrins is determined by ligand affinity and receptor density. *EMBO J* **12**, 1887–95.

Travier, L., Guadagnini, S., Gouin, E., Dufour, A., Chenal-Francisque, V., Cossart, P., Olivo-Marin, J.-C., Ghigo, J.-M., Disson, O. & Lecuit, M. (2013). ActA promotes Listeria monocytogenes aggregation, intestinal colonization and carriage. *PLoS Pathog* **9**, e1003131.

Treille, G.-F. & Yersin, A. (1894). La peste bubonique á Hong Kong. *Ann IInstitut Pasteur* **8**, 662–667.

Triadafilopoulos, G., Pothoulakis, C., O'Brien, M. J. & LaMont, J. T. (1987). Differential effects of Clostridium difficile toxins A and B on rabbit ileum. *Gastroenterology* **93**, 273–9.

Trinchieri, G. (1995). Interleukin-12: a proinflammatory cytokine with immunoregulatory functions that bridge innate resistance and antigen-specific adaptive immunity. *Annu Rev Immunol* **13**, 251–76.

Trülzsch, K., Sporleder, T., Igwe, E. I., Rüssmann, H. & Heesemann, J. (2004). Contribution of the major secreted yops of Yersinia enterocolitica O:8 to pathogenicity in the mouse infection model. *Infect Immun* **72**, 5227–34.

Tsang, T. M., Felek, S. & Krukonis, E. S. (2010). Ail binding to fibronectin facilitates Yersinia pestis binding to host cells and Yop delivery. *Infect Immun* **78**, 3358–68.

Tsukano, H., Kura, F., Inoue, S., Sato, S., Izumiya, H., Yasuda, T. & Watanabe, H. (1999). Yersinia pseudotuberculosis blocks the phagosomal acidification of B10.A mouse macrophages through the inhibition of vacuolar H(+)-ATPase activity. *Microb Pathog* **27**, 253–263.

Uliczka, F., Pisano, F., Kochut, A., Opitz, W., Herbst, K., Stolz, T. & Dersch, P. (2011). Monitoring of gene expression in bacteria during infections using an adaptable set of bioluminescent, fluorescent and colorigenic fusion vectors. *PLoS One* **6**, e20425.

Viboud, G. I. & Bliska, J. B. (2001). A bacterial type III secretion system inhibits actin polymerization to prevent pore formation in host cell membranes. *EMBO J* **20**, 5373–82.

Viboud, G. I. & Bliska, J. B. (2005). Yersinia outer proteins: role in modulation of host cell signaling responses and pathogenesis. *Annu Rev Microbiol* **59**, 69–89.

Visvikis, O., Boyer, L., Torrino, S., Doye, A., Lemonnier, M., Lorès, P., Rolando, M., Flatau, G., Mettouchi, A. & other authors. **(2011).** Escherichia coli producing CNF1 toxin hijacks Tollip to trigger Rac1-dependent cell invasion. *Traffic* **12**, 579–90.

Vogelsgesang, M., Pautsch, A. & Aktories, K. (2007). C3 exoenzymes, novel insights into structure and action of Rho-ADP-ribosylating toxins. *Naunyn Schmiedebergs Arch Pharmacol* **374**, 347–60.

Wachtel, M. R. & Miller, V. L. (1995). In vitro and in vivo characterization of an ail mutant of Yersinia enterocolitica. *Infect Immun* **63**, 2541–8.

Wennerberg, K. & Der, C. J. (2004). Rho-family GTPases: it's not only Rac and Rho (and I like it). *J Cell Sci* **117**, 1301–12.

Winder, S. J. & Ayscough, K. R. (2005). Actin-binding proteins. *J Cell Sci* **118**, 651–4.

Winter, S. E., Keestra, A. M., Tsolis, R. M. & Bäumler, A. J. (2010). The blessings and curses of intestinal inflammation. *Cell Host Microbe* **8**, 36–43.

Wolters, M., Boyle, E. C., Lardong, K., Trülzsch, K., Steffen, A., Rottner, K., Ruckdeschel, K. & Aepfelbacher, M. (2013). Cytotoxic necrotizing factor-Y boosts Yersinia effector translocation by activating Rac protein. *J Biol Chem* **288**, 23543–53.

Wong, K.-W. & Isberg, R. R. (2005). Yersinia pseudotuberculosis spatially controls activation and misregulation of host cell Rac1. *PLoS Pathog* **1**, e16.

Wong, K.-W., Mohammadi, S. & Isberg, R. R. (2006). Disruption of RhoGDI and RhoA regulation by a Rac1 specificity switch mutant. *J Biol Chem* **281**, 40379–88.

Yang, Y. & Isberg, R. R. (1997). Transcriptional regulation of the Yersinia pseudotuberculosis pH6 antigen adhesin by two envelope-associated components. *Mol Microbiol* **24**, 499–510.

Yang, Y., Merriam, J. J., Mueller, J. P. & Isberg, R. R. (1996). The psa locus is responsible for thermoinducible binding of Yersinia pseudotuberculosis to cultured cells. *Infect Immun* **64**, 2483–2489.

Ye, Z., Kerschen, E. J., Cohen, D. A., Kaplan, A. M., van Rooijen, N. & Straley, S. C. (2009). Gr1+ cells control growth of YopM-negative yersinia pestis during systemic plague. *Infect Immun* **77**, 3791–806.

Yip, C. K., Kimbrough, T. G., Felise, H. B., Vuckovic, M., Thomas, N. A., Pfuetzner, R. A., Frey, E. A., Finlay, B. B., Miller, S. I. & Strynadka, N. C. J. (2005). Structural characterization of the molecular platform for type III secretion system assembly. *Nature* **435**, 702–7.

Yother, J. & Goguen, J. D. (1985). Isolation and characterization of Ca2+-blind mutants of Yersinia pestis. *J Bacteriol* **164**, 704–11.

Young, G. M. & Miller, V. L. (1997). Identification of novel chromosomal loci affecting Yersinia enterocolitica pathogenesis. *Mol Microbiol* **25**, 319–328.

Young, G. M., Amid, D. & Miller, V. L. (1996). A bifunctional urease enhances survival of pathogenic Yersinia enterocolitica and Morganella morganii at low pH. *J Bacteriol* **178**, 6487–6495.

Young, R. (1992). Bacteriophage lysis: mechanism and regulation. *Microbiol Rev* **56**, 430–81.

Young, R. (2002). Bacteriophage holins: deadly diversity. *J Mol Microbiol Biotechnol* **4**, 21–36.

Zhang, Y. & Bliska, J. B. (2005). Role of macrophage apoptosis in the pathogenesis of Yersinia. *Curr Top Microbiol Immunol* **289**, 151–73.

Zhang, Y. & Bliska, J. B. (2003). Role of Toll-like receptor signaling in the apoptotic response of macrophages to Yersinia infection. *Infect Immun* **71**, 1513–9.

Zhang, Y. & Bliska, J. B. (2010). YopJ-promoted cytotoxicity and systemic colonization are associated with high levels of murine interleukin-18, gamma interferon, and neutrophils in a live vaccine model of Yersinia pseudotuberculosis infection. *Infect Immun* **78**, 2329–41.

Zhang, Y., Ting, A. T., Marcu, K. B. & Bliska, J. B. (2005). Inhibition of MAPK and NF-kappa B pathways is necessary for rapid apoptosis in macrophages infected with Yersinia. *J Immunol* **174**, 7939–49. American Association of Immunologists.

Zheng, D., Constantinidou, C., Hobman, J. L. & Minchin, S. D. (2004). Identification of the CRP regulon using in vitro and in vivo transcriptional profiling. *Nucleic Acids Res* **32**, 5874–93.

Zheng, Y., Lilo, S., Brodsky, I. E., Zhang, Y., Medzhitov, R., Marcu, K. B. & Bliska, J. B. (2011). A Yersinia effector with enhanced inhibitory activity on the NF-κB pathway activates the NLRP3/ASC/caspase-1 inflammasome in macrophages. *PLoS Pathog* **7**, e1002026.

Zlokarnik, G., Negulescu, P. A., Knapp, T. E., Mere, L., Burres, N., Feng, L., Whitney, M., Roemer, K. & Tsien, R. Y. (1998). Quantitation of transcription and clonal selection of single living cells with beta-lactamase as reporter. *Science* **279**, 84–8.

Supplementary material

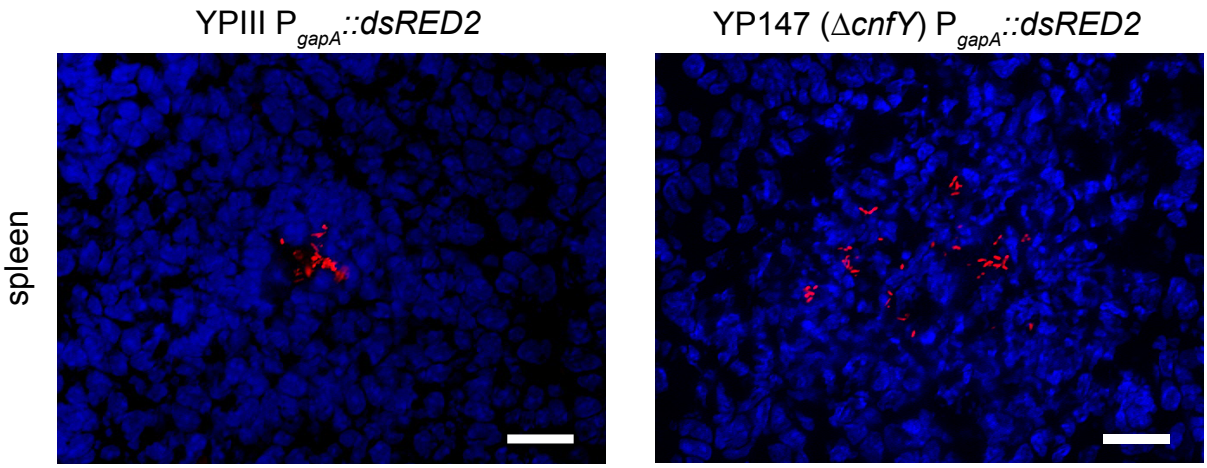

Figure S1: Microcolonies of *Y. pseudotuberculosis* in the spleen.
Groups of 3 BALB/c mice were infected orally with 2 x 10^8 bacteria of *Y. pseudotuberculosis* YPIII of YP147 (Δ*cnfY*), harbouring the plasmid pFU228 (P_{gapA}::*dsRed2*). Three days post infection, the mice were sacrificed and the spleen isolated. Cryosections (6 μm) have been prepared and analyzed by fluorescence microscopy. Sections were screened for bacteria expressing the reporter protein DsRed2. White bars indicate 20 μm.

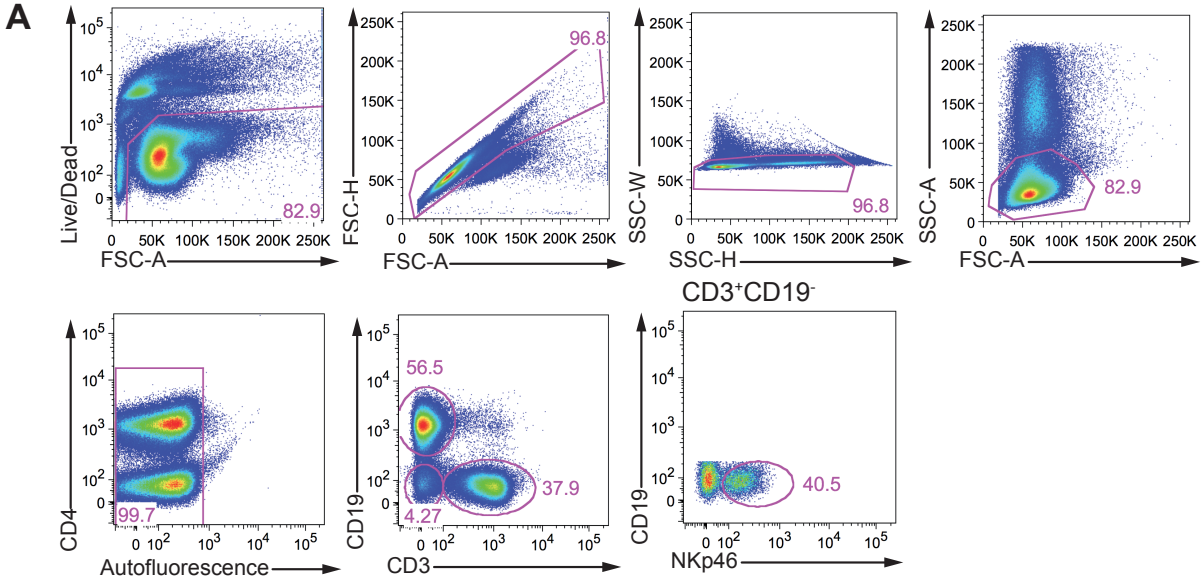

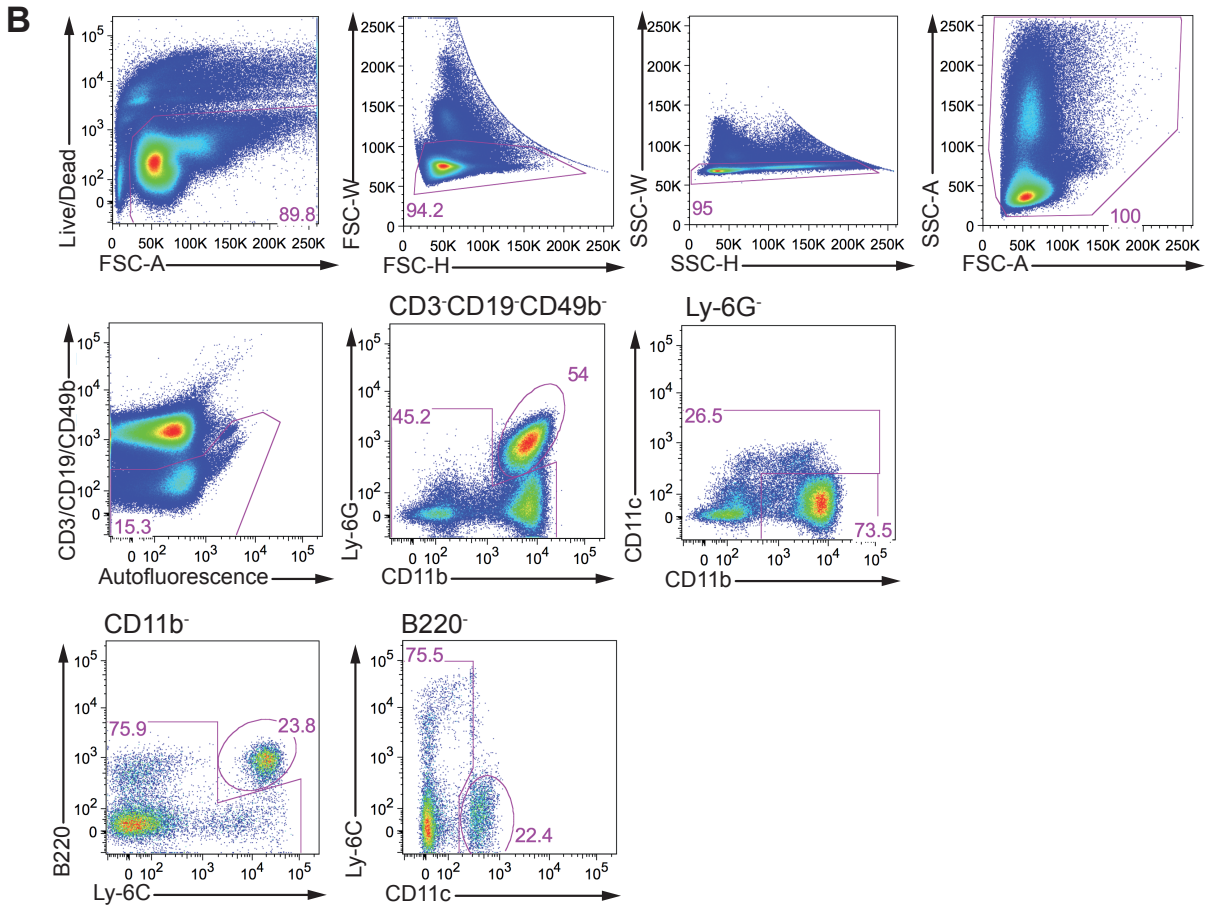

Figure S2: Gating strategies for immune cell contents in PP, MLNs, and spleen after infection with *Y. pseudotuberculosis* YPIII or YP147 (Δ*cnfY*).

Exemplary gating strategies of splenocytes from YP147 (Δ*cnfY*)-infected mice at day three post infection. (A) Lymphoid panel: T cells ($CD19^-CD3^+$), B cells ($CD19^+CD3^-$), NK cells ($CD19^-CD3^-NKp46^+$). (B) Myeloid panel: neutrophils ($CD49b^-CD19^-CD3^-Ly\text{-}6G^+CD11b^+$), DCs ($CD49b^-CD19^-CD3^-Ly\text{-}6G^-CD11b^-Ly\text{-}6C^-CD11c^+$), macrophages/monocytes ($CD49b^-CD19^-CD3^-Ly\text{-}6G^-CD11c^-CD11b^+$).

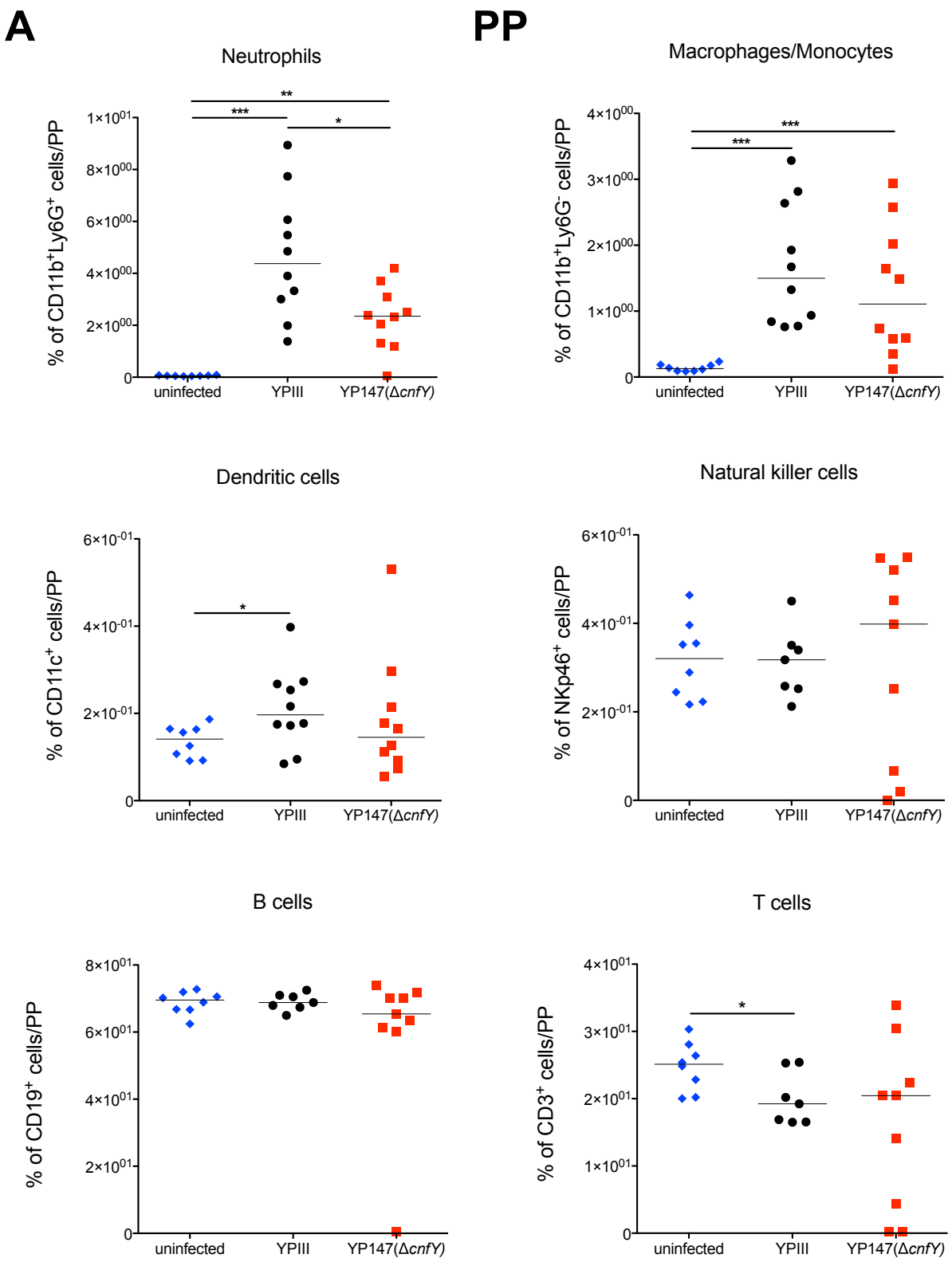
A
PP
Neutrophils
% of CD11b+Ly6G+ cells/PP
Macrophages/Monocytes
% of CD11b+Ly6G- cells/PP
Dendritic cells
% of CD11c+ cells/PP
Natural killer cells
% of NKp46+ cells/PP
B cells
% of CD19+ cells/PP
T cells
% of CD3+ cells/PP
uninfected
YPIII
YP147(ΔcnfY)

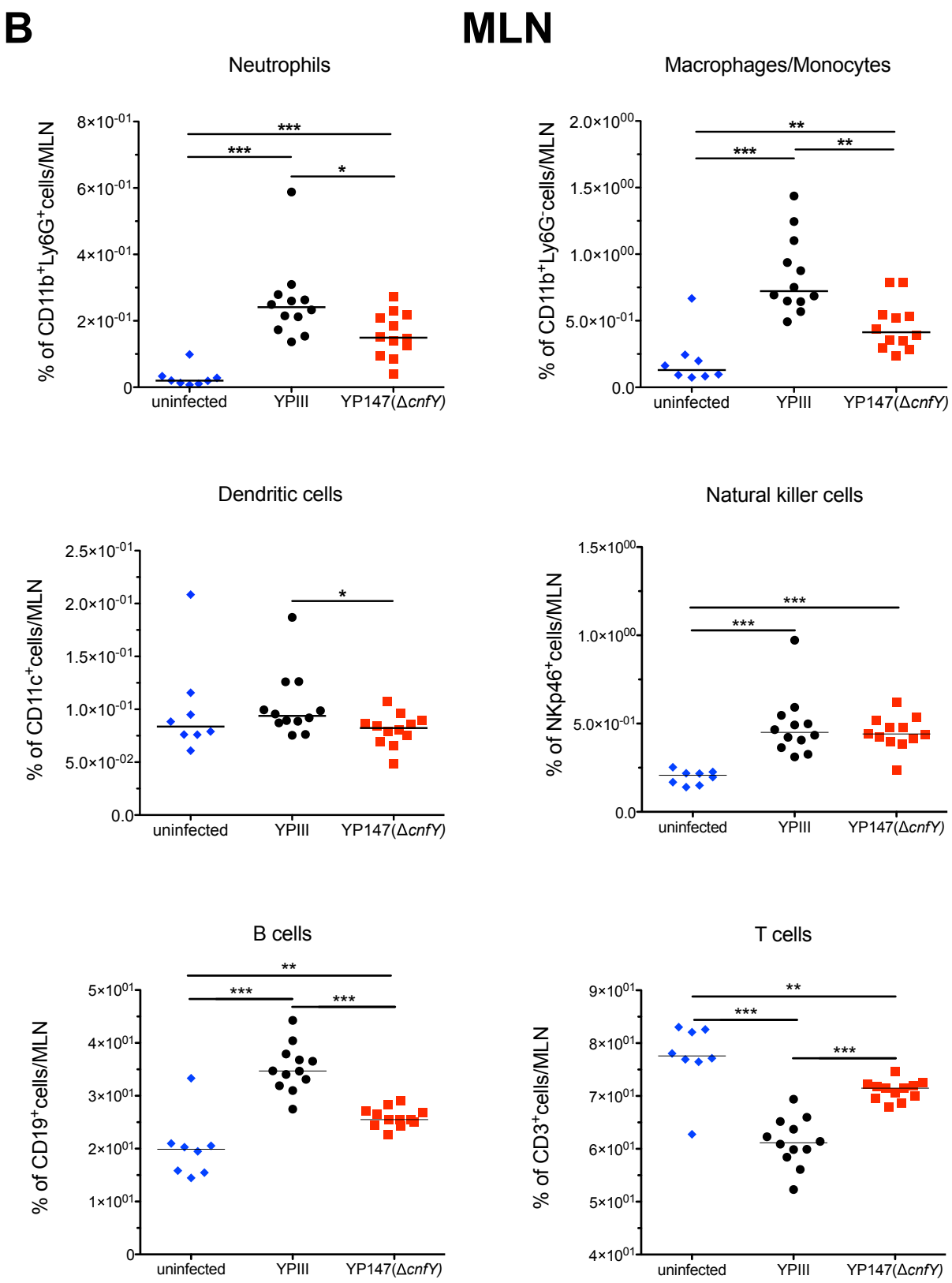
B
MLN
Neutrophils
% of CD11b+Ly6G+cells/MLN
8×10-01
6×10-01
4×10-01
2×10-01
0
***
***
*
uninfected
YPIII
YP147(ΔcnfY)
Macrophages/Monocytes
% of CD11b+Ly6G-cells/MLN
2.0×10+00
1.5×10+00
1.0×10+00
5.0×10-01
0.0
**
***
**
uninfected
YPIII
YP147(ΔcnfY)
Dendritic cells
% of CD11c+cells/MLN
2.5×10-01
2.0×10-01
1.5×10-01
1.0×10-01
5.0×10-02
0.0
*
uninfected
YPIII
YP147(ΔcnfY)
Natural killer cells
% of NKp46+cells/MLN
1.5×10+00
1.0×10+00
5.0×10-01
0.0
***
***
uninfected
YPIII
YP147(ΔcnfY)
B cells
% of CD19+cells/MLN
5×10+01
4×10+01
3×10+01
2×10+01
1×10+01
0
**
***
***
uninfected
YPIII
YP147(ΔcnfY)
T cells
% of CD3+cells/MLN
9×10+01
8×10+01
7×10+01
6×10+01
5×10+01
4×10+01
**
***
***
uninfected
YPIII
YP147(ΔcnfY)

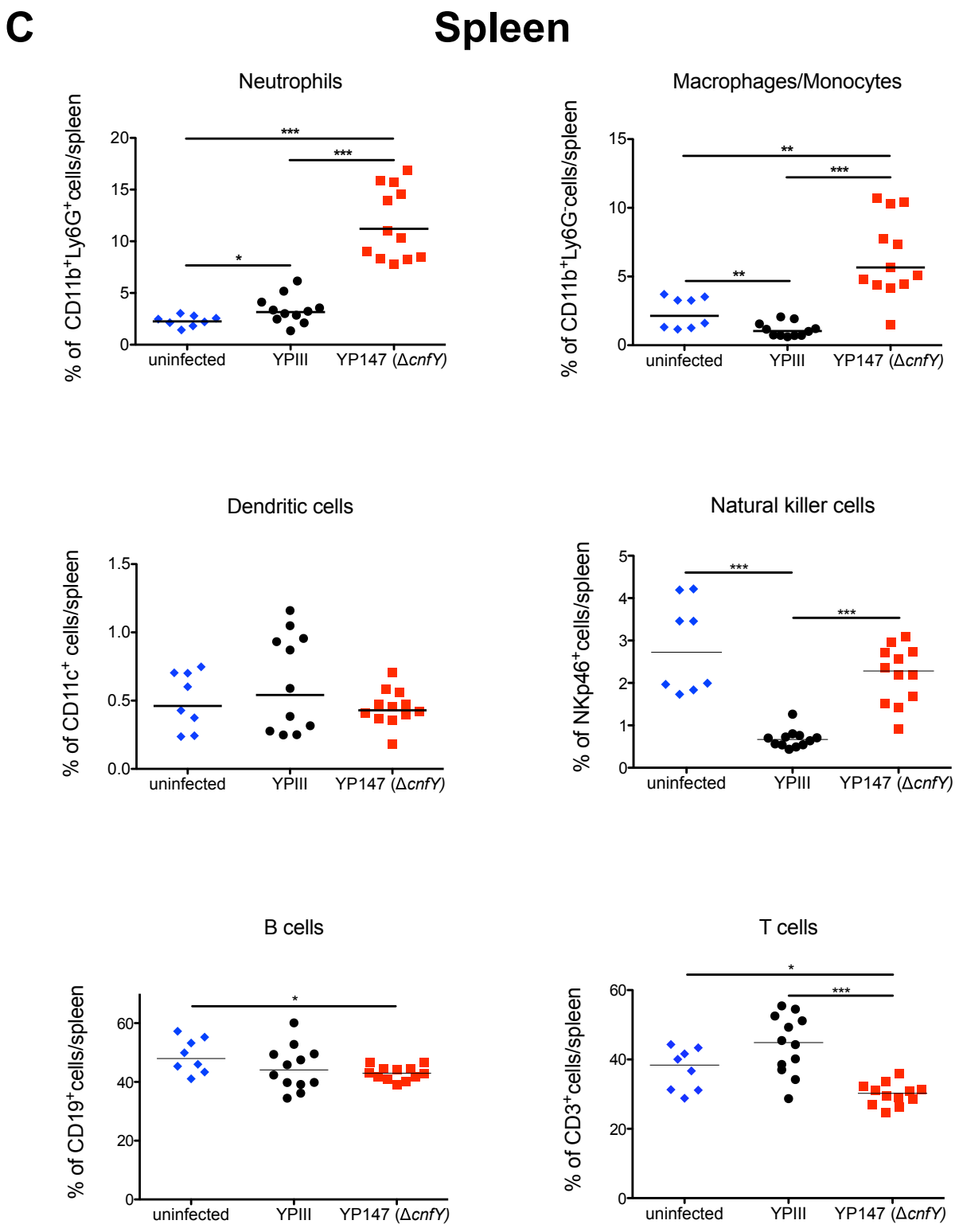

Figure S3: CNF$_Y$ modulates the host immune response in the infected mice.
Groups of 5 - 6 BALB/c mice were infected orally with 2 x 10^8 bacteria of *Y. pseudotuberculosis* YPIII or YP147 (Δ*cnfY*). Three days after infection, mice were sacrificed and organs (PP, MLNs, and spleen) isolated. Prepared cell suspensions were stained with fluorescently labeled antibodies to detect the different immune cells with flow cytometry: neutrophils ($CD11b^+/Ly6G^+$), macrophages/monocytes ($CD11b^+Ly6G^-$), DCs ($CD11c^+$), NK cells ($NKp46^+$), B cells ($CD19^+$), and T cells ($CD3^+$). Data plotted on the y axis indicate the percentages of the different immune cells isolated from uninfected, YPIII-infected or YP147 (Δ*cnfY*)-infected organs as the absolute cell amounts in the organs could differ due to tissue

damage or splenomegaly. Scatter dot plots show the median of two independent experiments for (A) PP, (B) MLNs, and (C) spleen. For statistical analysis, a Mann-Whitney test was applied to determine significant differences in the numbers of indicated cell types in the whole organ between YPIII-infected, YP147 (Δ*cnfY*)-infected or uninfected mice. Asterisks indicate the significances, with * (P<0.05), ** (P<0.01) and *** (P<0.001).

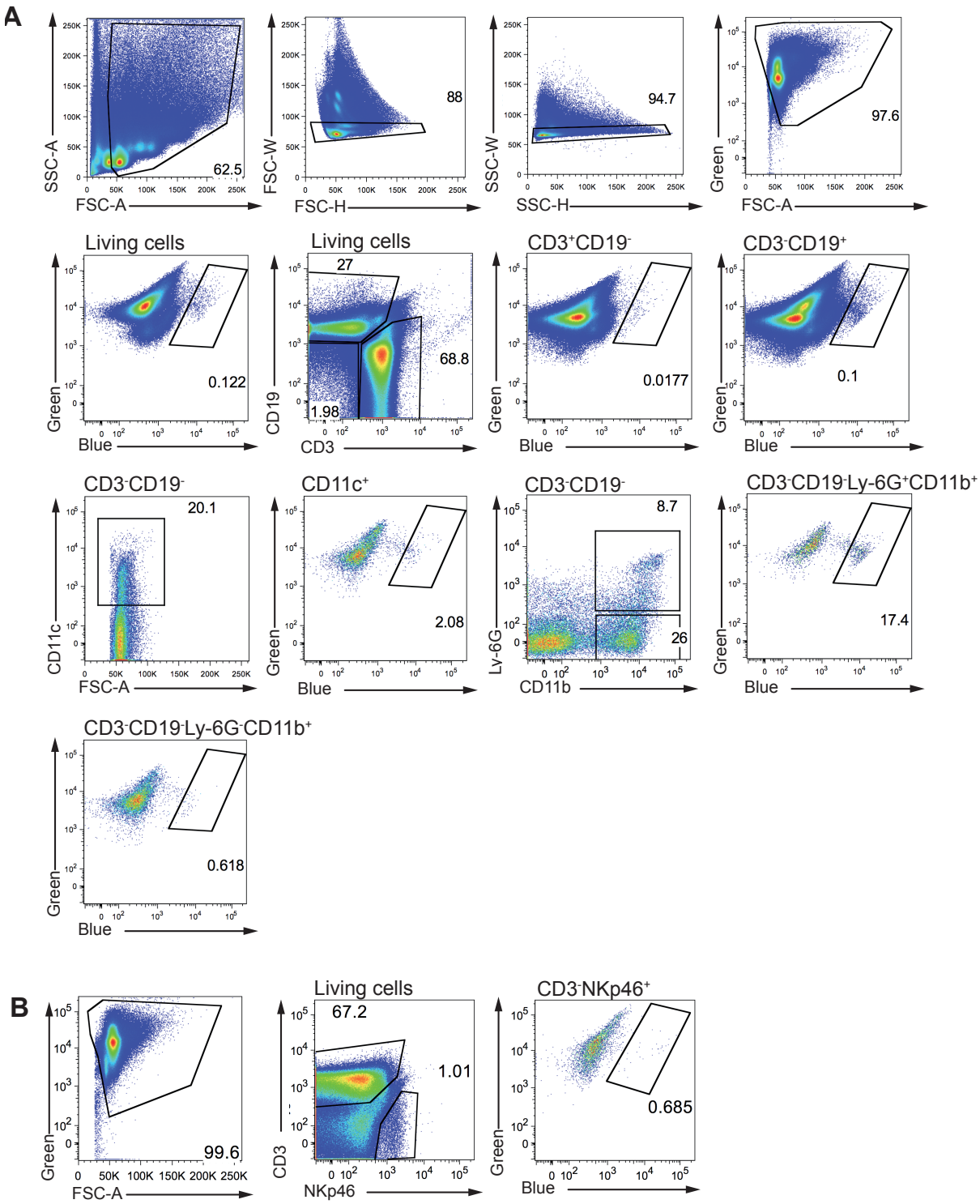

Figure S4: Gating strategies for the analysis of CNF_Y impact on Yop delivery.

Exemplary gating strategies of MLNs cells of YPIII-ETEM infected mice at day three post infection. Isolated cells were stained with fluorescently labeled antibodies and additional subjected to CCF4-AM treatment.

Living cells are „green“, Yop translocated cells are „blue“. (A) T cells ($CD19^-CD3^+$), B cells ($CD19^+CD3^-$), neutrophils ($CD19^-CD3^-Ly\text{-}6G^+CD11b^+$), DCs ($CD19^-CD3^-CD11c^+$), macrophages/monocytes ($CD49b^-CD19^-CD3^-Ly\text{-}6G^-CD11b^+$) (B) NK cells ($CD19^-CD3^-NKp46^+$).

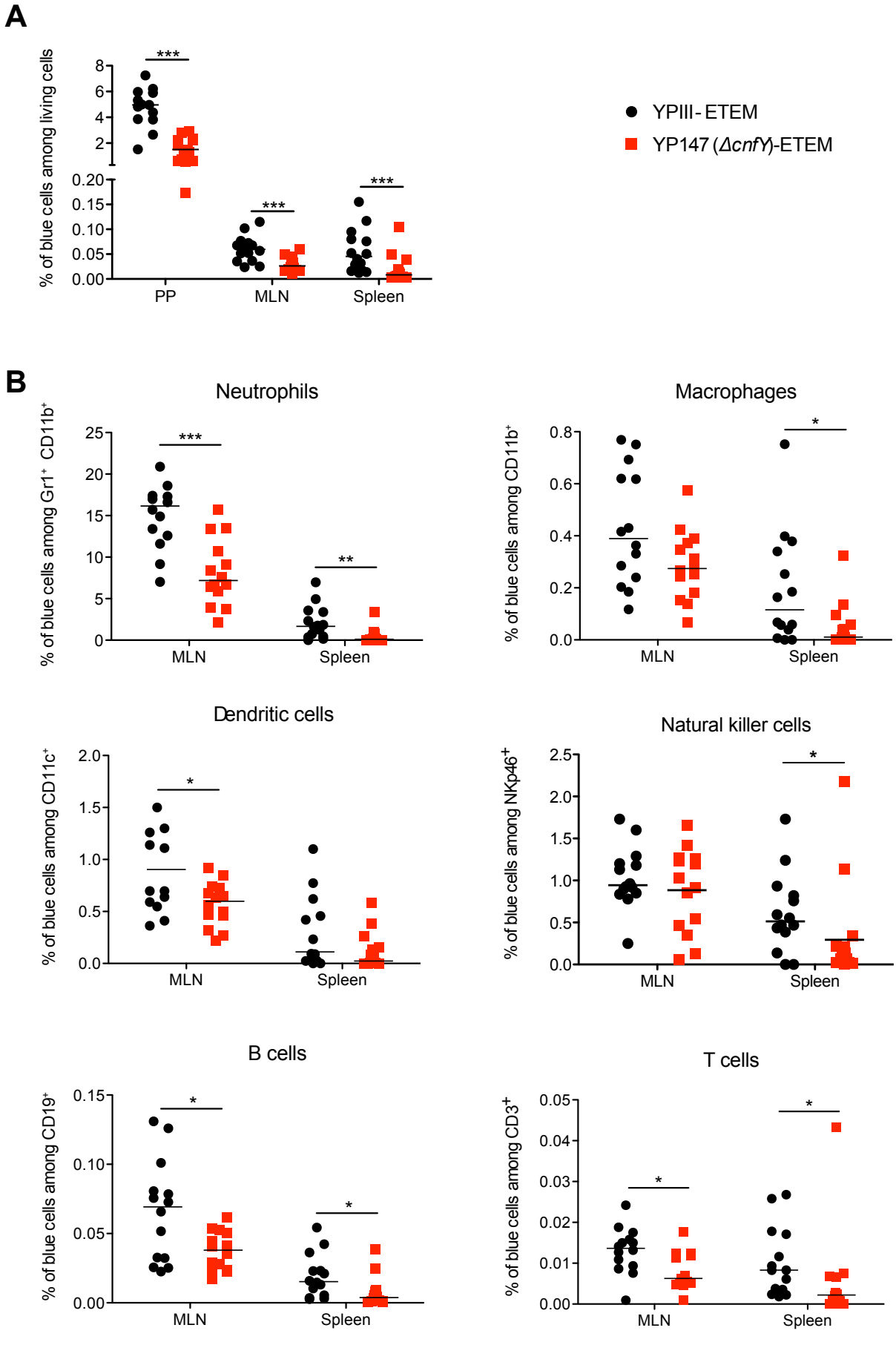
A
% of blue cells among living cells
PP
MLN
Spleen
YPIII-ETEM
YP147 (ΔcnfY)-ETEM
B
Neutrophils
% of blue cells among Gr1+ CD11b+
Macrophages
% of blue cells among CD11b+
Dendritic cells
% of blue cells among CD11c+
Natural killer cells
% of blue cells among NKp46+
B cells
% of blue cells among CD19+
T cells
% of blue cells among CD3+

Figure S5: Deletion of *cnfY* diminishes Yop delivery predominantly into neutrophils, macrophages and DCs in MLNs and spleen *in vivo*.

Groups of 6 - 8 BALB/c mice were infected orally with 2 x 10^9 bacteria of *Y. pseudotuberculosis* YPIII-ETEM (YP173), YP147 (Δ*cnfY*)-ETEM (YP217), YPIII or YP101 (Δ*yscS*)-ETEM (YP174). Three days after infection, mice were sacrificed and the organs (PP, MLNs, and spleen) isolated. Prepared cell suspensions were stained with fluorescently labeled antibodies to detect the different immune cells with flow cytometry: neutrophils ($Gr1^+$/$CD11b^+$), macrophages ($CD11b^+$), DCs ($CD11c^+$), NK cells ($NKp46^+$), B cells ($CD19^+$), and T cells ($CD3^+$). Subsequently, cells were additionally dyed using CCF4-AM. The percentage of blue cells was analyzed by multi-colour flow cytometry of two independent experiments. (A) Percentages of blue (translocated) cells among living cells of PP, MLNs, and spleen of mice infected with YPIII-ETEM (YP173) or YP147 (Δ*cnfY*)-ETEM (YP217) are illustrated. (B) Percentages of blue (translocated) cells among different living immune cell subsets of MLNs and spleen of mice infected with YPIII-ETEM (YP173) or YP147 (Δ*cnfY*)-ETEM (YP217) are illustrated. For statistical analysis, a Mann-Whitney test was applied to determine significant differences in translocation in (A) the different organs and (B) cell types between YPIII-ETEM (YP173)- and YP147 (Δ*cnfY*)-ETEM (YP217)-infected mice. Asterisks indicate the significances, with * (P<0.05), ** (P<0.01) and *** (P<0.001).

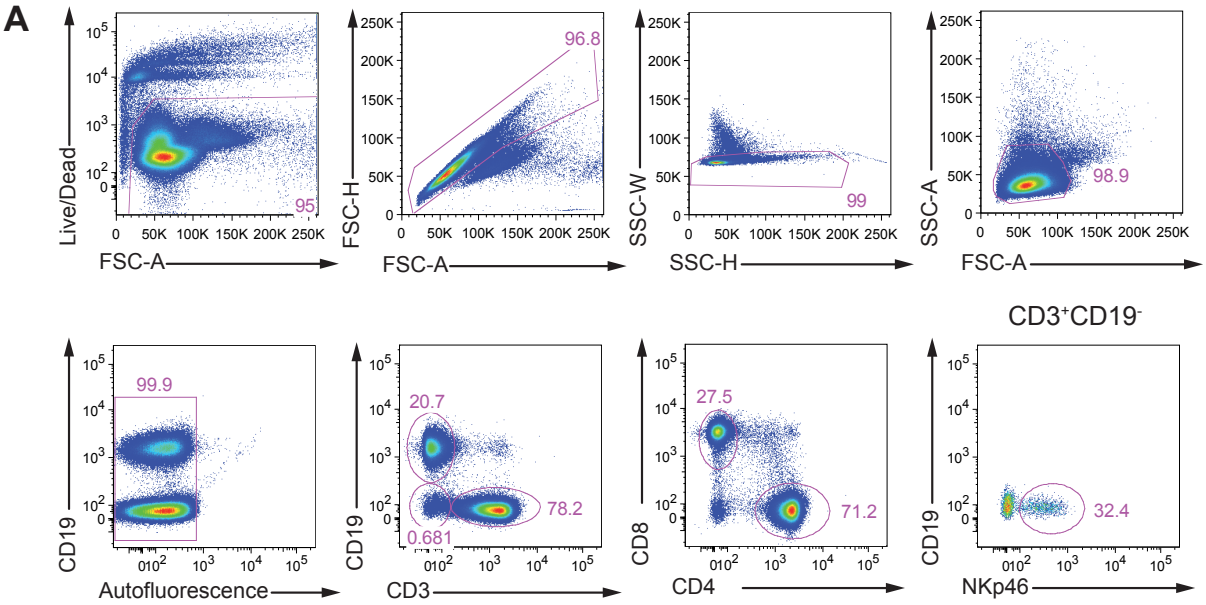

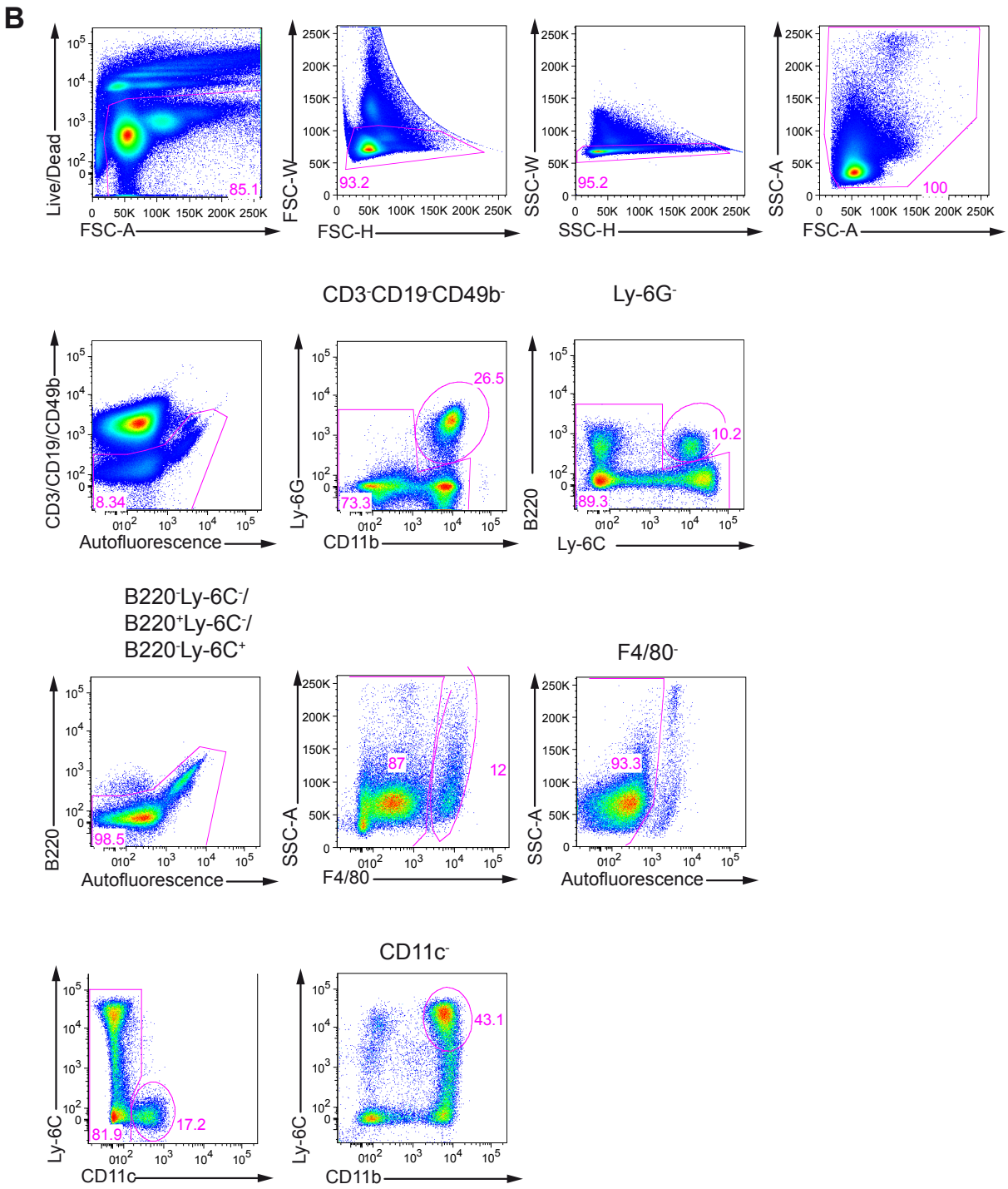

Figure S6: Gating strategies for immune cell contents in PP, MLNs, and spleen after infection with different *Y. pseudotuberculosis* strains.

Exemplary gating strategies of splenocytes from uninfected mice at day three post infection. (A) Lymphoid panel: T cells ($CD19^-CD3^+$), T helper cells ($CD3^+CD4^+$), cytotoxic T cells ($CD3^+CD8^+$) B cells ($CD19^+CD3^-$), NK cells ($CD19^-CD3^-NKp46^+$). (B) Myeloid panel: neutrophils ($Lin^-Ly\text{-}6G^+CD11b^+$), macrophages ($Lin^-Ly\text{-}6G^-pDC^-F4/80^{hi}$), DCs ($Lin^-Ly\text{-}6G^-pDC^-F4/80^-CD11c^+$), monocytes ($Lin^-Ly\text{-}6G^-pDC^-F4/80^-CD11c^-CD11b^+Ly\text{-}6C^+$). Lin (lineage) = $CD3^+CD19^+CD49b^+$; pDC (plasmacytoid dendritic cells) = $Ly\text{-}6C^+B220^+$.

Danksagung

Zuerst möchte ich mich an dieser Stelle bei meiner Mentorin Prof. Dr. Petra Dersch möchte ich mich an dieser Stelle bedanken. Danke dafür, dass du mich so freundlich in deiner Arbeitsgruppe willkommen geheißen hast, für dein Vertrauen in meine Arbeit sowie für die Betreuung und tatkräftige Unterstützung in jeglicher Hinsicht bei der Entstehung dieser Arbeit. Mein besonderer Dank gilt deinem Einsatz bei der Veröffentlichung meiner Ergebnisse.

Zusätzlich bedanke ich mich bei Prof. Dr. Michael Steinert für die Übernahme des Koreferates und die ständige Unterstützung durch die Teilnahme an meinen *Thesis Committees*. Ebenfalls möchte ich mich bei Prof. Dr. André Fleißner für die Teilnahme an der Promotionskommission und an meinem *Thesis Committee* bedanken.

Ein Danke auch an die „Helmholtz International Graduate School for Infection Research“ für die Finanzierung der Teilnahme an Konferenzen und Weiterbildungen.

Weiterhin bedanke ich mich bei Dr. Annika Kochut für die Einarbeitung und die Betreuung im ersten Jahr meiner Doktorarbeit. Ein besonderer Dank geht an Dr. Fabio Pisano, der mir immer mit Rat und Tat zur Seite stand. Der restlichen Arbeitsgruppe danke ich für die entspannte Arbeitsatmosphäre, vor allem im „großen Labor“ und insbesondere Rebecca Geyer, die mir sowohl beruflich als auch privat immer zur Seite stand. Zudem möchte ich mich bei Tanja Krause für die Unterstützung bei den Tierversuchen bedanken.

Vielen Dank auch an meine Eltern für jegliche Unterstützung, vor allem an meinen Vater, der sich Stunden mit dieser Arbeit beschäftigen musste. Danke dafür, dass ich immer auf euch zählen kann. Ebenfalls bedanke ich mich bei meinem großen Bruder Felix, dem mein Wohl immer wichtig war und ist. Meinen Freunden danke ich für die schöne Zeit.

Ein ganz besonderer Dank geht an meinen Partner André Hajek für die letzten neun Jahre fortwährender Unterstützung in allen Lebenslagen!